STRUCTURE FUNCTION OF ACTIN AND TROPOMYOSIN ISOFORMS AND DISCOVERY OF A UNIQUE ACTIN ISOFORM

WASANA A.K.A. MUDALIGE

Your file Votre référence
ISBN: 978-0-494-33475-1
Our file Notre référence
ISBN: 978-0-494-33475-1

Structure function of actin and tropomyosin isoforms and discovery of a unique actin isoform

by

Wasana A. K. A. Mudalige
Department of Biochemistry
Memorial University of Newfoundland
St.John's, NL
Canada
A1B 3X9

A thesis submitted to the School of Graduate Studies in partial fulfillment of the requirement for the degree of Doctor of Philosophy.

Abstract

1. Tropomyosin [TM] was isolated from following sources; shark fast skeletal muscle, which contains a single, partially phosphorylated, alpha type isoform, and salmonid fast, slow and cardiac muscle. At 50mM ionic strength [pH 7.0, room temperature], thin filaments composed of shark phosphorylated TM produce a higher steady-state activation of the myosin-S1MgATPase compared to those containing the unphosphorylated protein. This difference is attributable to the extra negative charge associated with phosphoserine 283 which, under certain conditions [neutral pH, low ionic strength], enhances the interaction of adjoining TM molecule. By comparison, none of the salmonid TMs are unphosphorylated. Of the substitutions, which are distributed throughout the molecule, one occurs within the overlap region [Asn276 in fast, His in slow and cardiac]. This correlates with observed weakening of the end-to-end association of the C-terminal histidine-containing isoforms [cardiac and slow] relative to one present in fast muscle (1). Surprisingly, however, thin filament activation of myosin-S1MgATPase increases in the order: fast TM < slow TM < cardiac TM. Since thin filaments composed of cardiac TM generate the greatest amount of activation it is apparent that tightness of the joint site is not the sole determinant for regulation. Thin filament based regulation is also sensitive to substitutions within the internal region of tropomyosin. The results of myosin binding show very little difference in the affinity of myosin for thin filaments containing non-identical

isoforms of tropomyosin. Therefore these data suggest that the observed changes in steady state rate are due to a change in a kinetic step in the actomyosin ATPase cycle.

2. Unlike other vertebrates, salmonids synthesize a unique isoform of actin in each type of striated muscle [fast, slow and cardiac]. Two are virtually identical to each other but one [slow actin] is divergent and is inferred to contain six or seven non-conservative substitutions depending on the pairing [out of a total of twelve] when compared to the other salmonid actins and rabbit actin. Four of these replacements are predicted to occur in sub-domain 3. The other two or three are in sub-domain 1. Of particular interest is the substitution at residue 360, where a neutrally charged amino acid in a variety of isoactins is replaced by Asp in slow actin. This is consistent with the observation that slow actin migrates ahead of other isoactins when analysed by alkaline urea PAGE. Of all actins tested, the one from slow muscle is the least conformationally stable G-actin [calcium form + ATP], as gauged by a number of techniques including electronic circular dichroism. The midpoint of the change in far-UV ellipticity versus temperature for this isoform is 10°C lower than that of other actins studied [transition temperature, 45°C versus 55°C]. The slow isoform also displays a reduced rate of polymerisation, a faster rate of nucleotide dissociation and a lower level of

myosin activation. These data suggest that actin heterogeneity is a source of thin filament diversity in some vertebrate skeletal muscle.

3. A survey was conducted to determine the distribution of slow muscle actin throughout the animal kingdom. Skeletal muscle actin extracted from certain species, selected on the basis of their taxonomical position, was characterized. Of the species surveyed, a unique isoform was identified in slow muscle of Chondrichthyes [mako shark] and Osteichthyes [teleosts, salmon, Atlantic herring and tuna] but not amphibians [frog] and avians [chicken]. In the latter two cases, the same isoform is present in both types of skeletal muscles. Further, a slow muscle actin gene is absent from the genomes of puffer fish and human. This suggests that a slow muscle actin gene starts to express randomly and then stops expressing after short period of time. This appearance and disappearance is a unique feature, which has occurred during the course of evolution in other genes as well. According to phylogenetic tree analyses performed using several methods [neighbour-joining, minimum evolution and MrBayes method] for selected amino acid and nucleotide sequences, a close relationship between salmon slow muscle actin and puffer fish cardiac actin which is considered one of the oldest actins, was observed. Finally, an actin clone was isolated from a dogfish shark skeletal muscle cDNA library and sequenced. The nucleotide sequence clusters with that

chicken actin, which again underlines the extraordinary degree to which the protein has been conserved.

Acknowledgements

First and foremost I would like to express my sincere gratitude to supervisor, Dr. D. H. Heeley, for continuous guidance, encouragements and patience. Thank you for giving a reasonable degree of independence with a common sense of justice and fairness while remaining true to the discipline of research.

I would like to thank the members of my supervisory committee, Dr. M. Mulligan and Dr. R. Rimsay for their effort in helping to make this project a success, especially in correcting my thesis.

I would like to express my appreciation to Ms. D. Jackman who was the most consistently friendly and supportive person I have known throughout the six years of this undertaking.

I am also grateful to my friends specially, Ms. Charitha Goonasekara who always held out a positive view for me, who assisted me with several tasks in the preparation of the thesis.

Contents

Chapter 1
Introduction

Chapter 2
Materials and Methods

Chapter 3

Effect of changes in primary structure on the regulatory properties of tropomyosin: examination of phosphorylation and isomorphism.

Chapter 4

Characterization of salmonid isoactins

Chapter 5
The distribution of slow muscle actin isoform in the animal kingdom.

Chapter 6
Conclusions

List of Tables

List of Figures

Abbreviations

$(NH4)_2CO_3$	Ammonium carbonate
$(NH4)_2SO_4$	Ammonium sulphate
$(NH4)HCO_3$	Ammonium bicarbonate
ADP	Adenosine diphosphate
Ala	Alanine
AMP	3'-5'-cyclic adenosine monophosphate
Arg	Arginine
Asn	Asparagine
Asp	Aspartic acid
ATP	Adenosine triohosphate
BCIP	5-bromo-4-chloro-3-indolyl-phosphate
BSA	Bovine serum albumin
$CaCl_2$	Calcium chloride
cAMP	Cyclic adénosine monophosphate
CAPS	(3-[N-Cyclohexylamino]-1-propanesulfonic acid
CNBr	Cyanogen bromide
Cys	Cystein
dH_2O	Distilled water
DTNB	5,5'-dithiobis-2-nitrobenzoic acid
DTT	1,4-Dithiothreitol
e-ATP	1-N^6-ethyladenosine-5'-triphosphate
EDTA	Ethylenediaminetetraacetic acid
EGTA	ethylene glycol bis(2-aminoethyl ether)-N,N,N'N'-tetraacetic Acid
ELC	Essential light chain
GdnHCl	Guanidine hydrochloride
Gln	Glutamine
Gly	Glycine
H_3PO_4	Phosphoric acid
His	Histidine
HPLC	High performance liquid chromatography
IAA	Iodo acetic acid
Ile	Isoleucine
K_2HPO_4	Dipotassium hydrogen phosphate
KCl	Potassium chloride
KH_2PO_4	Potassium dihydrogen phosphate
KNO_3	Potassium nitrate
KOH	Potassium hydroxide
Leu	Leucine
LMW	low molecular weight
Lys	Lysine
Met	Methionine

$MgCl_2$	Magnesium chloride
MHC	Myosin heavy chain
MLC	Myosin light chain
MOPS	3-Morpholinopropanesulfonic acid
Na_2CO_3	Sodium carbonate
Na_2HPO_4	Sodium dihydrogen phosphate
$NaHCO_3$	Sodium bicarbonate
NaN_3	Sodium azide
NaOH	Sodium hydroxide
NBT	4-nitroblue tetrazolium chloride
NH_2OH	Hydroxylamine
NMR	Nuclear Magnetic Resonance Spectroscopy
NOE	Nuclear Overhauser Enhancement
PAGE	Polyacrylamide gel electrophoresis
Phe	Phenylalanine
Pi	Inorganic phosphate
PMSF	Phenylmethylsulphonylfluoride
Pro	Proline
PVDF	Polyvinylidene hydrochloride
RLC	Regulatory light chain
RT	room temperature
SDS	Sodium dodecyl sulfate
Ser	Serine
TEMED	N,N,N',N'- tetramethyl ethylene diamine
Thr	Threonine
Tm	transition temperature
TM	Tropomyosin
Tn	Troponin
TnC	Troponin C
TnI	Troponin I
TnT	Troponin T
Tris-HCL	Tris[hydroxymethyl]aminomethane hydrochloride
Trp	Tryptophan
Tyr	Tyrosine
UV	Ultra-violet and visible
Val	Valine

Chapter 1

Introduction

1.0 An overview

Movement is essential to life, and takes many forms, from cytoplasmic streaming and the growth of neurons at the molecular level, to the long distance flight of the albatross or the explosive performance of a sprinter. Although only a few families of proteins are responsible for movement in the biological world, muscle, which is an organ specializing in the transformation of chemical energy into movement, has developed to optimize this function.

Muscles are categorized as striated [skeletal and cardiac muscle] or unstriated [smooth muscle] depending on whether alternating dark and light bands or striations can be seen when the muscle is viewed under the light microscope. Muscles are classified as voluntary [skeletal muscle] or involuntary [cardiac and smooth muscle] depending respectively upon whether they are innervated by the somatic nervous system and are subject to voluntary control or are innervated by the autonomic nervous system and are not subject to voluntary control (2 and 3). The rest of the discussion will be restricted to striated muscle unless otherwise noted.

Skeletal muscle is composed of long cylindrical cells [fibers], each measuring 10 to 100μm in diameter and up to several centimeters in length. These cells arise during embryonic development from the fusion of myoblast cells. Each muscle fiber is enclosed within a single plasma membrane referred to as the sarcolemma. The cytoplasm is occupied largely by

cylindrical filaments, which contain the contractile protein machinery of the muscle cell. Three types of fibers can be recognized based on numerous parameters, including speed of contraction [slow or fast] and genre of enzymatic machinery used for the synthesis of ATP [oxidative or glycolytic]. These are: slow-oxidative, fast- oxidative and fast-glycolytic. Further classification and characteristic features of muscle fibers are summarized in Table 1.0 (4). Slow-oxidative fibers [dark fibers], rich in myoglobin, cytochromes and mitochondria synthesize ATP predominately by oxidative phosphorylation. In contrast, glycolytic fibers contain very little myoglobin, and hence are pale in colour [white fibers]. In addition to their high myosin ATPase content, these fibers are also larger in diameter than the slow-oxidative fibers. Fast-oxidative fibers have high myosinATPase activity and also high oxidative capacity. However, the rate of ATP production of these fibers cannot keep pace with the high rate of ATP hydrolysis, because they rely partially on glycolysis and are more prone to fatigue than the slow-oxidative fibers. In mammals, most muscles contain a mixture of all three fiber types, the proportions of which depend on the type of muscle and the physiological demands placed upon it. Slow-oxidative fibers are in muscles specialized for maintaining low-intensity contractions for a long period of time without fatigue, such as muscles of the back and legs, while fast-glycolytic fibers can be seen in the arm muscles, which are adapted for performing rapid, forceful movements (2, 5).

In the early 1800s, it was first noted that muscle fibers exhibit a series of alternating light and dark bands or striations, when viewed with a light microscope. Later, it was determined that myofibrils of each muscle fiber are aligned with their bands in register, giving the cell a striated appearance consisting of alternating light and dark bands called I band [Isotropic

Table 1.0 Diversity of vertebrate striated muscle fibers

Fiber type	Twitch fibers		
	IIB	IIA	I
Color	White	Red	Red
Contraction speed	Fast twitch	Fast twitch	Slow twitch
Fatigue resistance	Low	Medium	High
Mechanism of ATP synthesis	Glycolytic	Glycolytic and oxidative	Oxidative

Extracted from "Calcium in muscle activation" by Ruegg, J. C. (4)

band] and A band [Anisotropic band] respectively. Running down the middle of each I band is a dense line known as the Z disk. The Z disks divide a myofibril into a series of repeating units called sarcomeres, each measuring about 2μm in length. Z discs also are implicated in mechanosensation and signalling to the nucleus. According to electron microscopy by Huxley (6 and 7), myofibrils are composed of two types of filaments: thin filaments [6nm in diameter] and thick filaments [15nm in diameter]. The I bands have a light appearance due to the presence of thin filaments only, while the A bands are dark because they contain overlapping arrays of both thick and thin filaments. There is a central region of the A band, called the H zone which does not contain thick filaments.

It is estimated that a single muscle fiber may contain 16 billion thick and 32 billion thin filaments, all arranged in a very precise pattern within the myofibrils. Each thick filament is composed of several hundred myosin molecules while thin filaments are comprised of three proteins: actin, tropomyosin [TM] and troponin [Tn]. The third filament system is made up of single molecules of titin, which span half sarcomeres. Another giant protein, nebulin, spans the length of the actin filaments and forms the fourth filament system in skeletal muscle. Apart from these major proteins found in filaments, numerous other proteins are also present in sarcomeres; for example, the filaments are capped at the pointed and barbed ends by tropomodulin and CapZ respectively.

1.1 Contractile proteins

1.1.1 Tropomyosin

Tropomyosin, discovered in 1946 (8 and 9), is a dimeric, heat-stable protein, having an isoelectric point of ~4.6 (10). Tropomyosin is present in every eukaryotic cell. There is no evidence so far of TM in prokaryotes. The most abundant source is striated muscle where it accounts for ~3% of total protein (11). In muscle, the protein is located within the thin filament where it exists as a continuous chain. Some of the characteristics of TM are: highly alpha-helical, rod-shaped, actin binding, and with a sequence repeat in which non-polar amino acids occur every first and fourth residue of a heptapeptide unit.

The complete primary structure of TM was reported in the early 1970s (12 and 13). Analysis of the sequence revealed two types of periodic repeats. As predicted by Francis Crick (14), there is a short-range repeat consisting of seven-residues in the form ***a-b-c-d-e-f-g*** [Fig.1.1], where positions ***a*** and ***d*** show a strong preference for non-polar side chains. The ***b,c,e,f*** and ***g*** positions are usually filled by polar or charged side chains. Crick also proposed that the side chains of ***a*** and ***d*** amino acids would interlock at the interface of the dimer, in a knobs-into-holes fashion (15). Because an alpha-helix encompasses 3.6 residues per turn [whereas the repeat unit is a heptapeptide], the hydrophobic seam does not run parallel to the long axis of the helix, but winds around it (16). The association of two molecules of TM reflects this, since they wind around one another producing a coiled coil structure (17-22). The two chains are parallel [i.e. having both N-termini at one end and both C-termini at the other] and in register [i.e. non-

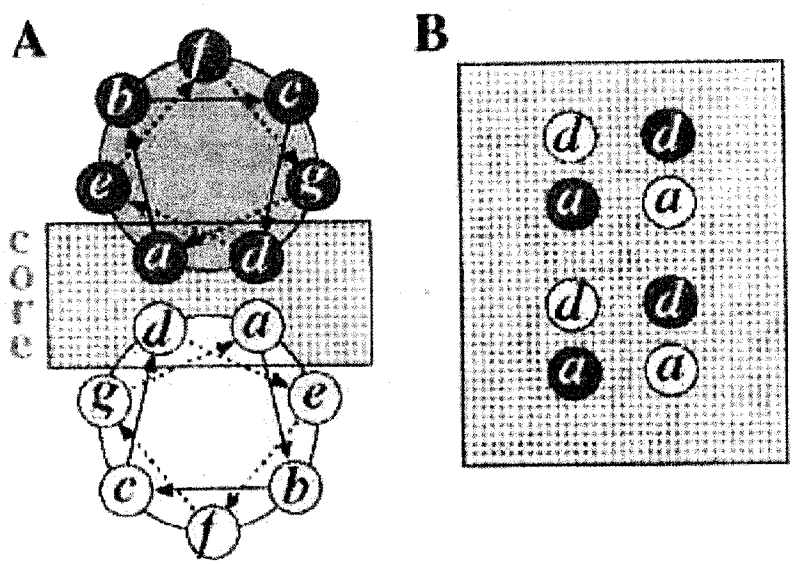

Fig. 1.1 Interactions between the two α-helices in the tropomyosin coiled-coil (16).

Each α-helix is shown with seven residues [***a-g***] in two turns. [A] End-on view looking from N terminus. The interface between the α-helices derives primarily from hydrophobic residues in core positions ***a*** and ***d***, although there are also some salt bridges formed between residues ***e*** and ***g***. [B] The core interface viewed parallel to the coiled-coil axis shows how residues from one chain occupy the spaces between the corresponding residues from the second chain to give "knobs in holes" packing (15). In tropomyosin there are slightly more than 3.6 residues per turn, which produces a left-handed super coil.

staggered]. One line of evidence for this arrangement of chains, is the fact that an interchain disulfide bond can be formed between Cystenes which occur at position 190 in both chains (23). This could only happen if the Cystenes were in close proximity. The basic features of the coiled coil as suggested by Crick were later confirmed by the crystal structure of the GCN4 leucine zipper (24). The long-range repeat is made up of alternating charged/polar and non-polar side chains and is considered to correspond to seven pairs of consecutive actin binding sites (25). Recently, an additional repeat involving core Ala residues has been identified. This is a semi-regular repeat, which is proposed to generate several bends in the molecule's axis (26).

The first 20 residues of the TM molecule are highly conserved, including the N-terminal Met, which is acetylated. A comparison of 11 vertebrate muscle TMs reveals two minor changes in this region of the protein, Glu2Asp and Leu19Ile (27-29). When *Drosophila* muscle TMs are included in the analysis, 14 of the first 20 residues are identical, including the first nine residues which contain three consecutive Lys at positions five, six and seven. These Lys are required for self-polymerization, a process that is conveniently demonstrated by viscometry (8). Polymerization, which is more pronounced for muscle TMs than non-muscle TMs, is thought to arise from a merger of different ends of contiguous molecules [end-to-end polymerization]. The basis of the 'overlap' is, in part, electrostatic. The N-terminus will possess a net positive charge at pH 7.0, while the C-terminus will possess a net negative charge. This is consistent with the ionic strength-dependence of polymerization and the observation that a phosphate group at Ser283 increases the viscosity in the neutral pH

range (30 and 31). An overlap of 8-9 residues would reduce the effective length of TM from 284 to about 275 residues, a length that is consistent with measurements from protein crystals (32) and the fact that removal of 12 residues from the C-terminus by carboxypeptidase results in non-polymerizable protein. (33-35). Interestingly, bacterially expressed TM, which is non-acetylated, exhibits substantially weaker end-to-end polymerization compared to wild type (36-39). This could be due to the N-terminal Met occupying an inner "***a***" position and/or repulsion with other positively charged side chains, notably one or more of the three aforementioned Lys. Restoration of polymerization can be achieved by the N-terminal fusion of two [Ala-Ser] or three [Ala-Ala-Ser] amino acids (40 and 41). It should be noted that there is evidence that changes within the central portion of the TM molecule can also influence overlap interactions (42 and 43). Despite the biochemical progress that has been made, the structure of the overlap region remains unsolved, as crystals of full length TM show low resolution in X-ray diffraction studies owing to their high water content [>90%] (44-46).

High-resolution structures of N- and C-terminal peptides have been obtained by X-ray crystallography and by ^{1}H-NMR (47 and 48). In the 2.7Å crystal structure of a 31 residue C-terminal fragment of TM fused to a fragment of the GCN4 leucine zipper, the helices formed by the last 22 TM residues [263-284] splay apart and two symmetrically related molecules make intermolecular contacts in a tail-to-tail manner (49). Further, evidence that the C-terminal 9 to 11 overlap residues are highly flexible and differ in structure from the rest of the molecule, comes from a ^{1}H-NMR study in which several sharp peaks [indicative of regions of high flexibility] were lost upon carboxypeptidase treatment (50). Phillip *et al.*, (51) suggested from examination of TM motion within crystals, that the C-terminal half is very

flexible and partially unfolded at physiological temperatures. In connection with these reports, is the recently published solution structure of a dimeric peptide containing the last 34 amino acids of TM [i.e. residues 251-284] (52). The peptide was cross-linked and contained a stabilizing mutation at position 279. In this study the residues 257-269 formed a coiled coil, residues 270-279 were helical but were not arranged in coiled coil and the last five residues [280-284] were non-helical (52-54).

The findings of a number of investigations have shown that the C-terminal half of the TM molecule is less stable than the N-terminal half (55 and 56). According to microcalorimetric analysis, TM thermal denaturation is interpreted as a multistep process in which specific segments called cooperative blocks unfold independently of one another (57). However, it has also been noted that the sum of the denaturation curves for two TM fragments, corresponding to predicted cooperative blocks [190-254 and 253-280], is not equal to the experimental curve for the fragment 190-254, arguing for long range cooperativity along the TM structure (58-60). Lee *et al.*, (61) have suggested that a complex combination of stabilizing effects along the sequence is a more general indicator of protein folding in coiled coils than the identification of a specific sequence. Even if TM folds either via independent cooperative blocks or nucleated by one or more specific sequences, it is clear that TM contains regions that are more intrinsically stable than others. The factors which may contribute to instability could be: inter-helix repulsion between ***g*** and ***e'*** positions of the heptad repeat, a charged residue at the hydrophobic coiled coil interface and a greater fraction of β branched residues located at ***d*** positions (62).

The role of TM remained unclear until the 1960s when Ebashi showed that TM is a regulator of the actomyosinATPase activity in striated muscle (63-66). This regulatory function stems from two fundamental properties of TM: [i] actin binding (67) and [ii] Tn binding. By interacting with both TnT [TM binding subunit of Tn] and actin, TM serves as a relay, conveying conformational information from Tn to actin (68 and 69).

Tropomyosin comprises a family of proteins. This was first demonstrated by electrophoresis. Using SDS-PAGE as a separation method, two isoforms α- and β- were reported in rabbit skeletal muscle (70). The heterogeneity was then characterized more rigorously, first by protein-level sequencing and then nucleic acid-level sequencing (29, 71). All muscle [skeletal, cardiac, smooth] TMs have been shown to contain a total of 284 amino acid residues. As would be expected from TM's extensive quaternary structure, the sequence has been strongly conserved. There are only 39 amino acid substitutions between rabbit -α and -β TMs (29). None of these substitutions significantly affect the short and long-range repeats discussed earlier. Non-muscle TMs are shorter in length, i.e. 245-251 amino acids. Yeast TMs are even shorter, containing 161 and 199 residues (72). Although, these TMs are dimeric, they polymerize less extensively than their muscle counterparts, primarily because of marked differences in the N-and C- terminal overlap sequences (71).

Four TM genes have been identified in mammals and from these at least 20 isoforms are generated by the use of alternative promoters and alternative RNA processing (73). The TPM1 and TPM2 genes give rise, respectively, to striated muscle α- and β- TMs (74 and 75). In addition, the TPM2 gene codes for the smooth muscle β-TM and fibroblast TM1. The

TPM3 gene [sometimes referred to as γ-TM] codes for fibroblast LMW tropomyosin and a slow twitch skeletal muscle α-TM (76). TPM4 [also known as the δ or TM4 gene] has so far only been shown to code for one isoform, fibroblast TM4.

The functional significance of this diversity is not fully understood and is one of the aims of this thesis. One of the problems that has been encountered is that, multiple TM isoforms often exist in the same muscle fiber. For example, certain fast-contracting mammalian skeletal muscles [psoas] contain a preponderance of α-TM [80%α, 20%β] while others [extensor digitorum longus] contain equal proportions of α- and β- TM isoforms (15, 77 and 78). Slow-contracting skeletal muscle contains an extra isoform, in addition to those found in fast muscle. The situation is made more complicated by the fact that the relative amount of each isoform changes during muscle development (79) and is also species-dependent. For example, the heart of small mammals [rabbit, rat, mouse], one of the rare instances of 'isoform-purity' contains only α-TM, whereas larger mammals [cow, pig] contain low levels [~15%] of the β-isoform. Studies involving the transgenic mouse heart have shown that heart containing only α- or β-TM exhibit differences in contraction and relaxation (80 and 81), despite the high homology between α- and β-TM [α- and β-TM are 86% identical at the amino acid level], Although the α- and β- TM isoforms are the major forms of the protein, additional variants have been observed in rabbit and rat skeletal muscle (15, 77 and 78). These extra isoforms may be products of the TPM3 gene (75). The complexity of this system will likely increase as more TM genes are characterized (79).

1.1.2 Actin

Discovered by Straub in 1942 (82), actin is one of the most abundant proteins in both the prokaryotic and eukaryotic world, having been identified in the cytoplasm of animal, plant, protozoan and fungal cells (83). One of the hallmarks of actin is its ability to activate the ATPase of myosin. It can also self-associate into long filaments which are called F-actin. These features are consistent with actin's involvement in motility [eg. muscle contraction, cytokinesis, organelle movement] and maintenance of cell shape (84). Actin represents 20% of the total protein in skeletal muscle. Virtually all of the actins are present within the thin filament, where it is required for the production of force.

Actin consists of a single polypeptide chain of, usually 373-375 (83), amino acid residues [mass, 42 kDa]. The sequence is one of the most highly conserved known. Side chains that are charged at pH 7.0 [i.e. Asp+Glu+Lys+Arg] account for roughly 25% of the total number of amino acids. Aromatic side chains, which include four conserved Trp, account for 10%. One Cys is removed by exolytic processing, yielding a final Cys content of five. Additional post-translational modifications are acetylation of the N-terminal amino acid and methylation of His73 (85). However, recently, unmethylated His73 was reported from *Naegleria gruberi, Candida albicans and Saccharomyces cerevisiae*, suggesting that methyl-His may be present only in multicellular eukaryotes (86). Other features of actin include one high affinity divalent cation-binding site, several low-affinity cation-binding sites (87) and one nucleotide [either ATP or ADP] binding site (88 and 89).

Filamentous actin is a non-covalent, double stranded polymer of actin monomers. The assembly process is sensitive to ionic strength and the type of divalent metal ion, and requires that the concentration of monomer be above a certain limiting value, which is known as the critical concentration (83). During polymerization the bound ATP is hydrolyzed. However, the involvement of ATP hydrolysis in polymerization is not completely clear (90). Previously, hydrolysis was assumed to play a key role in the steady-state treadmilling of actin filaments (91). Alternatively, Carlier (92) suggested that the hydrolysis of ATP upon polymerization facilitates rapid de-polymerization. Since ADP-actin can also polymerize (93 and 94), although the rate and the extent of polymerization are lower (95-97) than for ATP-actin, especially in the cold (98), it is evident that nucleotide hydrolysis is uncoupled from polymerization (94 and 95). The polymerization process can be conveniently divided into two major steps: the slow thermodynamically unfavored formation of nuclei, [the rate-limiting step], and the rapid elongation of nuclei to long filaments. The first step appears to involve a rapid conformational change of the actin monomer to a state referred to as F-monomer or G*-actin which is assumed to be a necessary intermediate in the polymerization process. (99 and 100). Self-assembly begins with the slow formation of G*-actin comprising three actin monomers (101-104).

Based on the arrowhead pattern created when rigor myosin heads bind to actin, one end is called the barbed end and the other the pointed end. The filament grows bidirectionally (105) with the monomer exchange rate being 20-fold faster at the barbed end than the pointed end

(106). Thus, the pointed end will have a terminal ADP monomer while the barbed end will have an ATP monomer, resulting in chemically different ends. At concentrations too low to cause polymerization, Mg^{+2} can exchange for Ca^{+2} at the high affinity site (107-110) with a resultant conformational change (87,108 and 109) that differs from, and is much slower than, that due to the association of cations with the low affinity sites (87,108). At micromolar levels of Mg^{+2} and Ca^{+2}, divalent metal ions have an opposite effect on actin polymerization; Ca^{+2} bound to the high affinity site inhibits spontaneous polymerization while Mg^{+2} enhances it (111-114). However, both Mg^{+2} and Ca^{+2} promote polymerization at concentrations in the millimolar range, apparently by binding to multiple lower affinity sites (115-117).

The three dimensional [3-D] structure of G-actin was first determined at low-resolution [i.e. 1.5 nm] from electron microscopy and from 3-D structure reconstruction (118). The atomic structure of rabbit skeletal muscle actin was solved to 2.8Å resolution in 1990 using crystals of actin complexed with DNase I (119). To facilitate the crystallization, the C-terminal three residues were removed using mild tryptic digestion (120). Later, two other actin structures were determined; undigested actin complexed with gelsolin segment I (121) and with profilin (122). There is a good qualitative agreement between these actin structures and the one derived from electron microscopy. Recently, Dominguez *et al.*, (123) succeeded in producing crystals of uncomplexed actin. They were also the first to crystallize actin with ADP present in the nucleotide-binding cleft (124). Collectively, these structural studies have revealed two major domains, each of which can be subdivided into two sub-domains. The overall dimension of the molecule, which is about 40% helical, is approximately 55 x 55 x 35Å .The protein chain initiates and terminates in sub-domain 1. This part of actin, as well as sub-

domain 3 has a repeat motif comprising a multi-stranded β-sheet, a β-meander, and a right handed βαβ-unit suggesting that they may have evolved by gene duplication, followed by insertion of sub-domains 2 and 4 [into sub-domains 1 and 3 respectively]. The high affinity divalent metal ion and the adenine nucleotide are located at the bottom of the central cleft between the major domains (119-122,125).

A major difference between these ATP and ADP structures occurs in sub-domain 2. The DNase I binding loop is folded as an α-helix or disordered or folded as a β turn [in ATP-actin]. In addition, minor differences can be seen in sub-domain 1, especially the interactions involved in the coordination of a divalent cation in the nucleotide binding cleft (124).

A notable feature of the structure is a two-stranded "hinge" at residues 140 and 338 joining the large and small domains. Tirion *et al.*, (126) described a "propeller" motion between these two domains that produces an opening and closing of the nucleotide cleft. The extensive contacts between the nucleotide cation complex and residues in all four sub-domains contribute to the stability of the protein. Interestingly, the actin structure is similar to a group of proteins, which includes sugar kinases and ATPase heat-shock proteins (127), although there is a very low sequence homology to actin.

It has been suggested from intrinsic fluorescence (107) and ^{1}H-NMR (115) studies that the conformation of the protein is sensitive to the type of bound metal ion. The Ca^{+2} and Mg^{+2} forms of the protein are not structurally equivalent. The removal of the bound metal ion upon addition of EDTA induces nucleotide dissociation and denaturation. One possible

explanation is that it is due to a loss of polymerization (128). However, in this inactivated state, actin retains much of its secondary structure. Complete unfolding is observed in high concentrations of urea and guanidine (129-132). It is possible to interconvert between the partially and completely unfolded states, but not between these states and the native conformation (131 and 132).

The structure F-actin has only been solved to low-resolution using electron microscopy and computed image analysis (133-136). The results from these investigations have not always been in agreement. According to the model of Holmes *et al.*, (134), in the left-handed helix, monomers rotate by –166° and have an axial translation of 27.5Åfrom one another. There are 13 monomers in six turns with a pitch of 59A° yielding a filament diameter of ~90-100A°. The larger sub-domains 3 and 4 are axially located across from and interaction with sub-domains 3 and 4 of the actin in the second strand. The smaller sub-domains 1 and 2 are located at the periphery of the filament exposed to the solvent and are available for interaction with myosin. Each actin monomer makes contact with four other monomer molecules of the preceding and following actins on the same long helix and the two across the filament on the other long pitch helix. Each actin uses 10 surface loops and 2 α-helices to make these interactions.

Actin activates myosin by speeding up the rate of product release through the isomerization [structurally] of myosin's active site between two states, the so-called 'open' and 'closed' conformations, depending upon the presence or absence of a phosphate group [Pi]. Upon binding ATP, it closes the site. Actomyosin dissociates and the bound ATP is hydrolyzed.

Reassociation opens the site. In this conformation myosin has reduced affinity for gamma phosphate affinity. The Pi dissociates, closely followed by ADP. At this time myosin is in the 'open' conformation and another molecule of ATP can enter the active site. Thus, actin's role is to lower the affinity of myosin for Pi (137).

Structural and chemical modification studies have revealed that the N-terminal acidic residues on actin could be covalently linked to myosin-S1 (133), troponin I [Inhibitory subunit of Tn] (138), TM (139) and several other proteins (140 and 141). Structural studies related to the docking of myosin-S1 at the surface of actin filaments led to a model of the actomyosin interface that involves a dominant component of hydrophobic interactions and several weaker sites of electrostatic interactions, which are located in sub-domain 1 and 2 of actin and include sequences 1-7, 18-29, 92-101, the helix 79-92 and N-terminal segment of the DNase I binding loop 38-52 (142 and 143). Chemical modification analysis of residues located between His40 and Try69 has shown their significance in actin-actin interactions (144-146). Actin binds with various other proteins. Actin monomer binding proteins such as profilin (147) and DNase I inhibit actin monomer ATPase activity and also polymerization while capping proteins [eg., gelsolin (148) and fragmin (149)] bind to one end of the actin filament and influence subunit interactions there. Moreover, cross-linkers or gelation proteins, which bind to the sides of actin filaments, act as spot welds to the different cross-link filaments. Fimbrin (150) and fascin (151) cause actin filaments to form bundles. While, actin was recently reported to occur in the nucleus, its function in the nucleus is not yet clear. However, Zhu *et al.*, (152) showed that nuclear actin interacts with RNA polymerase II. Hence it may have a function in RNA polymerase II mediated transcription.

A small multigene family encodes actin. In vertebrates, particularly mammals, the expression of each iso-actin gene is regulated in a developmental and tissue specific manner. The various iso-actins are grouped into α, β and γ forms on the basis of their iso-electric point (153) which is ~5.6 and can be further classified into six variants on the basis of amino acid sequence and site of expression: these are two striated muscle [α-skeletal and α- cardiac], two smooth muscle [α-vascular and γ-enteric], and two non-muscle [β-and γ-cytoplasmic] actins (154-158). It has been suggested that muscle actin genes have arisen from non-muscle actin genes by gene duplication and subsequent divergence events once within the deuterostome branch and once within the protostome branch (159-161). Furthermore, all metazoan cytoplasmic actins and the muscle actins of invertebrates appear to be direct descendants of the cytoplasmic actins found in protozoa and fungi (162). Even though actin is a remarkably conserved protein it does not appear to be interchangeable *in vivo* and numerous results using a variety of approaches suggest a functional diversity even within the same cell (163).

1.1.3 Troponin

The contraction of vertebrate striated muscle is regulated by Ca^{+2} through its binding to a specific regulatory protein complex, troponin [Tn], which is distributed at regular intervals along the entire thin filament (164-168). The Tn complex, which was discovered in 1959 by Ebashi (169), is composed of three subunits: the Ca^{+2} binding subunit, troponin C [TnC]; the tropomyosin binding subunit, troponin T [TnT]; and the inhibitory subunit, troponin I [TnI]. This complex can be dissociated by denaturants and reassembled into its functional complex

(170). It has been demonstrated that co-expression of all three Tn subunits in bacteria yields a functional ternary complex that can be purified under non-denaturing conditions (171). The overall structure of the troponin complex consists of two domains: a globular domain, which is comprised of subunits TnC, TnI and the C-terminal portion of TnT, and a highly extended region, or tail, containing the remainder of TnT (172 and173). Recently, the 3-D structure of the core domain of human cardiac Tn in the calcium-saturated form was reported (174). The core domain is mainly composed of α-helices and it can be further subdivided into two structurally distinct sub-domains, denoted as the regulatory head [consisting of TnC residues 3-84 and TnI residues 150-159] and the IT arm [IT arm: consists of TnC residues 93-161, TnI residues 42-136 and TnT residues 203-271]. These sub-domains are connected by flexible linkers making the entire molecule highly flexible (174).

1.1.3.1 Troponin C

Troponin C [18,000 Da], the smallest component of the Tn complex, was isolated in the 1960s (175 and 176). It is a very acidic protein owing to its high content of Glu and Asp residues. Rabbit skeletal troponin C contains no Trp residues, only two Tyr residues and only one residue each of Pro, Cys and His (177). The crystal structure of avian TnC, determined at pH 5.0, revealed a dumb-bell shaped molecule that consists of two N- and C-terminal lobes connected by a nine turn α-helix composed of two fused helices called D and E containing a centrally located Gly residue [Gly92] (178-181). Each lobe has two Ca^{+2} binding helix-turn-helix motifs known as EF hands (182-184). These sites have been numbered I-IV, starting from the N-terminus. Sites I and II are called "low affinity" sites which are specific for Ca^{+2},

and they have an association constant of $5x10^5$ M^{-1}. Sites III and IV, the "high affinity" sites, have a binding constant of $2x10^7$ M^{-1} and, in addition, bind Mg^{+2} with an apparent affinity constant of $3x10^3$ M^{-1} (185-187). Unlike skeletal TnC, cardiac TnC has only one Ca^{+2} specific site and two high affinity Ca^{+2}-Mg^{+2} sites (188). Further, there is a very hydrophobic region in the D-helix, which is buried within the amino terminal domain (177). It is possible that the Gly residue in the center of D-E helices may allow the molecule in the solution to fold over, which would bring the Ca^{+2} specific and Ca^{+2}-Mg^{+2} sites into close proximity to interact (177). Resonance energy transfer experiments support this suggestion (189)

^{1}H-NMR studies of tryptic fragments of TnC indicate that both halves of the molecule retain a structure in the apo and Ca^{+2} saturated forms, which resemble that of the intact protein (190). Additional work by Wang & Gergely (191) and Grabarek *et al.*, (192) suggests that the interactions between two halves of the TnC molecule in Tn occur via interactions with TnI and TnT subunits and may have a vital role in thin filament activation. Kinetic studies using dansylaziridine labelled TnC revealed rapid Ca^{+2} binding to both low and high affinity sites but the rate of Ca^{+2} release from the high affinity sites was considered to be too slow, suggesting that it may not participate in the dynamic regulation of contraction (193 and 194).

1.1.3.2 Troponin I

Troponin I [21 kDa] is a basic protein containing one Trp, two Tyr and three Cys, which may need to be reduced to maintain activity in reconstituted complexes (195). Troponin I inhibits the magnesium-dependent ATPase activity of actomyosin (170,175,196) through interactions with both actin and TM-actin (167,197) and also interactions with TM. The inhibition of the

actomyosinATPase is neutralized when calcium-saturated TnC forms a complex with TnI (196,198 and 199), an effect requiring a lower concentration of TnI in the presence rather than in the absence of TM. Studies have indicated that residues 1-21 and 96-116 of TnI interact with TnC (200-202). Residues 104-115 of TnI [Gly-Lys-Phe-Lys-Arg-Pro-Pro-Lys-Arg-Arg-Val-Arg] comprise the minimum sequence necessary for the inhibition of actomyosinATPase activity (203-205). This TnI peptide is basic and contains alternating basic and hydrophobic residues. Two residues of TnI can be phosphorylated: Thr11 by phosphorylase kinase and Ser118 by cardiac 3', 5'-cyclicAMP dependent protein kinase (200,206). Skeletal TnI is not phosphorylated in whole Tn complex. The main structural difference between cardiac and skeletal muscle TnI is an N-terminal extension unique to cardiac TnI containing phosphorylation sites for cAMP-dependent protein kinase. While phosphorylation of cardiac TnI appears to reduce the affinity of cardiac TnC for Ca^{+2} (207), no role has yet been established for skeletal TnI phosphorylation. The structure of the TnI peptide bound to calcium-saturated TnC, derived from 2D NOE ^{1}H-NMR spectroscopy, reveals an amphiphilic helix-like structure, distorted in the centre by the two Pro residues (208). The central bend in the peptide functions to bring the residues on the hydrophobic face into closer proximity with each other to form a small hydrophobic pocket with the hydrophilic basic residues extending off the opposite face of the peptide. The reversal of inhibition is related to Ca^{+2} dependent TnI-TnC interactions elucidated in part at the atomic level (209).

1.1.3.3 Troponin T

Troponin T, the largest subunit of the Tn complex, is a highly polar, structurally asymmetric molecule with a high content of acidic amino acids near the N-terminal half of the molecule and a predominance of basic residues within the C-terminal half. Troponin T isoforms isolated from vertebrate muscle are composed of a single polypeptide chain with a molecular weight in the 31-36kDa range, consisting of about 250 to 300 amino acids. Cardiac TnT usually contains a larger number of amino acids than its skeletal equivalents (210). Invertebrate forms exhibit significant homology with vertebrate skeletal TnT, but are often of higher molecular weight because of the addition of a C-terminal extension of about 100 amino acids, roughly half of which are polar (211). Troponin T can be phosphorylated at Ser position 1 in the native Tn complex (212 and 213). However, no physiological role for this posttranslational modification has been recognized (214). Troponin T binds TM at two sites (212-215). The globular C-terminal domain [TnT-2] mediates its interactions with TnI and TnC, as well as binding near residue Cys190 of TM. The N-terminal domain of TnI [TnT-1] appears to bind to sequences within the C-terminal one-third of TM, from Cys190 of one molecule to the N-terminus of the adjoining molecule (215). The central region and C-terminal domain of TnT contain a helical segment, which may stabilize interaction with TM by the formation of a triple helix (212).

1.1.4 Myosin

Myosins are a diverse super family of molecular motors capable either of translocating actin or of translocating cargo along a fixed actin filament. The first myosin was discovered in

1864 (216). It is a ubiquitous protein found in all eukaryotic cells, the highest concentration occuring in muscle (217) and comprises almost 50% of the total protein in skeletal muscle. Based on sequence homology this superfamily is currently known to fall into 17 different classes (218). According to the classification scheme suggested by Cheney *et al.,* (219), all new classes of myosins discovered after the myosin I and myosin II classes are assigned a Roman numeral in order of their discovery. The closeness of numerical numbers does not imply that those myosins are closely related. All types of myosins that have been identified are multimeric and are activated by actin, yet the functions are diverse. All myosins possess at least three functional domains, a head, a neck and a tail. Striated muscle myosin [myosin II] is capable of forming thick filaments at low ionic strength. It is a hexameric protein comprised of two heavy chains [MHC, MW = 171-241 kDa](220) and four light chains [MLC, MW = 15-30 kDa](221). The N-terminal sequence [720-780 amino acid residues] of the heavy chain forms the head region, which contains the actin and nucleotide binding sites. The C-terminal portions of the two heavy chains associate to form the tail; a highly elongated coiled coil (222 and 223). Two of the light chains belong to the essential light chain [ELC] family, which are related to Calmodulin and the other two are regulatory light chains [RLC](224 and 225). Within the class of essential light chains, which cannot be removed without loss of ATPase activity (226-228), two isoforms have been identified (229). The myosin head with ELC-1 can bind actin more tightly than the head with ELC-2 that has the same amino acid sequence except for the N-terminal 41 residues (230-233). The rigid elongated neck region that contains the tight binding sites amplifies small conformational changes in the globular motor domain, thus producing force and a step movement of approximately 5-10nm/ATP hydrolysed (234 and 235). The myosin II fragment, consisting of

the motor domain and the neck region, is referred to as myosin subfragment-1 or myosin-S1. Two prominent trypsin sensitive surface loops of myosin-S1 form the borders of the 25, 50, and 20kDa sub domains (236 and 237). The first loop, loop-1, spanning the 25/50kDa junction is situated near the nucleotide binding site and is involved in determining the rate of ADP release (238 and 239). The 50/20 junction, also called loop-2, plays a central role in actin binding and consequently in tuning the motor activity (240-242). Skeletal myosin contains two reactive thiols, SH-1 and SH-2, which are near each other in both the primary (243-245) and tertiary structures (246 and 247) and are released in a 20kDa tryptic peptide that constitutes the C-terminal region of myosin-S1 (248). Their precise locations are now known to be 66 [SH-1] and 56 [SH-2] residues from the N-terminus of the 20kDa fragment. Chemical modification of these thiols alters the ATPase activity of myosin. In addition, myosin-S1 contains one highly reactive Lys residue that on, modification, also affects the ATPase activity (249 and 250). While mapping of myosin-S1 has been pursued mainly through these biochemical techniques, investigations of the structure and function of myosin have been undertaken using numerous organisms and a variety of tissues within these organisms. Image reconstruction studies provided information on the general shape of the myosin-S1 (132, 251-256). The dimensions of the myosin-S1 in the region proximal to actin are 6.2-6.5nm x 4.8-5.6nm and the overall length is ~12-15nm in the absence of RLC. The angle of myosin-S1 attachment is suggested to be almost perpendicular to the filament axis and the arrowhead appearance, which was observed in the electron microscope, attributed to the curved nature of myosin-S1.

The characteristic feature, which is common to all myosins that have been identified so far, is the ability to bind with actin reversibly and hydrolyze ATP. Typically Mg^{+2}ATPase activity of myosin alone is very low and is increased significantly by the interaction with actin. The functional form of myosin in both muscle and non-muscle systems is the aggregated state. Myosin molecules are systematically organized into bipolar structures, the thick filaments whose length and diameter vary depending on the species. Myosin found in striated muscle has high ATPase activity (257) and actin sliding velocity, and requires the thin filament regulatory proteins [Tn/TM], for its regulation. Striated muscle myosin shows its motor activity without light chain phosphorylation and the Tn/TM system inhibits myosin motor activity when Ca^{+2} is dissociated from TnC molecule. However, the motor activity of vertebrate smooth muscle and non-muscle myosin is regulated by phosphorylation of its regulatory subunit and generally has lower ATPase activity and actin translocating activity (258). The phosphorylation takes place at Ser19 of the 20kDa light chain subunit and it is a prerequisite for smooth/non-muscle myosin motor activity. Furthermore, smooth muscle/non-muscle myosins are characterized by their change in the conformation, known as 10S-6S conformational transition (259). The 10S myosin has a folded conformation that is not found in striated muscle myosin, and the formation of this conformation is characterized by the inhibition of Mg^{+2} or Ca^{+2}ATPase activity and thick filament formation. Of interest is that phosphorylation destabilizes the formation of 10S conformation (260).

1.2 Muscle Contraction

The contraction of striated muscle is under neural control. Action potentials traveling along a nerve trigger the release of acetylcholine into the neuro-muscular junction. The neurotransmitter then binds to its receptor causing the wave of depolarization to spread over the muscle plasma membrane [the sarcolemma]. This electrical stimulation is transmitted to the sarcoplasmic reticulum, a calcium storage compartment which surrounds the myofibrils, by invaginations in the sarcolemma known as transverse tubules [T-tubules]. Upon excitation, calcium is released from the sarcoplasmic reticulum into the cytoplasm where it interacts with the Tn complex (261). The muscle then contracts and generates force.

It is well established that muscle shortening [and relaxation] involves the relative sliding of the thick and thin filaments into [or out of] each other, changing the degree to which they are interdigitated (262) Another widely accepted theory, the swinging cross bridge hypothesis, provides a basis for understanding how sliding occurs. Under activating conditions, a myosin head makes contact with the thin filament and then undergoes an ATP-driven swinging motion that rows the actin filament along (263). One of the difficulties with the swinging cross-bridge hypothesis was a lack of evidence for movement of the head. This problem was eventually overcome by determining the structure of the head with different nucleotides in the active site (264-268). Owing to the wealth of structural information, it is now believed that the entire head does not roll on the surface of actin during the power stroke but that the bulk of the movement occurs in the lever arm (269) [Fig.1.2].

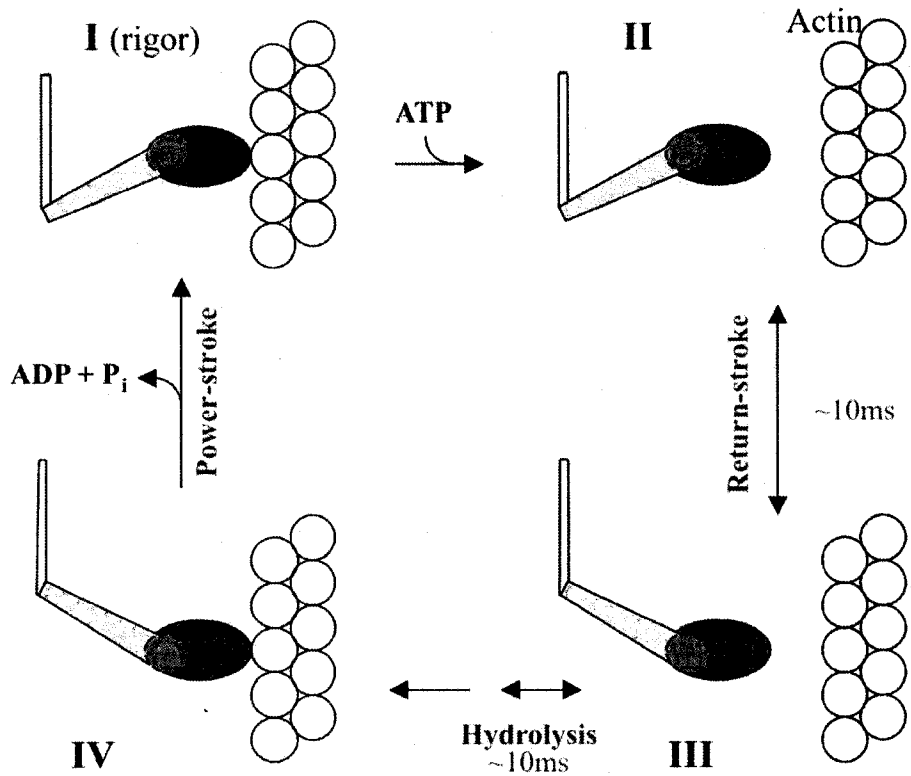

Fig.1.2 The Lymn-Taylor cycle (269).

The myosin cross-bridge is bound to actin in the rigor, 45° "down" position [state 1]. ATP binds, which leads to very fast dissociation from actin [state 2]. The hydrolysis of ATP to ADP and Pi leads to a return of the myosin cross-bridge to the 90°"up" position, whereupon it rebinds to actin [state 4]. This leads to release of the products and return to state 1 in the last transition actin is "rowed" past myosin.

The question of how the interaction between myosin and actin is regulated is more controversial. In the original Steric Blocking model (263), TM-Tn physically blocked the binding of myosin to actin at low Ca^{+2} concentrations. Calcium binding to Tn then induced a series of conformational changes within the thin filament that repositioned the TM molecule. This shift in TM led to the exposure of myosin-binding sites on the actin surface, strong stereospecific actomyosin binding and ultimately the generation of force. However, it was subsequently shown that Ca^{+2} has only a small effect on the binding of myosin to the thin filament, which is inconsistent with the model, at least in its original form (270). Another complicating factor is that Ca^{+2} is not the only ligand that can activate the actomyosin ATPase activity by binding to the thin filament. Rigor myosin, either nucleotide-free myosin or myosin-ADP, can also activate the actomyosinATPase activity (271 and 272).

Throughout the 1980s, increasing attention was given to the allosteric nature/properties of the thin filament. The Hill model (273) envisaged the thin filament to adopt two configurations: inactive and active, with the equilibrium between them poised in accordance with the concentration of ligand [either calcium or rigor myosin]. In this scheme, myosin is able to bind to each thin filament conformer but only the 'active' form is capable of a productive interaction, that is, an interaction which results in myosin activation. There is also a difference in the affinity of binding. The active conformer binds strongly to myosin-ATP [or myosin-ADP-Pi], whereas the inactive conformer is referred to as the weakly binding state.

The three-state model (274) proposes that the thin filament can adopt an additional conformation, referred to as 'blocked'. This state, which arises when no ligands are associated

with the thin filament, does not bind myosin. Although the other two states [referred to as 'closed' and 'open'] are assumed to have a similar affinity for myosin, only the 'open' state is proposed to be capable of producing force (275). The McKillop-Geeves model, which is supported by both X-ray diffraction and helical three-dimensional reconstruction of electron microscopic images (276-279), also segregates the effects of ligand binding. Calcium binding is postulated to stabilise the 'closed' conformer, whereas rigor myosin is required for production of the 'open' conformer. In effect, the three state model combines the allosteric effects of ligand binding with a modified steric blocking scheme. In the 'blocked' state [no ligands bound], TM is assumed to lie on the outside of the actin filament on sub-domains 1 and 2. Upon calcium binding, TM moves azimuthally by 25° towards sub-domains 3 and 4 thus attaining the 'closed' state. Here TM is positioned such that it only partially occludes the myosin-binding site on actin thus allowing an interaction to take place. Attachment of rigor myosin produces an additional shift in TM uncovering the entire myosin binding surface on actin. A more recent investigation into the problem has involved the use of double-mixing stopped-flow analysis to measure the effect of thin filament ligand binding on the rate of dissociation of the products of ATP hydrolysis from myosin (280 and 281). As predicted by other researchers (282), the main mode of regulation is the variation in the rate of product dissociation. Thin filaments saturated with Ca^{+2} and rigor myosin accelerate the rate of this step by ~200-fold relative to thin filaments devoid of bound ligand. At the same time, there was little change in the affinity of myosin-ADP-Pi for actin. Interestingly, both ligands are required to achieve the maximum rate of product release. Rigor myosin binding alone was insufficient, which is inconsistent with the model of McKillop and Geeves. A key difference between the experiments of Heeley *et al.,* (280) and those, on which the two-, and three-,

state models are based, is that the stopped-flow measurements were carried out with myosin-ATP/ADP-Pi. In the other cases (272 and 273), the active site was either empty or contained non-hydrolysable nucleotide. Because myosin, which does not contain true substrate, cannot produce a power stroke, the authors (279 and 280) argue that it may not give an accurate description of regulation.

1.3 Purpose of study

An important source of diversity in striated muscle is the synthesis of chemically related, non-identical, forms of the thin filament proteins; actin, TM and TnC, TnI and TnT. However, the structural and functional significance of this heterogeneity is unclear.

This problem is investigated by using salmonid fish as a model system. The salmonids have a simple musculature, such that the fast and slow swimming muscles of the trunk are anatomically segregated. Further, these muscles, together with cardiac muscle, synthesize unique isoforms of TM and actin.

A major concern of the project is the characterization of the properties of these cell-type specific proteins. In addition, the identification of a slow muscle actin isoform prompted the study of the distribution of slow actin in the animal kingdom and its evolutionary relationship with other actin isoforms.

Chapter 02

Materials and Methods

2.1 Extraction of muscle proteins

For protein extractions, fresh muscle was used except in the case of myosin, salmonid cardiac TM and Tn preparations where frozen muscle was used occasionally. All the steps in the procedures were carried out at or below 4°C unless otherwise noted. To prevent proteolytic breakdown ~2mM phenymethylsulphonylfluoride [PMSF] was added to the first extraction step [except in the case of myosin and myosin-S1 preparations]. Centrifugation was performed at the following speeds using the indicated instrument and rotor: 2000-4200rpm [Beckman J6HC, JS-4.2], 8000-10,000rpm [Sorval Superspeed RC2-B, GS-3] and 40,000-50,000rpm [Beckman Coulter Optima^{TM} L-90K, 70Ti]. Volumes less than 1ml were centrifuged at 160,000 x g in an Eppendorf-5415C microfuge.

2.1.1 Preparation of actin acetone powder

The following protocol was used to prepare actin acetone powder of salmon fast and salmon slow from Atlantic salmon [*Salmo salar*], and salmon cardiac from Rainbow trout [*Salmo gairdneri*]. Salmon were purchased from a local commercial outlet while trout hearts [frozen] were provided by a local hatchery. Light [fast] muscle and dark [slow] muscle were dissected from longitudinally sectioned salmon, taking care to minimise cross contamination. According to the method of Bollag and Edelstein (283) ground muscle [~500g] was stirred in

12-volumes [1kg = 1 volume] of distilled water [dH_2O] for about 30min. After allowing the solution to settle out for an additional 30min, the filtrate of the decanted solution was spun at 4200rpm for 5min. The residue was then resuspended in 3 volumes of 0.4%[w/v] $NaHCO_3$, pH 8.0, followed by stirring for about 15min, and centrifuged at 4200rpm for 10min. This step was then repeated in the presence of 0.05M Na_2CO_3 and 0.05M $NaHCO_3$ [pH 8.0] instead. After stirring for 2min in 0.2mM $CaCl_2$, the residue was centrifuged at 4200rpm for 10min, then stirred in 3 volumes of cold [4°C] 95%[v/v] ethanol for 2min. After filtering the solution, the residue was resuspended in acetone [-20°C] and stirred for 2min again. The resultant solution was filtered through cheesecloth and this step was repeated twice. Finally, the residue was dried in a fume hood overnight. Typically 1kg of muscle [either fast or slow] will yield 90g of acetone powder.

2.1.2 Preparation of Tropomyosin/troponin acetone powder

The method of Cartson and Mommearts (284) was followed. First, minced rabbit back and leg muscles [~500g] were stirred in 3 volumes of ice-cold Guba-Straub buffer [0.3M KCl, 0.1M KH_2PO_4, 0.05M K_2HPO_4] for 15min. After pelleting muscle by centrifugation at 2000rpm for 10min, this step was repeated. Then the residue was blended in one volume of 0.4% [w/v] $NaHCO_3$ followed by rinsing the blender with 3 more volumes of 0.4% [w/v] $NaHCO_3$. The solution was then spun at 2000rpm for 15min. After resuspending the pellet in one volume of 0.05M Na_2CO_3 and 0.05M $NaHCO_3$, 8L of 0.5mM $CaCl_2$ was added. After stirring for 10min, the muscle solution was strained through cheesecloth. The pellet was then

stirred in 1.5-2L of cold acetone [-20°C] for 5min and drained through cheesecloth. This step was repeated twice and the resulting residue was dried in a fume hood overnight.

Note: pH of buffers was not adjusted.

2.1.3 Preparation of actin

Actin was prepared by polymerization and depolymerization according to the method of Spudich and Watt (285) with some modifications. Acetone powder [10g] prepared in section 1.1 was gently stirred in 100ml of actin extraction buffer [2mM Tris-HCl, 0.2mM $CaCl_2$, 0.2mM ATP and 0.1mM DTT, pH 8.0] with the addition of solid DTT to a final concentration of 0.5mM for 30min. The resulting supernatant, after centrifugation at 4200rpm for 15min was then filtered through 8.0μm, 0.45μm and 0.22μm Millipore filters sequentially. Polymerization was initiated by the addition of KCl and $MgCl_2$ [0.05M and 0.002M respectively] to the filtrate. After one hour of stirring, solid KCl was added to a final concentration of 0.8M and stirring was continued for further 90min. The above two steps were carried out at room temperature. Afterwards, polymerized actin was sedimented by spinning at 45,000rpm for 90min, the polymerized actin pellet was dissolved in 3-6ml of cold actin extraction buffer and dialyzed against 4L of the same buffer for 2-3 days at 4°C with one change of buffer per day. Finally, depolymerized actin was clarified by centrifuging again at 45,000rpm for 90min. The resulting G-actin was in Ca form [Ca-G-actin].

2.1.4 Preparation of tropomyosin

Acetone powder [100g] as prepared in section 2.1.2 was continuously stirred in 700ml of buffer A [Buffer A: 1M KCl, 25mM Tris-HCl, 0.25mM DTT and 0.5mM EDTA, pH 8.0] for 2hrs. The supernatant of the sedimented solution [8000rpm, for 20min] was retained and the previous step was repeated, stirring for 60min. Taking the extinction coefficient as 1.00 for a 1mg/ml solution as suggested in Smillie (286), the concentration of the combined supernatants was adjusted to 1-2mg/ml using buffer A. Tropomyosin was isoelectrically precipitated by lowering the pH to 4.6 with 1M HCl, stirring for about 30min and then sedimenting at 8000rpm for 30min. The pellet was redissolved in 5X buffer B [Buffer B: 0.2M KCl, 20mM Tris-HCl, 0.25mM DTT and 0.5mM EDTA, pH 7.9] with a few drops of 1M Tris-HCl; pH 8.0 to maintain the pH at 7.9, clarified by centrifuging at 8000rpm for 20min., salted out between 40% and 70% $(NH_4)_2SO_4$ and centrifuged at 8000rpm for 45min. The precipitated protein was dissolved in dH_2O and, following dialysis against 4-5 changes of 10L of dH_2O in the presence of ~5mM (NH_4) HCO_3 and ~2mM mercaptoethanol, was lyophilized. The impure TM was loaded onto a Q-Sepharose Fast Flow [Pharmacia] column for further purification [section 2.4.1].

2.1.5 Preparation of troponin

Following the method of Potter (287), acetone powder [40g] prepared as described in section 2.1.2, was stirred continuously in 300ml of buffer C [Buffer C: 1M KCl, 25mM Tris-HCl, 0.1mM $CaCl_2$ and 0.1mM DTT, pH 8.0] over a period of 3hr, centrifuged at 4200rpm for 10min and the supernatant was reserved. The residue was re-extracted with 150ml of 1M

KCl and stirred for 60min, before recentrifugation. Tropomyosin was removed by lowering the pH to 4.6 using 1M HCl, stirring for 30min and centrifuging at 4200rpm for 30min. Following the adjustment of the supernatant pH to 8.0 using 1M KOH, protein was salted out with 40%[w/v] $(NH_4)_2SO_4$ while maintaining the pH of the solution between 7 and 8. The retained supernatant of the centrifuged solution [4200rpm for 10min] was again salted out by raising the $(NH_4)_2SO_4$ concentration to 50%[w/v] and then to 60%[w/v]. Finally, both 50% and 60% precipitates were dissolved in imidazole buffer [10mM Imidazole, 50mM KCl, 0.1mM $CaCl_2$ and 0.02%NaN_3, pH 7.0] and dialyzed extensively [2-3 days with several changes of dH_2O] in the presence of ~5mM $(NH_4)HCO_3$ and ~2mM mercaptoethanol. Protein, which precipitated during dialysis, was removed by centrifugation at 8000rpm for 30min. The combined pellets [both 50% and 60%] and individual supernatants of Tn were then lyophilized. Calcium sensitivity of Tn was determined as explained under section 2.6.4

2.1.6 Preparation of myosin

Myosin was extracted from New Zealand rabbit leg and back muscles according to Perry (288). Rabbit muscle [~500g] was minced by running through a cold meat grinder and stirred in 3 volumes [3 volumes of buffer per gram of tissue] of ice-cold Guba-Straub buffer [0.3M KCl, 0.1M KH_2PO_4, 0.05M K_2HPO_4] for 15min. The supernatant of the sedimented solution [2000rpm for 1min] was filtered and placed in a 12L container. Care was taken to maintain the temperature at 4°C. Then, 10L of cold dH_2O was slowly added, while stirring gently, to lower the ionic strength and induce myosin precipitation. The solution was then set aside to permit myosin to settle out. After siphoning away as much dH_2O as possible, the remaining

solution was centrifuged at 2000rpm for 20min. The myosin-containing pellet was dispersed in buffer [5mM MOPS, 2mM $MgCl_2$, 0.2mM DTT and 1M KCl, pH 7.0], and adjusted to 15-20 mg/ml with 1M KCl [to the final concentration of 0.5M KCl], as determined from its absorbance at 280nm [see section 2.5.4.1]. After overnight dialysis against 8L of sodium phosphate buffer [0.12M NaCl, 20mM Na_2HPO_4, 4mM EDTA and 1mM DTT, pH 7.0], the myosin solution was used to prepare myosin-S1 as outlined in the next section.

2.1.6.1 Preparation of myosin-S1

Myosin was cleaved proteolytically using chymotrypsin [Sigma, dissolved in 1mM HCl] as described by Heeley *et al.*, (242). An initial test digestion was performed on a spectrophotometrically determined amount of myosin. The conditions were: enzyme: substrate ratio, 1:200 [w/w]; sodium phosphate buffer [0.12M NaCl, 20mM Na_2HPO_4, 4mM EDTA and 1mM DTT, pH 7.0] at 4°C. The reaction was terminated by addition of a 2-fold mass excess of lima bean trypsin inhibitor [Sigma, dissolved in dH_2O] to the enzyme miture. The liberation of myosin-S1 was assessed by the measurement of the steady state ATPase rate [see section 2.6.4] in the supernatant after centrifuging at 40,000rpm for 30min. After ~6min, ~50% of total myosin was judged to have been proteolyzed. The procedure was then scaled up. Any intact myosin remaining after the digestion was removed by overnight dialysis against 8L of 20mM Tris-HCl, pH 8.0 at 4°C followed by centrifugation [40,000rpm for 1hr]. Impurities were removed [10,000rpm for 30min] from the myosin-S1 containing supernatant by adding solid $(NH_4)_2SO_4$ to a saturation of ~24%[w/v]. Myosin-S1 was then collected [10,000rpm for 30min] by precipitation at ~36%[w/v] $(NH_4)_2SO_4$. The pellet was

resuspended in 5mM MOPS, 2mM $MgCl_2$ and 0.2mM DTT, pH 7.0 and dialyzed extensively against the same buffer to remove salt. After the final centrifugation [40,000rpm for 1hr] myosin-S1 was either lyophilized in the presence of 10%[w/w] sucrose or further purified on a Q-Sepharose fast-flow column [section 2.4.1].

Note: The activity of myosin was checked at each step as explained in section 2.6.4

2.2 Electrophoretic methods

Electrophoresis in polyacrylamide slabs was performed using a Bio-Rad mini-Protean II apparatus [Bio-Rad, Richmond, CA]. Gels were 7cm long, 10cm wide and either 1.0mm or 0.75mm thick. Polymerization was initiated by the addition of N, N, N', N'-tetramethylethylenediamine [TEMED] and 10%[w/v] ammonium persulfate. Acrylamide, 30%[w/v] and bis-acrylamide, 0.8%[w/v] were used to prepare gels.

2.2.1 Sodium dodecyl sulfate polyacrylamide gel electrophoresis [SDS-PAGE]

The SDS gels consisted of 12%[w/v], 15%[w/v] or 20%[w/v] polyacrylamide (289). All protein samples were dissolved in sample buffer [13% [v/v] glycerol, 1.3%[w/v] SDS, 0.02%[w/v] NaN_3, and 0.79%[w/v] Tris-HCl; pH 6.8] to a final dilution of ~1μg/μl. Gels were stained in 0.25%[w/v] Coomassie Brilliant Blue R-250 [Bio-Rad], 50%[v/v] methanol and 10%[v/v] acetic acid and destained in 15%[v/v] acetic acid and 20%[v/v] methanol.

2.2.2 Alkaline Urea polyacrylamide gel electrophoresis [Alkaline Urea-PAGE]

Alkaline urea-polyacrylamide gels comprised of 10%[w/v] polyacrylamide: 33%[v/v] acrylamide solution {Stock solution: 30%[w/v] acrylamide: 0.8%[w/v] bis-acrylamide}, 8%[v/v] 12X glycine buffer [1.49M glycine and 0.24M Tris-HCl] and 8M urea (290). All protein samples were dissolved in a freshly-made solution of saturated urea, containing DTT and Bromophenol blue to a final dilution of approximately 1μg/μl. The gel was prerun for 15min and samples were loaded into the flushed wells. Electrophoresis was carried out at 220volts for the indicated predetermined times [actin, 700volt hr and TM, 450 volt hr]. The gel was stained and destained as described in section 2.2.1.

2.2.3 Safer gel electrophoresis

2.2.3.1 Native Safer gel electrophoresis

The method described in Bollag and Edelstein (291) was followed. The separating phase consisted of 7.5%[v/v] acrylamide, 0.2%[v/v] bis-acrylamide, 10%[v/v] 10X Safer buffer [250mM Tris-HCl, 1.94M glycine and 5mM $CaCl_2$], 0.2mM ATP and 0.1%[v/v] Triton. Samples were dissolved in sample buffer [2.0mM Tris-HCl, 0.05mM $CaCl_2$, 0.1mM ATP, 0.05mM DTT, pH 8.0] in 50% glycerol to a final concentration of 0.5-1μg/μl. Electrophoresis was carried out at 140volts for 60min.

2.2.3.2 Urea Safer gel electrophoresis

The protocol was as described in 2.2.3.1 except that gels contained a uniform concentration of urea varying from 2M to 8M. Gels were prerun at 140volts for 60min.

2.2.4 Two dimensional gel electrophoresis

Glass tubes [internal diameter ~1mm] were filled with a solution containing 5.5g urea, 4.0ml degassed dH_2O, 1.35ml acrylamide [30% [w/v] acrylamide and 1.8%[w/v] bisacrylamide], 0.5ml ampholines [from LKB], pH 4-6, 0.22ml NP40. Isoelectric focusing was performed in a Bio-Rad [model 175] unit [lower chamber: 0.1%[v/v] H_3PO_4, 0.1mM thioglycolate and upper chamber: 0.08%[v/v] 5M NaOH]. Gels were prerun at 850volts for 15min. Protein dissolved in a saturated urea solution was electrophoresed for 2500volt hrs. Finally gels were extruded from the tubes by hydrostatic pressure and placed onto a 15% [w/v] SDS-polyacrylamide gel and run as in section 2.2.1

2.3 Blotting techniques

2.3.1 Western blotting

Western transfer was carried out after either SDS–PAGE or alkaline urea PAGE to polyvinylidene difluoride [PVDF] membrane. The gel and membrane were soaked in transfer buffer [10mM CAPS, pH 11.0 in 10%[v/v] methanol] for 30min, assembled into a sandwich and electrophoresed for 2.5hr at 60volts at room temperature in transfer buffer. To confirm complete transfer of protein, the gel was stained with Coomassie Brilliant Blue R250

as outlined in section 2.2.1. The membrane was briefly stained using 0.025%[w/v] Coomassie Brilliant Blue R250 in 40%[v/v] methanol and destained in 50% [v/v] methanol. Finally, the membrane was air-dried.

2.3.2 Immunoblotting

Electrotransfer was performed from an alkaline urea gel [section 3.1] to PVDF. The blotted membrane was incubated in blocking reagent [3%[w/v] casein], washed twice with TTBS [20mM Tris-HCl, 0.5M NaCl, 0.05%[v/v] Tween 20, pH 7.5] for 5min and then probed with primary antibody of rabbit anti-actin [Sigma], [1:2000[v/v] in TTBS]. Actin was then detected using anti-rabbit IgG [whole molecule]-alkaline phosphatase antibody [1:6000[v/v]] with 5-bromo-4-chloro-3-indolyl-phosphate [BCIP [Promega], 0.15mg/ml] and 4-nitroblue tetrazolium chloride [NBT, 0.3mg/ml] [Promega] in 0.1M $NaHCO_3$, 1.0mM $MgCl_2$, pH 9.8 as the colour reagent (292).

2.4 Chromatographic techniques

2.4.1 Ion exchange chromatography

Ion exchange chromatography was carried out to purify TM isoforms and myosin-S1. Impure myosin-S1 [170ml] was loaded onto a Q-Sepharose Fast Flow [Pharmacia] column [2.5cm x 14.5cm; volume 80ml], which had been equilibrated against two column volumes of start buffer [100mM Tris-HCl, 2mM EDTA, pH 7.9 at 4°C]. The partially purified myosin was eluted using a linear salt gradient from 0.0 - 0.5M NaCl [volume, 800ml]. Protein-containing

fractions were analyzed by absorbance at 280nm, and SDS-PAGE. After dialyzing against 2mM Tris-HCl, pH 8.0, myosin-S1 was lyophilized in the presence of 10% [w/w] sucrose. In the case of TM, freeze-dried protein [300mg] was first dissolved in start buffer [20ml], centrifuged to clarify and then loaded onto the column.

2.4.2 Hydroxylapatite chromatography

The pooled fractions of TM from the ion exchange column were loaded onto a hydroxylapatite column [Bio-Rad] for further purification. The pooled fractions were directly loaded onto the column [2.5cm x 14.5cm; volume, 80ml] that had been previously equilibrated against two column volumes of column buffer [1M NaCl, 0.01% [w/v] NaN_3, 10mM NaH_2PO_4, pH 7.0]. Protein was eluted at room temperature using a 70-250mM NaH_2PO_4, pH 7.0, linear gradient [total volume, 800ml]. Protein-containing fractions which were detected by absorbance at 280nm and SDS-PAGE, were dialyzed against dH_2O in the presence of ~5mM $(NH_4)HCO_3$ and ~2mM mercaptoethanol and then freeze-dried.

2.4.3 Affinity chromatography

To study the interaction of various TM isoforms with Tn, predialyzed samples of TM [10-15nmol] were applied to a cyanogen bromide activated Sepharose 4B column [column dimensions, 0.9 x 8 cm] which had been equilibrated against 10mM MOPS, 50mM NaCl, 1.0mM EGTA, 1.0mM DTT, 0.01%[w/v] NaN_3, pH 7.0, at 4°C according to Spudich and Watt (293). Protein was eluted by application of a linear gradient [0.05 - 0.5M NaCl, total

volume, 100ml] using a flow rate of 5ml/hr. Fractions [1.75ml] were analyzed by absorbance at 230nm, by the method of Bradford [section 5.4.2] and by SDS-PAGE and alkaline urea PAGE as well.

2.5 Spectroscopic techniques

2.5.1 Mass spectroscopy

The molecular weights of proteins were determined using an Applied Biosystems, Matrix-Assisted Laser Desorption/Ionisation-Time Of Flight Mass Spectrometer (MALDI-TOF MS). Freeze-dried actin samples, which were dissolved in 0.2%[v/v] trifluoro acetic acid and 50%[v/v] acetonitrile, were embedded in a low molecular weight UV absorbing matrix of Sinapinic acid. The matrix material was present in vast excess [10mg/ml] of sample in order to isolate individual sample molecules. Desorption and ionization was induced by 3 nanosecond pulses of a nitrogen laser that was operated at 337nm. To obtain TOF spectra, Delayed Extraction mode [Voyager-DE PRO model] was used. The time at which the extraction pulse was applied was 750 nanoseconds. The flight tube is a field free region in which ions drift at a velocity inversely proportional to the square root of their masses. A linear detector was used to detect ions that travel down the flight tube and to measure the abundance of ions over time. Data Explorer™ software was used for data acquisition and processing. The acquisition mass range was 10,000-70,000Da. To obtain a spectrum, 100 laser pulses per spectrum were applied to the sample at a rate of 3.0Hz. Using Data Explorer™, software spectra and chromatogram [multispectra] data were manually calibrated [Calibration mixture: Insulin [bovine]- molecular mass 5734.59Da for the +1 ion and 2867.80

for the +2 ion, Thioredoxin [E.*Coli*], 11674.48Da for the +1 ion and 5837.74Da for the +2 ion and Apomyoglobin [horse], 16,952.56Da for the +1 ion and 8476.78Da for the +2 ion]. The Voyage–De-500mHz digitizer converted these analog data to digital data that allowed the signal from the mass spectrometer to be transferred to the computer and to present the data for each individual protein sample in a single peak on a true molecular mass scale.

2.5.2 Circular Dichroism spectroscopy [CD spectroscopy]

2.5.2.1 Far, and Near, -UV CD spectroscopy

Electronic circular dichroism spectra were recorded in the near-ultraviolet region [250-340nm] and far-ultraviolet region [190-300nm] using a Jasco-810 spectropolarimeter. For far-UV CD measurements, a protein concentration of ~1.5mg/ml was most commonly used. In the case of experiments conducted in the near-UV, a protein concentration of ~3.0mg/ml was most commonly used and the sensitivity of the instrument was adjusted to normal or low accordingly. Actin samples were dialyzed overnight against either actin extraction buffer [see section 2.1.3] or HEPES buffer [5mM Hepes, 0.2mM $CaCl_2$, 0.2mM ATP, 0.01%[w/v] NaN_3 and 2mM DTT, pH 8.0] at 4°C. The absorbance of the protein/reagents mixture at 222 nm was checked to ensure that it did not exceed 1.0. The temperature [5-65°C] was controlled by a CTC-345 circulating water bath. Water-jacketed cells varying in light path 0.2mm [far-UV experiments] and 5mm [near-UV experiments] were used. The heating rate was varied from 15°C/hr to 60°C/hr to confirm that the protein was at equilibrium. The scanning speed of the instrument was set at 100nm/min with normal sensitivity. The temperature-dependence of the signal at 222nm [far-UV] and 292nm [near-

UV] was observed by continuous monitoring at these wavelengths between 5-65°C. The melting temperature [Tm] was then obtained by converting the progress curve $\{[\theta]_{222 \text{ or }} [\theta]_{292}$ vs. T} to the first differential form $d[\theta]_{222 \text{ or }} d[\theta]_{292}/dT$ vs. T, where, T, absolute temperature; $d[\theta]_{222/292}$, changing ellipticity at 222/292nm.

2.5.2.2 Far-UV CD spectroscopy [Chemical unfolding]

Electronic circular dichroism spectra in the far-UV spectra of Ca-G-actin [1.5mg/ml] were recorded as a function of GdnHCl concentration from 0.2M to 4.0M in 0.2M intervals. The stock concentration of chemical denaturant was 6M and was prepared fresh each time. Experiments were carried out at 25°C. Ellipticity of the spectra at 222nm was recorded as in section 2.5.2.1.

2.5.2.3 Far-UV CD spectroscopy [Rate of unfolding]

As discussed in section 2.5.2.2, electronic circular dichroism spectra of Ca-G-actin were recorded by varying the concentration of of Ca-G-actin [1-4mg/ml] as function of time. Samples were incubated on ice in a 0.1mm light path cell prior to being subjected to a temperature of 65°C. Ellipticity at 222nm was then recorded as a function of time. The rate of unfolding of Ca-G-actin was then determined.

2.5.3 Fluorescence spectroscopy

2.5.3.1 Displacement of ATP from etheno ATP [e-ATP] in G- actin

The Ca-G-actin [~2.0mg/ml] was first converted into "Mg" form [Mg-G-actin] as described in section 2.6.7. According to the method of Kinosian *et al.*, (125), following the removal of excess ATP by swirling with Dowex A 1-8x 20%[v/v] for about 30min on ice, Mg-G-actin was filtered through a 0.2μm Millipore filter and incubated with 1-N^6-ethenoadenosine 5' triphosphate [e-ATP] at 4°C for 2hr adjusting the final concentrations of Mg-G-actin and e-ATP to 10μM and 140μM respectively using 2mM Tris-HCl, pH 8.0. The decrease in fluorescence emission was monitored as a function of time upon addition of ATP [0.28-1.12mM] using a Shimadzu RF-540 spectrofluorophotometer. Excitation and emission were set at 340nm and 410nm respectively and the temperature was at 25°C. Sensitivity was set to 1 [high mode] and the scan speed was set to 2 [fast mode].

2.5.3.2 Extrinsic fluorescence spectroscopy

Following the same procedure described in section 2.5.3.1, N-methylantraniloyl-ATP [mant-ATP; a gift from Dr. H. White, Eastern Virginia Medical School] Mg-G-actin was prepared using mant-ATP instead of e-ATP to the final concentrations of 15μM Mg-G-actin and 1μM mant-ATP. Visible spectra were recorded on all samples before and after excited state measurements to ensure that the samples did not photodegrade. Mant-ATP was excited at 340nm and emission was measured at 440nm. A wavelength scan from 350nm to 600nm was carried out using a Photon Technology International (PTI) model QM-2001-6 QuantaMaster emission spectrometer equipped with a Hamamatsu R-928 photomultiplier tube housed in a

Products for Research Inc. PC177CE refrigerated chamber. All emission spectra were collected with a 1mm slit width, 90° to excitation source and are uncorrected for instrument response. Excitation spectra were obtained in an analogous geometry and then corrected in real time using a procedure provided by PTI.

2.5.3.3 Intrinsic fluorescence spectroscopy

Ca-G-actin [0.9mg/ml] in buffer minus ATP was prepared as described in section 2.5.3.1 and tryptophan excitation spectra of these samples were recorded as indicated in Potter (294) using the same apparatus as in 2.5.3.2. Settings were the same as above. Tryptophan was excited at 275nm and emission was recorded at 330nm.

2.5.4 UV/Visible spectroscopy

2.5.4.1 Determination of protein concentration – [1] Near-UV absorbance

A Beckman DU-64 Spectrophotometer was used to measure absorbance. Protein was dialysed overnight against a given buffer at 4°C and then, if necessary, samples were clarified by centrifugation in an Eppendorf 5415 C Microfuge [2min at 14,000rpm, at room temperature]. The instrument was calibrated against dH_2O and the absorbances of both the dialysis buffer and the protein [diluted with the buffer] were read at the relevant wavelengths. When sample quantity was not limiting, measurements were in the 0.1-1.0 range. Light scattering at 320nm was subtracted from the reading at relevant wavelength.

Extinction coefficients and molecular masses for the indicated proteins are:

Tropomyosin [66, 000Da], $A_{280\,nm}$ of a 1mg/ml solution = 0.33 (295)

Troponin [70,000Da], $A_{280\,nm}$ of a 1mg/ml solution = 0.47 (242)

Myosin-S1 [115,000Da], $A_{280\,nm}$ of a 1mg/ml solution = 0.71 (296)

Myosin, $A_{280\,nm}$ of a 1mg/ml solution = 0.53 (297)

Ca/Mg-G-Actin [42,000Da], $A_{290\,nm}$ of a 1mg/ml solution = 0.69 (298)

2.5.4.2 Determination of protein concentration – [2] Bradford assay

The Bradford assay (299) was employed to determine the affinity chromatography elution profile as described in section 4.3. Column fractions [100µl] and dH_2O [700µl] were mixed carefully with 200µl of Bradford reagent [Bio-Rad] by gentle inversion. Absorbance at 595nm was recorded using Beckman DU-64 Spectrophotometer. Column buffer [100µl] in dH_2O [900µl] was used to calibrate the spectrophotometer.

2.6 Biochemical methods

2.6.1 Amino acid analysis

Amino acid analysis was used to verify cDNA sequence data obtained for dogfish shark actin and to determine whether any posttranslational modifications were present in dogfish shark actin. Hydrolysates [24, 48 and 72hr] of dogfish shark Ca-G actin [80nmol] were analyzed as described in Heeley and Hong (300) on a Beckman model 121 MB amino acid analyzer

using Benson D-X8.25 cation exchange resin, bed size 200 x 2.8mm. A single column, three buffer sodium citrate elution method was used. The flow rate was 8ml/h with buffers and column temperature as per Beckman 118/119 CI AM 001 application notes. All analyzes were done in triplicate. Values for Ser and Thr were extrapolated back to zero time. Val and Ile were taken from the 72hr sample. Tyrosine was taken from 24hr sample. Tryptophan was measured by hydrolysis in mercaptoethane sulphonic acid (301). Methionine was determined as methionine sulphone and half-cystine as cysteic acid after oxidation in performic acid prior to acid hydrolysis (302). The cysteine was also determined by conversion to carboxymethyl-cysteine in the presence of 6M GdnHCl (303). The compositions were then calculated relative to the number of Ala residues, which produced a total nearest to 375 residues.

2.6.2 Determination of free sulfhydryls in G-actin - Ellman's assay

Protein was pretreated with 2mM DTT for 2hr at 4°C and dialyzed overnight against Buffer D [20mM Tris-HCl, 0.2mM $CaCl_2$ and 0.2mM ATP, pH 7.5] at 4°C as described in (304). The reaction was initiated by adding 0.4mM of 5,5' dithiobis - 2-nitrobenzoic acid [DTNB], which was dissolved in 100mM Tris-HCl, pH 8.0, to Ca-G-actin [1mg/ml]. Colour development, as a function of time was measured at 412nm. To avoid air oxidation of the product, the cuvette was filled to capacity and covered with the lid. Taking the extinction coefficient of the product formed at 0.337 [$A_{412\ nm}$ of a 1mg/ml solution], the total number of reactive sulphydryls was determined at various temperatures.

2.6.3 NH_2OH cleavage

First, the C-terminal Cys374 of Ca-G-actin [2.0mg/ml] was blocked by reacting overnight with iodoacetic acid [final concentration, 10mM] at 25°C in the dark. The pH of the solution was adjusted to 8.0 by adding 1M Tris-HCl, pH 8.0. Incubating for 30min at room temperature with 80mM DTT to stop the reaction, the solution was dialyzed overnight against actin extraction buffer at 4°C, followed by radiolabelling with ^{14}C-iodoacetamide [2.5μCi/ml] overnight at the respective transition temperatures [i.e. salmon fast actin at 55°C and salmon slow actin at 45°C]. After dialyzing against actin extraction buffer at 4°C for 24hrs, the labelled Ca-G-actin [final concentration, 1.0mg/ml] was then reacted with 0.2M hydroxylamine [NH_2OH] in the presence of 4M urea for about 2hr according to Bornstein (305), run on 15%[w/v] SDS-polyacrylamide gel and subjected to autoradiography. Prior to the exposure of the gel, it was dried using a Bio-Rad gel dryer model 583. The same procedure was followed without radiolabelling, when Ca-G-actin was reacted with iodoacetamide [10X excess], transferred on to a PVDF membrane [section 3.1] and sent to Research Accounting facility at Hospital for Sick Children in Ontario for amino terminal sequencing of the desired fragment.

2.6.4 ATPase activity measurements

Tropomyosins and myosin-S1 were dissolved and dialyzed against 30mM NaCl, 6mM $MgCl_2$ and 5mM MOPS, pH 7.0 [Higher ionic strength buffer E]. Following a centrifugation step to remove any insoluble material, TM samples were stored frozen at –20°C. Myosin-S1 was stored at 4°C. The EDTA activated ATPase activity [$10s^{-1}$] did not decrease substantially

over a two week period. A stock solution of Tn was prepared in 5 X buffer E [absence of EGTA], dialyzed overnight against 1 X buffer E [absence of EGTA] at 4°C and clarified by sedimentation and used immediately. Ca-G-actin was converted to the polymerized, actin by dialysis against buffer E in the presence of 1mM ATP. A stock solution of ATP [100mM] was prepared by dissolving the disodium salt in 1M NaOH to a final pH of 7.9. The final volume of the reaction mixture [$CaCl_2$ or EGTA [1mM]], F-actin, TM and Tn in a ratio of 7:4:4 respectively] was 600µl. After incubating the reaction solution at 4°C for 30min, myosin-S1 [1µM] was added, incubated at 25°C for 10min and the reaction was started by adding ATP [1mM]. Buffer E was used to do necessary dilutions. Aliquots of 200µl were withdrawn at various time points, quenched by the addition of 100µl of EDTA/SDS [0.12M EDTA and 13.3%[w/v] SDS] and, following the addition of 700µl of ammonium molybdate reagent {0.5%[w/v] $FeSO_4$ and 5%[v/v] molybdate stock solution [10%[w/v] ammonium molybdate in 10M H_2SO_4]}, colour development was measured at 550nm. Reaction rates were calculated from linear records over 2-8min intervals. The same assays were carried out at lower ionic strength as well [Lower ionic strength Buffer F: 4.5mM $MgCl_2$ and 5mM MOPS, pH 7.0]

To determine the Ca-sensitivity of Tn, ATPase assay was performed at higher ionic strength with reconstituted thin filaments in the presence of $CaCl_2$ [1mM] and EGTA [1mM] separately and the ratio of the rates was calculated. Only Tn samples, which had a ratio above 10, were used for the assays. In order to check the activity of myosin, myosin ATPase assay was carried out at higher ionic strength in the presence of ATP, myosin-S1 [1µM] and 2mM EDTA only.

2.6.5 Myosin binding assay

Myosin-S1 [1μM] was added to the reconstituted thin filaments [F-actin, TM and Tn in a ratio of 7:4:4 respectively] as described in section 2.6.4 in the absence of ATP. Upon addition of ATP [1mM], the mixture was sedimented in the Airfuge at 167,000 x g for 10min. The amount of myosin-S1 remaining in the supernatant was determined by ATPase assay using 5mM ATP in 0.4M NH_4Cl, 35mM EDTA and 25mM Tris-HCl, pH 8.0. Then the rate of ATP hydrolysis was calculated. Further verification was obtained by SDS-PAGE. This assay was done in both buffer E and F systems.

To confirm the results of the above experiment, the following experiment was carried out. Thin filaments and myosin-S1 were reconstituted at higher ionic strength [50mM] in the absence of ATP as above. Immediately before centrifugation at 50,000rpm for 25min at 4°C, ATP [10mM] was mixed with the solution. To 400μl of the supernatant, 600μl of a reaction mixture containing 20μM F-actin, 1.7mM EGTA and 1.7mM ATP was added and equilibrated in a 25°C water bath. As explained before [section 2.6.4], 200μl aliquots were pipetted out at 0, 8, 14 and 18min intervals and added to 100μl of EDTA/SDS quenching solution. The amount of inorganic phosphate released was determined as in section 2.6.4.

2.6.6 DNase I binding affinity for G-actin

DNase I binding with Ca-G-actin was carried out according to Young *et al.*, (306) with some modifications. A solution of DNase I [Sigma] was prepared in 2mM Tris-HCl, pH 8.0 to a final concentration of 4μg/μl. To each 10μl of Ca-G-actin [1.0mg/ml], 1μl, 5μl and 10μl of DNase I was added. Bringing the final volume to 20μl by adding appropriate volumes of

2mM Tris-HCl, pH 8.0, samples were incubated at 4°C for 30min. After adding 5µl of Safer sample buffer, a 5µl of the solution was analyzed on 7.5%[w/v] native Safer gel as described in section 2.2.3.1. The experiment was repeated at 25°C as well.

2.6.7 Actin polymerization

Studies on the polymerization of actin isoforms were carried out by taking advantage of the polymerization capability of actin at higher ionic strength. By incubating for 30min at 4^0C in the presence of 0.2mM EGTA and 0.1mM $MgCl_2$, Ca-G-actin [2mg/ml] was first converted into Mg-G-actin (307 and 308). Polymerization was induced at room temperature by the addition of 2mM $MgCl_2$ and 0.05M KCl to Mg-G-actin [1mg/ml]. At various time intervals 100µl of solution was airfuged [167,000 x g] or centrifuged at 45,000rpm for 30min at 25°C. Supernatants were analyzed by 15% [w/v] SDS-PAGE as in section 2.2.1. In order to determine the polymerization kinetics, light scattering studies were carried out using a Shimadzu RF-540 spectrofluorophotometer. Following a set period of 30s, samples [Ca-G-actin] were loaded into a pre-positioned cuvette. The increase in signal at 320nm as a function of time was measured. Polymerization was also investigated using an Ostwald [capillary-flow] viscometer. Freshly prepared samples of Ca-G-actin were dialyzed against 100mM KCl, 1mM $MgCl_2$, 0.1mM $CaCl_2$, 1mM $NaHCO_3$ and 1mM NaN_3, pH 7.6 overnight at 4°C in the presence of different concentrations of ATP [0.05-0.3mM]. The next day, each solution was adjusted to a protein concentration of 24µM using the appropriate buffer and passed through the capillary at room temperature. The flow times were expressed as specific viscosity.

Relative viscosity = Flow time of the sample/Flow time of the buffer

Specific viscosity = Relative viscosity –1

2.7 Nucleic acid biochemistry

2.7.1 Preparation of cDNA library

A Dogfish shark, [*Scyliorhinus retifer*] cDNA library was prepared by Donna M. Jackman using a Superscript™ plasmid System for cDNA Synthesis and Cloning [Gibco BRL] following the specifications of the manufacturer. Dogfish shark muscle tissue was a donation of the Marine Sciences laboratory [Virginia Beach, VA]. Restriction enzymes were purchased from either Pharmacia or Promega. All reagents were molecular biology grade.

In summary, mRNA was separated from total RNA using an affinity oligo [dT] cellulose column. A [poly T] *Not I* primer adapter was added to provide a substrate for both reverse transcriptase and Rnase H during first strand synthesis and to facilitate ligation to the vector following second strand synthesis. The resulting cDNAs, synthesized by nick translational replacement of mRNA, were ligated into pSport [4.1 kb], transformed into *Escherichia coli* DH5α and plated on Luria Broth [LB: 10g/L tryptone, 5g/L yeast extract, 10g/L NaCl and 15g/L Bacto agar], ampicillin [100μg/ml] plates. Approximately, 1100 colonies were individually transferred to 96 well Microtitre plates in TYPGN [2%[w/v] tryptone, 1%[w/v] yeast extract, 0.8%[w/v] glycerol, 5g/L Na_2HPO_4, 10g/L KNO_3] media and incubated overnight at 37°C (309). After making duplicate plates, a 2X glycerol solution [65%[w/v] glycerol, 0.1M $MgSO_4$, 0.025M Tris-HCl, pH 8.0] was added to the archive plates and frozen at –70°C.

2.7.2 cDNA library Screening

Bacterial suspensions [25µl] from duplicate plates were immobilized by vacuum suction onto nylon Hybond-N^+[Amersham] nucleic acid transfer membranes, which had been prewet with 10%[w/v] SDS using a dot blot apparatus. The cells were lysed in 100µl of solution A [solution A: 0.5M NaOH and 1.5M NaCl], neutralized by the addition of 100µl of solution B [solution B: 0.5M NaCl, 0.5M Tris-HCl, pH 8.0] at room temperature (309) and rinsed in 4X SSC [SSC: 0.15M NaCl and 15mM sodium citrate], then air-dried. An 18 base mixed oligonucleotide [Queen's Oligonucleotide Synthesis Facility], which had previously been made for sequencing salmonid actins, was radiolabelled using bacteriophage T4 polynucleotide kinase [Pharmacia], $\gamma^{32}P$ ATP [Mandel][12.5mCi/ml] and polynucleotide kinase buffer [50mM Tris-HCl, 10mM $MgCl_2$, 5mM DTT, 0.1mM spermidine and 0.1mM EDTA, pH 7.6]. After incubating at 37°C for 45min, the reaction was heated to 68°C to inactivate polynucleotide kinase. Following the removal of unincorporated radioactive phosphate by ethanol precipitation of DNA, the pellet was washed with 70%[v/v] ethanol and added to 10ml of prehybridization solution [5X SSPE: 150mM NaCl, 10mM Na_2HPO_4, pH 7.4 and 1.25mM EDTA, 5X Denhardt's reagent: 0.5% of each of Ficoll, polyvinylpyrrolidine and BSA, 0.5%[w/v] SDS]. A 2hr prehybridization at 42°C followed by overnight hybridization was carried out with the actin probe at 42°C, and then membranes were washed as follows, with all procedures at room temperature unless otherwise stated. The membranes were first washed in 2X SSPE and 0.5%[w/v] SDS, followed by 2X SSPE and 0.1%[w/v] SDS. The membranes were then subjected to two cycles of washes of 0.1X SSPE and 0.5%[w/v] SDS, the first at room temperature and the second at 42°C. Finally the membranes were rinsed in 0.1X SSPE, covered with plastic wrap and exposed to X-ray film

for ~ 6hr at –70°C (310). Positives from dot blot hybridization were verified by Southern analysis (311). The insert was excised from the plasmid using Hind III and EcoRI, subjected to agarose [10% [w/v]] gel electrophoresis and alkaline [0.4M NaOH] transferred to a nylon membrane. Prior to probing, the membranes were neutralized in 0.2M Tris-HCl, pH 7.5, 2X SSC [150mM NaCl and 15mM sodium citrate]. Hybridization conditions and stringency were identical to those for dot blot hybridizations.

2.7.3 Isolation and sequencing of DNA

Pelleted cells from overnight cultures [5ml] of positive clones were resuspended in 200µl of GTE [50mM glucose, 50mM Tris-HCl, 10mM EDTA, pH 8.0 and 100µg/ml RNase A], lysed with 400µl of 0.2M NaOH, 1.0%[w/v] SDS and neutralized with 300µl of KacF [5M $K^+CH_3COO^-$ and 88%[v/v] formic acid]. The supernatant of the centrifuged solution [14,000rpm for 2min] was extracted with an equal volume of phenol: chloroform [1:1] followed by the extraction of DNA from the aqueous layer using 0.5 volume 7.5M ammonium acetate and 2 volumes of ice cold ethanol (311). The purification of DNA was carried out using Wizard^R Minipreps [Promega] according to the manufacturer's instructions. Dideoxynucleotide sequencing (312) was performed using a T7^{TM} Sequencing kit [Pharmacia] with $\gamma^{35}S$ dATP [Mandel]. Sequencing gels were run at 32 watts at a temperature ~ 50-55°C in TBE [0.1M Tris-HCl, 0.1M boric acid and 2mM EDTA, pH 8.3]. Following electrophoresis, gels were fixed in 10%[v/v] methanol, 10%[v/v] CH_3COOH, dried and autoradiographed overnight at room temperature.

Chapter 3

Effect of changes in primary structure on the regulatory properties of tropomyosin: examination of phosphorylation and isomorphism.

Tropomyosin isoforms originate from multiple genes as well as through alternative splicing of a common transcript (73). In each TM gene studied thus far, TM is encoded by 9 exons, and 4 out of the 9, exons 1, 2, 6, and 9, are alternatively spliced [Fig.3.1]. The unique striated muscle exon 9, which is specialized for the interaction of TM with Tn on the thin filament encodes for amino acids 258-284, is part of the TnT binding site. Paulucci *et al.*, (62) have shown that this region is very important for the stability of the C-terminal region of the molecule. It is interesting that a phosphorylation site [Ser 283] (29), which was first discovered in the course of identification of the ^{32}P-labeled proteins in live frog muscle (313), was identified in this region. In the following studies the functional significance of this phosphorylation and isomorphism was investigated. Thin filaments were reconstituted from rabbit actin, rabbit whole Tn and a given form of TM. The regulatory properties of each type of thin filament were then assessed in a steady-state actomyosin-S1Mg^{+2}ATPase assay.

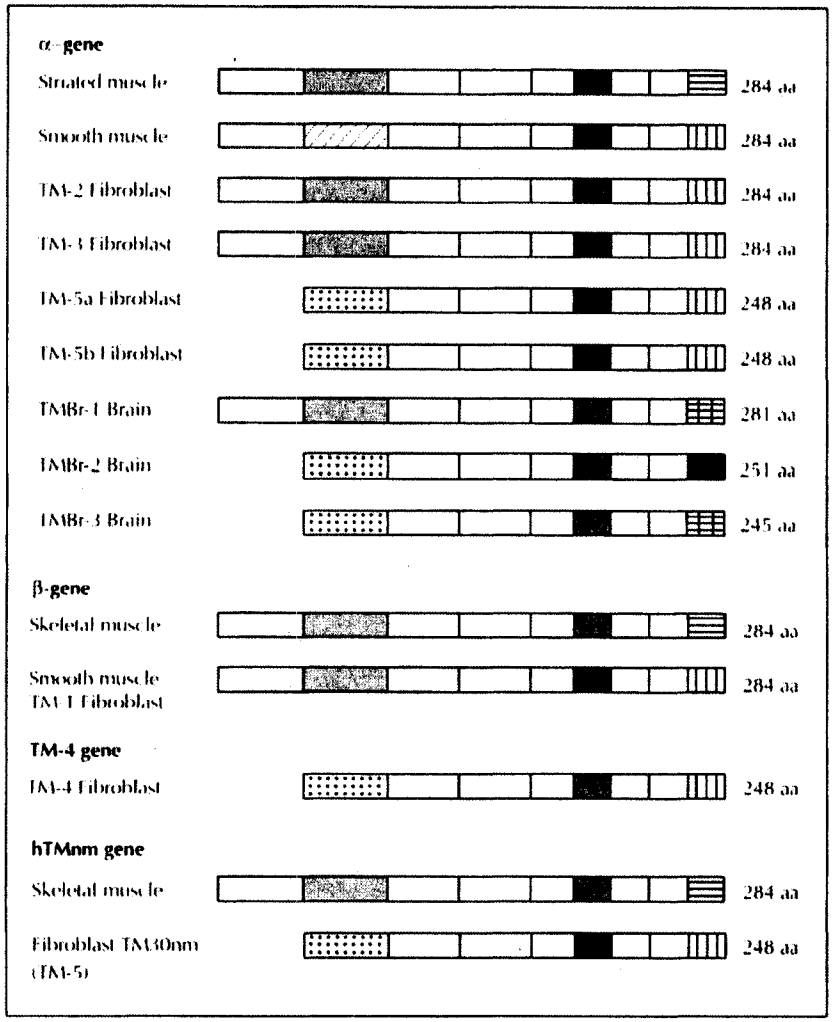

Fig.3.1 Schematic representation of the tropomyosin isoforms (73)

The exons are represented by boxes and represent only the coding portions of the exons. The empty boxes common to all genes.The α-gene straighted muscle isoform is frequently refrred to as the α-fast-twitch isoform, while the hTMnm gene encodes a skeletal muscle isoform which correspond to the α-slow- twitch muscle isoform. Fibroblast TM-4 corresponds to the human platelet TM30. Finally, the human TM30nm isoform has been identified in mouse and rat [W Guo, DM Helfam unpublished data], and also referred to as TM-5.

3.1 Regulatory properties of thin filaments containing unphosphorylated and phosphorylated tropomyosins.

Myosin activation by thin filaments, which were reconstituted from purified proteins, was measured as described in Materials and Methods [Section 2.6.4]. Myosin, Tn and actin were isolated from rabbit skeletal muscle, while phosphorylated [PTM] and unphosphorylated TM [UnPTM] were purified from blue shark skeletal muscle. The steady state actomyosin-S1Mg^{+2}ATPase activity was determined by measuring the rate of release of inorganic phosphate [Materials and Methods, section 2.6.4]. In Fig.3.2 the time-dependent change in absorbance at 550nm at 50mM ionic strength was plotted for mixtures of myosin-S1 plus thin filaments consisting of 25μM actin + shark PTM or UnPTM + rabbit Tn at a ratio of 7:2:2. It is apparent that thin filament [+Ca^{+2}] preparations activate myosin-S1 to a different extent. In light of this observation, the experiment was repeated at different concentrations of reconstituted thin filaments, using the same buffer conditions. It is important to note the linearity of the rate of reaction with time, which indicates substrate was not limiting over the duration in which these measurements were taken.

When specific activity was plotted [Fig.3.3] as a function of the concentration of reconstituted thin filament in the presence of Ca^{+2}, the production of a 2-fold greater activation of thin filaments containing PTM was observed compared to those consisting of UnPTM at higher ionic strength, 50mM [Vmax; 10.4s^{-1} (PTM) vs 5.8s^{-1} (UnPTM)]. However, the apparent binding constants [K_d] of reconstituted thin filaments containing either PTM or UnPTM did not show a significant difference [78.88μM (UnPTM) Vs 72.08μM (PTM)].

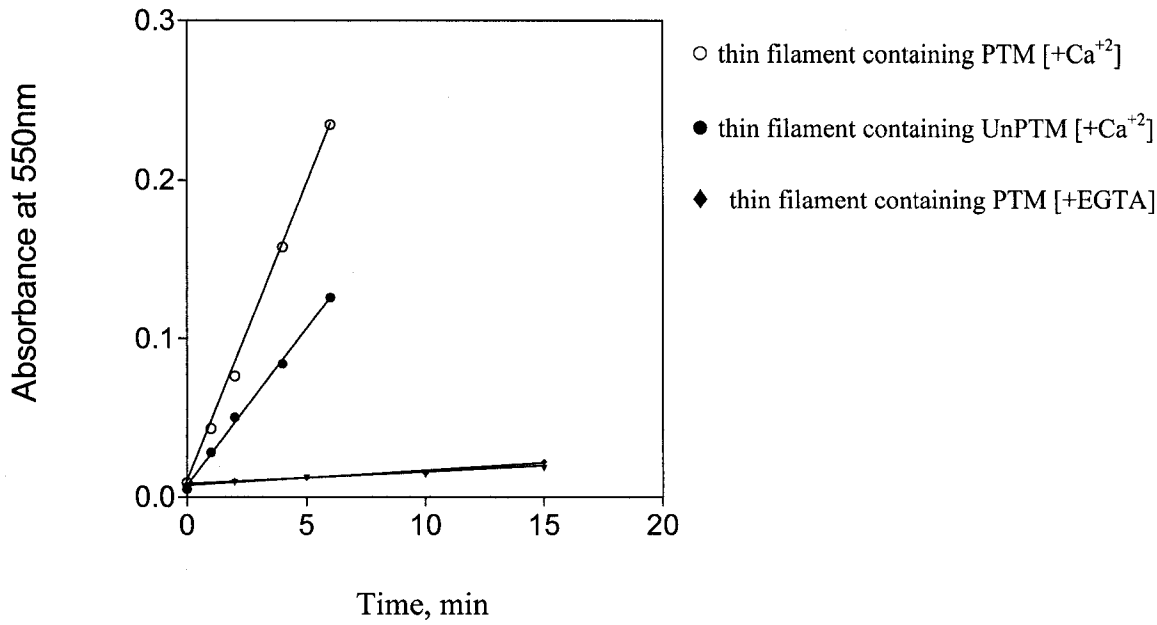

Fig.3.2 Regulated actomyosin-S1Mg^{+2}ATPase assay using either phosphorylated or unphosphorylated tropomyosin.

The regulated actin [25μM] was reconstituted with either PTM or UnPTM [7.14μM] and Tn [7.14μM]. Each reaction mixture contained either $CaCl_2$ [1mM] or EGTA [1mM]. The concentration of myosin-S1 was 1.0μM. The amount of inorganic phosphate generated by the reaction in buffer, 30mM NaCl, 6mM $MgCl_2$ and 5mM MOPS, pH 7.0 [ionic strength, 50mM], was monitored measuring the absorbance of produced phosphomolybdate at 550nm at 25°C.

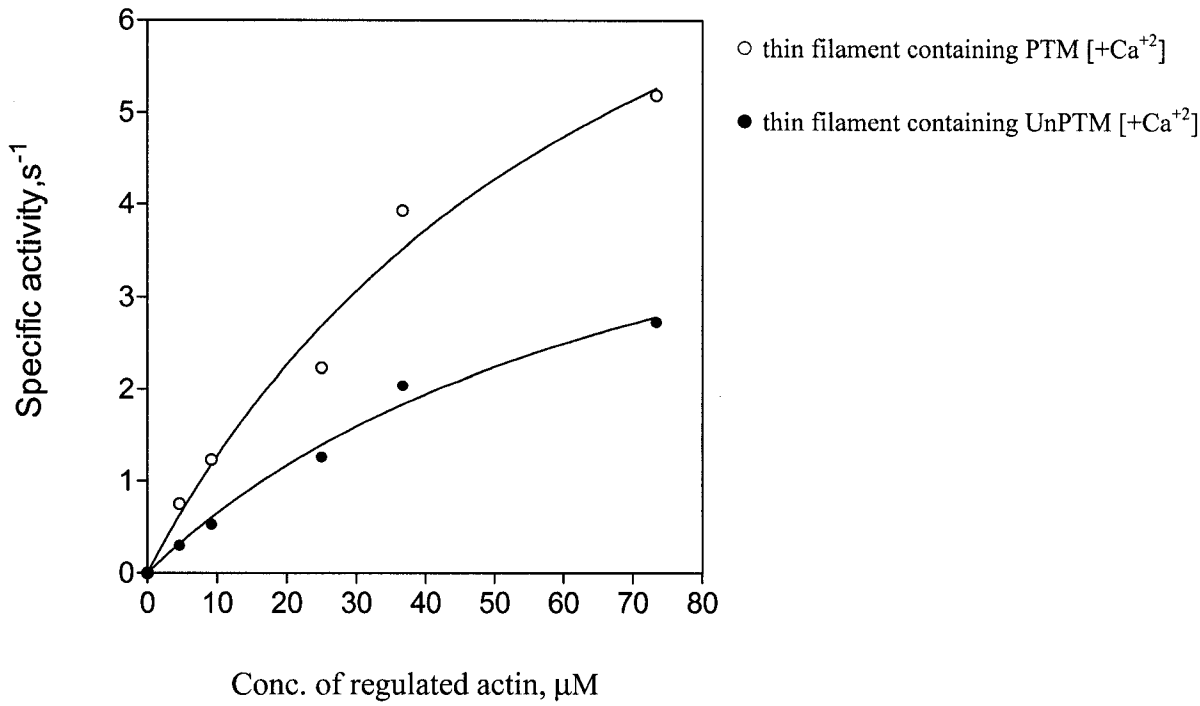

Fig.3.3 Dependence of actomyosin-S1Mg^{+2}ATPase rate on concentration of reconstituted thin filaments that contain either phosphorylated or unphosphorylated tropomyosin at 50mM ionic strength.

The concentrations of PTM, UnPTM and Tn were 2/7th that of the actin concentration. The concentration of myosin-S1 was 1.0μM. To avoid complexity, the rates of actomyosin-S1Mg^{+2}ATPase activities in the presence of PTM/UnPTM [+EGTA] are not shown. Buffering conditions: 30mM NaCl, 6mM $MgCl_2$ and 5mM MOPS, pH 7.0. The rate of release inorganic phosphate was determined as explained in Fig.3.2. The actomyosin-S1Mg^{+2}ATPase rate of myosin-S1 alone has been deducted. The graph pad software, PRIZM was used to draw plots. The Vmax values of PTM and UnPTM are 10.4 and 5.8s^{-1} respectively.

Therefore, it is apparent that under certain conditions [eg. Ionic strength of the buffer, pH], a change at a single site [i.e. phosphorylation] in the TM molecule can alter the regulatory properties of the thin filament.

3.2 Myosin-S1 binding affinity of reconstituted thin filaments containing either phosphorylated or unphosphorylated tropomyosin.

To ascertain whether the observed difference presented in Fig.3.3 is a result of a change in myosin affinity, myosin binding was assessed by measuring the myosin NH_4^+ATPase activity in the supernatant following sedimentation of different reaction mixtures in the Airfuge [see section 2.6.5 in Material and Methods] and confirmed electrophoretically in the presence of SDS [Fig.3.4]. The results showed an insignificant difference in the affinity of myosin for thin filaments containing non-identical TM isoforms [Fig.3.5], and this observation was compatible with the K_d values obtained from the kinetic data.

3.3 Myosin activation of reconstituted thin filaments in the presence of salmonid isotropomyosins.

Salmonid fish have a simple TM phenotype. Salmon and trout synthesize unique TM isoforms: fast skeletal, slow skeletal and cardiac (300). The sequences of these TM isoforms have been previously determined [Genbank accession numbers: fast skeletal, L25609; slow skeletal, Z66490; cardiac, Z66527].

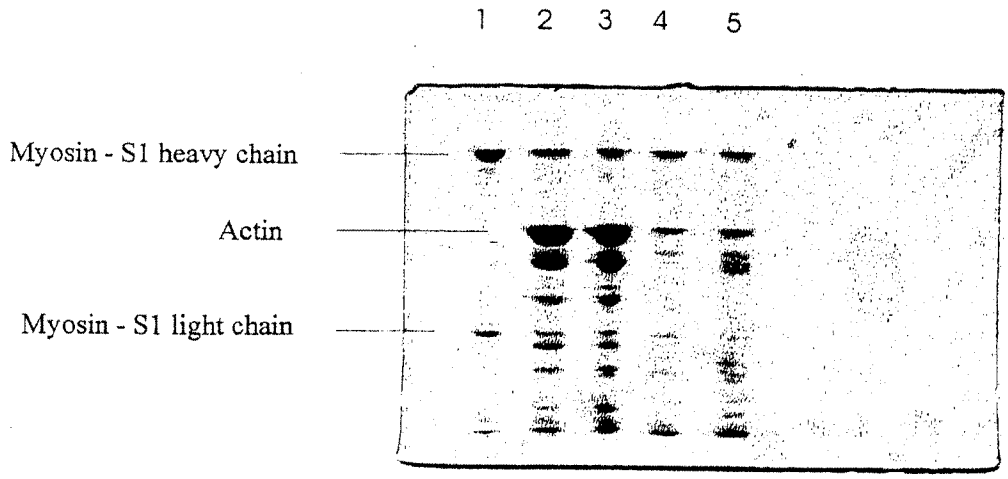

Fig.3.4 SDS-polyacrylamide gel analysis of myosin-S1 binding affinity of thin filaments containing either phosphorylated or unphosphorylated tropomyosin as determined by sedimentation method.

Lane 1-myosin-S1 standard;

Lane 2-thin filaments containing UnPTM [pre centrifugation]

Lane 3-thin filaments containing PTM [pre centrifugation]

Lane 4-thin filaments containing UnPTM [post centrifugation]

Lane 5-thin filaments containing PTM [post centrifugation]

Thin filaments, F-actin [25μM], Tn and TM [either PTM or UnPTM] were reconstituted at a ratio of 7:4:4 in the presence of 0.8μM myosin-S1 at 25°C. Upon addition of 1mM ATP, samples were Airfuged for 10min at 167,000 x g. The dilution factor of samples in lanes 2 and 3 is 1:1 [sample buffer: protein solution] while it is 1:4 for samples in lanes 4 and 5.

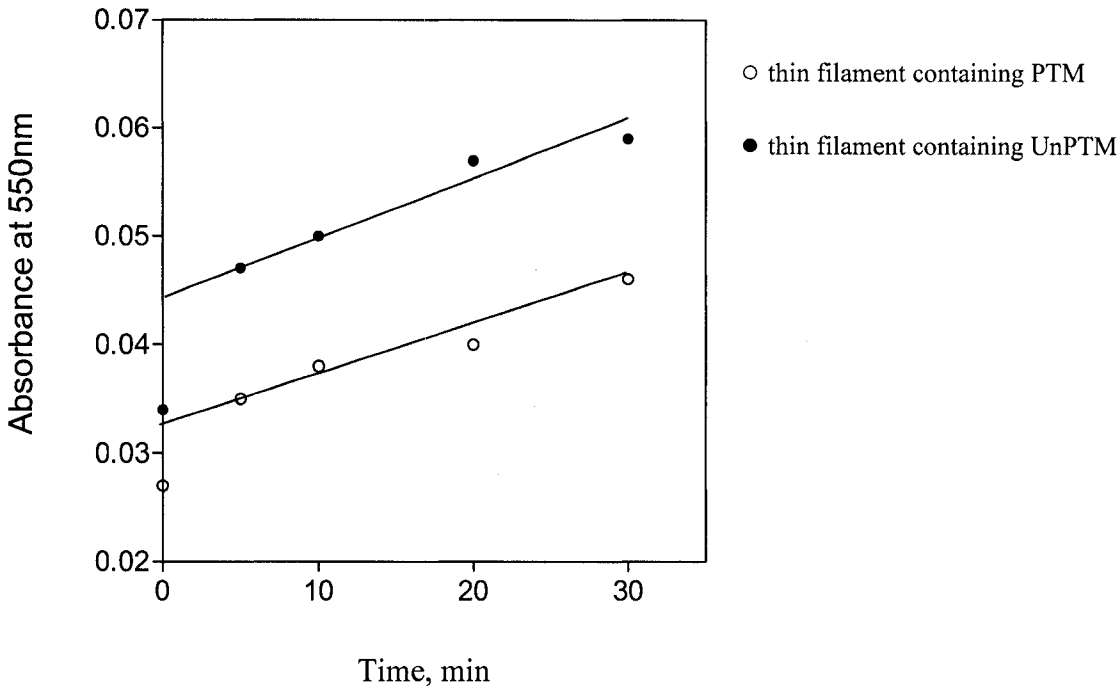

Fig.3.5 Myosin NH_4^+ATPase activity remaining in the supernatant fraction after sedimentation of a mixture of myosin-S1 and thin filaments [$+Ca^{+2}$] in the presence of ATP at 50mM ionic strength.

The thin filaments were reconstituted as denoted in Materials and methods [section 2.6.5] and the amount of inorganic phosphate released at a given time period of time was determined as noted in Fig. 3.2. The buffering system used was 30mM NaCl, 6mM $MgCl_2$ and 5mM MOPS, pH 7.0.

The amino acid substitutions within these isoforms [Fig.3.6] are distributed along the length of the molecule but a considerable number are confined to the Tn binding region and head-to-tail overlapping region. Therefore, the focus of this part of the study was to understand the effect of this heterogeneity on thin filament regulation.

A thin filament titration was carried out as before [Fig.3.2] using the three salmonid TMs: fast, slow and cardiac. As shown in Fig.3.7, thin filaments containing cardiac TM yield approximately 4-fold higher activation of actomyosinMg^{+2}ATPase [Vmax, $21.3s^{-1}$(salmon cardiac TM) vs $5.4s^{-1}$ (salmon fast TM)] than those containing fast TM at the higher ionic strength [50mM]. The presence of salmon slow muscle TM in the thin filament produces an intermediate level of activation [Vmax, $12.5s^{-1}$]. The same trend was observed at lower ionic strength [Vmax; $19.3s^{-1}$ (salmon cardiac TM) vs $7.6s^{-1}$ (salmon fast TM)] [Fig.3.8].

3.4 Dual regulation of reconstituted thin filaments containing salmonid Tropomyosin isoforms.

In this experiment, the concentration of myosin-S1 was varied from 1 to 10μM while maintaining the TM isoform [either salmon fast, slow or cardiac], Tn, and F-actin concentrations at 1.14, 1.14 and 4μM, respectively. Under these conditions, which were far away from Vmax, there was a linear dependence of actomyosin-S1Mg^{+2}ATPase activity on myosin-S1 concentration [Fig.3.9].

```
fast            MDAIKKKMQMLKLDKENALDRAEGAEGDKKAAEDKSKQLEDDLVALQKKLKGTEDELDKY 60
slow            MEAIKKKMLMLKMDKETALEAADQSEIDKKAAEDKSKQHDDALIQMQKKLKGTEDELDKY 60
cardiac         MEAIKKKMQMLKLDKENAIDRAEQAETDKKAAEDKCKQLEDELLSLQKNLKGTEDELDKY 60
                *:****** ***:***.*:: *: :* ********.** :* *: :**:************


fast            SESLKDAQEKLEVAEKTATDAEADVASLNRRIQLVEEELDRAQERLATALTKLEEAEKAA 120
slow            SEALKDAQEKLEVADKKAADAEAEVASLNRRIQLVEEELDRAQERLATALQKLEEAEKAA 120
cardiac         SEALKDAQEKLEQSEKTAADAEGDVAGLNRRIQLVEEELDRAQERLSTALQKLEEAEKAA 120
                **:********* ::*.*:***.:**.******************:*** *********


fast            DESERGMKVIENRASKDEEKMELQDIQLKEAKHIAEEADRKYEEVARKLVIIESDLERTE 180
slow            DESERGMKVIENRASKDEEKMEMQEIQLKEAKHIAEEADRKYEEVARKLVIIEGDLERTE 180
cardiac         DESERGMKVIENRASKDEEKMEIQELQLKEAKHIAEEADRKYEEVARKLVILEGELERAE 180
                **********************:*::*************************:*.:***:*


fast            ERAELSEGKCSELEEELKTVTNNLKSLEAQAEKYSQKEDKYEEEIKVLTDKLKEAETRAE 240
slow            ERAELAEGKCAELEEELKNVSNNLKSLEAQAEKYSQKEDKYEEEIKILTDKLKEAETRAE 240
cardiac         ERAEVSELKCSDLEEELKNVTNNLKSLEASSEKYSEKEDKYEEEIKVLSDKLKEAETRAE 240
                ****::* **::******.*:********.:****:**********:*:************


fast            FAERSVAKLEKTIDDLEDELYAQKLKYKAISEELDNALNDMTSI 284
slow            FAERSVAKLEKTIDDLEDELYAQKLKYKAISEELDHALNDMTSI 284
cardiac         FAERTVAKLEKSIDDLEDELYAQKLKYKAISEELDHALNDMTSL 284
                ****:******:**********************:*******:
```

Fig.3.6 Amino acid sequence comparison of salmonid tropomyosin isoforms.

The inferred amino acid sequences of TMs from salmonid fast skeletal, slow skeletal and cardiac muscle have been aligned. Identities in all three sequences have been indicated with an asterisk. Positions where amino acids are not identical are highlighted in red.

Fig.3.7 Dependence of actomyosin-S1Mg^{+2}ATPase activity on changing concentration of regulated actin in the presence of various forms of salmonid tropomyosin isoforms at 50mM ionic strength.

Actin, Tn and either salmon fast, slow or cardiac TM were reconstituted at a ratio of 7:2:2. The concentration of myosin-S1 was 1.0μM. Buffering conditions: 30mM NaCl, 6mM $MgCl_2$ and 5mM MOPS, pH 7.0. Temperature: 25°C. The rate of release inorganic phosphate was determined as explained in Fig.3.2. The myosin-S1Mg^{+2}ATPase rate of myosin-S1 alone has been deducted. The Vmax values of thin filaments containing salmon cardiac, fast and slow TM were 21.3, 5.4 and 12.5s^{-1} respectively.

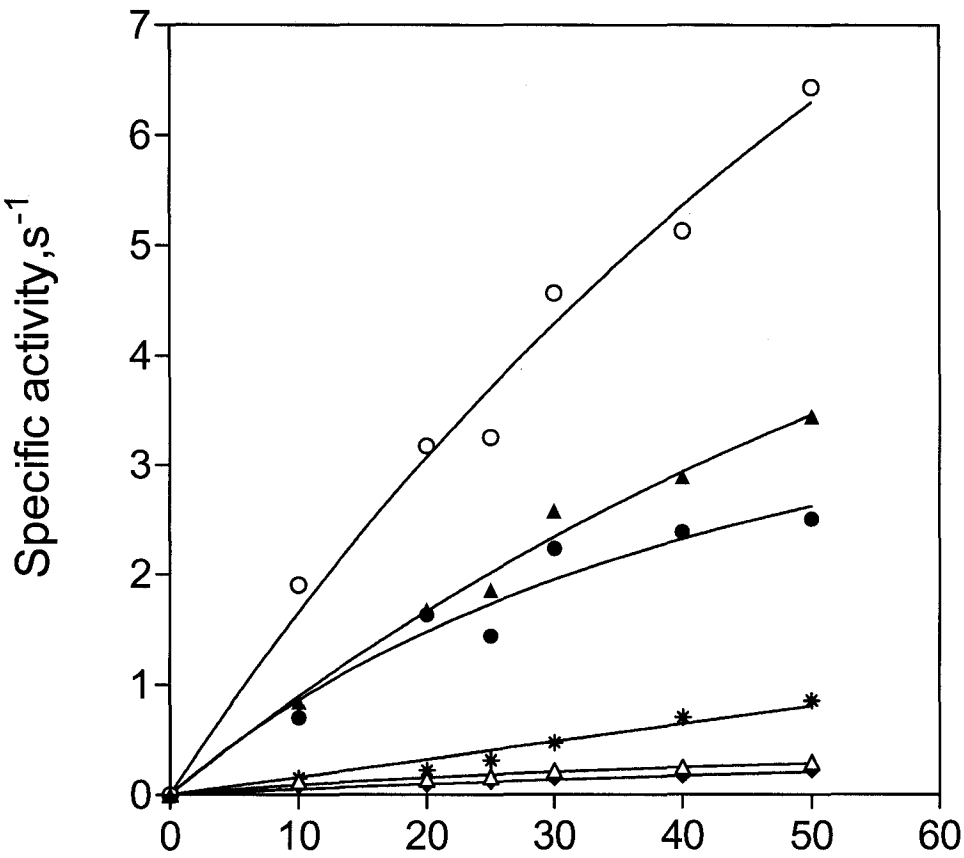

○ thin filaments containing salmon cardiac TM + Ca^{+2}

□ thin filaments containing salmon slow TM + Ca^{+2}

● thin filaments containing salmon fast TM + Ca^{+2}

* thin filaments containing salmon cardiac TM + EGTA

Δ thin filaments containing salmon slow TM + EGTA

♦ thin filaments containing salmon fast TM + EGTA

Fig.3.8 Activation of actomyosin-S1Mg^{+2}ATPase activity by regulated actin in the presence of variant salmonid tropomyosin isoforms at 22mM ionic strength.

The thin filaments were reconstituted as noted in Fig.3.7 in a buffer consisting of 4.5mM $MgCl_2$ and 5mM MOPS, pH 7.0 buffer at 25°C. The determination of the amount of inorganic phosphate released was the same as in Fig.3.2. The myosin-S1Mg^{+2}ATPase rate of myosin-S1 alone has been deducted. Vmax: 19.31s^{-1}[salmon cardiac TM] and 7.64s^{-1}[salmon fast TM]. Binding constants of thin filaments containing salmon cardiac and fast TM were 64.09 and 19.87μM respectively.

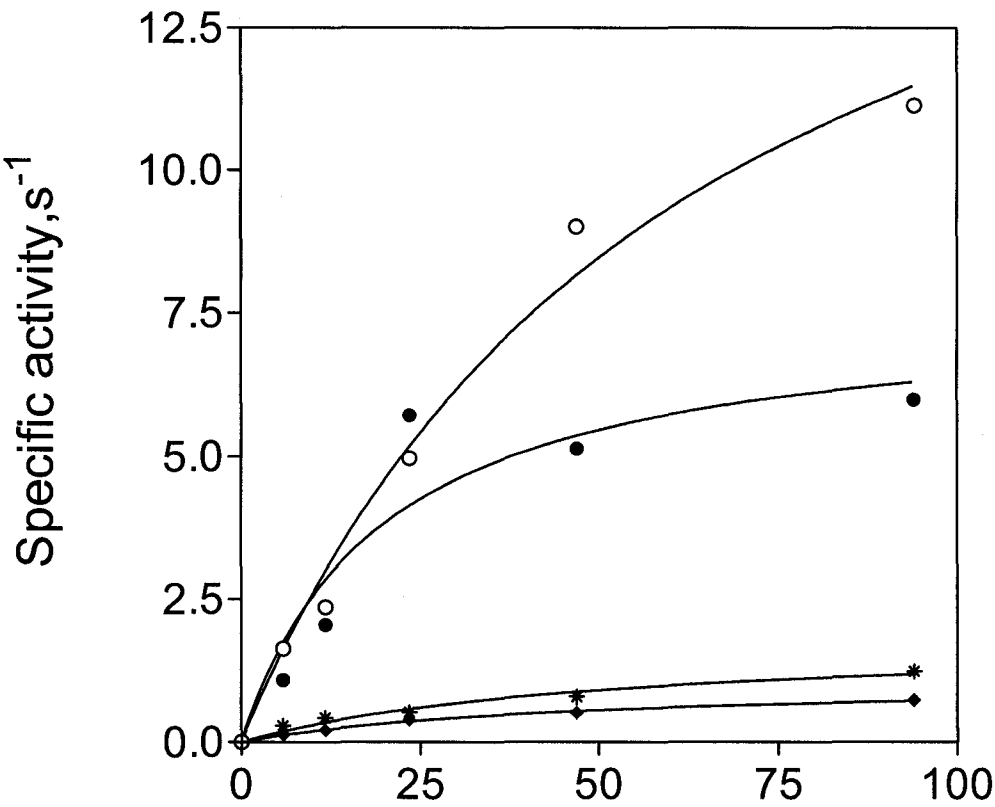

○ thin filaments containing salmon cardiac TM +Ca^{+2}

● thin filaments containing salmon fast TM + Ca^{+2}

* thin filaments containing salmon cardiac TM + EGTA

♦ thin filaments containing salmon fast TM + EGTA

Fig.3.9 The actomyosin-S1Mg^{+2}ATPase activity with regulated F-actin containing variant forms of salmonid tropomyosin and rabbit troponin, as a function of myosin-S1 concentration.

The concentration of myosin-S1 was increased from 0 to 10μM while the concentrations of F-actin, TM and Tn were maintained at 4, 1.14 and 1.14μM respectively. The buffering conditions: 30mM NaCl, 6mM $MgCl_2$ and 5mM MOPS, pH 7.0. Temperature: 25°C. The values for activity were corrected for the rate of myosin-s1 alone.

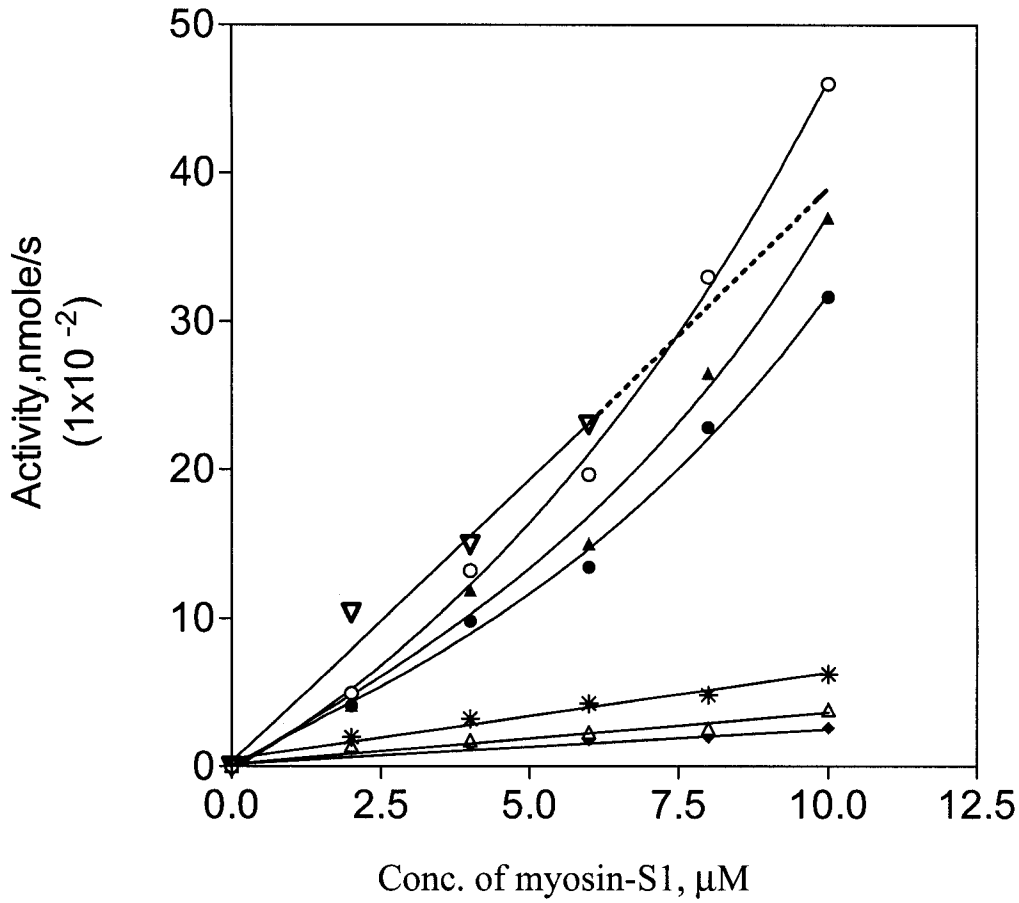

∇ myosin-S1actin alone

○ thin filaments containing salmon cardiac TM + Ca^{+2}

□ thin filaments containing salmon slow TM + Ca^{+2}

● thin filaments containing salmon fast TM + Ca^{+2}

* thin filaments containing salmon cardiac TM + EGTA

Δ thin filaments containing salmon slow TM + EGTA

♦ thin filaments containing salmon fast TM + EGTA

It has been shown previously that addition of TM-Tn [$+Ca^{+2}$] results in a departure from linearity with inhibition at low myosin-S1 concentration and potentiation at high myosin-S1 concentration, relative to F-actin alone (314). A similar behaviour was observed in Fig.3.9. As was demonstrated earlier [Fig.3.7], the highest activation occured with thin filaments reconstituted with salmon cardiac TM. In this particular case, potentiation was observed at a lower myosin-S1 concentration ratio than with the other two types of thin filament; ~7μM [salmon cardiac TM], 10μM [salmon slow TM] and > 10μM [salmon fast TM]. In conclusion, the order of decreasing actomyosin-S1Mg^{+2}ATPase activation is: cardiac > slow > fast.

Myosin-S1 binding experiments were carried out in identical fashion to those described earlier in the chapter. As before, changing the TM component of the thin filament produced no change in myosin-S1 binding [data not shown]. This suggests that the observed differences in thin filament regulation may be the result of a variation[s] in a kinetic step[s].

3.5 Effect of tropomyosin heterogeneity on the binding of rabbit troponin.

Tropomyosin was chromatographed on whole Tn Sepharose 4B using a linear gradient of NaCl. Eluted protein was determined by Bradford assay (299) or by Coomassie R-250 staining of electrophoretically separated protein bands. To facilitate the comparison of the variant salmon TM isoforms, a mixture of isoforms was loaded onto the column and co-

chromatographed. This method was employed to obviate run-to-run variation observed for chromatography of the same TM. Figure 3.10 [A],[B] and [C] shows the elution profiles of salmon fast +slow, fast+cardiac and slow + cardiac TM, respectively. The asymmetry of the profiles is evidence for a variable affinity of TM isoforms towards Tn. As shown in Fig.3.11 [A] salmon slow TM starts to elute prior to salmon fast TM indicating that, of the two, fast TM is more tightly bound to Tn. Further, salmon cardiac TM released from the column later in the salt gradient than salmon slow TM [Fig.3.11 [B]] and fast TM [Fig.3.11[C]]. Therefore, Tn binding affinity increases in the order: slow < fast < cardiac TM. Thus, substitutions in the Tn binding region of salmonid TM must be responsible for this variant degree of binding affinity with Tn.

3.6 Discussion

3.6.1 Effect of phosphorylation on the regulatory properties of tropomyosin.

Striated muscle TM [but not smooth muscle or non-muscle TMs] contains a single phosphorylation site: Ser residue 283, which is located in the overlapping region (9). This covalent modification, which gives the molecule a higher negative charge at pH 7.0 (9, 315), has been demonstrated in amphibians (316), mammals (77), birds (317) and fish (300). It is more prevalent in α-TM than in β-TM (313, 318-320) and requires a unique protein kinase, which is not activated by cAMP or Ca^{+2} (317-320).

Fig.3.10 Chromatography profiles of mixtures of salmonid Tropomyosin isoforms from rabbit skeletal muscle troponin Sepharose 4B.

[A] A mixture of salmon fast +slow TM

[B] A mixture of salmon slow + cardiac TM

[C] A mixture of salmon fast+cardiac TM

Samples [10-15nmol] which were dialyzed against 10mM MOPS, 50mM NaCl, 1.0mM EGTA, 1.0mM DTT, 0.01% [w/v] NaN_3, pH 7.0, at 4°C were loaded on to the column. The proteins were eluted with a linear gradient [0.05-0.5M NaCl, total volume, 100ml]. Protein was determined by Bradford assay as outlined in Materials and Methods [section 2.5.4.2].

A

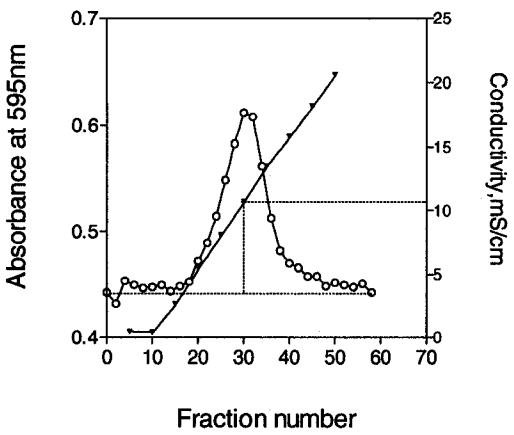

Conductivity at the peak of absorbance

11mS/cm

B

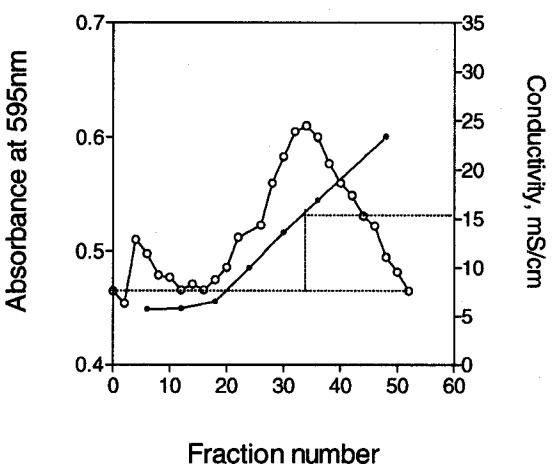

15.5mS/cm

C

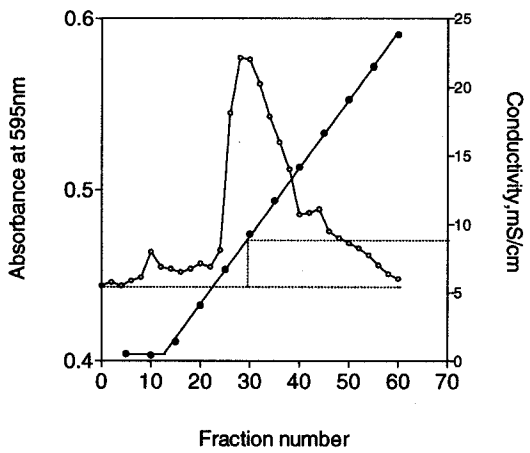

8.5mS/cm

Fig.3.11 SDS and alkaline urea polyacrylamide gel electrophoresis of eluted fractions from troponin Sepharose 4B.

Gel A, fractions of the mixture of salmon fast and slow TM

Gel B, fractions of the mixture of salmon slow and cardiac TM

Gel C, fractions of the mixture of salmon fast and cardiac TM

The fractions and standard proteins were loaded on the gels as noted. Sample [80μl] was mixed with 20μl of sample buffer and applied to the gel [20μl]. Binding affinity is apparent from the change in stained band intensity as a function of fraction number.

A

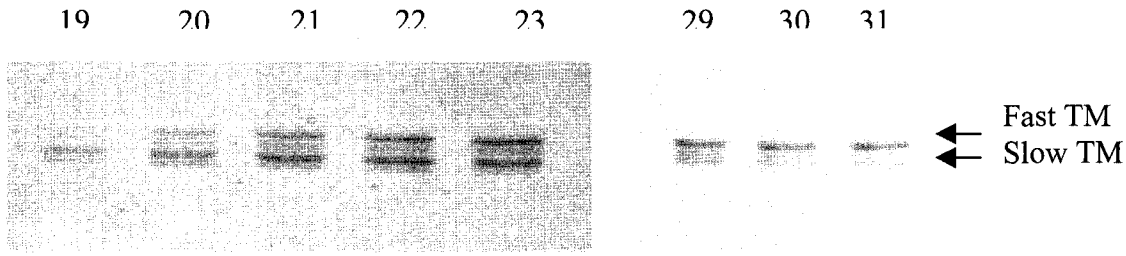
19
20
21
22
23
29
30
31
Fast TM
Slow TM

B

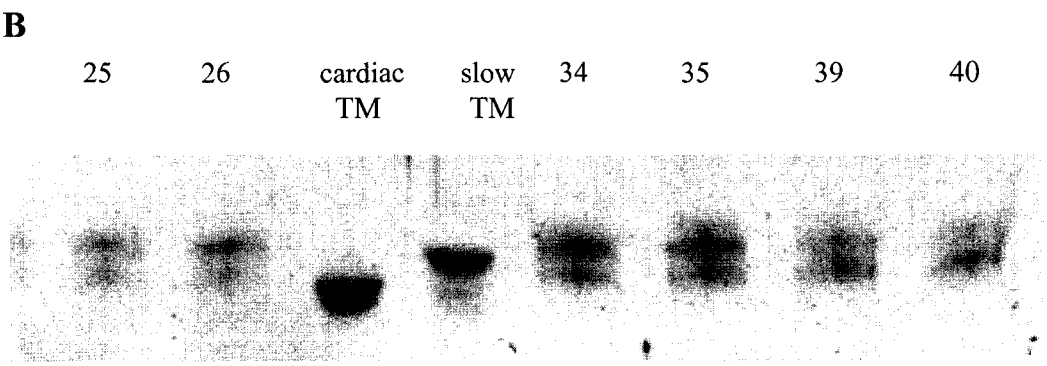
25
26
cardiac TM
slow TM
34
35
39
40

C

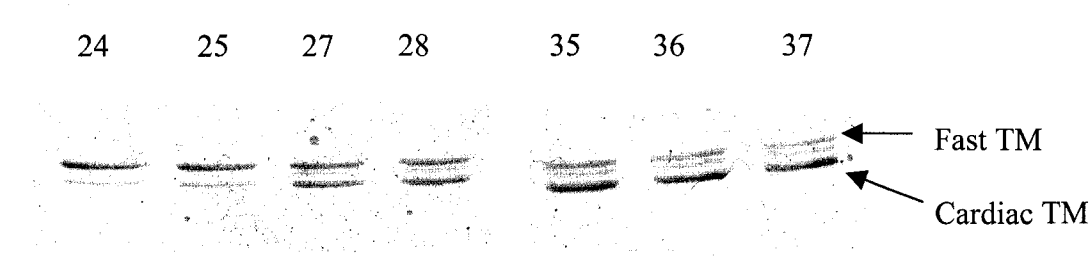
24
25
27
28
35
36
37
Fast TM
Cardiac TM

In the neutral pH range and at low ionic strength, phosphorylation strengthens the end-to-end interaction of adjoining TM molecules (321) an effect that can be mimicked by mutating the Ser with Glu (322).

Serine 283 is in a *c* position of the heptad repeat, which is predicted to fall on the outside of a coiled coil structure, hence the phosphate group is exposed to solvent. According to a ^{1}H- NMR analysis of the secondary structure of a C-terminal fragment of TM, $^{1}H^{\alpha}$ and $^{13}C^{\alpha}$ chemical shift displacements showed that residues 252-279 are α-helical but residues 280-284 are non-helical (323). The same researchers later reported that residues 270-279 are arranged in an unusual parallel, linear arrangement with the last five amino acids splayed apart (52). The functional consequences of phosphorylation have been studied previously in regards to mammalian α-TM (214), but not the fish protein. Studies conducted in the Heeley lab have shown that the phosphorylation site is conserved in shark TM (324).

At 50mM ionic strength, reconstituted thin filaments [$+Ca^{2+}$] containing shark PTM [which comprises a single α-type isoform] showed approximately 2-fold higher activation than the unphosphorylated version [Fig.3.3], consistent with the findings of previous experiments conducted with rabbit TM under similar conditions (321). Further, there was no observable change in myosin-S1 binding affinity. These data are included in this chapter to show that TM phosphorylation may be of physiological importance in fish, as well as other animal classes. In addition, they also demonstrate the critical nature of

the overlapping region. A single change in this region alters the properties of the entire thin filament.

Tropomyosin, together with Tn, is required for ligand [either Ca^{2+} or rigor myosin-S1]-dependent regulation of the actomyosin-S1Mg^{+2}ATPase. In the absence of bound ligand [presence of EGTA and ATP] the thin filament is in an inhibited state and unable to form a productive interaction with myosin (274). Ligand binding changes the conformation of the thin filament such that it can now activate myosin. The three state model (274) envisages that Ca^{2+} binding produces an intermediate state [the 'closed' state], which can partially activate myosin. Conversion to the fully activating state, or 'open' state, requires the binding of rigor myosin heads. By contrast the two-state model predicts that Ca^{2+} and myosin binding influence a single equilibrium defining two states in which myosin is either weakly ['off' state] or strongly ['on' state] bound. The difference in actomyosin-S1Mg^{+2}ATPase activity observed in Fig.3.3 can be explained by proposing that thin filaments composed solely of PTM have more regulatory units in an activating conformation than those containing UnPTM.

3.6.2. Effect of isomorphism on the regulatory properties of tropomyosin.

The study of naturally occurring protein isoforms can provide valuable insights into which regions of a protein are key to its function, as well as how these regions can be altered in order to modulate function. The location and characteristic features of the side

chains of the amino acids that are substituted in different TMs will be major factors in this regard.

When thin filaments were reconstituted with a different isoform of TM, different levels of myosin-S1 activation were observed [Figs.3.7-3.9]. Interestingly, the maximal level of myosin activation cannot be predicted from inspecting only the overlap sequences, as with the simple case of PTM and UnPTM. For example, at neutral pH [low ionic strength, 5°C] salmon fast muscle TM polymerizes end-to-end more strongly than salmon cardiac and slow muscle TMs on account of the substitution at position 276 [Asn in fast, His in slow and cardiac, (214)]. However, thin filaments containing this TM generate less than half the maximal activation of those containing cardiac TM, 7.6 vs $19s^{-1}$. A similar result was obtained at low thin filament concentration, conditions where inhibition and potentiation of the myosin-S1Mg^{+2}ATPase occurs (69, 313, 325-327). Thus, as was observed with PTM [Fig.3.3], thin filaments containing salmon cardiac TM have a greater fraction of units in the activating state compared to other thin filaments (272,326,328). However, unlike PTM, from these findings, it can be suggested that changes away from, as well as within, the overlap site [Fig.3.3 and (38)], also have a bearing on the regulatory properties of TM.

Since the regulatory properties of TM are connected to its interactions with actin and Tn, it is reasonable to assume that the three salmonid TM isoforms do not bind actin and Tn in precisely the same way. The interaction with actin requires Mg^{+2}. It is thought that carboxylate groups on each protein interact via Mg^{+2} salt bridges. The ability of one TM molecule to bind 7 molecules of actin has been accounted for by the presence within the

primary structure of stretches of approximately twenty amino acids having either a preponderance of hydrophobic [discounting the ***a*** and ***d*** positions] or hydrophilic side-chains, the so-called α and β bands (25). There is also evidence to suggest that these actin-binding sites are not equivalent (25). For example, the β-band has been implicated in the 'on' state of myofilament activation, and the positive zones are primarily filled with hydrophobic residues allowing for close contact between TM and actin (272,329 and 330). The N- and C-terminal regions of TM are particularly important determinants of actin affinity (331). When the sequences of the salmonid TMs are compared with each other, the first and last 50 residues are found to contain a number of substitutions, including charge changes at positions 21, 42, 49 and 276 [Table 3.2]. The substitution at position 49, Lys [in salmon fast TM] to Asn [salmon cardiac TM], will give this region of the cardiac isoform one fewer positive charge at cellular pH than that of fast muscle TM. Conversely, the presence of the C-terminally located His in salmon cardiac TM will impart a partial positive charge. Changes in the actin affinity of TM have also been attributed to alternatively spliced exons. In α-TMs, approximately 2-fold differences in affinity for actin can be attributed to the type of second [residue 39-80] and sixth exon [residue 189-214] (332 and 333). It is interesting to note that the salmonid TMs also possess variability in these sections of the molecule [Table 3.2].

There are four replacements of Ala involving an hydroxyl-containing side chain between residues 45-79 of the salmon cardiac and fast muscle TM sequences. Further, a charge substitution exists at residue 216; Gln in fast, Glu in salmon cardiac TM. Because changes in these regions of TM have been linked to a change in actin binding (334-336)

the salmon cardiac and fast muscle TM are predicted to have different actin affinity. Although this was not verified experimentally, the interaction of the various TM isoforms with Tn was investigated and differences were demonstrated [Figs.3.12 and 3.13].

As mentioned in the introduction, Tn spans more than one-third of the length of TM [Fig.3.14]. It binds to TM via the Tn-T subunit at two sites. One of these is located towards the center of TM, between residues 175-190. The other encompasses the C-terminal 25 amino acids [residues 258-284], and perhaps the N-terminal region of the next TM molecule on the actin filament (172 and 173). The main substitution in the terminal sections of salmonid TMs is at 276, which is located within the overlap, where a His in cardiac TM [which exhibits the strongest affinity for Tn] is switched for Asn in fast TM. It is possible that the partial positive charge associated with the His enhances the binding of the negatively charged N-terminal portion of Tn-T. The weak Tn affinity exhibited by slow TM can be speculated to be partially due to the loss of an Arg residue at 21. When attention is given to the other binding site, residues 175-190, salmon cardiac muscle TM is seen to contain three substitutions compared to fast muscle TM, specifically, at positions 174, 179 and 188. In the first two cases, a hydroxyl-containing side-chain in fast TM is replaced by Gly [residue 174] or Ala [residue 179]. The latter may be especially important because it is a core position. It is possible that the fast muscle isoform is destabilized relative to the cardiac muscle form in this region. Finally, it is worth noting the substitution at 188 where a Gly in fast TM is exchanged for a Leu in cardiac TM.

Table 3.2 The distribution of substituted amino acids in salmonid tropomyosin.

The denoted comparison was carried out with respect to salmon fast TM. The substitutions highlighted in violet are in the Tn binding region, charge substitutions are in grey colour. The positions ***d*** and ***g*** are highlighted in orange and green respectively.

Location of the amino acid	Salmon fast TM	Salmon cardiac TM	Salmon slow TM	Location in the heptad sequence
9	Gln	-	Leu	b
17	Asn	-	Thr	c
21	Arg	-	Ala	
24	Gly	Gln	Gln	c
25	Ala	-	Ser	
27	Gly	Thr	Ile	f
36	Ser	Cys	Ser	
39	Leu	-	His	
42	Asp	-	Ala	
45	Ala	Ser	Gln	c
49	Lys	Asn	-	
63	Ser	Ala	Ala	
74	Ala	Ser	Ala	
79	Thr	Ala	Ala	b
83	Ala	Gly	-	f
87	Ser	Gly	-	c
107	Ala	Gly	-	b
111	Thr	Gln	Gln	f
	Ser	Gly	Gly	f
	Thr	Ala	-	
	Ser	-	Ala	
	Gly	Leu	-	f
	Ser	-	Ala	b
	Thr	Asn	Asn	c
	Gln	Ser	-	
	Ala	Ser	-	a
	Gln	Glu	-	f
276	Asn	His	His	c

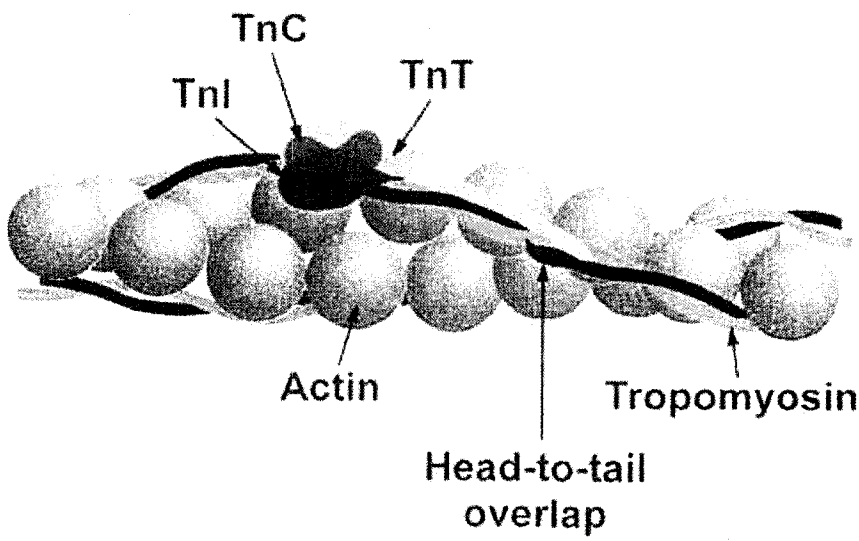

Fig.3.14 A model of the molecular arrangement of Tn subunits, TM, and actin in skeletal muscle thin filament (39).

Note the adjacent TM molecules overlap head to tail with the N-terminus of TnT lying along the overlap region. The C-terminus of TnT interacts with TnC and TnI, and TnI also interacts with actin.

Another consideration is the proximity of substitutions to alanine clusters. The seven Ala clusters in TM's helical structure impart conformational bends and yield flexibility to TM's coiled-coil design, thus allowing more effective interactions with actin (26). Charge changes in salmonid TM residue, 39Leu/His, 42Asp/Ala, 49Lys/Asn, 216Glu/Gln and 276Asn/His can be expected to have repercussions on nearby amino acid side chains and thus could alter the conformational bends in TM imparted by Ala clusters [Table 3.3].

Residue 179, which occurs within the fifth Ala cluster, is occupied by Thr in salmon fast TM. The presence of a bulky hydrophilic side chain could disrupt the local conformation in this part of the molecule. More importantly, this residue is located in part of the TnT binding region. On the other hand residue 276, which lies adjacent to Ala277, the seventh cluster, is Asn instead of His as in salmon cardiac and slow TM. This substitution could minimize steric repulsion due to reduced size and neutrality of the side chain at pH 7.0.

Position 24, which is adjacent to the first Ala cluster, is occupied by Gln in cardiac and slow TM while it is Gly in fast TM. Further, the second Ala cluster consists of residues Ala67, Ala74, Ala78 and Ala81 and of those residues, hydrophilic Ser in cardiac TM substitutes 74Ala. In addition, Ala211which is located in position ***a*** in the heptad repeat is also substituted by Ser. It is possible that this change, combined with His276 could make the conformation unstable. Gaffin *et al.*, (337) have determined the distance between native and mutant of His276Asn of transgenic mouse using atomic coordinates available from a protein data bank and minimizing the mutant structure in the Insight II suite, using Discovery [Accelrys].

Table.3.3 The comparison of amino acid substitutions near alanine clusters.

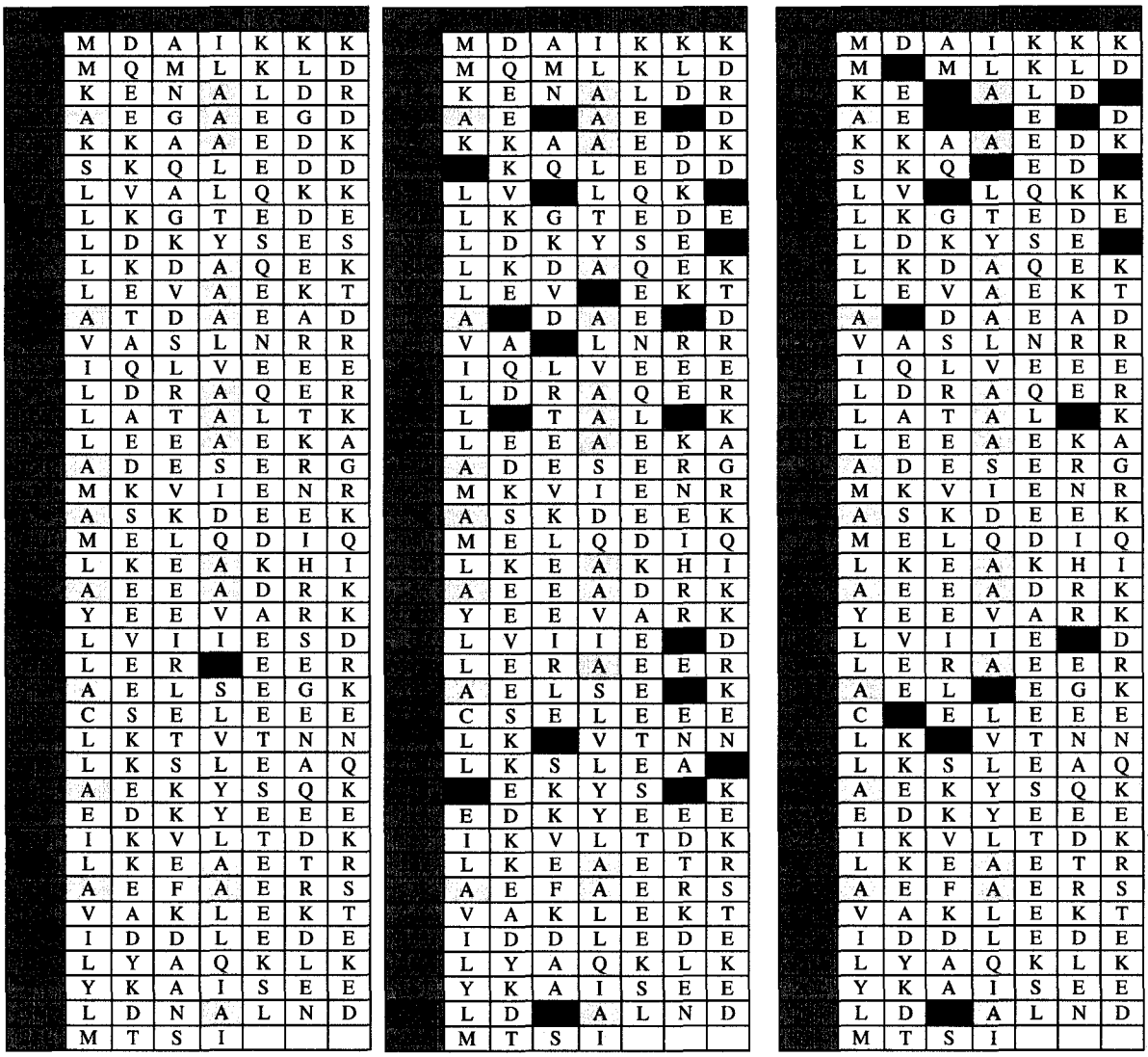

Fast TM							Cardiac TM							Slow TM						
M	D	A	I	K	K	K	M	D	A	I	K	K	K	M	D	A	I	K	K	K
M	Q	M	L	K	L	D	M	Q	M	L	K	L	D	M		M	L	K	L	D
K	E	N	A	L	D	R	K	E	N	A	L	D	R	K	E		A	L	D	
A	E	G	A	E	G	D	A	E		A	E		D	A	E			E		D
K	K	A	A	E	D	K	K	K	A	A	E	D	K	K	K	A	A	E	D	K
S	K	Q	L	E	D	D		K	Q	L	E	D	D	S	K	Q		E	D	
L	V	A	L	Q	K	K	L	V		L	Q	K		L	V		L	Q	K	K
L	K	G	T	E	D	E	L	K	G	T	E	D	E	L	K	G	T	E	D	E
L	D	K	Y	S	E	S	L	D	K	Y	S	E		L	D	K	Y	S	E	
L	K	D	A	Q	E	K	L	K	D	A	Q	E	K	L	K	D	A	Q	E	K
L	E	V	A	E	K	T	L	E	V		E	K	T	L	E	V	A	E	K	T
A	T	D	A	E	A	D	A		D	A	E		D	A		D	A	E	A	D
V	A	S	L	N	R	R	V	A		L	N	R	R	V	A	S	L	N	R	R
I	Q	L	V	E	E	E	I	Q	L	V	E	E	E	I	Q	L	V	E	E	E
L	D	R	A	Q	E	R	L	D	R	A	Q	E	R	L	D	R	A	Q	E	R
L	A	T	A	L	T	K	L		T	A	L		K	L	A	T	A	L		K
L	E	E	A	E	K	A	L	E	E	A	E	K	A	L	E	E	A	E	K	A
A	D	E	S	E	R	G	A	D	E	S	E	R	G	A	D	E	S	E	R	G
M	K	V	I	E	N	R	M	K	V	I	E	N	R	M	K	V	I	E	N	R
A	S	K	D	E	E	K	A	S	K	D	E	E	K	A	S	K	D	E	E	K
M	E	L	Q	D	I	Q	M	E	L	Q	D	I	Q	M	E	L	Q	D	I	Q
L	K	E	A	K	H	I	L	K	E	A	K	H	I	L	K	E	A	K	H	I
A	E	E	A	D	R	K	A	E	E	A	D	R	K	A	E	E	A	D	R	K
Y	E	E	V	A	R	K	Y	E	E	V	A	R	K	Y	E	E	V	A	R	K
L	V	I	I	E	S	D	L	V	I	I	E		D	L	V	I	I	E		D
L	E	R		E	E	R	L	E	R	A	E	E	R	L	E	R	A	E	E	R
A	E	L	S	E	G	K	A	E	L	S	E		K	A	E	L		E	G	K
C	S	E	L	E	E	E	C	S	E	L	E	E	E	C		E	L	E	E	E
L	K	T	V	T	N	N	L	K		V	T	N	N	L	K		V	T	N	N
L	K	S	L	E	A	Q	L	K	S	L	E	A		L	K	S	L	E	A	Q
A	E	K	Y	S	Q	K		E	K	Y	S		K	A	E	K	Y	S	Q	K
E	D	K	Y	E	E	E	E	D	K	Y	E	E	E	E	D	K	Y	E	E	E
I	K	V	L	T	D	K	I	K	V	L	T	D	K	I	K	V	L	T	D	K
L	K	E	A	E	T	R	L	K	E	A	E	T	R	L	K	E	A	E	T	R
A	E	F	A	E	R	S	A	E	F	A	E	R	S	A	E	F	A	E	R	S
V	A	K	L	E	K	T	V	A	K	L	E	K	T	V	A	K	L	E	K	T
I	D	D	L	E	D	E	I	D	D	L	E	D	E	I	D	D	L	E	D	E
L	Y	A	Q	K	L	K	L	Y	A	Q	K	L	K	L	Y	A	Q	K	L	K
Y	K	A	I	S	E	E	Y	K	A	I	S	E	E	Y	K	A	I	S	E	E
L	D	N	A	L	N	D	L	D		A	L	N	D	L	D		A	L	N	D
M	T	S	I				M	T	S	I				M	T	S	I			

The comparison was done with respect to salmon fast TM. The Ala clusters are shaded ash in colour and all the substitutions are shaded green in colour.

The carbonyl atoms distance at residue 275,276 and 277 is 12.92, 11.19 and 6.20Å in the native versus 13.33, 11.07 and 6.53Å in the mutant molecule. Thus this mutation causes a significant change in the distance between the monomer strands in localized regions of the TM molecule and this change in turn could affect the interactions of the TM molecule with neighboring thin filament molecules such as actin and TnT. Later, using the same model, Gaffin *et al.*, (338) have reported that the mutant His276Asn does not alter Ca^{+2} sensitivity or thin filament regulation. Further, work by Jagatheesan *et al.*, (339) have shown contradicting results obtained from transgenic mice expressing chimeric α-/-β TM where there are only 5 amino acid differences between the C-terminal 27 amino acids of α-TM and β-TM, of which two are highly conservative [Leu260Val, Ile284Leu]. Of the remaining 3 amino acids [Leu265Met, His276Asn and Met281Ile], all have substantial differences in the size of the side chain group and one introduces a charge change as well. Using recombinant TM, mutational studies on Gln111Trp, which is located in the ***f*** position in the heptad repeat, have not shown any significant difference in actin binding and myosin-S1Mg^{+2}ATPase inhibitory activity (340). Therefore, the observed variations in myosin- S1Mg^{+2}ATPase activation and binding affinity with Tn appears to reflect the contributions of several substitutions spread throughout the molecule as opposed to heterogeniety in one particular region such as the overlap. Therefore, more research is required to explain the basis of the non-identical regulatory properties of the salmonid TM isoforms. The experiments reported in this chapter are to be viewed as a first step in this process.

Chapter 4

Characterization of salmonid isoactins

4.0 Introduction

Salmon striated muscle contains three different types of actin isoforms: fast, slow and cardiac. Clones from cDNA libraries for each muscle type were identified from cDNA libraries and sequenced by Donna Jackman [Heeley lab]. The nucleotide sequences are registered with GenBank [accession numbers are as follows: salmon fast, AF 304406; slow, AF 267496; cardiac, AF 303985]. As expected, the inferred amino acid sequences of salmonid actins have been highly conserved [Fig.4.1]. However, the slow actin isoform appears to be surprisingly divergent from the other two. Cardiac and fast actins differ in only two positions, but both differ from slow actin at 12 positions [Table 4.1]. The slow muscle and fast muscle isoactins have six non-conservative changes between them: [i] Val103Thr [Val in slow, Thr in fast, and the residue position is based on processing of the first two amino acids to produce a stable 375 amino acids]; [ii] Ala155Ser; [iii] Thr278Ala; [iv] Gly281Ser [v] Gly310Ala and [vi] Asp360Gln [Table 4.2]. The slow-cardiac pairing has an additional replacement [making a total of seven]; Ala354Gln. This particular substitution is also the only significant difference between the fast and cardiac sequences. Of interest is that, compared to the fast muscle isoform, slow actin is predicted to contain a charge at position 360, to have lost hydrogen bonding side chains at positions 103 and 155, and to have gained one such group at position 278.

Table 4.1 Comparison of the number of amino acid substitutions between salmonid isoactins.

	Slow	Fast	Cardiac
Slow	-	12 (6)	12 (7)
Fast	12 (6)	-	2 (1)
Cardiac	12 (7)	2 (1)	-

The number of non-conservative substitutions is shown in parentheses.

Table 4.2 The non-conservative amino acid substitutions in salmonid isoactins.

Residue	Fast actin	Slow actin	Cardiac actin
103	Thr	Val	Thr
155	Ser	Ala	Ser
278	Ala	Thr	Ala
281	Ser	Gly	Ser
310	Ala	Gly	Ala
354	Ala	Ala	Gln
360	Gln	Asp	Gln

The residue position is based on processing of the first two amino acids to produce a stable 375 amino acid protein, consistent with protein mass spectrometric measurements.

```
fast            MCDDDETTALVCDNGSGLVKAGFAGDDAPRAVFPSIVGRPRHQGVMVGMGQKDSYVGDEA 60
cardiac         MCDDDETTALVCDNGSGLVKAGFAGDDAPRAVFPSIVGRPRHQGVMVGMGQKDSYVGDEA 60
slow            MCDEEETTALVCDNGSGLVKAGFAGDDAPRAVFPSIVGRPRHQGVMVGMGQKDSYVGDEA 60
                ***::************************************************************

fast            QSKRGILTLKYPIEHGIITNWDDMEKIWHHTFYNELRVAPEEHPTLLTEAPLNPKANREK 120
cardiac         QSKRGILTLKYPIEHGIITNWDDMEKIWHHTFYNELRVAPEEHPTLLTEAPLNPKANREK 120
slow            QSKRGILTLKYPIEHGIITNWDDMEKIWHHTFYNELRVAPEEHPVLLTEAPLNPKANREK 120
                ****************************************.***************

fast            MTQIMFETFNVPAMYVAIQAVLSLYASGRTTGIVLDSGDGVTHNVPIYEGYALPHAIMRL 180
cardiac         MTQIMFETFNVPAMYVAIQAVLSLYASGRTTGIVLDSGDGVTHNVPIYEGYALPHAIMRL 180
slow            MTQIMFETFNVPAMYVAIQAVLSLYASGRTTGIVLDAGDGVTHNVPVYEGYALPHAIMRL 180
                ***********************************:*********:*************

fast            DLAGRDLTDYLMKILTERGYSFVTTAEREIVRDIKEKLCYVALDFENEMATAASSSSLEK 240
cardiac         DLAGRDLTDYLMKILTERGYSFVTTAEREIVRDIKEKLCYVALDFENEMATAASSSSLEK 240
slow            DLAGRDLTDYLMKILTERGYSFVTTAEREIVRDIKEKLCYVALDFENEMATAASSSSLEK 240
                ************************************************************

fast            SYELPDGQVITIGNERFRCPETLFQPSFIGMESAGIHETAYNSIMKCDIDIRKDLYANNV 300
cardiac         SYELPDGQVITIGNERFRCPETLFQPSFIGMESAGIHETAYNSIMKCDIDIRKDLYANNV 300
slow            SYELPDGQVITIGNERFRCPETLFQPSFIGMESAGIHETTYNGIMKCDIDIRKDLYANNV 300
                ************************************:**.*****************

fast            LSGGTTMYPGIADRMQKEITALAPSTMKIKIIAPPERKYSVWIGGSILASLSTFQAMWIT 360
cardiac         LSGGTTMYPGIADRMQKEITALAPSTMKIKIIAPPERKYSVWIGGSILASLSTFQQMWIS 360
slow            LSGGTTMYPGIGDRMQKEITALAPSTMKIKMIAPPERKYSVWIGGSILASLSTFQAMWIS 360
                ***********.******************:************************ ***:

fast            KQEYDEAGPSIVHRKCF 377
cardiac         KQEYDEAGPSIVHRKCF 377
slow            KDEYEEAGPSIVHRKCF 377
                *:**:************
```

Fig.4.1 Amino acid sequence comparison of salmonid isoactins.

The inferred amino acid sequences of actin from salmonid fast, slow and cardiac muscle have been aligned.

Positions where amino acids are not identical are highlighted in red.

Further, slow actin has a higher Gly content on account of the changes at position 310, as well as an extra Met residue via a conservative switch at 329. When considering the conservative substitutions, a total of six substitutions are distributed in each isoform [Table 4.3]. As a final point, it should be noted that both the non-conservative and conservative substitutions are confined to actin sub-domains 1 and 3 [Fig.4.2, Table 4.3]. These two domains of the molecule are thought to have arisen as a result of gene duplication and are structurally similar (119).

The surprising sequence diversity of the salmonid slow muscle actin prompted an investigation into the possibility that this actin might have different properties compared with other striated muscle actins. In view of the near-identity of the salmonid fast and cardiac actin isoforms, the investigation was limited mostly to the fast and slow isoforms.

Note: For convenience salmonid fast and slow actins are denoted as F and S respectively.

4.1 Charge substitution in salmonid isoactins.

As shown in Fig.4.3, there is a distinct difference in the mobility of slow and fast actin, when they are separated by electrophoresis in the presence of 8M urea at alkaline pH, confirming the presence of a charge substitution in slow actin. This is consistent with the amino acid substitution at position 360. According to the available sequencing data in the GenBank slow actin is the only actin that has Asp at position 360.

Table 4.3 The distribution of conservative and non-conservative amino acid substitutions in salmonid isoactins with respect to secondary structure.

Substitution	Sub-domain	Location
Asp2Glu	1	loop Asp1-Leu8
Asp3Glu	1	loop Asp1-Leu8
Ile163Val	3	helix Thr160-Tyr166
Ile329Met	3	helix Lys328-Ala331
Thr358Ser	1	helix Lys359-Ala365
Asp363Glu	1	helix Lys359-Ala365
Val103Thr	1	loop Asn92-Thr103
Ala155Ser	3	loop Ser155-Thr160
Thr278Ala	3	helix Ile274-Ile282
Gly281Ser	3	helix Ile274-Ile282
Gly310Ala	3	helix Ile309-Leu320
Ala354Gln	1	loop Met355-Lys359
Asp360Gln	1	helix Lys359-Ala365

The first amino acid of a given pair corresponds to that residue in fast muscle actin. The second corresponds to slow muscle actin. For example, Asp2Glu: Asp in salmon fast and Glu in salmon slow actin.

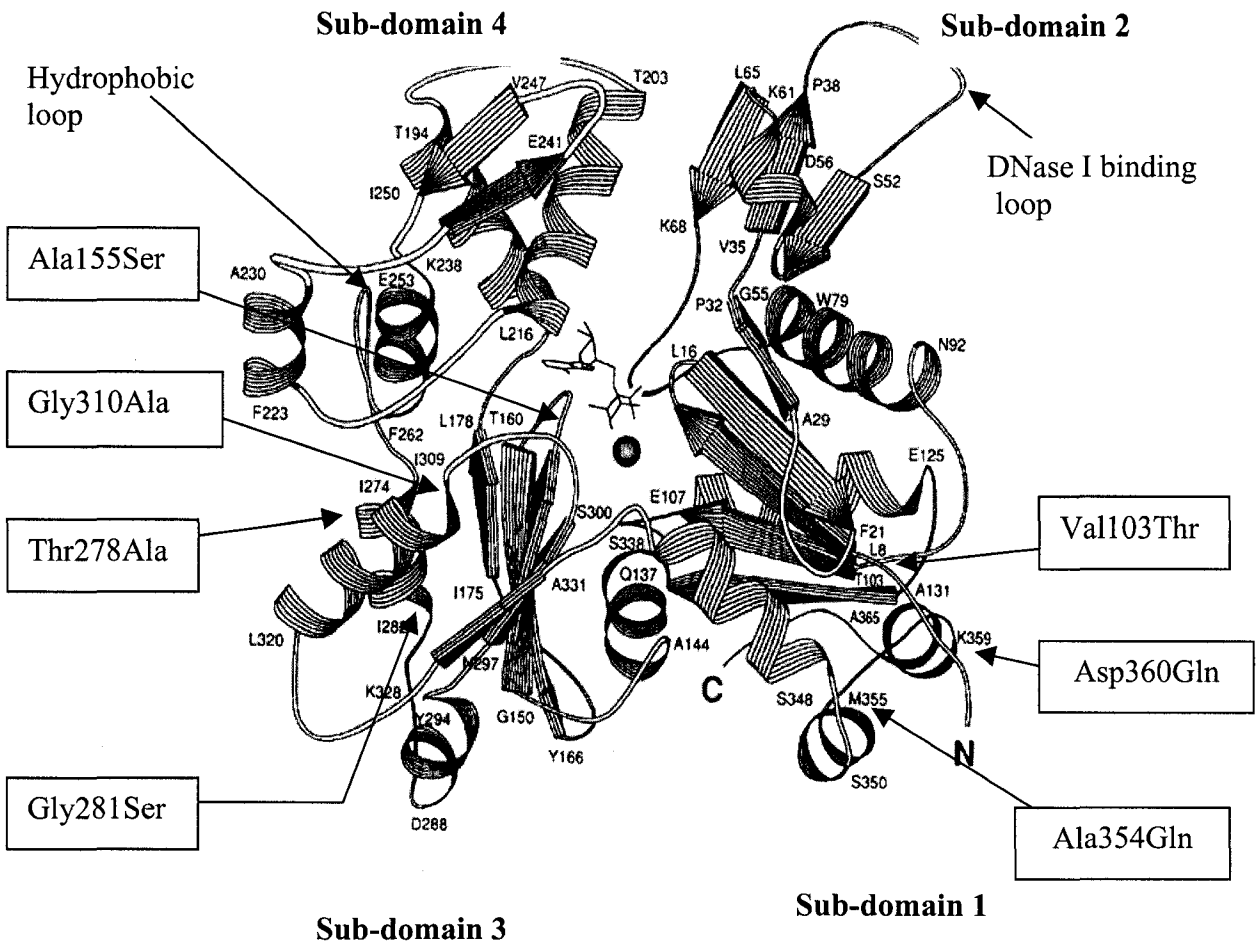

Fig.4.2 The distribution of non-conservative amino acid substitutions in salmonid isoactins with respect to tertiary structure solved by Kabsch et al (119).

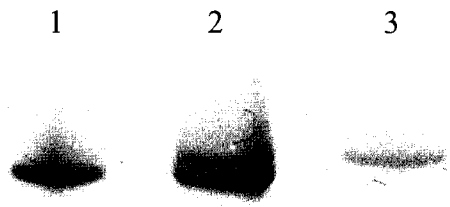

Fig.4.3 Alkaline urea polyacrylamide gel electrophoresis of purified salmonid iso- actins.

Samples [0.5-2mg] of slow muscle actin [lane 1], a mixture of slow and fast muscle actin [lane 2], and fast muscle actin [lane 3] were applied to the gel, which had been pre-run for 15min at 220V and electrophoresed (290) at the same voltage for a total of 650Vhr at room temperature. Protein containing bands were detected by staining with Coomassie Brilliant Blue R-250. This gel was run by Donna Jackman.

4.2 Polymerization of salmonid isoactins.

One of the characteristic features of G-actin is its ability to undergo salt induced polymerization into a filamentous form, F-actin. ATP hydrolysis accompanies ATP-actin polymerization but takes place on the polymer as a first order reaction (341-343). Nucleation of filament formation is thought to occur by the slow association of two monomers followed by stabilization of the complex with the fast addition of a third monomer (109,344). The filament then elongates from this complex. The rate of actin polymerization is known to be determined primarily by the nucleation rate. Actin nucleation rates are strikingly dependent on the ionic strength of the solvent while the elongation and dissociation reactions show only moderate sensitivity to ionic strength (103).

Actin polymerization was investigated in different ways. The steady state extent of polymerization was assessed by a sedimentation assay. As described in Materials and Methods [section 2.6.7], polymerization of Mg-G-actin was initiated by addition of KCl and $MgCl_2$ to a final concentration of 0.05M and 2mM respectively, at room temperature and in the presence of ATP. Aliquots of the reaction mixture were removed at set times, centrifuged in an Airfuge at room temperature [167,000 x g, 30min] and the supernatant fraction was analyzed by SDS-PAGE. As shown in Fig.4.4, more slow actin than fast actin remains in the supernatant at all time points following initiation. This result may be due to a slower rate of nucleation, or a reduced elongation rate. Either scenario would produce a larger pool of non-sedimentable protein.

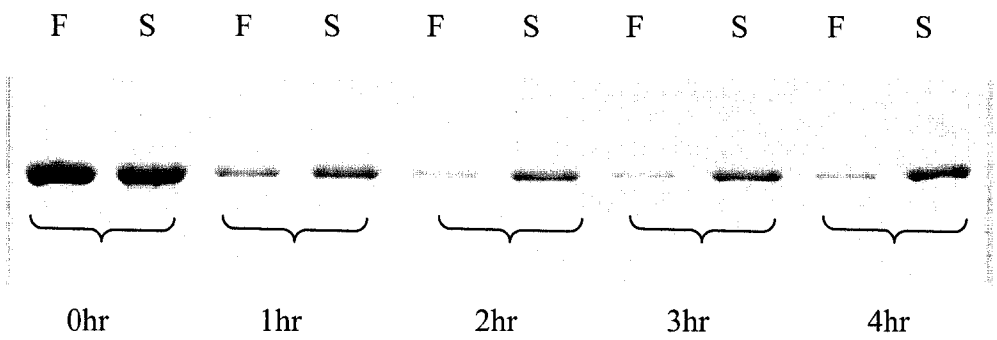

Fig.4.4 Time course of salmonid isoactin polymerization.

F- salmon fast actin; S-salmon slow actin

G-actin [Ca^{+2}] samples [~1.0mg/ml] were converted into the Mg^{+2} form in the presence of 0.1mM $MgCl_2$ and 0.2mM EGTA. Polymerization was initiated by increasing the ionic strength. At selected time intervals [0, 1, 2, 3 and 4hr], aliquots [100µl] were Airfuged and 20µl of the resulting supernatant was subjected to SDS-PAGE analysis [see section 2.6.7 in Materials and Methods].

Alternatively, it can not be ruled out that a portion of the slow actin is denatured, even though freshly prepared protein was used. A number of batches of protein [n=5] were analyzed and a significant amount of non-sedimentable slow actin was consistently detected. Also apparent from the stained gel, is the fact that there is a slight increase in the amount of actin [slow] in the supernatant after three hours.

Light scattering was used to examine actin polymerization in the pre-steady state phase. Subunit association was initiated as above and then, following a set period of 30s, samples were loaded into a pre-positioned cuvette and the scattering at 320nm was monitored. The increase in signal as a function of time for a protein concentration of 15μM is presented in Fig.4.5. Under these conditions the two isoactins yield clearly different progress curves. In the case of fast actin, more than 75% of the light scattering increase occurred before the first measurement can be taken. This was followed by an increase having an observed rate, k_{obs}, of $0.15min^{-1}$ [Fig.4.5 open symbols]. By contrast, the change in light scattering of slow actin is sufficiently time-resolved to be fit to a double exponential where k_{obs}, is $2.45min^{-1}$ and $0.5min^{-1}$ [Fig.4.5 closed symbols]. The dependence of the observed rates of these phases upon protein concentration is presented in Figs 4.6 and 4.7. Since fast actin polymerizes at a very fast rate even at low concentrations, it was not possible to conduct a complete titration. However, the available data demonstrates that salmonid fast actin polymerizes at least three times faster than salmonid slow actin. Since the increase in light scattering did not exhibit a lag [Fig.4.5], it can also be concluded that the difference between the fast and slow isoactins which was

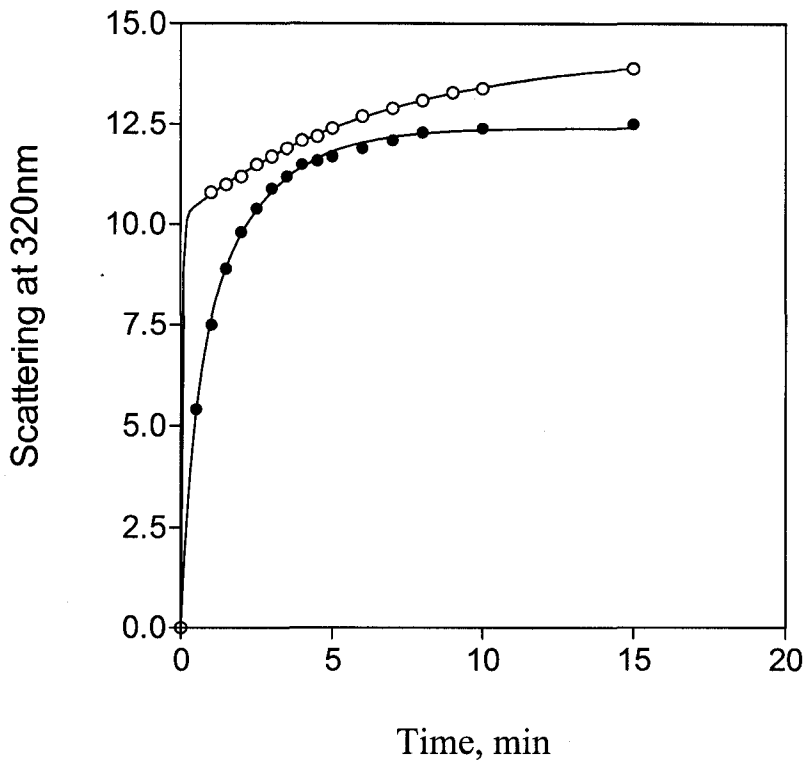

Fig.4.5 Change in light scattering at 320nm of actin solutions after induction of polymerization.

Purified Ca-G-actin [15μM], which was first converted into Mg-G-actin in the presence of 0.2mM EGTA and 0.1mM $MgCl_2$ at 4°C, was induced to polymerize at room temperature by adding KCl and $MgCl_2$ to final concentrations of 50 and 2mM, respectively. The change in light scattering, which is taken to be an index of subunit association, conforms to a biphasic process. The fast components of salmonid fast actin account for 75% [open circles] and it is 60% for salmonid slow actin [closed circles] of the total spectral change. The observed rate constants for slow actin subunit association are: $2.45min^{-1}$ and $0.5min^{-1}$. The rate of the fast phase of fast actin subunit association is not resolved by the current method, which has a dead time of 30s. The observed rate of the slow phase is $0.15min^{-1}$

Fig.4.6 Polymerization of isoactins at different concentrations as determined by light scattering.

A- salmon fast actin

B- salmon slow actin

Experimental conditions were the same as to Fig.4.5. Because of the almost instantaneous change in light scattering signal associated with polymerization of salmon fast actin, lower concentrations of protein were used compared to salmon slow actin. The graph pad PRIZM was used to fit the curves.

A

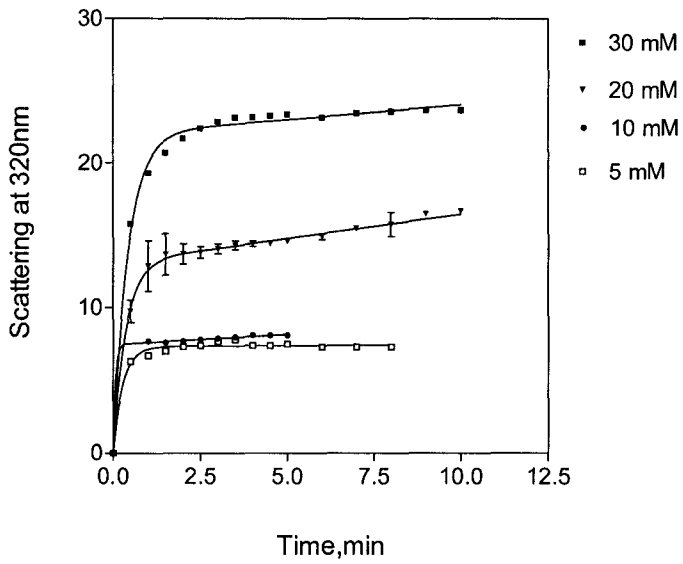
30
20
10
0
0.0
2.5
5.0
7.5
10.0
12.5
Scattering at 320nm
Time,min
30 mM
20 mM
10 mM
5 mM

B

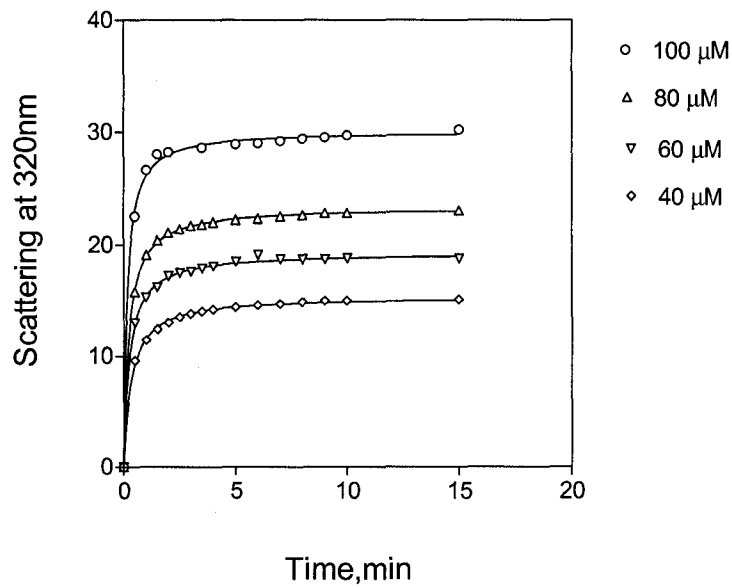
40
30
20
10
0
0
5
10
15
20
Scattering at 320nm
Time,min
100 μM
80 μM
60 μM
40 μM

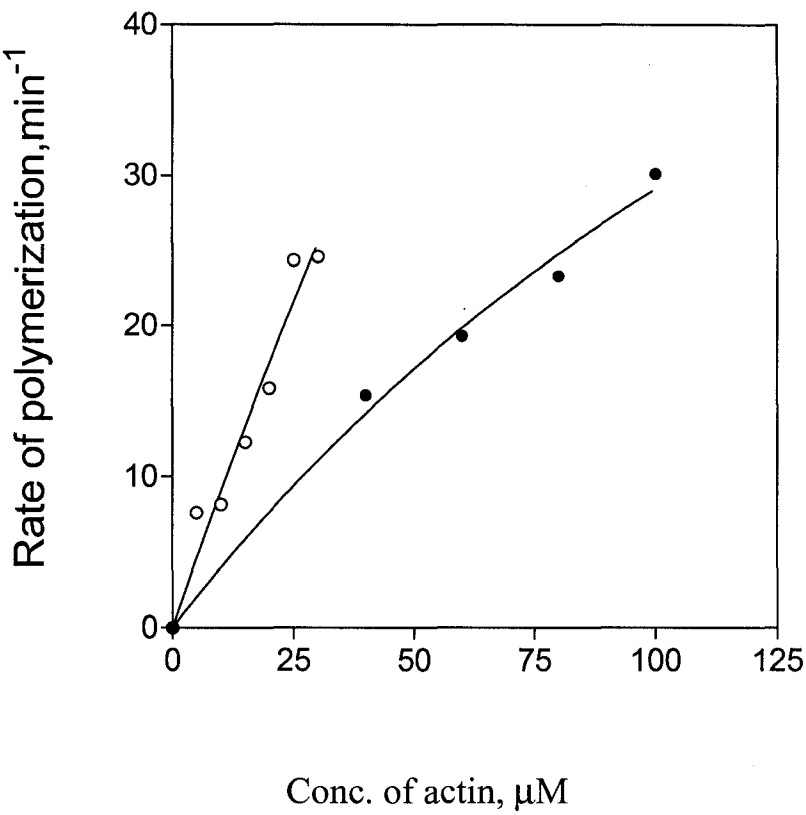

Fig.4.7 Dependence of light scattering increase with time at 320nm on actin concentration.

The fast component of the light scattering change for slow actin [closed circles] observed was fit to a hyperbolic function using PRIZM graph pad software. The data for fast actin [open circles] could not be extrapolated to plateau and is included only for comparison.

observed in the sedimentation assay [Fig.4.4] was not due to a difference in nucleation rate.

Polymerization was also investigated using an Ostwald [capillary-flow] viscometer. Freshly prepared samples of G-actin were dialyzed overnight in the cold against a high ionic strength solution in the presence of different concentrations of ATP. The next day, each solution was adjusted to a protein concentration of 24μM using the appropriate buffer and passed through the capillary at room temperature. Flow times, expressed as specific viscosity, are presented in Fig.4.8. Fast actin showed higher specific viscosity than slow actin regardless of the ATP concentration. This is most noticeable at very low concentrations of nucleotide, where the flow time of the slow actin solution is virtually the same as that of the buffer. The difference between the two isoforms is diminished by raising the ATP concentration. The observed increase in specific viscosity levels off at 0.05mM, whereupon there is 3-4 fold difference. Although, viscometry is a crude measure of filament formation, these data, which have been reported in preliminary form (345), are consistent with a difference in the steady state extent of polymerization. This is further supported by electrophoretic analysis [Fig.4.9.] of the supernatants arising from sedimentation of the various samples used in Fig.4.8.

It is of interest to identify the individual or group of substitutions in slow actin that is or are responsible for the observed functional variability. The DNase I binding loop [residues 38-52 in sub-domain 2], the hydrophobic loop [residue 262-274 in sub-domain

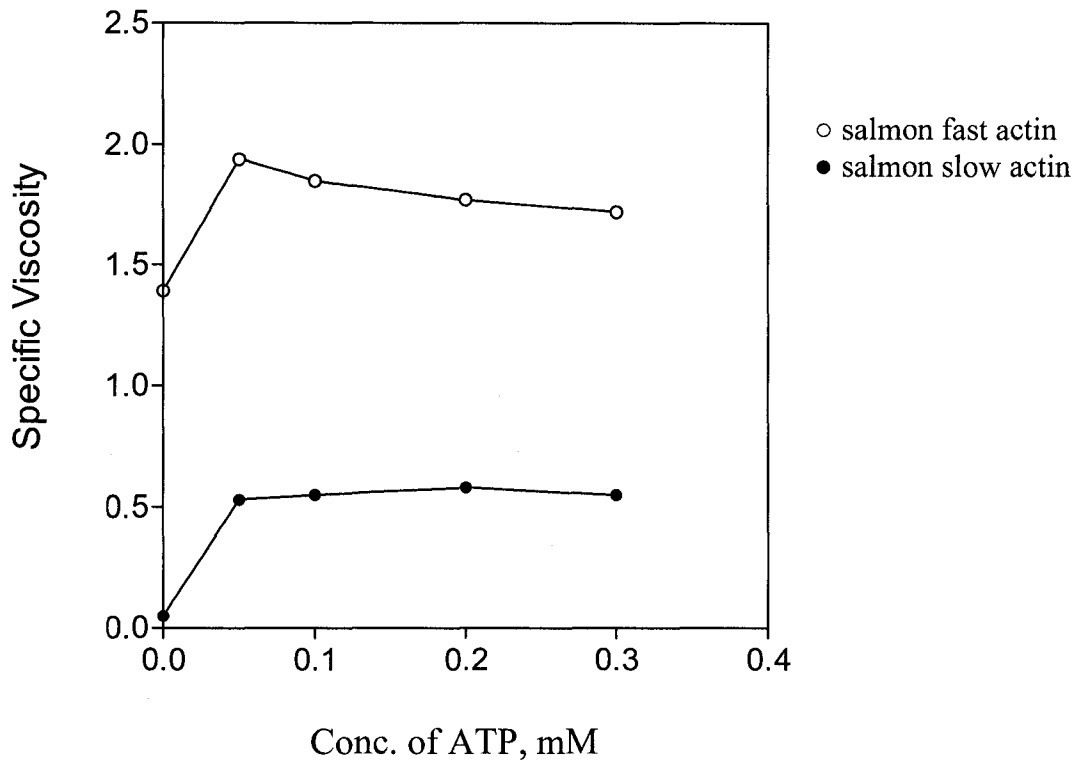

Fig.4.8 Dependence of specific viscosity of salmonid actin on ATP concentration as analyzed by viscometry.

G-actin [24μM] was polymerized in 100mM KCl, 1mM $MgCl_2$, 0.1mM $CaCl_2$, 1mM $NaHCO_3$ and 1mM NaN_3, pH 7.6 in the presence of different concentrations of ATP [0-0.3mM] as described in Materials and Methods [section 2.6.7]. Viscosity of these samples was assayed at 25°C.

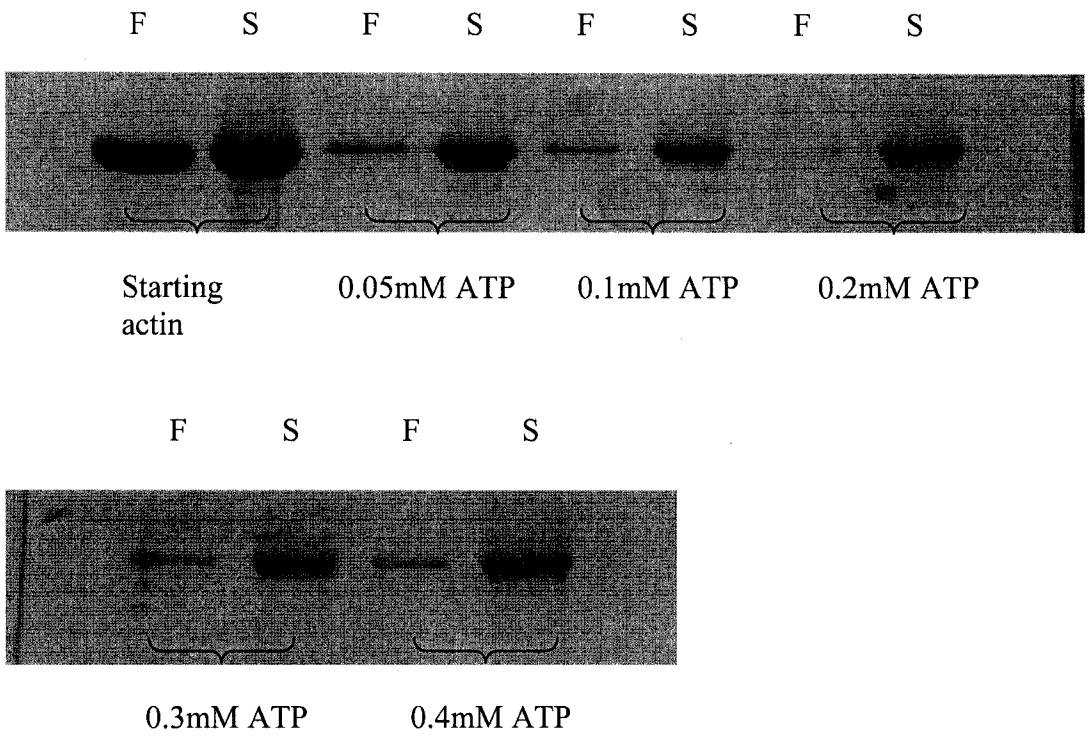

Fig.4.9 SDS-polyacrylamide gel analysis of salmonid isoactins polymerized at different concentrations of ATP.

F-salmon fast actin; S-salmon slow actin

Salmonid isoactins [24μM, 100μl], which were polymerized at various concentrations of ATP as described in Fig.4.8 were sedimented in an Airfuge and 10μl of 1:1[v/v] diluted supernatants with SDS-sample buffer were loaded on to the gels. Staining and destaining of gels were carried out as described in Materials and Methods [section 2.2.0]. There was a loading error in the sample of salmon fast actin polymerized in the presence of 0.2mM ATP.

4], and the C-terminus region [in sub-domain 1] are among the structural elements of monomeric actin proposed to form the inter-monomer interface in F-actin. In the atomic model of F-actin, amino acids 40-45 of one monomer interact with residues 166-169 of the neighbouring subunit and with the hydrophobic loop of the subunit from the opposite strand. In addition, common contact areas for monomer/monomer interactions mapped by x-ray diffraction studies (119,134) include a loop at positions 61-65 in sub-domain 2 and segment 202-204 on the top of sub-domain 4 of the monomer.

In order to assess the binding affinity of G-actin with DNase I, actin [2μg] was incubated with varying amounts of DNase I [1μg-6μg] and analyzed by electrophoresis as described in section 2.6.6 under Materials and Methods [Fig.4.10]. No difference was observed in banding intensities of DNase I bound G-isoactins. Since there are no amino acid substitutions in the DNase I binding loop of salmonid isoactins, it can be suggested that amino acid substitutions close to the DNase I binding loop have no effect on DNase I binding.

4.3 Thermal unfolding of salmonid isoactins

Circular dichroism was used to determine the conformational stability of salmonid isoactins [G-actin-Ca in ATP form] by monitoring their ellipticity at 222nm as a function of temperature. Figure 4.11 shows that approximately 27% of the secondary structure of salmon fast actin was lost after thermal unfolding. Similar results were obtained for

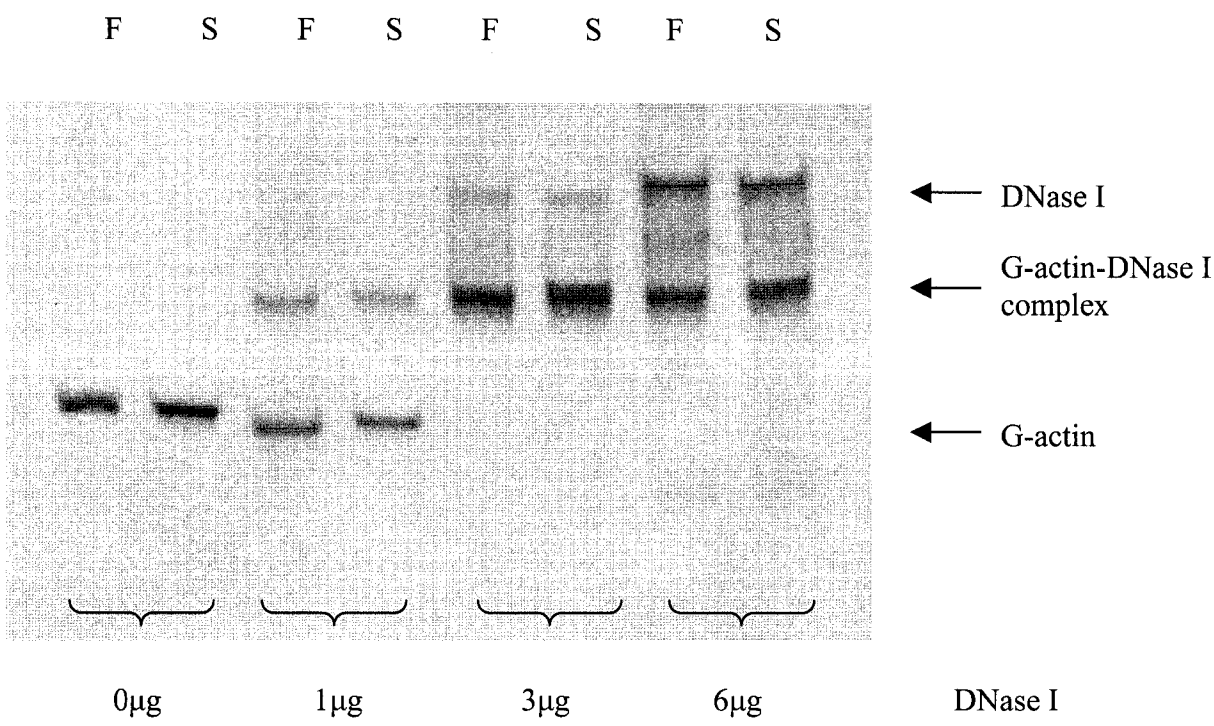

Fig.4.10 DNase I binding affinity of salmonid isoactins as determined by non-denaturing polyacrylamide gel analysis.

F-salmon fast actin; S-salmon slow actin.

To a fixed concentration of salmonid G-actin [2μg] various amounts of DNase I, which was dissolved in 2mM Tris-HCl, pH 8.0, were added. After incubating at 4°C for 30min, samples [5μl] were loaded onto a nondenaturing polyacrylamide gel. Electrophoresis was carried out as per Materials and Methods [section 2.6.6]. Note the similar banding intensities of DNase I complex with salmon fast and slow-G-actins.

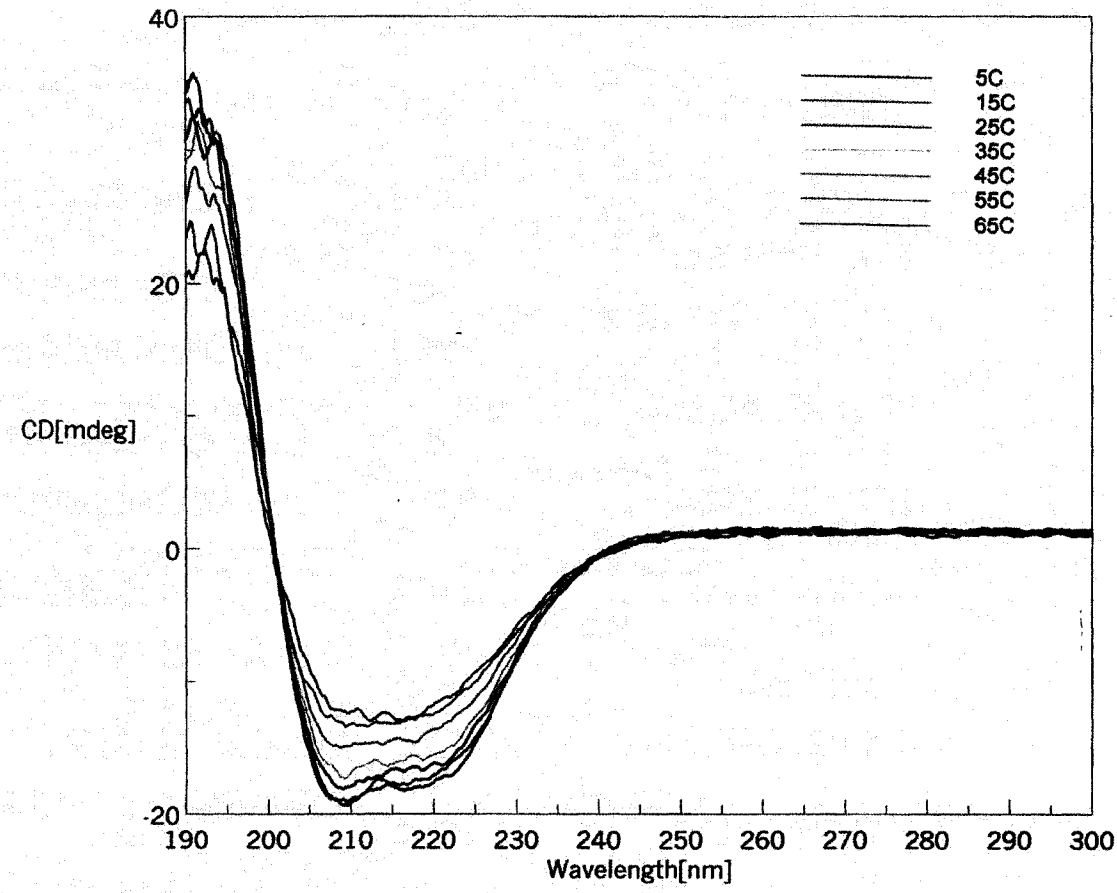

Fig.4.11 Far-UV circular dichroism spectra of salmon fast G-actin at different temperatures.

Circular dichroism UV spectra [190-350nm] of salmon fast actin [~1.5mg/ml], which has been dialyzed against 5mM Hepes, 0.2mM $CaCl_2$, 0.2mM ATP, 0.01%[w/v] NaN_3 and 2mM DTT, pH 8.0 at 4°C, were recorded at 5 to 65°C temperature range at a rate of 30°C/hr. The scan speed was 100nm/min.

Light path, 0.1mm.

salmon slow actin [Fig.4.12], rabbit fast actin and mako shark fast actin as well [data not shown]. The change in relative ellipticity at 222nm as a function of temperature showed that the transition temperature [Tm] for unfolding of slow and fast salmon isoactins are 45 and 55°C [Fig.4.13], respectively, when heated at a rate of 30°C/hr, indicating that slow actin is the least conformationally stable of the two. Similar results were observed when the experiment was carried out at a heating rate of 60°C/hr. Interestingly, when thermal unfolding was monitored at 293nm the Tms of fast and slow salmonid muscle actins are 58°C and 48.6°C, similar to the values obtained from main-chain unfolding [Fig. 4.14]

Since salmonid isoactins showed a significant difference in conformational stability, it was of interest to study the rates of thermal-induced unfolding of these isoactins. Towards this end samples were incubated on ice in a 0.1mm light path cell prior to being subjected to a temperature of 65°C. Ellipticity at 222nm was then recorded as a function of time and data were analyzed using PRIZM graph pad. As shown in Fig.4.15 the rate of unfolding of slow actin is much faster than fast actin, again suggesting that slow actin is less conformationally stable. Similar studies involving ADP-G-actin were hampered due to the instability of slow G-actin in ADP form [data not shown].

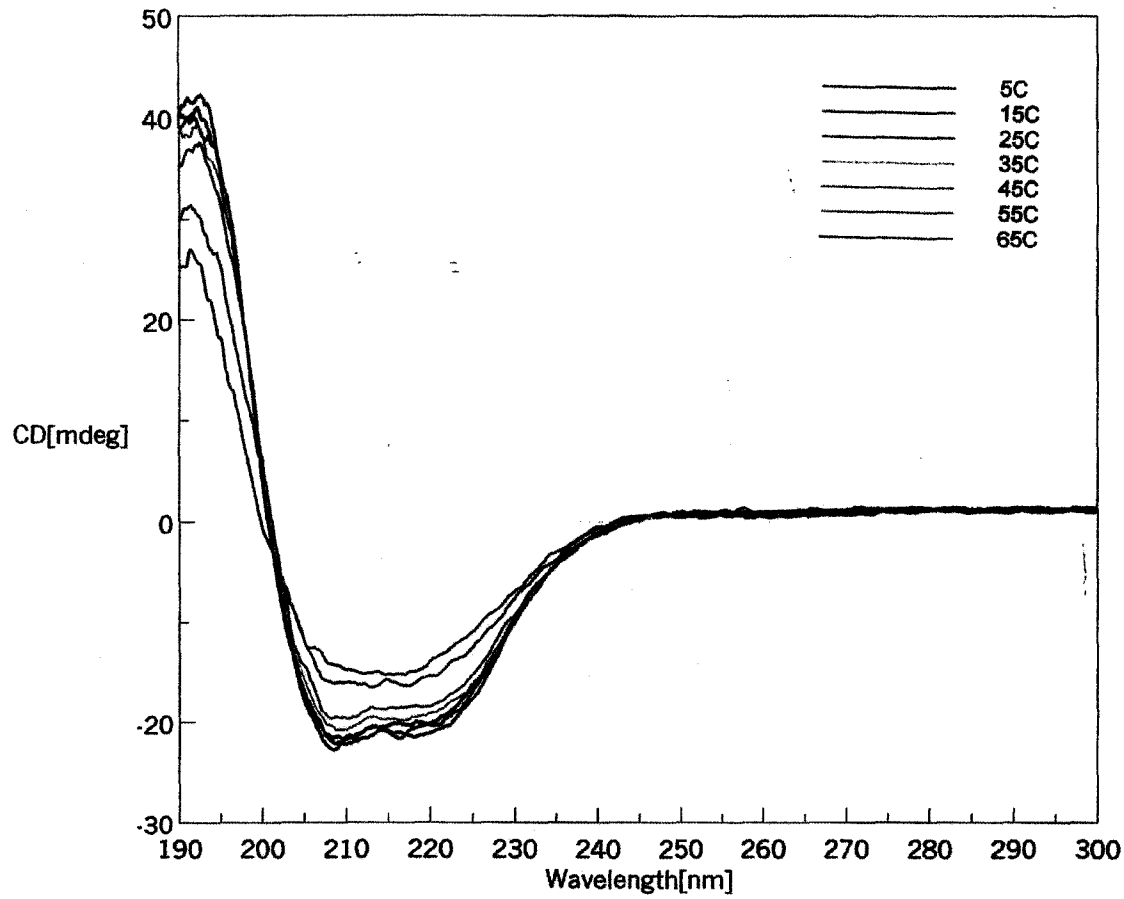

Fig.4.12 Far-UV circular dichroism spectra of salmon slow G-actin at different temperatures.

Circular dichroism UV spectra of salmon slow actin [~1.5mg/ml] were recorded. The experimental conditions were the same as in Fig.4.11.

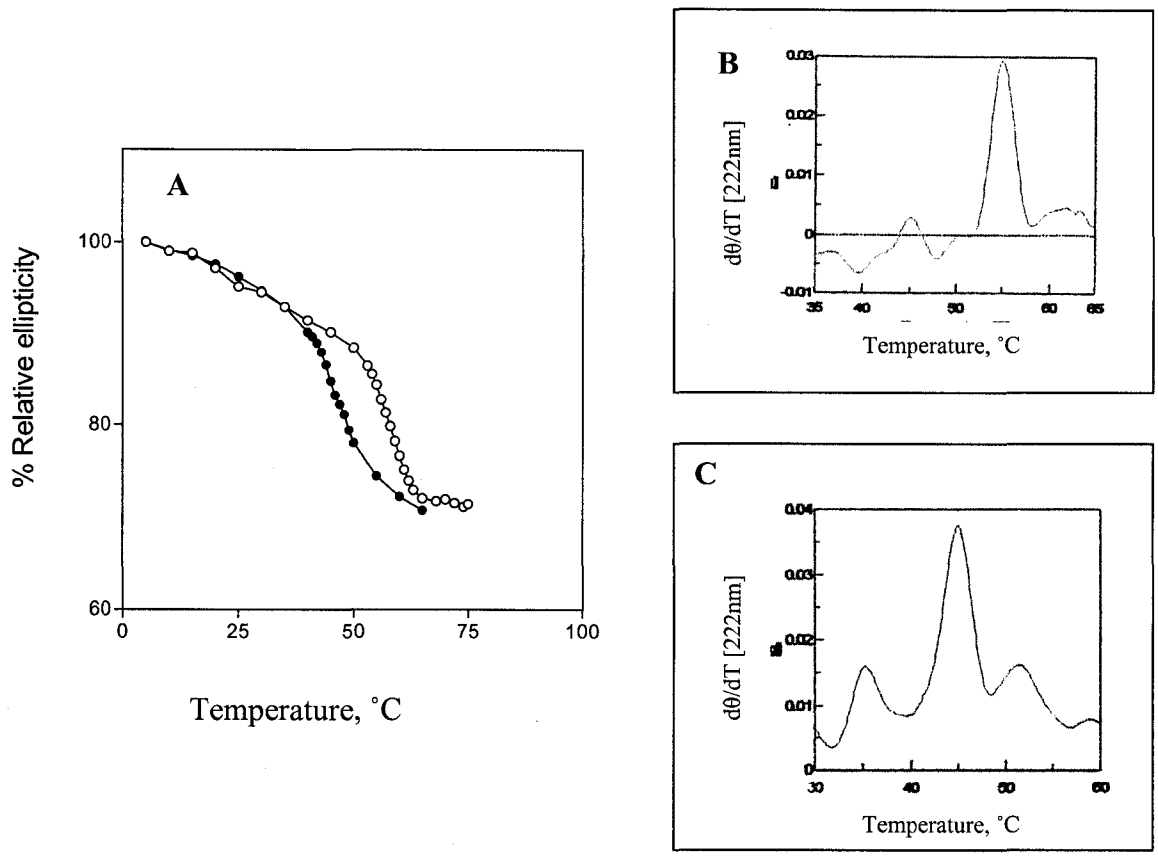

Fig.4.13 The thermal unfolding of salmonid isoactins.

Figure, A: The relative ellipticity of salmon fast [open circles] and slow actin [closed circles] at 222nm is plotted as a function of temperature;

Figure, B and C: The first derivative of the change in ellipticity at 222nm [dθ/dT [222nm] of fast and slow muscle actin, respectively.

Tms are: fast actin; 55°C; slow actin, 45°C. [n=5]. At 5°C, starting ellipticity of fast actin, -29.867mdeg; slow actin, -19.156mdeg. The first derivative of the change in ellipticity was calculated according to the instrument software.

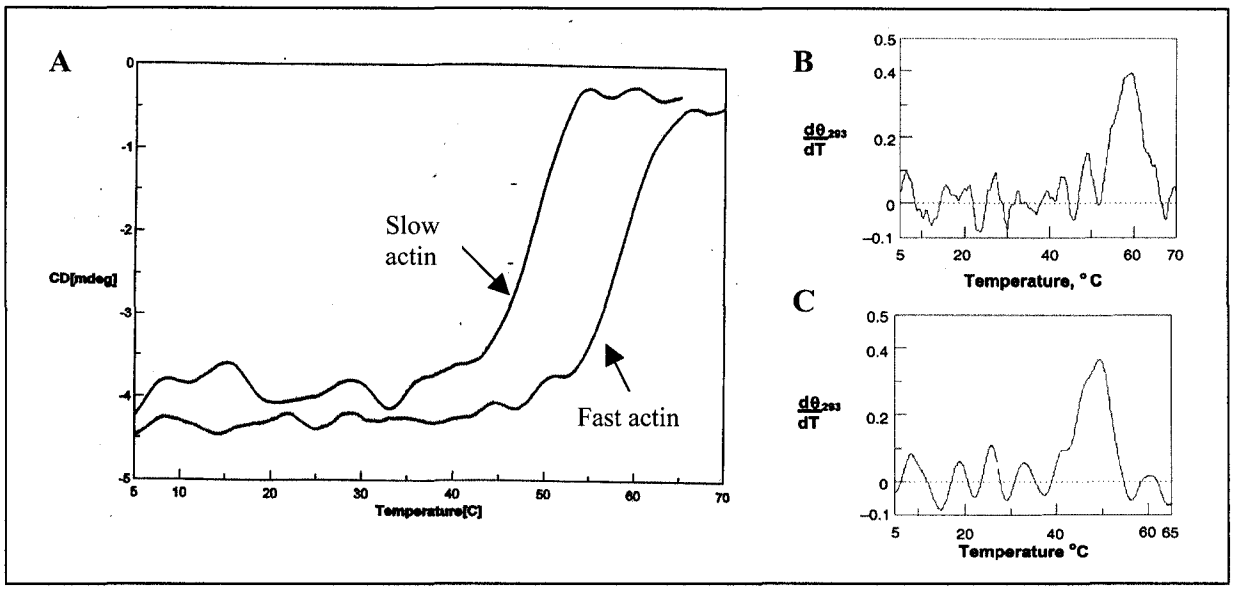

Fig.4.14 Near-UV circular dichroism progress curve of the first differential of salmonid isoactins.

Figure A: The change in ellipticity [at 293nm] of slow and fast muscle salmon actin [3.4mg/ml], was recorded as a function of temperature. Path length of the cell is 5.0mm.

Figures B and C: The first derivative of the change in ellipticity at 293nm of fast and slow muscle actin, respectively.

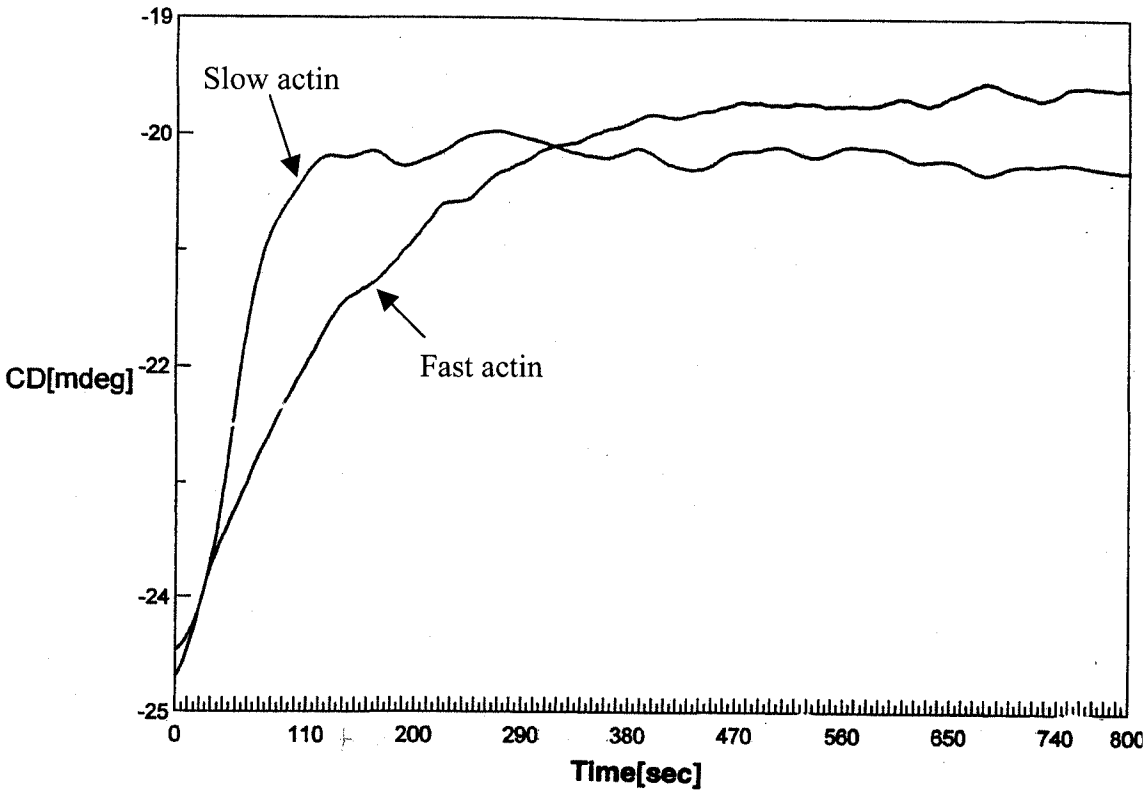

Fig.4.15 Time dependent unfolding of salmonid isoactins following a temperature jump.

The change in ellipticity [at 222nm] of salmonid isoactins [concentration, 1mg/ml], was recorded as a function of time following a temperature jump from 0 to 65°C. Path length of the cell was 0.1mm. Prior to the temperature jump, samples were incubated on ice. This experiment was repeated changing the concentration of actin from 1 to 4mg/ml. No concentration dependence on the rates of unfolding was observed. The time taken to reach maximum ellipticity at 222nm of slow and fast muscle actins was 55 and 105s respectively.

Actin contains four Trp residues that are the primary fluorophores in the molecule. All of them are located in sub-domain 1 (119). According to the resolved rabbit G-actin-DNase I structure (119), Trp79, Trp86 and Trp340 are located in α-helices; Trp79-Asn92 and Ser338-Ser348, whereas Trp356 is located in the loop between α-helices Ser350-Met355 and Lys359-Ala365. Of these Trp residues, Trp79 is the only one that can be regarded as being exposed to the solvent.

The intrinsic fluorescence spectra of salmonid isoactins [14μM] were recorded at 25°C in order to study the effects of substituted amino acids on protein conformation. As shown in Fig.4.16 the emission spectrum of slow actin is equivalent to that of fast actin with λ_{max} at 330nm, indicating that the immediate environment around the fluorophore is similar in the different isoactins. The intrinsic fluorescence spectra [Fig.4.16] of native and thermally unfolded salmonid isoactins are also equivalent, indicating that the conformation of sub-domain 1 is similar. Unfolding of both isoactins resulted in a red shift of the emission maximum from 330nm to 336nm. However, this result is not in good agreement with near-UV circular dichroism spectra of these isoactins [Fig.4.17]. Since the signal in this region of the UV is also dominated by Trp, the observed spectral difference suggests that one or more of these groups occupy a different environment in slow actin compared to fast actin. Unfortunately, it is difficult to explain these conflicting results.

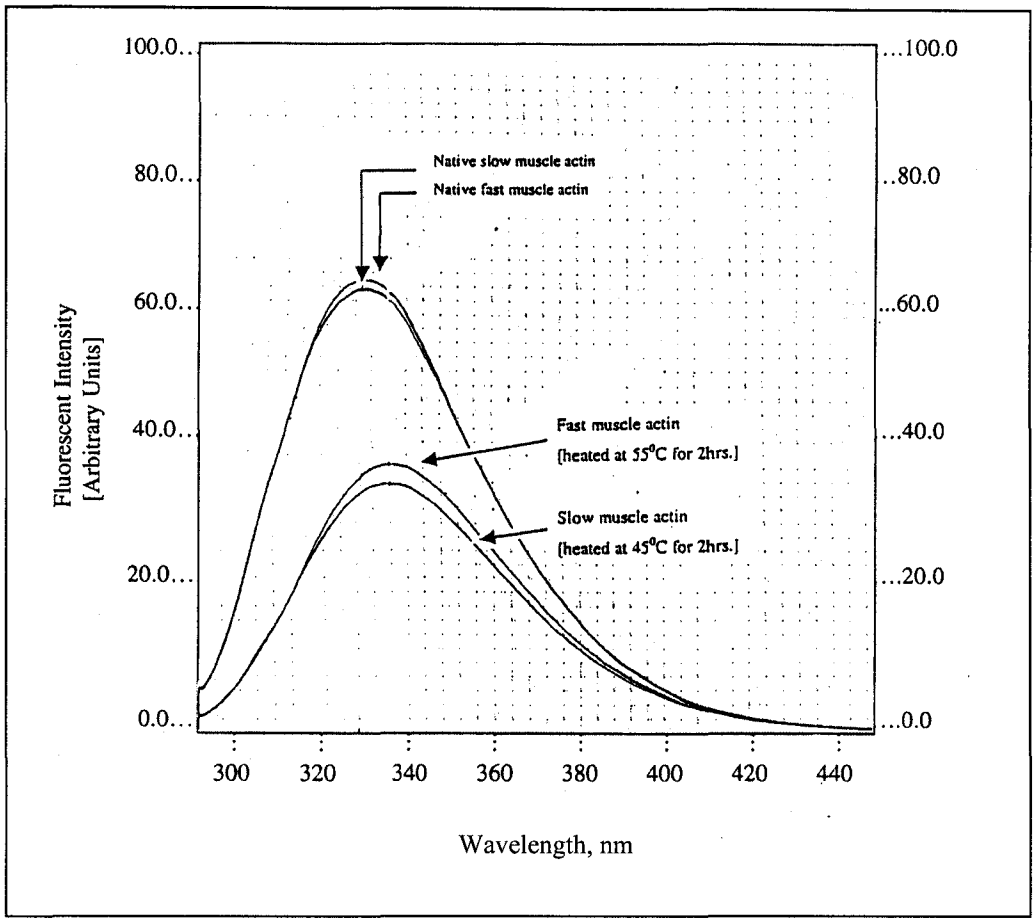

Fig.4.16 The fluorescence emission spectra of thermally unfolded salmonid isoactins.

Actin [0.9mg/ml], which was incubated for 2hrs at either 45°C [slow actin] or 55°C [fast actin] in 5mM Hepes, 0.2mM $CaCl_2$, 0.2mM ATP, 0.01%[w/v] NaN_3 and 2mM DTT, pH 8.0, was excited at 270nm [at 25°C] and the emission was recorded. Both actin isoforms have red shifted to the same extent. The λ_{max} values of native and unfolded salmonid isoactins were 330nm and 336nm, respectively.

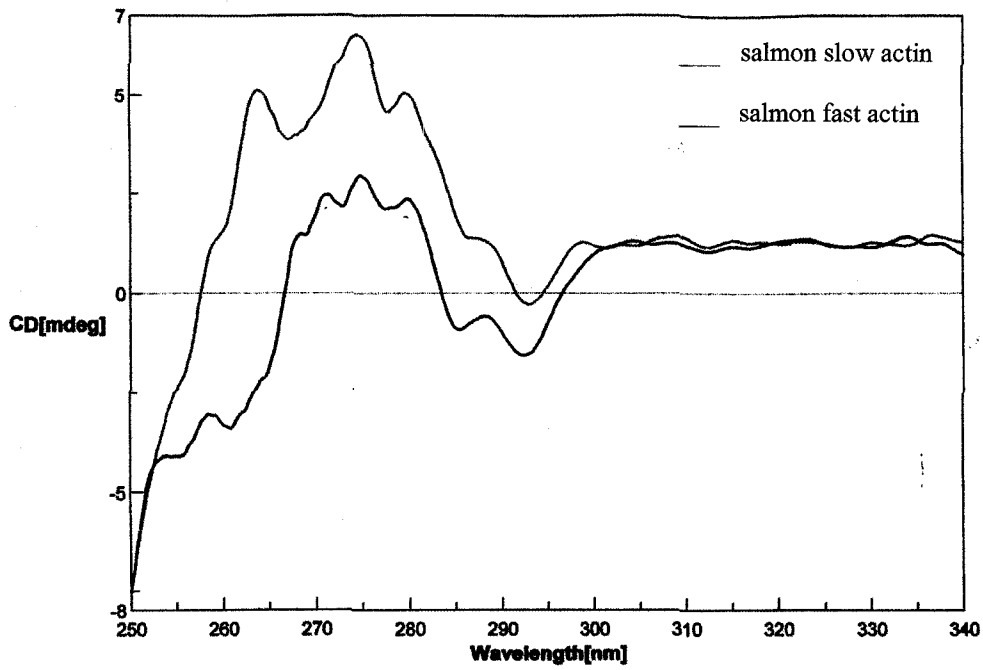

Fig.4.17 Near-UV circular dichroism spectra of salmonid isoactins.

Circular dichroism UV spectra [250-340nm] of salmonid iso-actins [1.2mg/ml], were recorded at a speed of 100nm/min. The temperature was maintained at 5°C and the path length of the cell was 5.0mm. The concentration of actins is 3.74mg/ml.

4.4 Chemical unfolding of salmonid isoactins

In order to study chemical sensitivity of salmonid isoactins, urea and GdnHCl-induced unfolding was carried out. The concentration of actin was maintained ~1mg/ml and in the presence of various concentrations of GdnHCl, the ellipticity at 222nm of far-UV circular dichroism spectra was recorded at 25°C. It can be seen in Fig.4.18 that the dependence of ellipticity at 222nm versus GdnHCl concentration represents two distinct cooperative transitions, reflecting the fact that the GdnHCl induced unfolding of G-actin is a two-step process. The first transition, which is similar in both isoactins, occurred at ~ 1.0M of GdnHCl. However, the second transition of slow actin starts at ~ 1.8M GdnHCl while it is 2.2M in the case of fast actin. With slow actin, the transition from native to inactivated actin [see discussion] takes place at low GdnHCl concentrations [0.0-1.0M], whereas the transformation of the inactivated actin into completely unfolded protein occurs between 1.8 and 4.0M GdnHCl concentrations. Salmon slow actin has a short range of inactivated form [1.0-1.8M] while the range is slightly higher for salmon fast actin [1.0-2.2M], indicating that slow actin is more sensitive to chemical unfolding than fast actin. Aiming to obtain more information about the change in conformation, which is induced by addition of GdnHCl, intrinsic fluorescence spectra of isoactins [0.1mg/ml] were recorded at various GdnHCl concentrations. As shown in Fig.4.19 the emission maximum of both fast and slow actins have red shifted to the same extent, *i.e* from 330nm to 345nm in the presence of 2M GdnHCl and to 350nm at 4M GdnHCl. Therefore it appears that although sub-domain 1 varies in stability depending on the isoform in question, the environments of the aromatic side chains are largely similar.

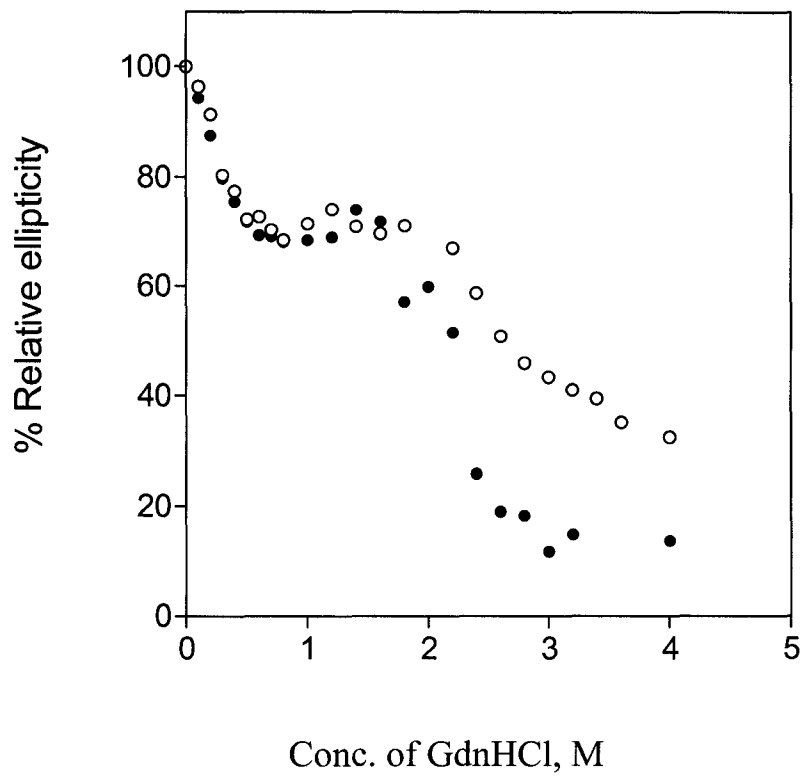

Fig.4.18 The chemical unfolding of salmonid isoactins as determined by Far-UV circular dichroism in the presence of varying concentrations of GdnHCl.

The changing ellipticity at 222nm of salmonid G-actin [1mg/ml] in the presence of varying concentrations of GdnHCl was recorded. The difference in incubation period of every sample in the presence of GdnHCl is minimal. Note the % relative ellipticity of both fast [open circles] and slow actin [closed circles] is similar in the range of 0-1.8M GdnHCl and rapidly decreases at higher concentrations of denaturant in the case of slow actin. The ellipticity at 0.0M GdnHCl of fast and slow muscle actins are –12.30 and –9.37mdeg, respectively.

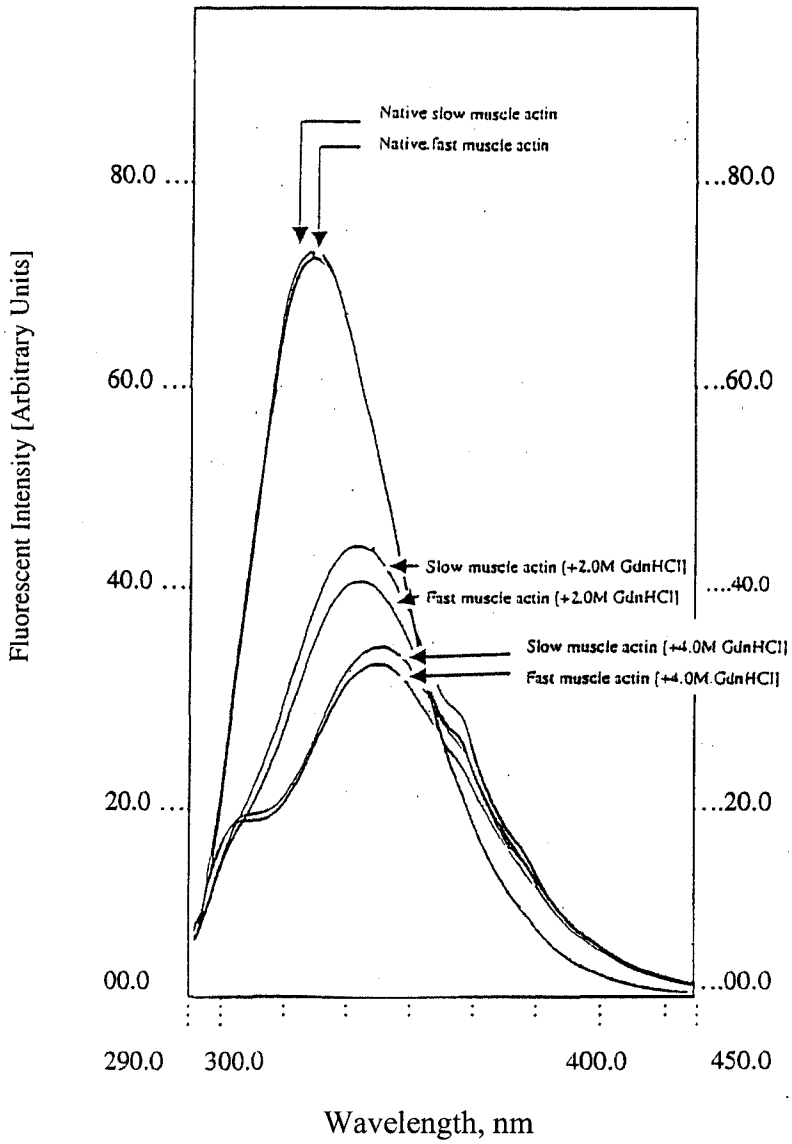

Fig.4.19 Intrinsic fluorescence spectra of unfolded salmonid isoactins in the presence of various concentrations of GdnHCl.

Tryptophan emission [330nm] of salmonid G-actin isoforms, which were reacted with 0, 2, and 4M GdnHCl were recorded at 25°C. The buffering condition: 2mM Tris-HCl, 0.2mM $CaCl_2$, 0.2mM ATP and 0.1mM DTT, pH 8.0.

Slow muscle actin also exhibits low resistance to urea-induced unfolding [Fig.4.20]. The midpoints of the change in relative ellipticity at 222nm are ~3M [slow actin] and 4M [fast actin]. At the highest concentrations of urea the relative ellipticity at 222nm of these two actins is similar, stabilising at ~30%. Compared to urea, guanidine has a greater effect on the conformation of slow muscle actin. This is consistent with GdnHCl, which is positively charged at pH 8.0, being a more powerful denaturant than urea.

Further to mapping the region(s) of instability in the isoactins, the number of reactive Cys residues was determined both at room temperature and at each respective transition temperature. Muscle actin contains five Cys residues at positions 10, 217, 257, 280 and 374. The changing intensity of yellow color was recorded as a change in absorption at 412nm with time following the addition of DTNB [0.4%w/v] to the actin [1mg/ml] solution. As shown in Fig.4.21, regardless of the type of isoactin present, there was only one reactive Cys residue at room temperature and only one additional Cys residue is exposed at the respective Tm. Holmes *et al.*, (134) reported that Cys374 is the only Cys that is exposed to solvent at room temperature. Since actin is a highly conserved molecule, it can be assumed that the reactive Cys of salmonid isoactins at room temperature is Cys374 as well. To identify the second reactive Cys residue, hydroxylamine, NH_2OH, cleavage reactions were carried out using actin in which Cys374 was blocked with ^{14}C-labelled iodoacetic acid. NH_2OH has a highly specific cleavage site between Asn-Gly. Specificity of this reagent was first tested on rabbit skeletal TM which lacks this sequence.

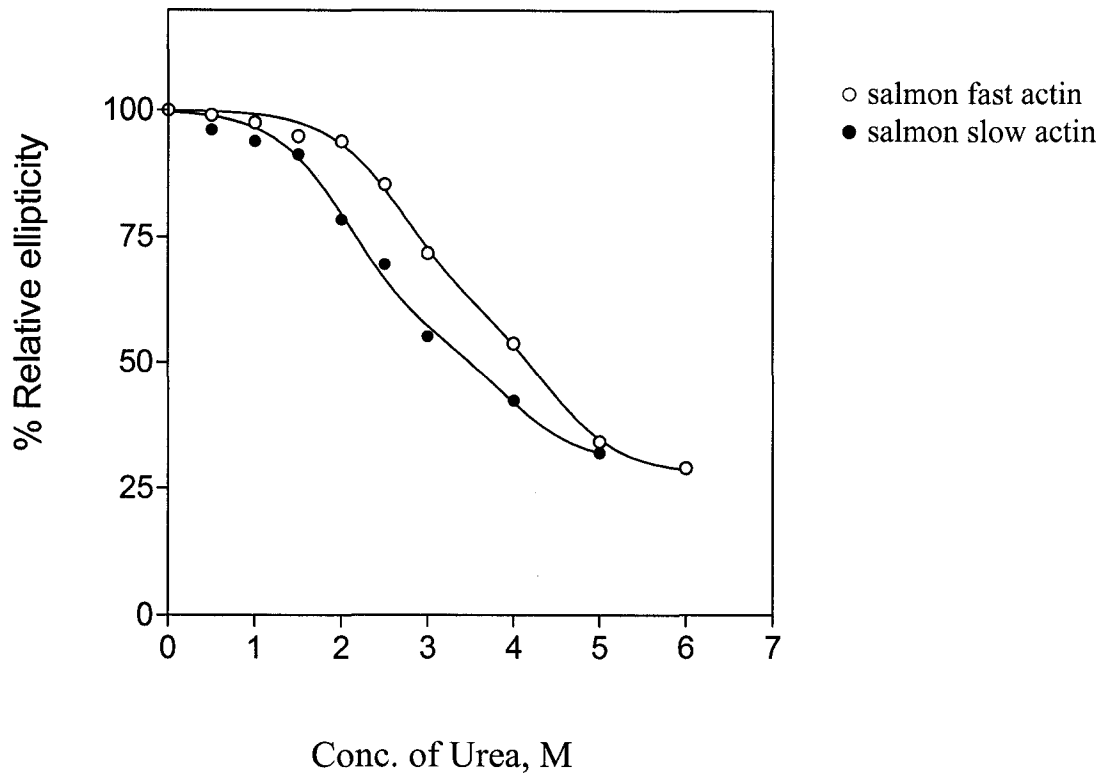

Fig.4.20 Far-UV circular dichroism analysis of salmonid isoactins unfolding in the presence of urea.

The ellipticity at 222nm of unfolded salmonid monomeric isoactins [0.5mg/ml], which has been dialyzed against 2mM Tris-HCl, 0.2mM $CaCl_2$, 0.2mM ATP and 0.1mM DTT, pH 8.0, was recorded at 25°C. Urea concentration varied from 0 to 6M and samples were incubated in urea for 30min. Using the ellipticity at 0M urea as 100%, %molar ellipticity was calculated for every concentration. For fast actin the ellipticity at 0M urea is -11.7mdeg while it is –12.5mdeg for slow actin.

Fig.4.21 The sulphydryl reactivity of salmonid isoactins with DTNB as a function of time.

Salmonid G-actin isoforms [1mg/ml], which were pretreated with 2mM DTT in 20mM Tris-HCl, 0.2mM $CaCl_2$ and 0.2mM ATP, pH 7.5, were reacted with 0.4mM DTNB at either 25, 45 or 55°C and the color development was recorded at 412nm as a function of time. The concentrations of isoactins were confirmed electrophoretically. For 1mg/ml protein, an absorbance change of 0.33 is equivalent to one reactive Cys [ε_{412} of DTNB, 14,000 $M^{-1}cm^{-1}$].

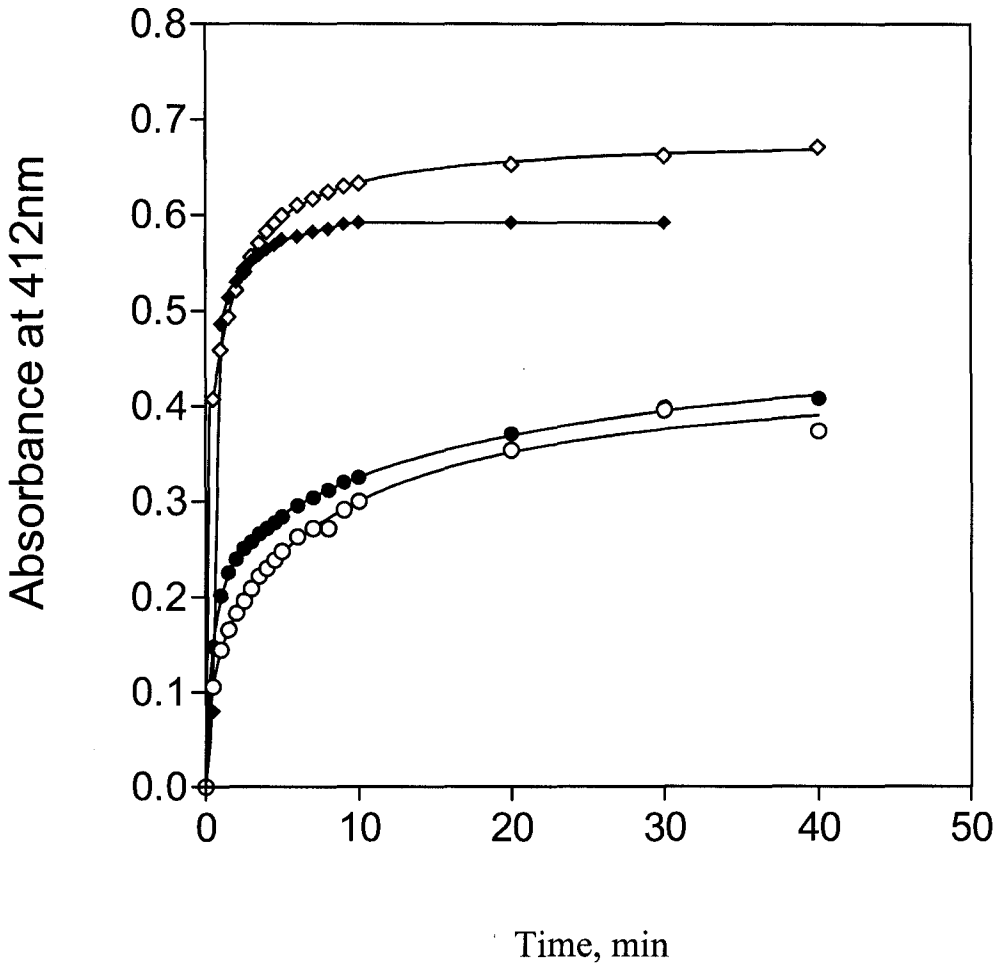

○ salmon fast actin reacted with DTNB at 25°C

● salmon slow actin reacted with DTNB at 25°C

◊ salmon fast actin reacted with DTNB at 55°C

♦ salmon slow actin reacted with DTNB at 45°C

No cleavage was observed [data not shown]. The sequence Asn-Gly can be found only in slow actin at positions 11-12 and 280-281 in the molecule. Due to partial cleavage, the reaction resulted in five fragments along with intact actin [Fig.4.22 [A].-Actin fragments 1-280, and 12-280 were labelled with ^{14}C but not the C-terminal fragment [Fig.4.22 [B]]. It was confirmed by sequencing that the C-terminal fragment contains both Cys285 and Cys374. Therefore, Cys10, which is located in sub-domain 1, or Cys217, or Cys257 could be the second reactive Cys residue, which is exposed to solvent upon thermal induced unfolding of the actin molecule. This is consistent with Konno and Morales (346) who reported that upon removal of Ca^{+2}, Cys10 is exposed first followed by Cys257. However, efforts to pinpoint the second reactive Cys by mass spectrometric analysis of tryptic, CNBr and subtilisin peptides [data not shown] were unsuccessful. Part of the difficulty was the complexity of the spectra which consisted of numerous unidentified components. If sub-domain 1 is the least-stable region of actin it is reasonable to suggest that the second reactive sulfhydryl is Cys10.

4.5 Nucleotide binding of actin

The nucleotide/cation complex has been shown by crystallographic studies, to be bound at the bottom of the cleft between the major domains of actin with the adenosine base located in a hydrophobic pocket formed between sub-domain 3 and 4. The triphosphate tail is bound tightly by two invariant β-hairpin loops, Asn12-Cys17 and Asp154-His161, protruding into the inter-domain cleft from sub-domain 1 and 3, respectively.

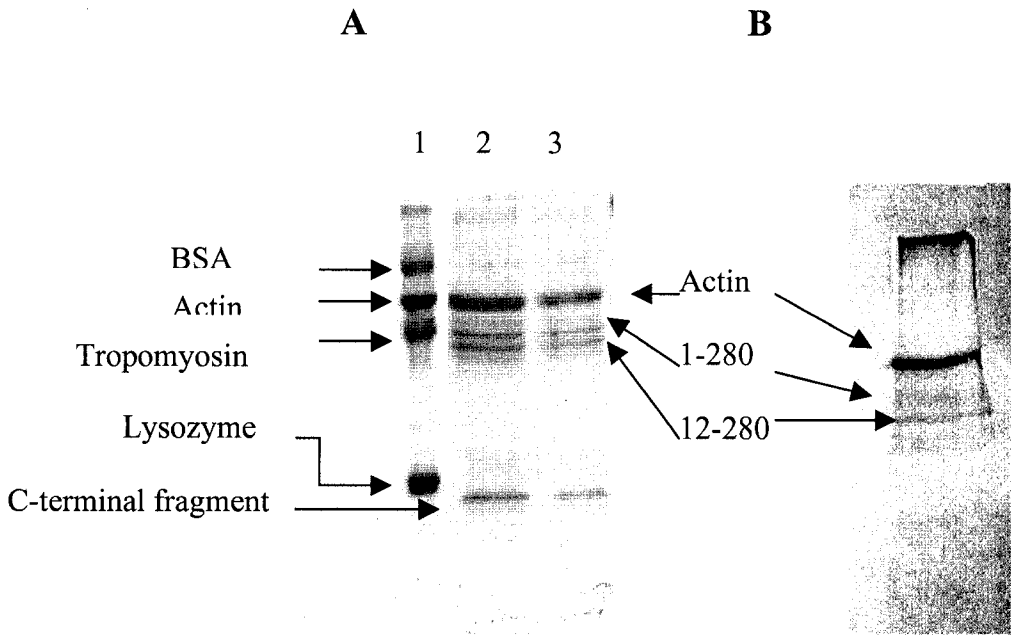

Fig.4.22 Electrophoresis and autoradiogram of hydroxylamine-treated, ^{14}C-labelled slow actin.

Figure A: SDS-polyacrylamide gel analysis of unlabelled, C-terminus blocked salmon slow G-actin [1mg/ml], which had been reacted with 0.2M NH_2OH in the presence of 4M urea for 2hrs. Lane 1, molecular weight marker; lanes 2 and 3, reacted salmon slow actin. Gel was electrophoresed as described in Materials and Methods [section 2.2.0].

Figure B: Autoradiogram of NH_2OH reacted salmon slow actin, that had been labelled with ^{14}C-iodo acetamide [2.5μCi/ml] overnight at 45°C before reacting with 0.2M NH_2OH in the presence of 4M urea.

In the 'opened' state the interactions between nucleotide and the loop in sub-domain 3 are somewhat weaker compared to the 'closed' state (347 and 348). Both loops are linked with sub-domain 2 and 4 by side chain interactions of Ser14 with Gly74, and Asp157 with Arg183, respectively. These amino acids, which interact with β- and γ- phosphate groups of the nucleotide, are highly conserved. In salmon slow actin there is a rare Ser155Ala substitution which can also be found in some other fish species *eg.* Gold fish [*Carassius auratus*], Thilapia [*Oreochromis mossambicus*], and Japanese puffer fish [*Takifugu rubripes*]. Because this replacement occurs in the vicinity of the nucleotide-binding site, it was of particular interest to determine whether there is a change in interaction with the nucleotide. To study this, bound nucleotide was first displaced with a fluorescent analogue of ATP [mant-ATP] as described in Materials and Methods [section 2.5.3]. To ensure that all of the fluorophore was bound, the concentration of actin was in 14-fold molar excess compared to the fluorescent analogue [14:1μM]. A spectral analysis of these fluorescent probe bound salmonid isoactins was then carried out. It is apparent that slow actin is blue shifted by about 8nm with respect to fast actin, indicative of non-identity in the nucleotide-binding cleft [Fig.4.23]. In order to further investigate the consequences of the Ser155Ala substitution on nucleotide affinity, bound ATP was first displaced with 10-fold excess of etheno-ATP in the absence of free ATP. Then, a time course of decreasing fluorescence intensity was determined by mixing the etheno-ATP-actin with excess ATP. At 0.56mM ATP, the rate of displacement, which is fit as a single exponential, was ~$0.02s^{-1}$ [fast actin] and $0.038s^{-1}$ [slow actin] [Fig.4.24].

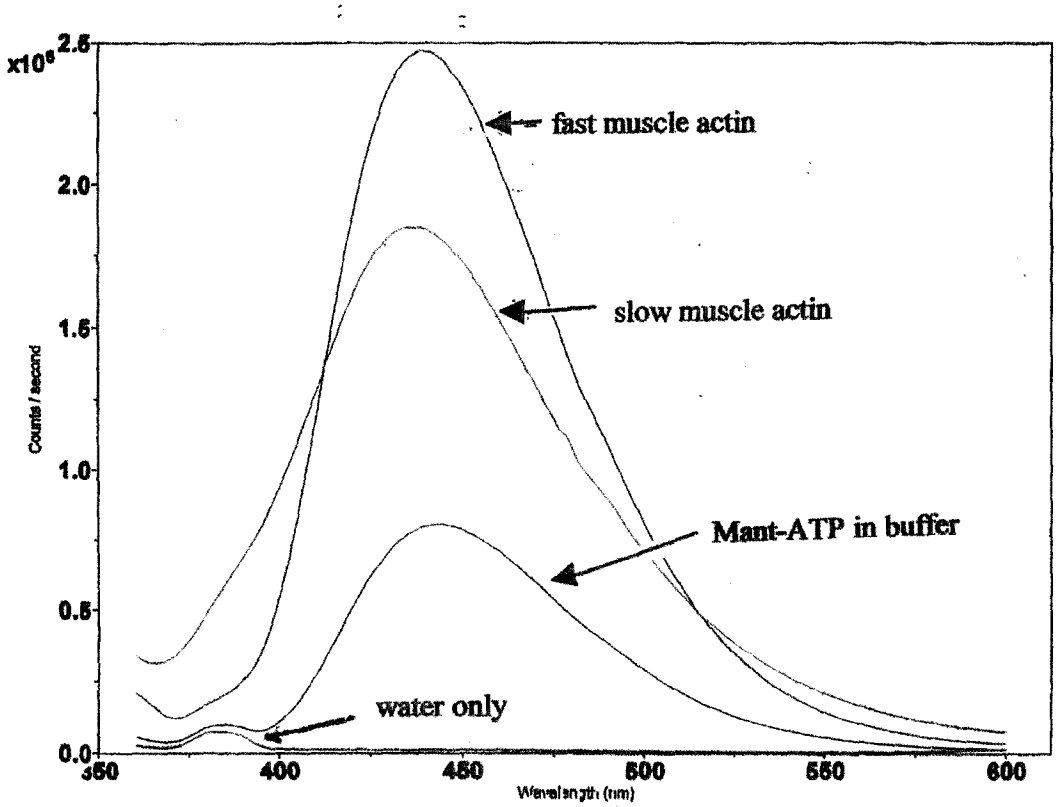

Fig.4.23 Extrinsic fluorescent spectra of salmonid mant-ATP-G-actin isoforms.

The emission spectra of salmonid mant-ATP-G-actins, which were prepared as explained in Materials and Methods [section 2.5.3], were recorded. Prior to analysis, the concentrations of isoactins were confirmed by UV-visible absorption. Mant-ATP was excited at 340nm and emission was measured at 440nm. Visible spectra were recorded on all samples before and after excited state measurements to ensure that the samples did not photodegrade.

The dependence of the observed rate on ATP concentration is presented in Fig.4.25. The results for the slow actin isoform can be fit to a hyperbola having a maximum observed rate of $0.093s^{-1}$ [K_d, 3.5mM]. In the case of fast actin, the conditions are far-removed from saturation and the observed rate shows a near-linear dependence on the ATP concentration. However, at sub-saturating ATP concentrations, approximately three times as much ATP is needed to produce the same rate of analogue displacement from fast actin as from slow actin. As a control, a far-UV circular dichroism spectrum of etheno-ATP-slow actin [in the absence of ATP] was recorded to confirm that the protein was in fact in the native conformation. This was important in view of the lower conformational stability of this isoactin.

4.6 Myosin activation by unregulated and regulated salmonid isoactins.

The ability of different isoactins to activate myosin was investigated in a steady-state ATPase assay [ionic strength, 50mM and T=25°C] First, actin from slow muscle or from fast muscle was mixed with rabbit skeletal muscle myosin-S1 in the absence of other thin filament proteins. Inorganic phosphate arising from the hydrolysis of MgATP was quantified by reaction with molybdate. The MgATPase rates, which were measured on the same day, are plotted against F-actin concentration in Fig.4.26.

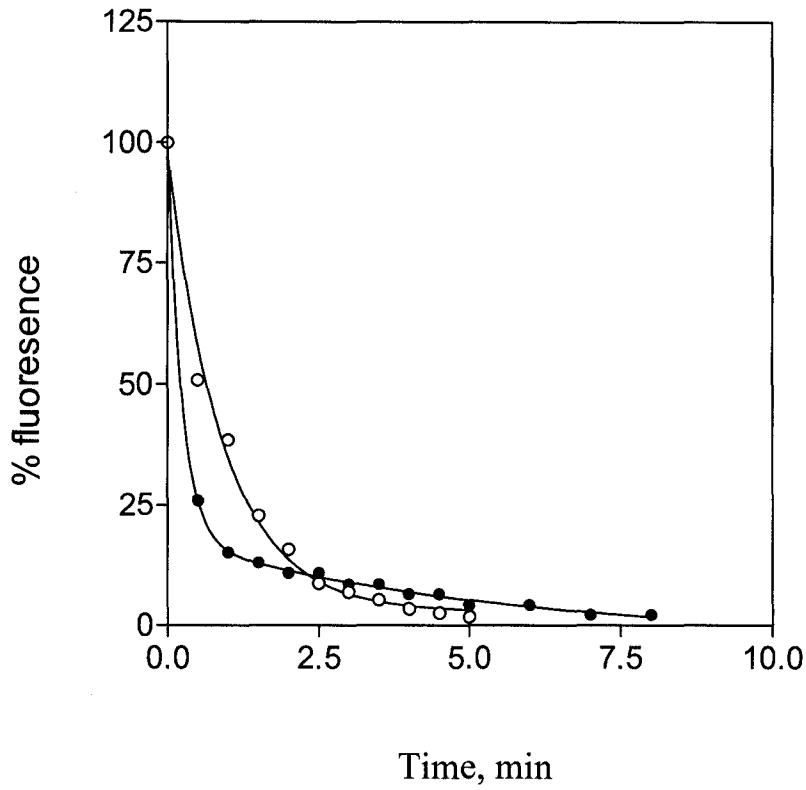

Fig.4.24 Time course study of displacement of etheno-ATP from etheno-ATP-G-actin by ATP.

The etheno-ATP-G-actin was prepared as discussed in Materials and Methods. The fluorescence of etheno-ATP was monitored at 410nm [excitation wave length, 340nm] at 25°C. The experiment was repeated at various ATP concentrations and the rate of fluorescence decline as a function of ATP concentration was determined by fitting plots to a single exponential decay curve [PRIZM graph pad software]. Fluorescence at zero time of fast [open circles] and slow [closed circles] muscle actins were 55.7 and 50.0 respectively [arbitrary units].

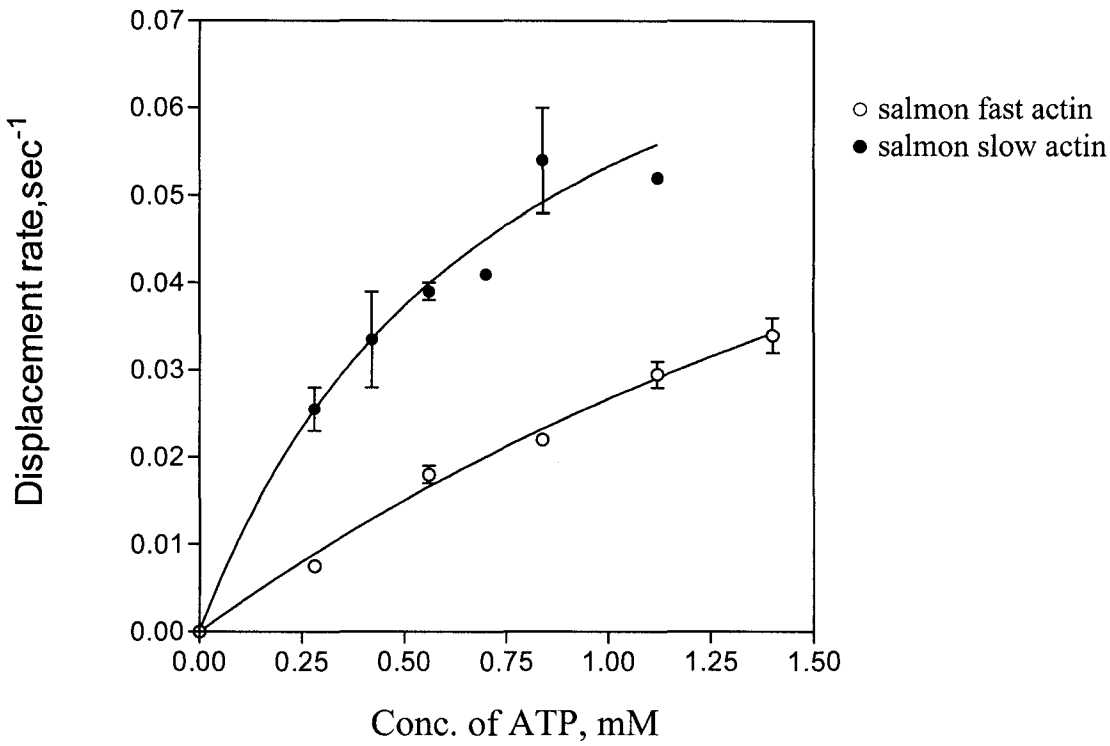

Fig.4.25 Dependence of etheno-ATP displacement from salmonid G-actin on the concentration of ATP.

The rate constants for displacement of etheno-ATP by ATP were determined from the best fits to single exponential decay curves as shown in fig.4.24. For slow actin the rate of displacement of ATP at saturation, Vmax, is $0.092s^{-1}$ and the ½Vmax is 0.74mM.

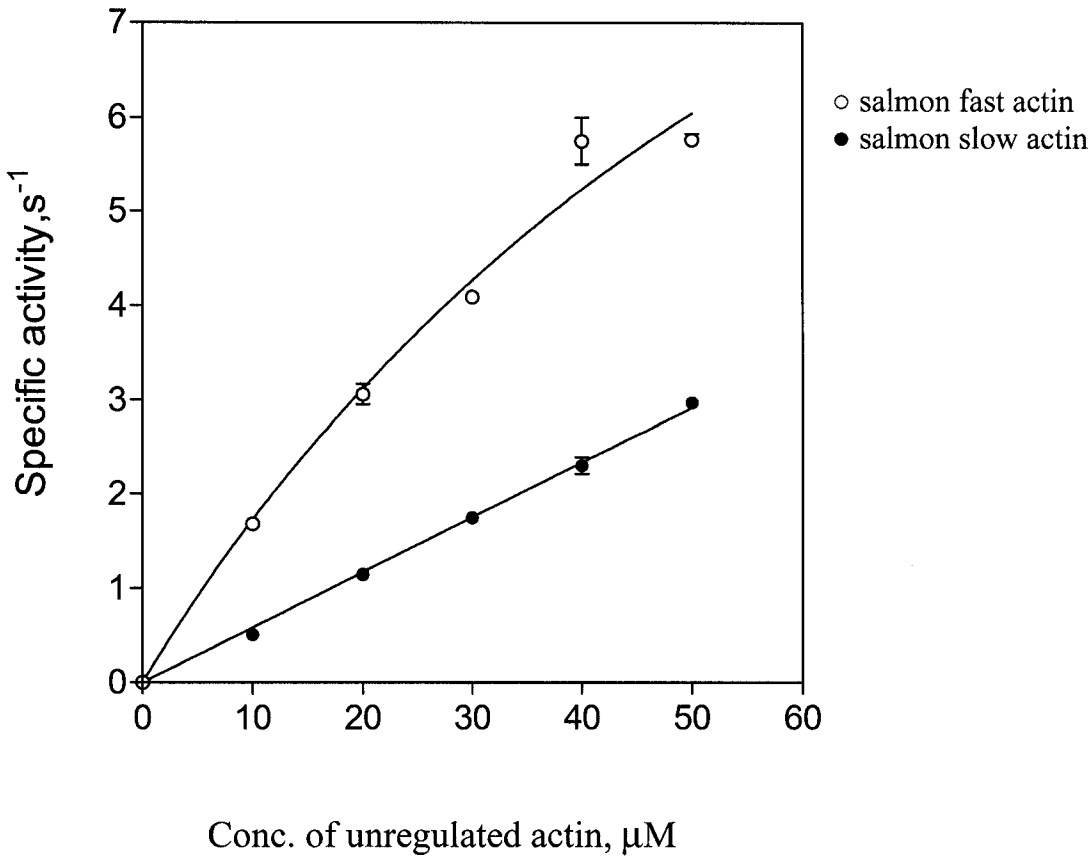

Fig.4.26 Dependence of the acto-myosin-S1ATPase activity on the unregulated salmonid isoactin concentration.

The rate of release of inorganic phosphate as a function of unregulated actin concentration was determined in 30mM NaCl, 6mM $MgCl_2$ and 5mM MOPS, pH 7.0 buffer at 25°C [ionic strength, 50mM] as described in Materials and Methods [section 2.6.4]. Myosin-S1 and ATP concentrations were 1μM and 1mM respectively. Myosin-S1ATPase activities were corrected for myosin-S1 alone. The experiment was repeated using different batches of actin [n>5] The Vmax and K_d of salmon fast unregulated actin are 16.18s^{-1} and 83.76μM, respectively.

In the case of fast actin, the curve can be fit to a hyperbola with a maximum rate of $16.18s^{-1}$. By contrast, the ATPase rate shows a linear dependence on the concentration of slow actin and extrapolation to saturation is not feasible. At the highest protein concentration used, slow actin produces ~50% of the activation that is generated by fast actin but we can not say whether this is due to a decrease in Vmax or affinity for myosin, or both. The experiment was repeated with other batches of protein. In all instances, slow actin activated myosin to a lower extent than fast actin. The difference varied between 25 – 35%.

The next step was to extend the comparison to thin filaments. These were prepared by addition of rabbit skeletal TM and Tn to a given isoactin. Rabbit Tn was used in the reconstitution because a reliable procedure for isolating whole Tn from salmon is currently unavailable [Heeley, personal communication]. The results are presented in Fig.4.27. It is apparent that thin filaments [$+Ca^{+2}$] composed of salmon fast actin activate myosin to a greater extent than those composed of slow actin. The same batches of actin were used in these experiments as in Fig.4.26 and the difference in rate at sub-saturating concentrations of protein is the same [~2-fold]. In the presence of EGTA, both sets of thin filaments inhibit the myosin MgATPase, indicating that the regulatory proteins are in fact bound to actin [Fig.4.27]. Thin filaments containing different salmonid isoactins were also compared by myosin-S1 titration [Fig.4.28]. In this case, the actin concentration was held constant at 4μM and the myosin-S1 concentration was varied between zero and 8μM.

Fig.4.27 The relationship between acto-myosin-S1ATPase activity and regulated actin concentration.

Thin filaments were reconstituted with salmonid isoactins, rabbit TM and rabbit Tn at a mole ratio of 7:4:4 in 30mM NaCl, 6mM $MgCl_2$ and 5mM MOPS, pH 7.0 at 25°C. Myosin-S1 and ATP concentrations were 1μM and 1mM, respectively. The amount of released inorganic phosphate was determined as noted under Materials and Methods [section 2.6.4].

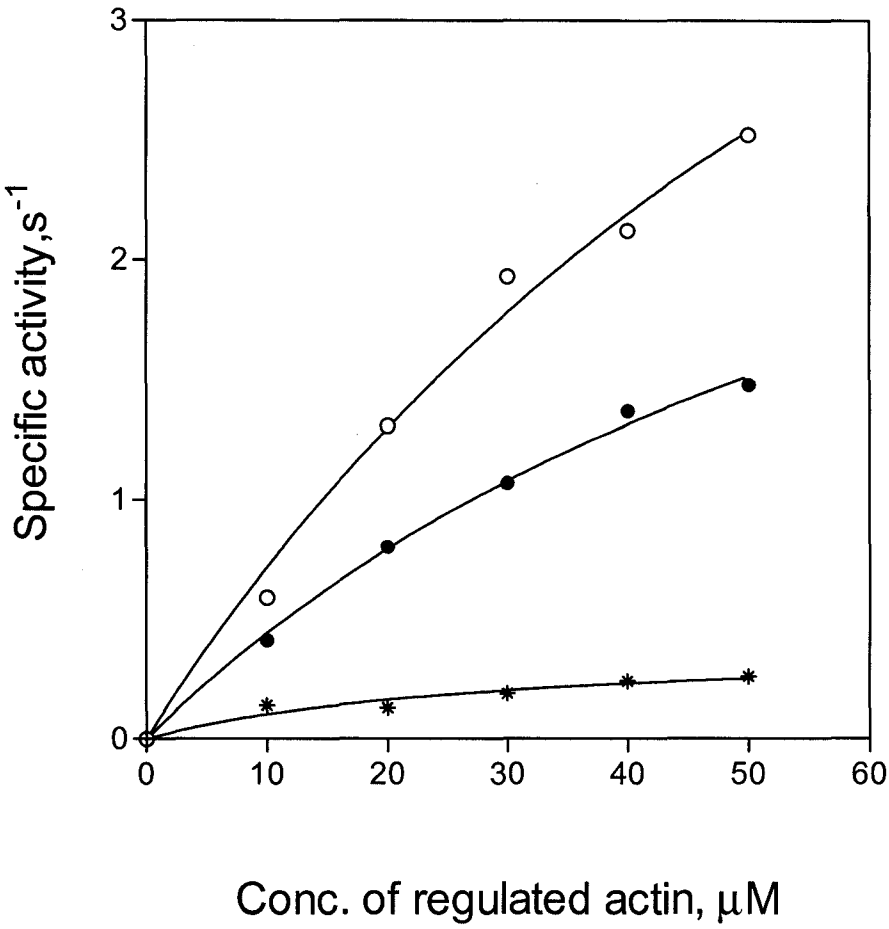

○ thin filament containing salmon fast actin + Ca^{+2}

● thin filament containing salmon slow actin + Ca^{+2}

* thin filament containing salmon fast actin + EGTA

Fig.4.28 The acto-myosin-S1ATPase activity in the presence of regulated salmonid isoactins as a function of myosin-S1 concentration.

The concentration of myosin-S1 was varied from 0 to 8μM while the concentration of F-actin [each isoform], TM and Tn were maintained at 4, 1.14 and 1.14μM, respectively. The experiment was carried out in 30mM NaCl, 6mM $MgCl_2$ and 5mM MOPS, pH 7.0 at 25°C as outlined in Material and Methods [section 2.6.4].

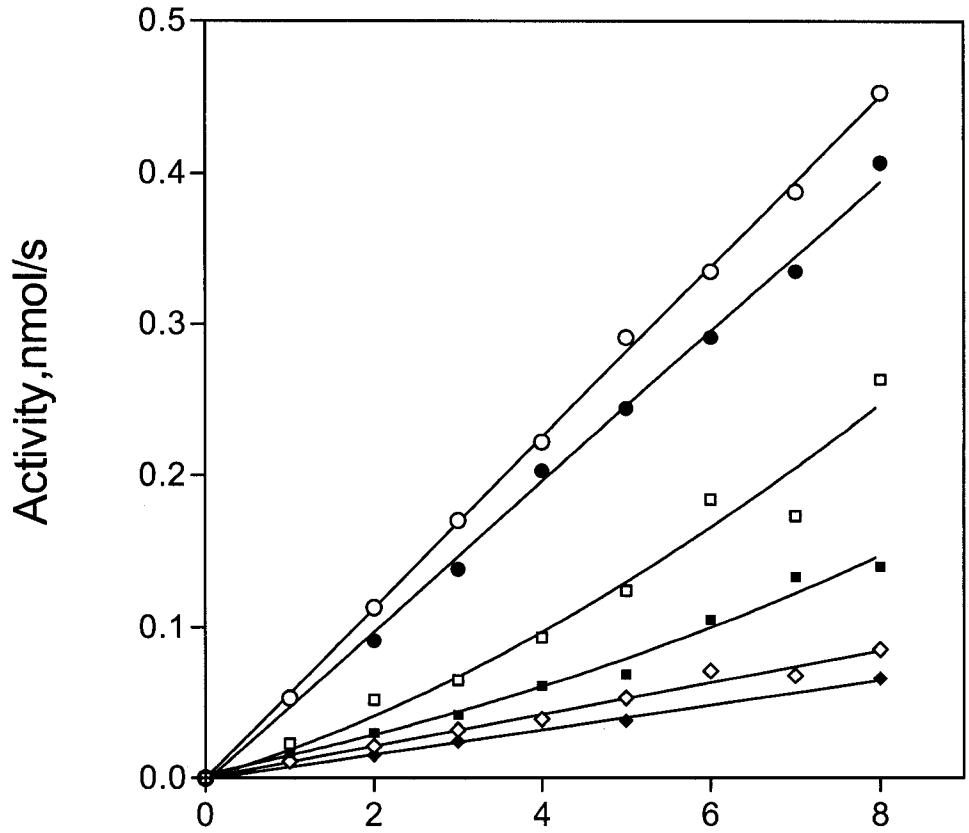

○ salmon fast actin

● salmon slow actin

□ regulated salmon fast actin + Ca^{+2}

■ regulated salmon slow actin + Ca^{+2}

◊ regulated salmon fast actin + EGTA

♦ regulated salmon slow actin + EGTA

The same trend that occurred in Fig.4.27 is again observed, although the difference in thin filament activation at the higher concentrations of myosin enzyme appears to be larger than the difference in activation by pure actin. The fact that the calcium-activated rates do not exceed the unregulated rate at the highest mole ratio of myosin-S1: actin, unlike what has been reported previously, can be attributed to an error in protein concentration, either S1 or thin filament or both.

Finally, a TM titration was performed in the absence of Tn. The conditions [2μM myosin-S1 and 7μM F-actin] were such that TM is expected to act as an inhibitor of the actomyosin ATPase (349). For this particular experiment, a given isoactin was paired with either rabbit TM or the corresponding salmon TM isoform. Fig.4.29 shows that the rate of ATP hydrolysis decreases with increasing concentrations of TM and that saturation is achieved at ~ 2μM. Interestingly, the maximal levels of inhibition are: > 75% [i.e. < 25% of the unregulated ATPase rate] for fast actin and < 50% for slow actin. It is also noticeable that salmon TM effects exerts more inhibition than does rabbit TM. The %ATPases at saturation for mixtures containing fast actin are: ~50% [+ rabbit TM] and < 25% [+salmon TM].

Fig.4.29 The effect of tropomyosin on the acto-myosin-S1ATPase activity.

The concentrations of myosin-S1, F-actin [either, salmon fast or salmon slow] and ATP were 2, 7μM and 1mM respectively. The concentration of TM [either, rabbit, salmon fast or salmon slow] was varied from 0 to 3.0μM. The buffering conditions are the same as in Fig.4.28. Rates are expressed relative to the actomyosin-S1ATPase activity in the absence of TM. After correction for the rate of myosin-S1 alone [0.2nmol/s], these are: $1.04s^{-1}$ [salmon fast actin] and $0.38s^{-1}$ [salmon slow actin].

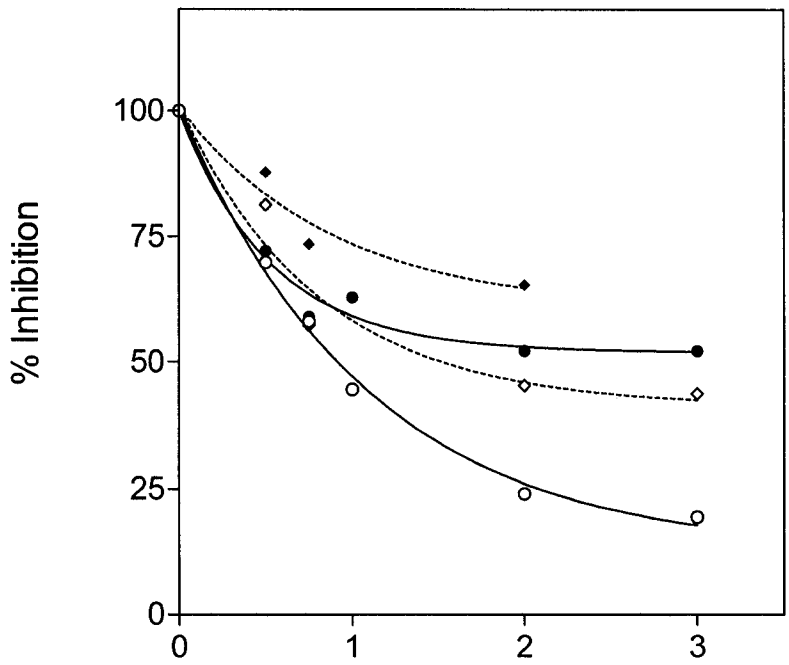

◊ salmon fast actin + rabbit TM

♦ salmon slow actin + rabbit TM

○ salmon fast actin + salmon fast TM

● salmon slow actin + salmon slow TM

4.7 Discussion

The focus of this chapter is to investigate the structural-functional consequences of the heterogeneity which is inferred from the sequences of salmon muscle actin cDNA. The possible importance of the non-conservative substitutions is summarized in Table 4.4. In addition, the conservative substitutions [Table 4.3] could also impose an effect on isoactins functions. To determine this, the following actin-related properties were investigated: [i] polymerization; [ii] conformational stability; [iii] nucleotide affinity and [iv] myosin activation.

4.7.1 Polymerization of salmonid isoactins

Polymerization, one of the fundamental properties of actin, was studied using sedimentation, viscometry and light scattering. After initiating the process of polymerization, more slow muscle actin remained in the supernatant following high-speed centrifugation than fast muscle actin [Fig.4.4]. This result, which is consistent with those from the viscometric analysis [Fig.4.7], demonstrates that there is a difference in the extent to which these two isoforms form sedimentable filaments. Because no lag was observed in the light scattering experiment [Fig.4.5 and 4.6], it can be deduced that the G-actin, which was used in the sedimentation experiment, already contained nuclei.

Table 4.4 The significance of non-conservative substitutions with regard to binding with other proteins.

Substitution	Location	Binding site
103	Start of β strand [sub-domain 1]	Near to myosin binding site [residues 95-100]
155	End of β strand [sub-domain 3]	Very near to nucleotide/metal ion
278	Middle of α-helix [sub-domain 3]	Near to actin binding site [residues 286-289]~3 helical turns away
281	End of α-helix [sub-domain 3]	Near to actin binding site [residues 286-289]~2 helical turns away
310	Start of α-helix [sub-domain 3]	Glu311Ala mutation is reported to change the affinity for TM.
354	[sub-domain 1]	-
360	End of final α-helix [sub-domain 1]	Glu360His mutation is reported to change the affinity for TM.

Thus, although, the two salmonid actins may possess non-identical nucleation rates, this can not explain the findings in Fig.4.8. Therefore, it is reasonable to conclude that the observed difference in polymerization arises due to a difference in the rate of elongation, which may have been imposed by the structural differences resulting from conservative and non-conservative substitutions within the primary structure.

In the actin filament, each actin monomer makes contact with four others, the preceding and following actins on the same long pitch helix and the two across the filament on the other long pitch helix. The larger sub-domains 3 and 4 are axially located with interactions across to the sub-domains 3 and 4 of the actin in the second strand. The smaller sub-domains 1 and 2 are located at the periphery of the filament exposed to the solvent and are available for interaction with myosin. The interface of F-actin is proposed to be encompassed by the DNase I binding loop [residues 38-52], the hydrophobic loop [residue 262-274] and the C-terminal region. The rest of the discussion is concerned with amino acid substitutions which may influence polymerization.

In the monomer, a hydrophobic loop extends from the surface of the protein and then hooks back towards the actin in the vicinity of Tyr188. However, this loop could be remodelled to represent two anti-parallel β-strands with a four residue hydrophobic plug in a direction perpendicular to the filament axis. The four residue "plug" consisting of three hydrophobic residues and a Gly, could insert into a hydrophobic pocket generated by the interface of two subunits on the opposing strand of the helix. Actin residues

Tyr143, Ala144, Gly146, Thr148, Gly168, Ile168, Ile341, Ile345, Leu346, Leu349, Thr351, Met355 and possibly the C-terminal region of actin, which is typically disordered in actin structures, line this hydrophobic cleft (350). Site directed mutagenesis studies have shown that partial disruption of the plug pocket interaction in this complex has a significant effect on the stability of the so called nucleus, since this hydrophobic interaction constitutes a major component of the inter-subunit interactions (109,351). Interestingly, the non-conservative substitutions Thr103Val and Asp360Gln, as well as the conservative substitutions, Ile163Val, Thr358Ser and Asp363Glu, are in the proximity of the hydrophobic cleft indicating that they may have direct contacts with these inter monomer binding regions thereby resulting in a lower rate of polymerization.

However, Schutt *et al.,* (348,352), have suggested a possible alternative model for the actin filament, based on their work with the crystal structure of the actin/profilin complex. According to their model, sub-domains 1 and 2 are in the interior of the filament where sub-domain 2 contacts the small domain [sub-domain 1 and 2] of one neighbouring monomer and the top of the large domain [sub-domain 4] of another monomer. The interface between sub-domains 3 and 4, where the hydrophobic loop is located, is on the exterior of the filament apparently not involved directly in inter-subunit contacts. Supporting this proposal, are studies on F-actin-ADP and F-actin-ADP-BeFx in which the release of phosphate following ATP hydrolysis in F-actin destabilizes the filament (93,353) by means of disordering sub-domain 2. Since there are no substitutions in, or in the vicinity of, sub-domain 2 [as confirmed by DNase I binding affinity], it is

difficult to explain the observed difference in polymerization using this model. However, the limited proteolysis studies done on the region of sub-domain 2 using subtilisin (354), chymotrypsin (355), and *E. coli* protease (356) and trypsin (357) are in agreement with Schutt's model of F-actin filament.

The mutations Arg177Asp (358), Ser14Cys (359) and the double mutation Ser14Cys/Asp157Ala (360) have been reported to reduce the rate of polymerization, indicating that the amino acids in sub-domains 1 and 3 also have interactions with each monomer in the F-actin filament. Therefore, it is reasonable to say that the charge substitution along with other conservative and non-conservative substitutions in sub-domains 1 and 3 of slow actin may have produced conformational changes in sub-domains 2 [without altering DNase I binding] and/or 4 that are large enough to cause a difference in interaction between actin monomers, resulting in a significant difference in polymerization.

When polymerization was investigated using Ostwald viscometry, salmonid fast actin showed higher specific viscosity than slow actin, regardless of the concentration of ATP present. Pantaloni *et al.,* (361) observed the same behavior of rabbit actin polymerization in the presence of varying ATP concentrations. Further, the authors found that the critical concentration of actin is 20-fold higher in 1mM Mg^{+2}, 0.2mM ADP than in 1mM Mg^{+2}, 0.2mM ATP, suggesting two possible mechanisms of polymerization. The association rate constant for the addition of ATP-G-actin to an ADP-F-actin might be

larger than that for the addition of ADP-G-actin, facilitating actin monomer assembly. Alternatively, the rate of actin dissociation from filaments might be lower in the presence of ATP than in the presence of ADP, which would imply the presence of an ATP "cap" at the ends of the filament. Later, Carlier *et al.,* (343) reported that both mechanisms do occur when actin is polymerizing in the presence of excess ATP. The growing filament consists of ADP subunits in the interior and ATP subunits near the ends forming a "cap". The size of the ATP cap increases with the rate of actin monomer addition to the filament and is larger when the polymer is in its equilibrium than in the steady state. Therefore, the authors proposed that the rate of actin dissociation from filaments might be lower in the presence of ATP, which would imply the presence of one or several subunits of ATP-F-actin at the ends of filaments forming a "cap" and that ATP hydrolysis is not tightly coupled to actin polymerization. In the presence of ATP, the association rate constant is greater, the dissociation rate constant is lower, and a stabilizing "cap" of ATP-F-actin subunits maintains the metastable ADP-F-actin filament. Above the critical concentration, the system is mainly dominated by the association-dissociation reactions of ATP-G-actin to form F-actin ends.

From this research it can be suggested that, for slow muscle salmonid actin, the critical concentration is higher and the rate of elongation is significantly lower than for salmonid fast actin resulting in a difference in the extent of polymerization. The lower viscosity of salmon slow actin may be due to the formation of shorter filaments as well. Due to the higher rate of ATP dissociation [to be discussed in the latter part of the chapter, section

4.7.3.] the slow actin may produce shorter F-actin filaments. It is clear that the amino acid substitutions in the primary structure of salmonid slow actin have a significant impact on polymerization but it is difficult to identify the responsible amino acids in this regard.

4.7.2 Conformational stability of salmonid isoactins

The actin protein chain transverses the various sub-domains in the order of: 1 → 2 →1 →3 → 4 → 3 → 1, thereby creating a small and a large domain [sub-domains 1+2 and 3+4, respectively] connected by two crossed helices at the bottom of the inter-domain cleft. This linkage provides the means whereby a change in structure in one part of the molecule may be communicated to another (347,362). In the present work, salmon slow muscle actin was found to be less stable than any other actin tested [salmon fast, rabbit skeletal and shark fast actin]. This isoactin was the one that is most susceptible to heat, urea, and GdnHCl-induced denaturation.

Prior to the current investigation, it had been shown that the composition of the N-terminal region of actin influences stability. This was established by comparison of cytoplasmic β-actin [Asp2, Asp3, Asp4....Val10] and γ-actin [Glu2, Glu3, Glu4...Ile10] (362). Interestingly, salmonid slow muscle actin carries two conservative substitutions in the N-terminal region [Asp2Glu and Asp3Glu, Asp in both salmon fast and cardiac]. In addition another unique substitution, Asp363Glu [Asp in both salmon fast and cardiac] is

found in sub-domain 1 in slow muscle actin. Thus, it is conceivable that heterogeneity at either end of the molecule could contribute to the observed difference in conformational stability [Table 4.3].

The clustering of tryptophan residues in sub-domain 1 provides a probe for this section of the protein. Of the four indoles [at position 79, 86, 340 and 365], Trp340 and 365 are the main fluorophores (363). Bertazzon *et al.,* (364) have reported that upon denaturation the intrinsic fluorescence of yeast actin is red shifted (364). Significantly, the emission maximum of the salmonid skeletal muscle actins is equivalent, below the Tm as well as above the Tm [Fig.4.16], suggesting that the tryptophan environment and, by extrapolation, the conformation of subdomain-1 is similar in both isoforms and that the extent of unfolding induced by heating beyond the Tm is the same. However, the differences in near-UV CD spectra, which were recorded at 5^0C indicate a different conformation of each sub-domain-1. Further, because the Tm associated with the thermal unfolding of both salmonid slow and fast muscle actin, as observed by near-UV CD, coincides within 2-3 degrees to that observed in the far-UV, the difference in thermal stability of the salmonid skeletal muscle actins appears to be due to a change in sub-domain-1 though its conformation is different in each isoform. Therefore, the only non-conservative substitutions in this part of the molecule at positions 103 [Thr/Val] and 360 [Gln/Asp]. It is interesting that the charge substitution, which is close to Trp356, makes no detectable contribution to intrinsic fluorescence.

The instability of salmon slow actin is also evidenced by the results of chemical unfolding experiments, in which both GdnHCl and Urea were used. Previously, Kuznetsova *et al.,* (365) observed the denaturation of rabbit actin by Gdn.HCl to result in two unfolding transitions where the second transition is completely reversible, unlike the first transition, suggesting that the process of equilibrium actin refolding from a GdnHCl-unfolded conformation is terminated at the stage of formation of an intermediate state.

However, recently Kuznetsova *et al.,* (366) and Turoverov *et al.,* (367) independently reported that the inactivated state is not an intermediate between the native and completely unfolded states. According to the phosphorescence studies on actin unfolding (368) inactivated actin which is a homogeneous association consisting of 15 macromolecules of actin (369), is not formed from single state transition of kinetic intermediate to inactive actin. Instead, inactivated actin is formed from the unfolded state by a gradual increase in the number of associates.

A specific association of actin macromolecules seems to be the main reason for the irreversibility of the native to intermediate state/inactivated actin transition (370 and 371). Inactivated actin has a unique structure where hydrophobic clusters are on the surface of the associate, while some polar regions and Trp residues are in the interior, (363). It is apparent that salmonid slow actin tends to form inactivated aggregates at lower concentrations of denaturing agents and quickly attains its irreversible unfolded state [Fig.4.18]. The similar extent of red shift in intrinsic fluorescent spectra of salmonid

isoactins at the respective melting temperature suggests that the unfolding region in the first transition state of both isoactins is the same [i.e. sub-domain 1] and that a further increase in the concentration of denaturant starts to exert a greater impact on slow actin leading to more inactivated actin. The regions which comprise the second transition are unknown.

4.7.3 Nucleotide binding of actin

It is well understood that dissociation of ATP from G-actin depends on various factors including the type and concentration of divalent metal ion present in the high affinity site, as well as the pH (372-374). Several reports show a wide range of affinities of actin for nucleotide, depending upon the phosphorylation state of the nucleotide and the solution conditions (375-377). Further, it is clear that the metal ion is located in a deep hydrophobic pocket formed by the phosphate groups of the adenine nucleotide and the actin residues, Asp11, Gln137 and Asp154 (134).

Nucleotide-free protein is unstable (130), consistent with the nucleotide-binding pocket being situated in the middle of the molecule. Likewise, unfolding can be induced by ion chelators such as EDTA (130). Leading on from this, it can be postulated that the substitution at position 155 [Ala in salmon slow muscle, Ser in fast muscle] contributes to the interaction with nucleotide-metal ion. This does not agree with crystal structure, however, where the Ser 155 side-chain is pointing away from the metal ion and too far removed to interact with it [Dr. Les Burtnick, Dept. of Chemistry, University of British

Columbia, personal communication]. On the other hand, we observed a shift in the fluorescence emission spectrum of mant-ATP [Fig.4.23] consistent with a change in polarity at the site of nucleotide binding. Specifically, association of mant-ATP with salmonid slow muscle actin produces a blue shift of ~8nm relative to that of fast muscle actin. We cannot, however, rule out the possibility that instability elsewhere in slow muscle actin, connected with one or more substitutions, is transmitted to the nucleotide-binding cleft.

Since G-actin inactivates rapidly in the absence of nucleotide, it is difficult to obtain absolute values for the nucleotide dissociation constants (126). For example, the ATP dissociation rate constant of rabbit Ca-G-actin at pH 7.0 is $0.015s^{-1}$ at very low concentration of Ca^{+2} and reaches a minimum value of $5 \times 10^{-4}s^{-1}$ at high Ca^{+2} concentration [0.001-100μM] (378). However, Strzelecka-Golaszewiska (379) reported a value of $4 \times 10^{-6}s^{-1}$ at pH 7.0 in the presence of an infinite concentration of Ca^{+2}. Using the experimental data for the ATP association rate constant (380), the ATP dissociation constant can be calculated as $0.2s^{-1}$ (109). At low ATP concentrations [<50μM], the rate of displacement is not exactly first order, but the major step has an apparent rate constant of $0.003\text{-}0.006s^{-1}$, and this value does not vary greatly with Ca^{+2} concentration. Frieden and Pantane (373) have reported that above ~100μM, the rate of etheno-ATP displacement as a function of the ATP concentration, is strictly first order. The rate constant markedly increased to about $0.15s^{-1}$ from $0.003S^{-1}$[<50μM] at 4mMATP [at 10μM Ca^{+2}]. In the current study, the ATP concentration was changed from 0 to 1.40mM

[in the case of salmon slow actin the ATP concentration was increased up to 1.18mM] in the presence of 0.2mM Mg^{+2} at 25°C. At 1.18mM ATP, the rate of displacement of etheno-ATP from salmon slow actin was $0.052S^{-1}$ and it was $0.026S^{-1}$ for salmon fast actin. Since the experimental conditions were different from above, the observed apparent rate constants are different from others. However, it is clear that the displacement rate constant of salmon slow actin is significantly greater than that of salmon fast actin and the major causative factor for the observed difference could be the substitution in the vicinity of the nucleotide binding region [Ser155Ala]. As observed in extrinsic fluorescence spectra of salmonid isoactins [Fig.4.23], the environment around the nucleotide binding region might have changed, thereby weakening the interactions of ATP with other amino acids. Another possibility is that the observed change in nucleotide affinity has been caused by a change in the strength of metal ion bonding. Finally, it is feasible that the substitutions at 360 and 363 have exerted a long range effect. In connection with this point researchers have shown that modification of Cys374 perturbs nucleotide binding and vice versa (381 and 382).

4.7.4 Myosin activation

The reconstituted thin filaments containing salmon fast actin in the absence of regulatory proteins showed 2-fold higher myosin activation than that of slow actin under steady state conditions [Fig.4.26]. A similar difference in myosin activation was also observed between these two proteins in the presence of rabbit TM and Tn [Fig.4.27]. However, a

maximum level of inhibition was observed for fast actin by increasing TM concentration to 3μM [Fig.4.28]. This indicates that, due to the influence of Tn, the interactions between actin and myosin-S1 in the presence of TM have changed drastically. Therefore, a clear understanding of the involvement of amino acids in actomyosin interactions gives insights into the functional variations that arise as result of amino acid substitutions.

The 3-D atomic model of F-actin decorated with *Dictyostelium* myosin-S1 (143) and rabbit chymotryptic S1-decorated actin (142) reveal three regions of close contact between single actin monomers and the myosin-S1 head. The first contact involves the N-terminal amino acids Asp1-Asp4, Asp24, Asp25, Glu99 and Glu100 [according to the rabbit actin sequence]. This contact is electrostatic in nature and may be responsible for the ionic strength dependent 'weak' interactions between actin and myosin (383). The second contact region has stereospecific interactions with hydrophobic residues Ala144, Ile341, Ile345, Leu349 and Phe352. The third contact region involves Pro332 and Pro333. These three regions define the primary site of actomyosin interaction and all occur in sub-domain 1. Truncated actin, devoid of the last two or three C-terminal residues has shed light on the importance of actin's C-terminus to inter-monomer communication as well. The critical concentration for actin polymerization and the activation of myosinS-1ATPase is also affected by the removal of C-terminal residues (384 and 385). It is further confirmed by fluorescence studies where the reactivity of Cys10 alone is very low in actin, but when the complex, [myosin-S1]-F-actin is formed, the reactivity of Cys10 is strongly increased (386). Actin's N-terminus is believed to play

a greater role in the formation of the weakly bound actomyosin states than in the formation of the strongly bound actomyosin states. However, mutations at Asp363His/Glu364His, and Glu360His/Glu361His resulted in a rather large increase of K_d values indicating that both mutations changed kinetic steps of the ATPase cycle to some extent (387). From this it is apparent that the conservative substitutions of salmonid isoactins [see table 4.3], substitutions Asp2Glu and Asp3Glu, which are located in sub-domain 1, might influence weak actomyosin-S1 binding Further, as confirmed by mutational studies (387), the involvement of charge substitution at position 360 and the conservative substitution Asp363Glu could also be substantial in salmonid thin filament regulation.

The sub-domain 2, and in particular its DNase I binding loop, possibly play a role in transmission of conformational changes between actin protomers in the filaments. Their conformational transitions strongly influence the inter-protomer interactions along the filament (388 and 389). Inhibition of *in vitro* motility assays by inter-protomer cross linking of actin filaments between various residues revealed the importance of conformational freedom of the sub-domain 2/sub-domain 1 interface for generation of motion with myosin. Charged actin side chains between residues 309 and 326 located in sub-domain 3 have been hypothesized to interact with TM in the absence of Tn by Lorenz *et al.*, (390). In accordance with the results of mutational studies [Lys315Ala/Glu316Ala and Glu311Ala/Arg312Ala] performed by Korman and Tabacman (391), the effect of these mutations on TM binding was insignificant,

suggesting that the interactions, if present must be weak. Hence, it can be suggested that the observed difference in thin filament regulation of salmonid isoactins is not a direct result of one substitution of amino acid, but a result of involvement of a few, if not all of the substitutions.

Chapter 5

The distribution of slow muscle actin isoform in the animal kingdom.

Actin comprises a small multigene family. Mammals have four distinct muscle actins [α-skeletal, α-cardiac, α-vascular and γ-enteric], and two distinct non-muscle actins [β- and γ-cytoplasmic] (154-159). In organisms that contain only a single actin gene, the sequence is more similar to vertebrate non-muscle actin genes than to muscle actin genes, so the non-muscle actins are considered to be ancestral. Kovilur *et al.,* (392) suggested that the evolution of muscle actin genes from non-muscle actin genes began in the prochordate lineage, even though they found a sea urchin actin gene as a sister to the chordate actin genes. The two actin genes from an early echinoderm led to the chordate muscle and non-muscle actin genes. However, actin sequences analyzed from a variety of animals including sea star [*Pisaster ochraceus*], have shown that actin genes are more closely related to vertebrate cytoplasmic actins than they are to vertebrate muscle actins. For this reason it is speculated that chordate muscle actin arose from non-muscle actin before the divergence of urochordates and vertebrates (393).

In the human genome, only a single gene for each of the six-actin isoforms have been mapped (394). A large number of actin pseudogenes have been identified in the human genome (395).Two striated muscle actins, skeletal and cardiac are found in both avians and

amphibians (397-399), but only one smooth muscle actin, α-aortic, has been identified in birds (400). A third form of cytoplasmic actin, denoted as type 5, has been reported in chicken (401). In early development of mice, skeletal and cardiac muscle actins are co-expressed in developing somites, but the cardiac actin withdraws from the skeletal muscle in later stages (402). Amphibian non-muscle cells synthesize five different isoforms of actin (403). Different regulatory mechanisms are thought to activate these tissue-specific genes. For example, in skeletal muscle, myogenic determination factors of the 'basic helix-loop-helix' [bHLH] that bind to E box [CANNTG], are the most notable muscle-specific transcription factors (404 and 405). Other important cis-regulatory sequences include CarG box, to which positive acting serum response factor [SRF] and negative actin YY1 factor competitively bind (406 and 407).

It has been reported that teleosts have two striated muscle actin genes [α-skeletal and α-cardiac]. Interestingly, a unique second skeletal actin gene in salmon was reported in our laboratory (408). Therefore, the focus of this study was to determine the existence of a slow muscle actin isoform in other animal species and to analyze the evolutionary relationships among those species. Actin was analyzed from the following species; chicken [*Gallus gallus*], frog [*Xenopus laevis*], yellowfin tuna [*Thunnus albacares*], Atlantic herring [*Clupea harengus harengus*] and mako shark [*Prionace glauca*].

Tunas are unique among teleosts because of their ability to elevate the temperature of their locomotor muscle, viscera, brain, and eye tissues above that of water temperature. Endothermy in tunas is compartmentalized in regions of high metabolic output (409-411).

Elevation of slow twitch [red] muscle temperature is facilitated by the more axial positioning of the aerobic muscle mass and the presence of counter-current heat exchangers in the circulatory system, which reduces conductive and convective heat loss at the gills and body surfaces. Many tunas have a higher proportion of slow twitch muscles, relative to fast twitch muscles than other teleosts (411). Mechanisms for heat retention in aerobic muscle are widespread in large pelagic fish. Telemetry and anatomical studies have shown that heat conservation strategies are present not only in tunas, but in lamnid sharks, alopiid sharks, blue sharks and swordfish as well (412).

Salmon and herring are round-bodied teleost fish. Herring are found mainly offshore in deeper water and spawn in the vicinity of bays, straights, estuaries and oceanic banks, while salmon are migratory fish that spawn in fresh water but spend a longer time in salt water. Unlike the tuna and shark, these fish do not have a mechanism to maintain body temperature, and hence they are cold-blooded fish.

The chicken has dark and red muscles related to the different types of fibres. Breast muscle has mainly white fibres, which contain a relatively small amount of myoglobin, while some leg muscles contain more red fibres with myoglobin. Certain birds such as the hummingbird have only red fibres and studies indicate that these fibres have high mitochondrial density and stored fat. As in mammals many avian muscles contain a mixture of different types of fibres.

Since the selected species represent vertebrates, amphibians, bony fish and cartilaginous fish, it was expected to get valid information on this slow muscle actin isoform pertaining to its existence and distribution in the animal kingdom.

For the study, fish and chicken were bought from a local store and frogs were donated by the Terry Fox Cancer Research Laboratory [Health Sciences-Memorial University of Newfoundland]. Chicken breast was used as the fast muscle while the anterior latissimus dorsi muscle [ALD] was used as the slow muscle. In the case of frog, sartorius and cruralis muscles were used as fast and slow muscles, respectively. All the extracted actins were in Ca-G-actin form. With the exception of the chicken and frog, the primary structures of the other actins have not yet been determined.

5.1Two-dimensional gel electrophoresis [2-D PAGE] of isoactins

To determine the existence of actin isoforms in a particular muscle type, 2-D PAGE was carried out using both muscle extracts and purified actins as discussed under Material and Methods. As shown in Fig.5.1 chicken ALD and breast muscle have a single actin isoform in each muscle extract while there are two isoforms present in mako shark, Atlantic herring [data not shown] and tuna slow muscle extracts. Due to the problem of smearing, some of the obtained results were inconclusive. However, the presence of actin isoforms was confirmed by various other methods as described below.

5.2 Alkaline urea polyacrylamide gel electrophoresis of isoactins

As mentioned in Mudalige *et al.,* (408), salmon slow muscle actin isoform has a unique charge substitution at the position of 360 [Asp/Gln; Asp in salmon slow actin and Gln in salmon fast actin]. Assuming all slow muscle actin isoforms contain this charge substitution, actin was extracted from a variety of muscles and subjected to alkaline urea-PAGE [Figure 5.2]. No difference was observed in the mobility of actins from chicken and frog muscles. However, tuna and Atlantic herring do possess a faster moving actin in their slow muscles. It is important to note that shark and tuna slow muscles are intermingled with fast type fibers thus showing two bands in the actin slow muscle extract. Secondly, the mobility of mako shark slow actin isoform is less when compared to the mobility of salmon slow actin.

5.3 Immunoblotting of isoactins

To confirm that the proteins electrophoresed under alkaline condition are actins, immunoblotting was carried out. From the results of immunoblotts [data not shown], it can be confirmed that not only salmonids, but Atlantic herring and tuna also carry a separate gene for slow muscle actin. Interestingly, the immunoblot of shark isoactins revealed a single band, indicating that the second protein observed in the alkaline urea gel was not actin.

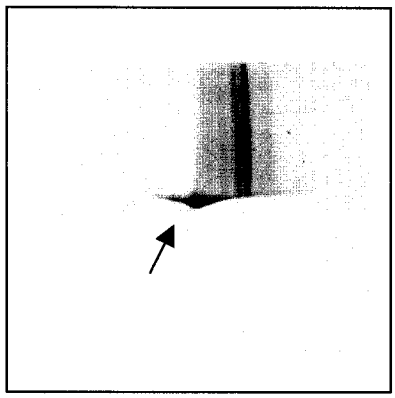

Gallus gallus [chicken]ALD purified muscle actin

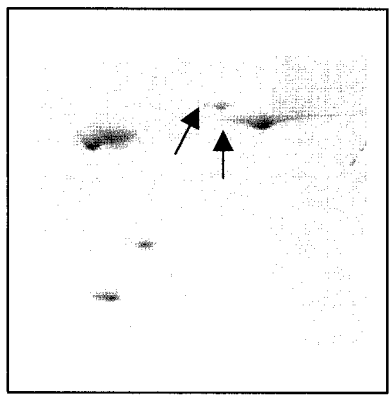

Prionace glauca [mako shark] slow muscle homogenate

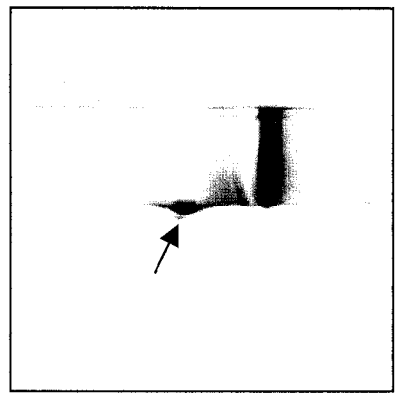

Thunnus albacares [Tuna] purified fast muscle actin

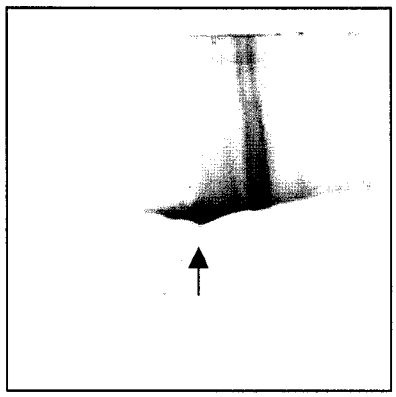

Gallus gallus [chicken] breast purified muscle actin

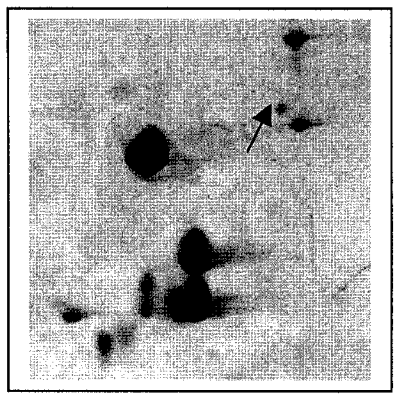

Prionace glauca [mako shark] fast muscle homogenate

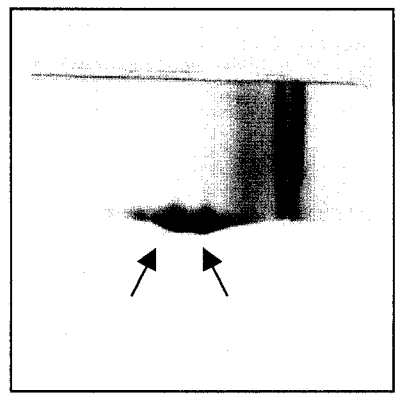

Thunnus albacares [Tuna] purified

Fig.5.1 Two-dimensional gel analysis of the isolated isoactins and muscle homogenates from various species.

Purified actins or muscle homogenates were subjected to 2-D gel electrophoresis. The pH gradient, 4-6; the concentration of polyacrylamide of the slab gel, 15% [w/v]. Coomassie blue stained protein patterns of the gels are shown here with the acidic end to the left. Arrowheads indicate the actin containing spots. As seen in all the gels, bilateral smearing obscured spot separation.

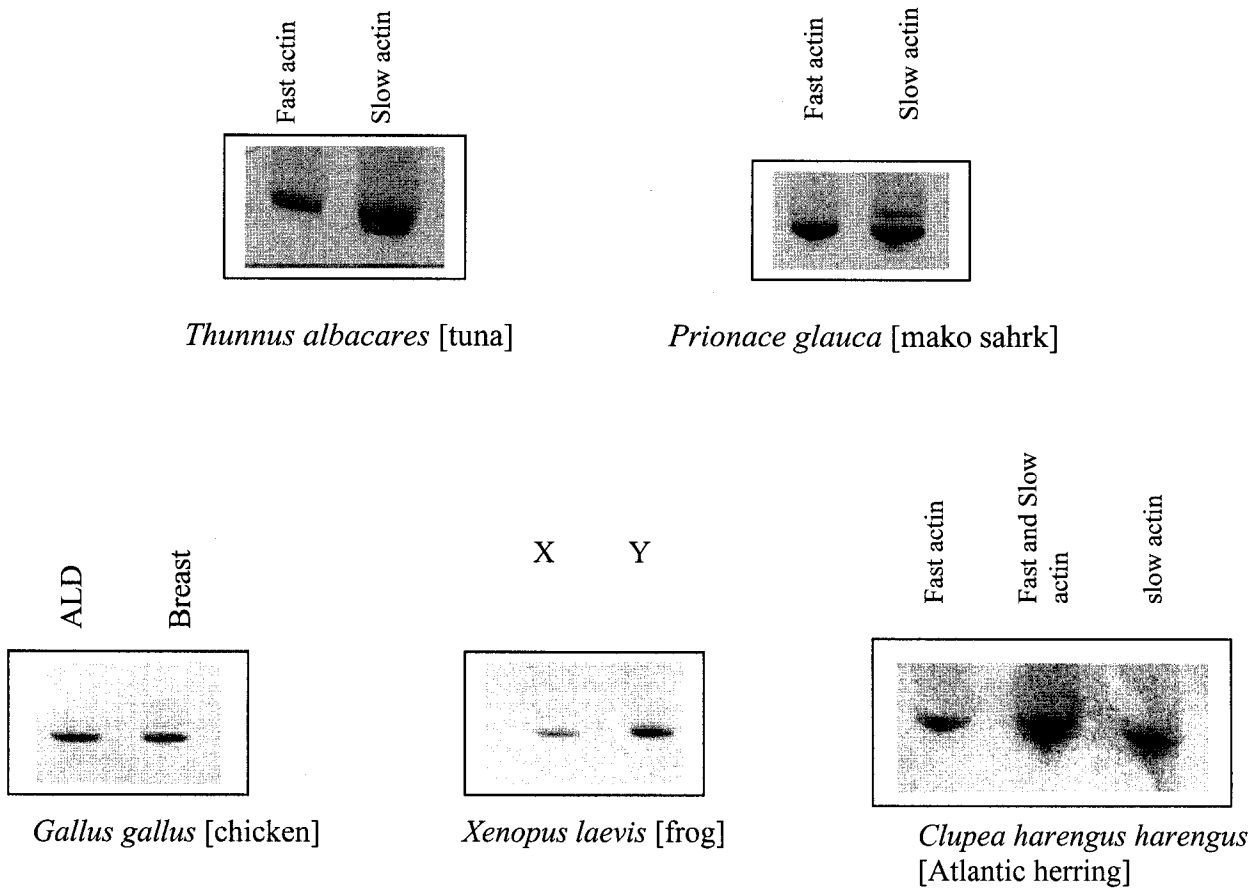

Fig.5.2 Alkaline urea polyacrylamide gel electrophoresis of purified isoactins extracted from fast and slow muscles of various species.

X-sartorius muscle actin; Y-cruralis muscle actin.

Samples [0.5-2mg] were applied to the gel, which had been pre-run for 15min at 220V and electrophoresed at the same voltage for a total of 650Vhr at room temperature. Protein containing bands were detected by staining with Coomassie Brilliant Blue R-250. As seen in the gel, the migration of mako shark slow actin differs from salmon, tuna and Atlantic herring slow actins [under the alkaline conditions].

5.4 Polyacrylamide gel electrophoresis of isoactins in the presence of 4M urea [Safer gel electrophoresis in the presence of 4M urea]

A significant difference was observed in the electrophoretic mobility of salmon slow actin in the presence of 4M urea, suggesting that salmon slow muscle actin has different conformation[s] of unfolded intermediate[s], when compared to salmon fast actin (408). At 4M urea, the extent of unfolding of salmon slow actin is greater and its conformation[s] is different from salmon fast actin resulting in a change in mobility in Safer gels (291). This observation can be used as a fingerprint in characterizing other isoactins. Tuna and Atlantic herring isoactins show a similar profile to salmonid isoactins under the same conditions [Fig.5.3], unlike chicken isoactins, indicating that the conformation[s] of unfolded salmonid, tuna and Atlantic herring slow muscle actin isoforms are similar.

5.5 Polymerization of isoactins

The sedimentation technique was utilized to study the extent of polymerization of isoactins. As shown in Fig.5.4 [A], the extent of polymerization of Atlantic herring slow actin was lower than salmonid slow actin [Fig 4.4]. However, possibly due to the presence of both isoactins in the tuna slow muscle actin extract, a different behaviour was observed, i.e. both isoforms polymerize to the same extent over a given time period [Fig.5.4 [B]].

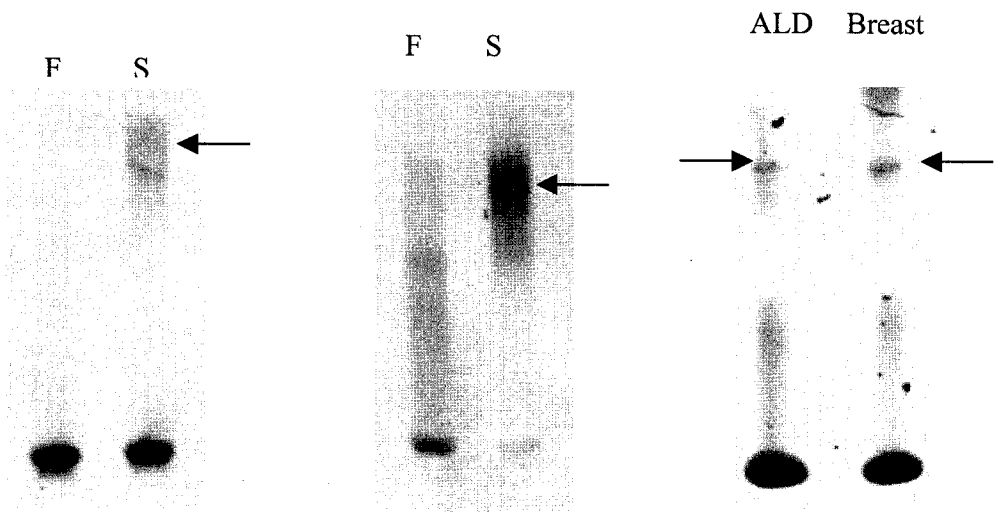

Thunnus albacares [tuna]

Clupea harengus harengus [Atlantic herring]

Gallus gallus [chicken]

Fig.5.3 Polyacrylamide gel electrophoresis of G-actin isoforms in the presence of 4M urea.

F- fast muscle actin; S-slow muscle actin.

Samples [2-4μg] diluted in 2mM Tris-HCl, 0.1mM $CaCl_2$, 0.2mM ATP, 2mM DTT, pH 8.0 in the presence of 10%[v/v] glycerol were loaded onto a pre-run [for 1hr at 140v] 6.5%[m/v] polyacrylamide gel containing 4M urea. Electrophoresis was for 1hr at 140v at room temperature. The gels were stained with Coomassie blue R-250. The arrows show the inactivated G-actin aggregates. As salmonid isoactins (408), Atlantic herring and Tuna slow muscle actins unfold at 4M urea forming inactivated aggregates while the proportion of the formation of these aggregates in fast muscle actins is much less.

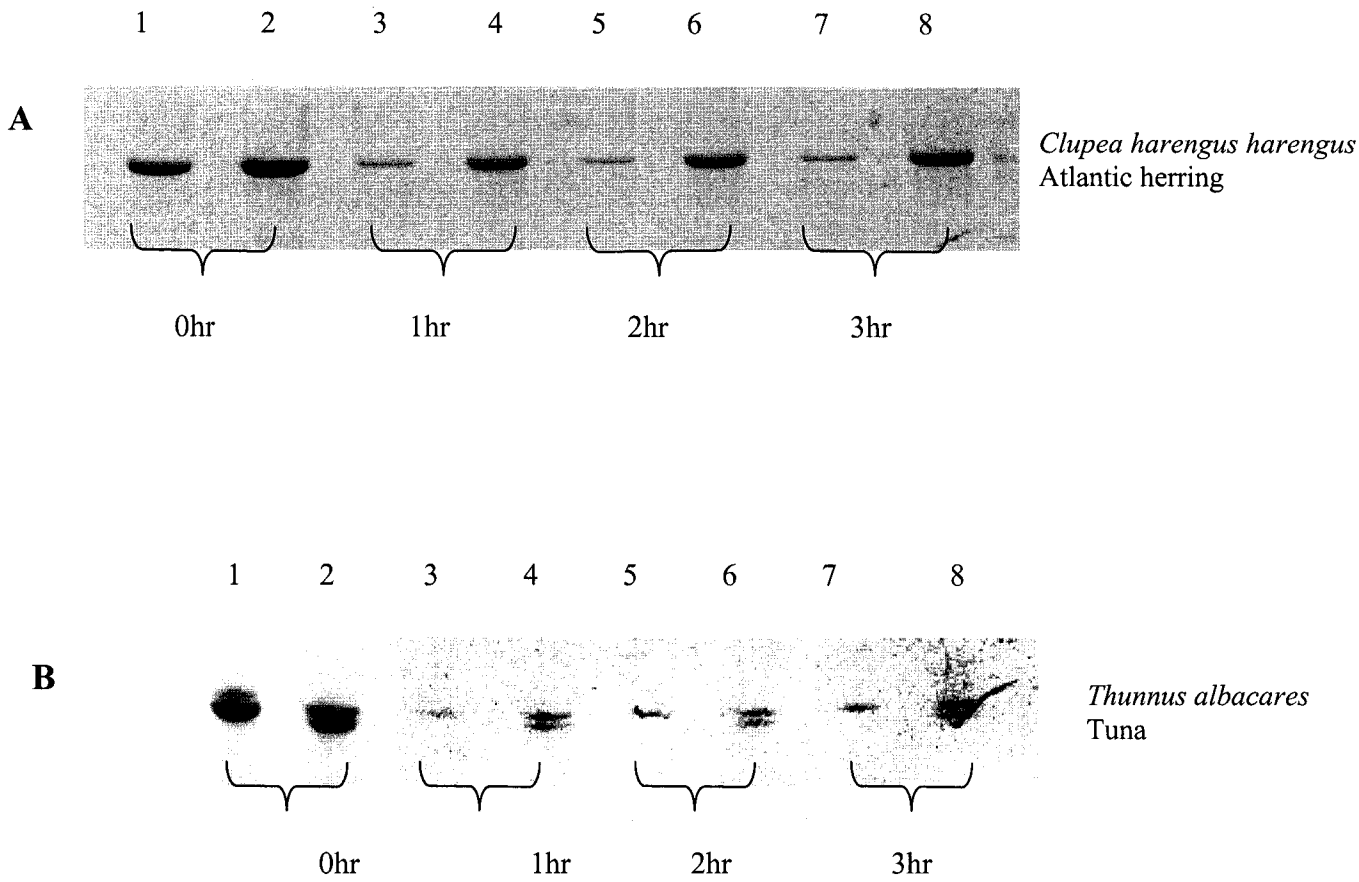

Fig.5.4 SDS-polyacrylamide gel analysis of time course polymerization of isoactins extracted from various species.

The experimental conditions were as outlined under Material and Methods. As shown in gel A, the pattern of polymerization is the same as salmon isoactins, while it is different in tuna, possibly due to presence of two isoforms in the slow muscle actin extract.

5.6Thermal unfolding of isoactins

Thermal unfolding was carried out using circular dichroism spectropolarimetry as discussed under Materials and Methods. The results are tabulated in Table 5.1. First, the transition temperature [Tms] of ALD, Atlantic herring fast, and mako shark fast actin are similar to salmon fast actin (408). Second, Atlantic herring slow muscle actin is more thermally stable than salmon slow muscle actin. Third, a higher Tm was observed in tuna fast muscle actin when compared to the salmon fast muscle actin. The endothermy in tunas may account for greater thermal stability of fast muscle actin. Surprisingly, two different Tms were observed in chicken breast and ALD isoactins even though there was no difference observed between these actins in other experiments, such as alkaline urea PAGE and PAGE in the presence of 4M urea and according to literature chicken contains only one skeletal muscle actin.

5.7 Mass spectrometric analysis of isoactins

Molecular masses of actin isoforms were determined using MALDI-TOF mass spectrometry. Freeze-dried samples were dissolved in 0.2% [v/v] trifluoro acetic acid and 50%[v/v] acetonitrile. Table 5.2 illustrates the molecular weights of isoactins. According to the amino acid sequence, the molecular weight of chicken breast actin is 41823Da [corrected for the N-terminal acetylation and methylation of His73], and the experimental value was 41808Da.

Table 5.1 The transition temperatures of fast and slow muscle isoactins as determined by circular dichroism spectroscopy.

Species	Transition Temperature [Tm],°C	
	Fast muscle actin	Slow muscle actin
Salmo salar [salmon]	55.0	45.0
Gallus gallus [chicken]	58.9	55.4
Xenopus laevis [frog]	59.6	59.2
Thunnus albacares [tuna]	57.6	-
Clupea harengus harengus [herring]	55.8	49.0
Prionace glauca [mako shark]	55.0	-

Proteins were dialyzed against HEPES buffer [5mM Hepes, 0.2mM $CaCl_2$, 0.2mM ATP, 0.01%[w/v] NaN_3 and 2mM DTT, pH 8.0] and concentration was adjusted to 1.5mg/ml. Temperature was increased from 5 to 65^{0}C and change in ellipticity at 222nm was monitored. The Tms were obtained from the 1st derivative of the change in ellipticity with temperature. The experiment was repeated at least twice from each batch of protein preparation. Number of batches = 2.

Table 5.2 Molecular weights of isoactins as determined by MALDI-TOF.

Species	Molecular mass of isoactins,Da	
	Fast muscle actin	Slow muscle actin
Gallus gallus [chicken]	41808	41817
Xenopus laevis [frog]	41763	41770
Thunnus albacares [tuna]	41767	-
Clupea harengus harengus [herring]	41787	41825
Prionace glauca [mako shark]	41822	-

The shown values are not averaged. Attempts to measure the molecular weight of tuna and mako shark slow muscle actins [which are contaminated with fast muscle isoform] were unsuccessful.

The difference of 23Da observed in frog skeletal muscle probably due to the presence of Na^+. The comparison for the other isoforms cannot be performed due to the unavailability of amino acid sequences in the protein data bank.

5.8 The cDNA library sequencing of dogfish shark skeletal actin

As a continuation of this study, a clone encoding dogfish shark actin was identified from a cDNA library. The cDNA and the amino acid sequences [accession no. AF388172] are given in Fig.5.5 and 5.6, respectively. As shown in Table 5.3, there is a greater homology of the dogfish shark actin to the salmonid fast and cardiac actins than to salmonid slow actin [when compared the non-conservative amino acid substitutions]. A comparison of amino acid substitutions [both conservative and non-conservative] is given in Table 5.4. Interestingly, dogfish shark actin also contains a unique substitution at position 51[Ala] where it is Ser in all the other amino acid sequences listed in the Genbank. Note that this residue is a part of the DNase I binding looping. Secondly, when comparing all the substitutions with salmonid isoactins, it is apparent that dogfish shark actin is more hydrophilic than that of salmon slow actin as it is comprised of Thr/Val, Thr/Ala, and Gln/Ala [Thr in dogfish shark and Val in salmon slow].

```
   1atgtgtgacg acgaggaaac cacagcactg gtctgtgaca acggctccgg tctggtaaag
  61 gctggctttg ccggtgatga cgctcccagg gctgtcttcc cttccatcgt gggccgaccc
 121 aggcaccagg gtgtcatggt tggtatgggt caaaaagacg cctatgtagg agatgaggcc
 181 cagagcaaga gaggtatcct gactttaaaa tacccaattg aacacggcat cattaccaac
 241 tgggatgata tggagaagat ctggcaccac actttctaca atgagctgcg tgtggcccct
 301 gaggaacatc ccaccctgct cactgaagcc cccctcaacc ccaaggctaa ccgagagaag
 361 atgacccaaa tcctgtttga gaccttcaac gtacccgcca tgtatgtcgc catccaagct
 421 gtgctgtccc tgtacgcctc cggtcgcaca actggtattg ttctggactc tggtgatggt
 481 gtgacccata acgtccccat ctatgaaggt tatgctctcc ctcacgccat catgcgcctg
 541 gatctggctg gtcgcgacct gactgactac ctgatgaaga ttctcacaga gcgtggttat
 601 tcatttgtca ccactgctga acgtgaaatt gtccgtgaca tcaaggaaaa actttgctac
 661 gtggctctgg actttgagaa tgagatggca acagctgcat catcttcatc tctggagaaa
 721 agttatgaac ttcccgatgg ccaggtcatc accattggca atgagcgttt caggtgccca
 781 gagaccctct ttcagccatc cttcattggt atggaatctg atggcattca tgagaccacc
 841 tacaacagca ttatgaagtg tgatattgac attcgtaagg atctgtacgc caacaatgtc
 901 ctatctggtg gtaccaccat gtaccccggt attgctgacc gcatgcagaa ggaaatcact
 961 gccctagccc ccagcactat gaagattaag attattgccc cacctgagcg taaatactcc
1021 gtctggattg gaggctccat cttagcttca ctgtccacct tccagcagat gtggattagc
1081 aaacaggaat atgatgaggc gggtccctct attgtacaca ggaaatgctt ctaa
```

Fig.5.5 The complete cDNA sequence of dogfish shark skeletal actin.

```
        10         20         30         40         50         60
MCDDEETTAL VCDNGSGLVK AGFAGDDAPR AVFPSIVGRP RHQGVMVGMG QKDAYVGDEA

        70         80         90        100        110        120
QSKRGILTLK YPIEHGIITN WDDMEKIWHH TFYNELRVAP EEHPTLLTEA PLNPKANREK

       130        140        150        160        170        180
MTQILFETFN VPAMYVAIQA VLSLYASGRT TGIVLDSGDG VTHNVPIYEG YALPHAIMRL

       190        200        210        220        230        240
DLAGRDLTDY LMKILTERGY SFVTTAEREI VRDIKEKLCY VALDFENEMA TAASSSSLEK

       250        260        270        280        290        300
SYELPDGQVI TIGNERFRCP ETLFQPSFIG MESDGIHETT YNSIMKCDID IRKDLYANNV

       310        320        330        340        350        360
LSGGTTMYPG IADRMQKEIT ALAPSTMKIK IIAPPERKYS VWIGGSILAS LSTFQQMWIS

       370
KQEYDEAGPS IVHRKCF
```

Fig.5.6 The predicted amino acid sequence of dogfish shark skeletal actin as determined by the dideoxy method.

The estimated molecular weight of the posttranslationally modified dogfish shark actin is 41840 Da.

Table 5.3 The comparison of total number of substitutions of dogfish shark skeletal actin with other isoactins.

	Dogfish shark	Salmon slow	Salmon fast	Salmon cardiac	Rodent skeletal
Dogfish shark	-	12	6	4	6
Salmon slow	12	-	12	12	12
Salmon fast	6	12	-	2	6
Salmon cardiac	4	12	2	-	4
Rodent skeletal	6	12	4	4	-

Table 5.4 The comparison of dogfish shark skeletal actin with salmonid isoactins.

Position in the sequence	Dogfish shark actin	Salmon fast actin	Salmon slow actin	Salmon cardiac actin
2	Asp		Glu	
3	Glu	Asp		Asp
51	Ala	Ser	Ser	Ser
103	Thr		Val	
155	Ser		Ala	
165	Ile		Val	
278	Thr	Ala		Ala
281	Ser		Gly	
310	Ala		Gly	
318	Ile	Thr	Thr	Thr
329	Ile		Met	
354	Gln	Ala	Ala	
358	Ser	Thr		
360	Gln		Asp	
363	Asp		Glu	

The comparison was carried out with respect to dogfish shark actin.

5.9 Evolutionary relationships of isoactins

To examine the evolutionary relationships of deuterostome actin isoforms, especially in relation to salmonid isoactins, a molecular phylogenetic analysis of actin amino acid and nucleotide sequences was performed. Deduced amino acid and nucleotide sequences were aligned using CLUSTAL W (413) and the phylogenies were constructed using the Neighbor-Joining [NJ] (414), Minimum Evolution [ME], or Bayesian analysis [BA] methods as implemented in the MEGA 3.1 or Mr.Bayes 3.1.2 programs. The analysis using Mr.Bayes 3.1.2 were carried out by Dr. D. Marshall [Department of Biology, Memorial University of Newfoundland].

One phylogenetic tree was constructed using the ME method and bootstrapping for support at the nodes, and the other with the NJ method and estimation of branch lengths for support of branches leading to nodes. About 95% or greater support on nodes is considered to be statistically valid. However, about 80% or greater is often considered as satisfactory as well. For this analysis amino acid sequences were obtained from GenBank [Fig.5.7]. The NJ [Fig.5.8 [A]] and ME [5.8[B]] analyses gave essentially similar results with respect to the major clusters identified. Due to the lack of statistical support observed in the results of these phylogentic trees, which were constructed using amino acid sequences, trees were again constructed using nucleotide sequences. To construct these trees, the NJ and BA methods were used and lamprey [*Lethenteron japonicum*] muscle actin was used as an out-group to root the nodes. To minimize the complexity of the tree, a reduced number of nucleotide sequences were utilized.

1.	*Bos taurus* alpha-aortic smooth muscle actin	P62739
2.	*Bos taurus* alpha-skeletal actin precursor	AAA82873
3.	*Cyprinus carpio* alpha-skeletal muscle actin	P53479
4.	*Fugu rubripes* alpha- cardiac muscle actin1	P53480
5.	*Fugu rubripes* alpha-skeletal muscle actin1	P68140
6.	*Gadus morhua* alpha-fast skeletal muscle actin	AAM21702
7.	*Gallus gallus* alpha actin	AAA98527
8.	*Gallus gallus* alpha-cardiac muscle actin	P68034
9.	*Homo sapiens* actin, alpha 1, skeletal muscle	CAI19051
10.	*Homo sapiens* actin, alpha 2- aorta smooth muscle actin	CAI13865
11.	*Homo sapiens* actin, alpha, cardiac muscle actin	P68032
12.	*Lethenteron japonicum* muscle actin	BAB79590
13.	*Mus musculus* alpha-cardiac muscle actin	P68033
14.	*Mus musculus* actin alpha 2- aorta smooth muscle actin	NP_031418
15.	*Mus musculus* alpha 1-skeletal muscle actin	NP_033736
16.	*Oryctolagus cuniculus* alpha-aortic smooth muscle actin	P62740
17.	*Rattus norvegicus* alpha, cardiac muscle actin	P68035
18.	*Rattus norvegicus* alpha-aortic smooth muscle actin	P62738
19.	*Rattus norvegicus*, alpha 1, skeletal muscle actin	NP_062085
20.	*Salmo salar* alpha-fast muscle actin.	AAG25672
21.	*Salmo trutta* alpha-cardiac muscle actin	AAG22822
22.	*Salmo trutta* alpha-slow muscle actin	AAF75784
23.	*Scyliorhinus retifer* alpha-fast muscle actin.	AAK70884
24.	*Sus scrofa* alpha-skeletal muscle actin	P68137
25.	*Takifugu rubripes* alpha1-skeletal muscle actin	P68140
26.	*Takifugu rubripes* alpha-cardiac muscle actin	P53480
27.	*Xenopus laevis* alpha-aortic smooth muscle actin	AAX85448
28.	*Xenopus laevis* alpha-cardiac muscle actin	P04751

Fig.5.7 Accession numbers taken from GenBank.

Fig.5.8 Molecular phylogenetic analysis of the amino acid sequences of isoactins of selected species.

The total number of amino acids [377] were subjected to phylogenetic analysis. [A] phylogenetic tree inferred by the neighbour-joining method. Branch lengths are proportional to evolutionary distances. *Scale bar* indicates an evolutionary distance of 0.005 amino acid substitutions per position in the sequence. [B] Phylogeny inferred by the minimum evolution method. Numbers shown in both trees are percentages of 1,000 bootstrap replicates. All the accession numbers are given in Fig.5.7

A

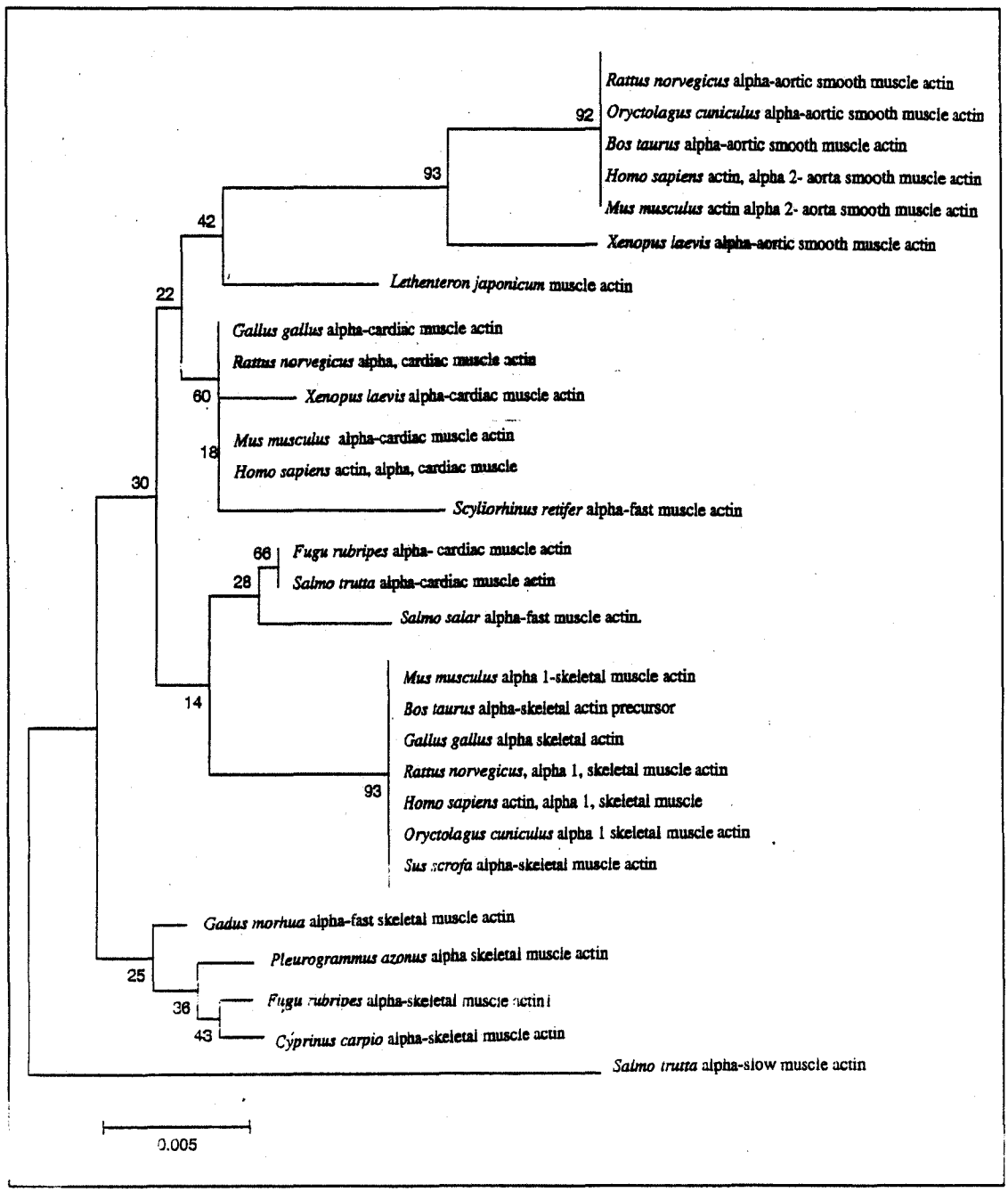

Fig.5.8 continued on the next page.

B

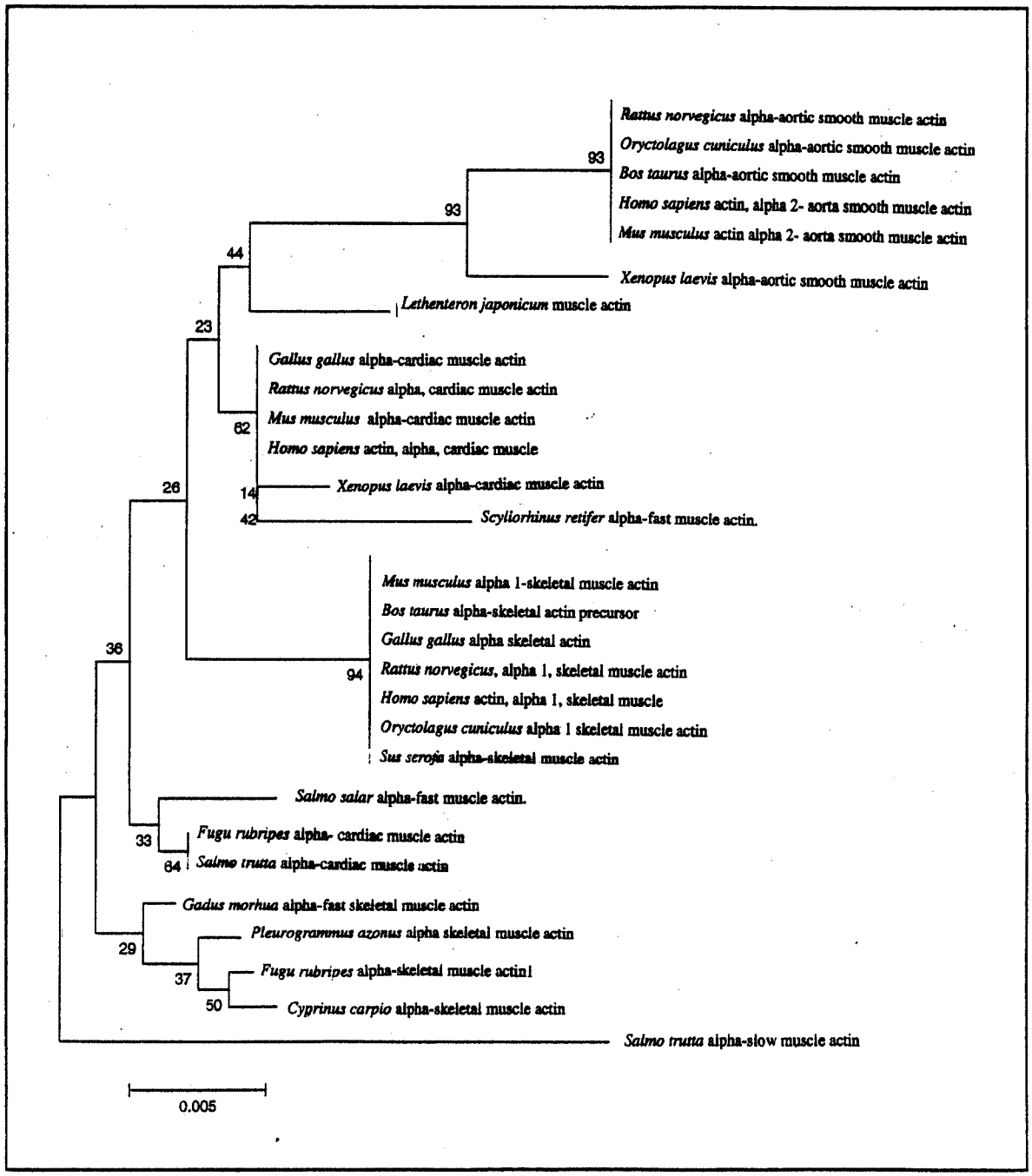
Rattus norvegicus alpha-aortic smooth muscle actin
Oryctolagus cuniculus alpha-aortic smooth muscle actin
Bos taurus alpha-aortic smooth muscle actin
Homo sapiens actin, alpha 2- aorta smooth muscle actin
Mus musculus actin alpha 2- aorta smooth muscle actin
Xenopus laevis alpha-aortic smooth muscle actin
Lethenteron japonicum muscle actin
Gallus gallus alpha-cardiac muscle actin
Rattus norvegicus alpha, cardiac muscle actin
Mus musculus alpha-cardiac muscle actin
Homo sapiens actin, alpha, cardiac muscle
Xenopus laevis alpha-cardiac muscle actin
Scyliorhinus retifer alpha-fast muscle actin.
Mus musculus alpha 1-skeletal muscle actin
Bos taurus alpha-skeletal actin precursor
Gallus gallus alpha skeletal actin
Rattus norvegicus, alpha 1, skeletal muscle actin
Homo sapiens actin, alpha 1, skeletal muscle
Oryctolagus cuniculus alpha 1 skeletal muscle actin
Sus scrofa alpha-skeletal muscle actin
Salmo salar alpha-fast muscle actin.
Fugu rubripes alpha- cardiac muscle actin
Salmo trutta alpha-cardiac muscle actin
Gadus morhua alpha-fast skeletal muscle actin
Pleurogrammus azonus alpha skeletal muscle actin
Fugu rubripes alpha-skeletal muscle actin1
Cyprinus carpio alpha-skeletal muscle actin
Salmo trutta alpha-slow muscle actin
93
93
44
23
82
26
14
42
36
94
33
64
29
37
50
0.005

As shown in Fig.5.9 [A] the phylogenetic tree constructed using the BA method gives high probabilities at the nodes, when compared to bootstrap support for nodes on the tree constructed using the NJ method [5.9[B]].

Discussion.

The alkaline urea gel and immunoblotting analysis confirmed that, in contrast to mako shark, frog and chicken, Atlantic herring tune and salmon contain a separate actin gene in its slow muscle implying that this gene expresses in some of the aquatic species. This is evidenced by the absence of a slow muscle actin isoform in other higher vertebrates including rat, mouse, pig and human (415-419). The existence of a single skeletal actin isoform in chicken and frog embryos (420) as well has been previously reported.

First, according to the amino acid phylogeny, first, using mid point rooting, salmon slow actin is the out-group to Atlantic cod [*Gadus* morhua] fast skeletal muscle actin. Secondly, all fish skeletal muscle actins cluster together except salmon fast and dogfish shark isoactins. Surprisingly, dogfish shark actin seems to be closely related to mammalian and frog [*Xenopus laevis*] cardiac isoactins. On the other hand,,salmon fast actin is grouped with salmon and puffer fish [*Fugu rubripes*] cardiac isoactins. Note that in particular this latter relationship is not strongly supported by bootstrap replicates. As to the grouping of mammalian aortic smooth muscle actins with frog aortic smooth muscle actin, this was strongly supported with 93% of the bootstrap replicates as was the grouping of mammalian and Atlantic cod skeletal muscle actins with 94%. However, the support for other nodes is

A

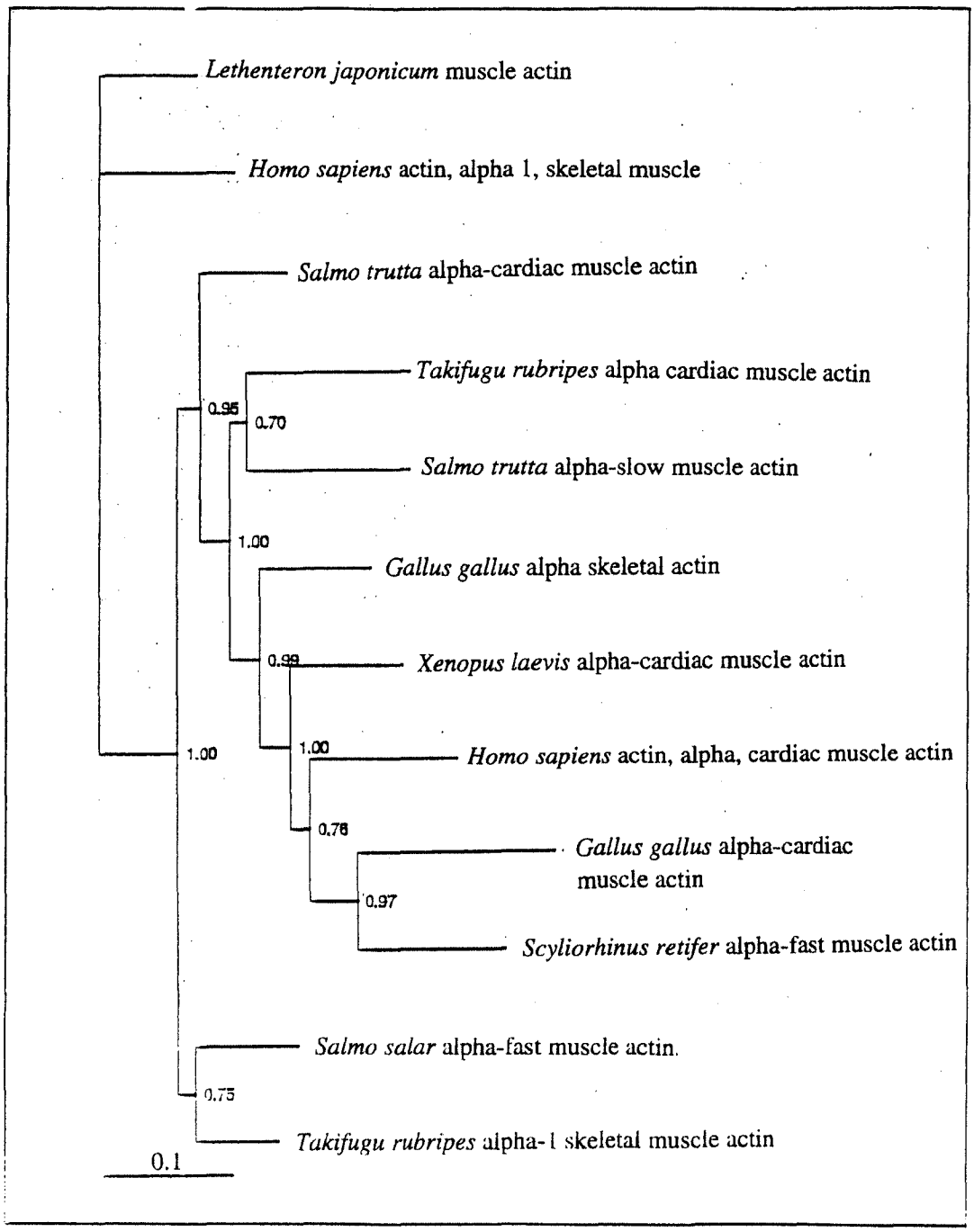

Fig.5.9 continues on the next page.

B

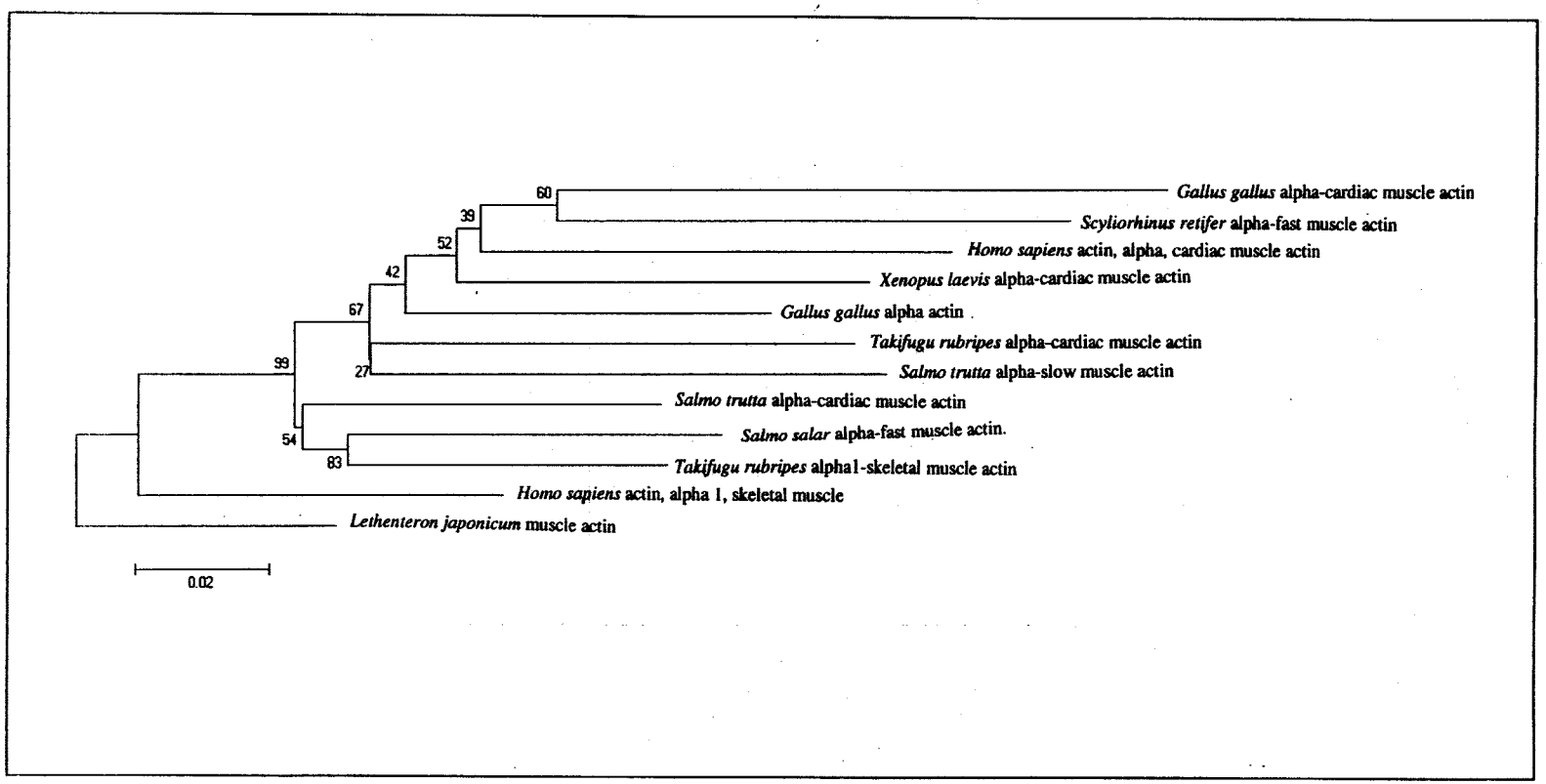

Fig.5.9 Phylogentic trees of the aligned actin nucleotide sequences of selected species.

[A]Phylogenetic analysis to generate phenograms via the Bayesian method was implemented with MrBayes 3.1.2 computer package. [B] Phylogentic tree inferred by the neighbour joining method as implemented in MEGA 3.1. Branch lengths are proportional to evolutionary distances. *Scale bar* indicates an evolutionary distance of 0.02 amino acid substitution per position in the sequence. All the accession numbers are given in Fig. 5.7.

considerably lower, such that the results do not fall into the statistically defensible range. This is mainly due to the limited number of amino acid substitutions in the actin molecule.

As seen in Fig.5.9, human skeletal and lamprey muscle actins are clearly separated from other isoactins. The nucleotide sequences of salmonid isoactins reported here clearly fall into different categories of vertebrates. In the Bayesian phylogenetic analysis, salmon slow muscle actin was clustered together with puffer fish cardiac alpha actin 1 isoform while salmon fast actin is clustered together with puffer fish skeletal alpha actin 1.

The salmon slow muscle actin seems to have diverged from the ancestral actin after it diverged from salmon cardiac muscle actin. Interestingly, with 97% support dogfish shark actin is grouped together with chicken cardiac actin. The comparison of amino acid sequences between salmon slow and puffer fish cardiac actin shows six non-conservative substitutions and it is only two for both between salmon fast and puffer fish skeletal actin and chicken cardiac and dogfish shark fast actin. Therefore, it is apparent that the amino acid sequence of dogfish shark fast muscle actin is well preserved for a very long period.

Japanese puffer fish have two skeletal actin isoforms containing three non-conservative substitutions (421). The substitutions unique to salmonid slow muscle actin such as the charge substitution at 360 and Ala residue at 155 do not appear in these sequences. The comparison of slow muscle actin amino acid sequence with the other available vertebrate actin sequences in the GenBank revealed the diversity of non-conservative substitutions in the animal kingdom [Table 5.5]. The charge substitution at 360 can only be found in salmon.

Table 5.5 The diversity of salmonid non-conservative substitutions in the animal kingdom.

Substitution	No. of species having the substitution	Remarks
Val103Thr	2	In zebra fish and sea squirt [Molgula oculata] skeletal muscle
Ala155Ser	17	In fish, desert iguana [Dipsosaurus dorsalis] and pelican [Sphyraena idiastes]
Thr278Ala	23	Found in terestial [frog, rat, mouse and human] and aquatic species [zebra fish, lamprey]
Gly281Ser	1	Zebra fish [Brachydanio rerio]
Gly310Ala	1	Zebra fish [Brachydanio rerio]
Asp360Gln	0	-

A total of 100 sequences were analyzed. All the sequence data are taken from GenBank.

Val103Thr – Val at position 103 of salmon slow actin and other species documented under the column "remarks" is substituted with Thr in salmon fast actin.

Further, the substitutions, Gly281Ser and Gly310Ala [Val in slow, Thr in fast] are only unique to salmon and zebra fish [*Brachydanio rerio*]. Interestingly, all the non-conservative substitutions of salmonid slow actin except the Asp360Gln, exist in zebra fish skeletal muscle actin. Therefore, zebra fish could be closely related to salmonids. The charge substitution at position 360 of salmon might have arisen as a result of a point mutation.

The nucleotide sequences of the 5' flanking region and the 3' untranslated region of actin genes have been reported to be isoform specific (422 and 423). Salmonid 5' and 3' untranslated sequences were compared with the few other available 5' and 3' untranslated sequences. The information, which can be gathered from this alignment, is very limited due to the fact that the salmonid non-coding sequences are short.

To study whether there is a relationship between the distribution of the slow muscle actin isoform in the phylogeny and the taxonomy of the species, a taxonomical study was carried out [Fig.5.10]. First, it is apparent that, as a result of the gene duplication, slow muscle actin isoform starts express in bony vertebrates [euteleostomi], hence it has not been observed in cartilaginous fish [e.g. mako shark]. Secondly, the expression of this isoform diverted towards teleostei [bony fish] and can only be found in some fish species such as salmon and Atlantic herring. However, the distribution of this isoform in fish is difficult to explain due to the lack of slow actin sequences in the Genbank.

In a comparison of the functional properties of salmon fast actin with slow actin it can be seen that fast actin is a thermally stable actin having greater ATPase activity and polymerization (408). This indicates that the existence of a second isoform [slow actin]

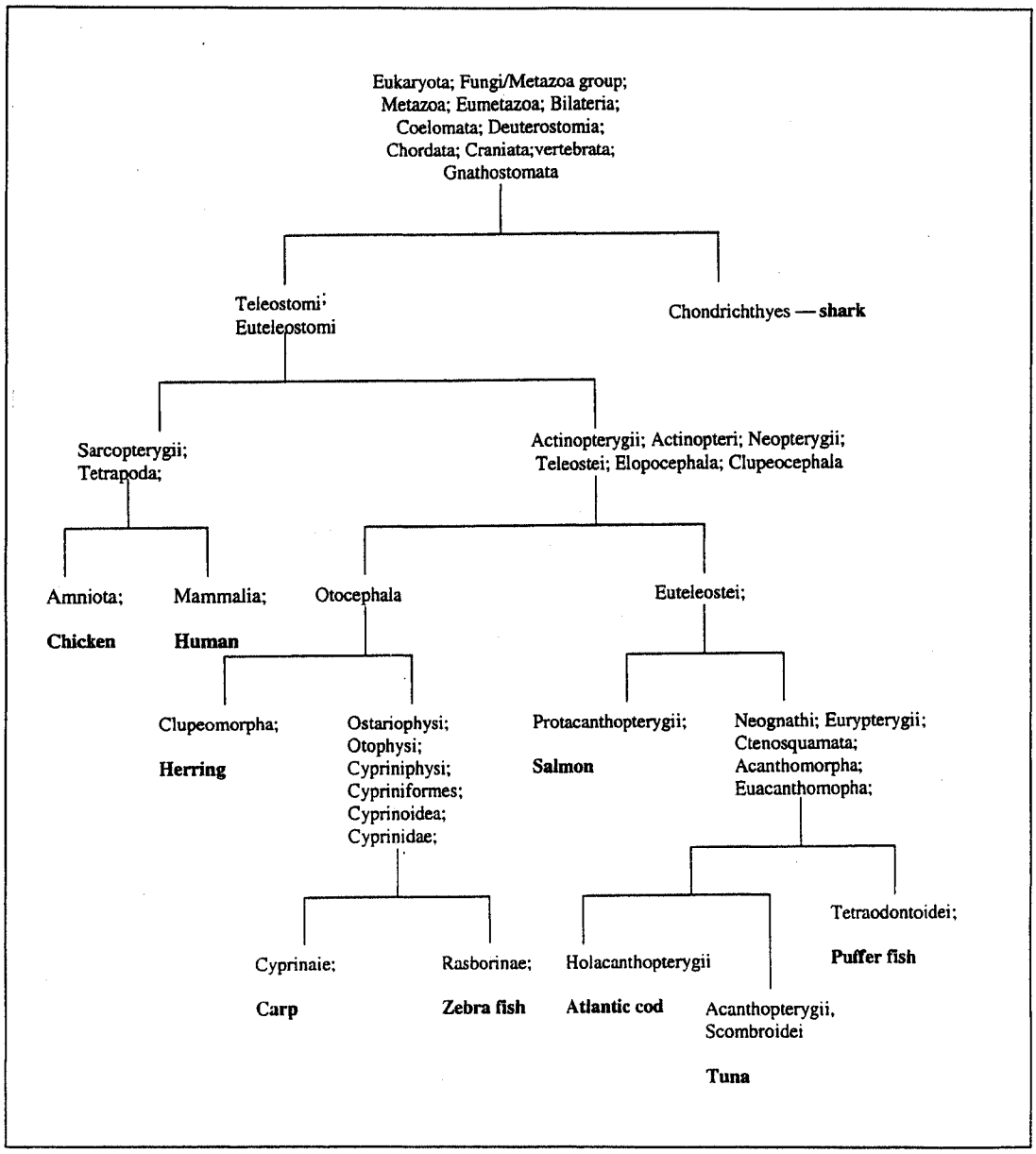

Fig.5.10 The distribution of selected species in the animal taxonomy

which is less effective is not important to the skeletal muscle system. Possibly due to this reason, and maybe due to environmental changes that occurred, the slow muscle actin gene stopped expressing in some species [e.g. tetrapodes].

Actin isoforms display very small differences in amino acid sequence across a diverse range of eukaryotic organisms, *e.g.* human, rat and chicken skeletal actin sequences are identical. This conservation is probably due primarily to selective pressure on the protein itself. However, an additional mechanism for maintaining homogeneity among members of gene families is gene conversion, the non-reciprocal exchange of portions of allelic or homologous non-allelic genes (424 and 425). Further, the nucleotide sequences of the 5' and 3' flanking regions and the location of introns are also helpful in determining the conservation of isoforms.

The factors that determine a particular protein's rate of change may be genetic, structural or functional. It has been shown that the evolutionary rates of molecules depend strongly on tissues where they are expressed specifically, and suggested the presence of functional constraints against molecular variations from the tissue level (426). Because family members often express tissue specifically and the evolutionary rates differ for different tissues, it is important to find the relationship between tissue and molecular evolution. The rate of change of eukaryotic actin is about 10% per billion years (427). One reason that actin changes slowly may have to do with the large number of macromolecular interactions that it possesses and those interactions must be preserved. For example, these include myosin, profilin, gelsolin etc. As such the various interactions are genetically interlocked, change in any one having a

potential consequence for the rest. This is evident in that, when muscle and non-muscle sequences are compared, the substitutions of an internal residue appear to be accompanied by another change in the vicinity, compensating for the effects of the first. Cys10/Val17 and Thr103/Val129 in muscle actins become, respectively, Val10/Cys17 and Val103/Thr129 in non-muscle actins. The exact symmetries of the compensatory pairs of the residues suggest that there are very specific requirements in the internal packing of amino acids in actin, probably to preserve and maintain the overall structure.

Chapter 6

Conclusions

The capacity for the diversity of striated muscle proteins is enormous. Numerous isoforms arise from the use of multiple genes, multiple promoters, and alternative splicing of individual genes. Additional diversity is supplied by the reversible phosphorylation of some of these proteins. Therefore, it is important to understand the difference in functionality of a given muscle protein variant. To this end, this thesis focuses on the evaluation of these phenomena as they apply to two striated muscle constituents namely, tropomyosin and actin. In addition, the distribution of a slow muscle isoform actin, thought not to exist in vertebrates, has been mapped.

As to the study on shark TM [Chapter 3], it is clear that phosphorylation at residue 283 exerts a significant impact on thin filament regulation. This is probably due to the strengthening of the end-to-end interaction which, in turn, may lead to the change in thin filament 'block' size [discussion – chapter 3]. As a result, a greater activation in thin filament regulation was observed in thin filaments containing PTM [2-fold activation over UnPTM; Figure 3.3, Chapter 3]. Further, the observed insignificant difference in myosin-S1 binding affinity [Figure 3.4, Chapter 3] with reconstituted thin filaments containing PTM/UnPTM is in good agreement with the above explanation. However, it cannot be ruled out that the observed difference in myosin-S1 activation could also be due to the difference in rate(s) in kinetic steps.

Heeley et al (1) reported the existence of two skeletal [fast and slow] and a cardiac muscle TM isoforms in salmon. From the results of Tn binding experiments [Chapter 3], affinity of these isoforms increases in the order: slow <fast < cardiac. It has been well documented that TM contains two binding regions for Tn in the thin filament [residues 10-30 and 174-216 (173)]. However, under the experimental conditions it is reasonable to assume that TM is in the monomeric form [no F-actin present either] and hence the end-to end interactions are absent. Therefore, it can be suggested that the non-conservative and conservative substitutions of the Tn binding region of these TM isoforms [174-216, see Table 3.2] are responsible for the observed difference in Tn binding affinity. When studying the amino acid substitutions in this region it is noted that salmon slow TM does not carry a single Ser residue in this region while salmon fast and cardiac TMs contained three and two Ser residues, respectively. However, while salmon cardiac TM does not contain any Thr residues in this region, but both salmon fast and slow TM carry Thr residues. Further, only cardiac TM, contains an amino acid with a charge substitution [216Glu in cardiac while it is Gln in fast and slow]. Secondly, it is possible to have long-range effect[s] from other non-conservative and conservative substitutions in the rest of the TM molecule on Tn binding. There are four charge substitutions in the N-terminal region [residues 9-50, see table 3.2]. Of these charge substitutions, three substitutions are located in the ***g*** position of the heptad sequence [residues 21, 42 and 49], while the fourth charge substitution [Leu39His, Leu in salmon fast vs His in salmon cardiac TM] is located in the ***d*** position. Interestingly, as a result of these substitutions the cardiac TM carries the least net charge in the N-terminal region while fast TM has the highest.

Therefore, the substituted amino acids in the region of 174- 216 along with rest of the substitutions could be responsible for the observed difference in Tn binding affinity.

Interestingly, the order of actomyosin-S1ATPase activities of reconstituted thin filaments of salmonid TMs is the same as the order of Tn binding affinity, implying that these substitutions which are in Tn binding region are involved in moving TM from the 'blocked' state to the 'open' state. Further, the other substitutions, including conservative and charge substitution at 276 [Asn/His], may also be involved in binding with actin giving a different level of ATPase activity.

When considering the results of all the experiments that have been carried out using salmonid isoactins, the uniqueness of salmon slow muscle actin is an eminent feature [Chapert 4], the uniqueness of salmon slow muscle actin is an eminent feature. Salmon slow muscle actin contains one dozen of substitutions compared to those isoforms present in salmon fast skeletal muscle, salmon cardiac muscle and rabbit skeletal muscle, and yet it shares considerably lower rate of polymerization resulting in a less viscous solution, and is less stable to both elevated temperature and chemical denaturants such as 8M urea and Gdn-HCl, thus having greater rate of unfolding compared to salmon fast actin. Under the steady state conditions salmon slow actin showed significantly less myosin activation. Further, its ability to displace ATP from the nucleotide binding pocket is greater with respect to salmon fast actn.

As mentioned in chapter 4, each G-actin monomer possesses several binding sites with other monomers in F-actin. Most of the substitutions are found in these interacting regions making it difficult to recognize one or a group of amino acids responsible for the change in the interactions. When considering the thin filament regulation, sub-domain-1 is of interest due to its carrying the myosin-S1 binding region. The changing interactions imposed by the charge substitution at 360, which is located in sub-domain-1, with other substitutions can account for the observed difference in thin filament regulation.

When considering the stability of ATP-G-actin, from the results of near and far-UV thermal unfolding [Fig. 4.25], it is reasonable to predict that the least stable region is sub-domain-1. Therefore, the exposed Cys residue [other than Cys374] at Tm could be Cys 10. However, the unfolded regions of the G-actin molecule in the presence of chemicals [8M urea and 4M Gdn-HCl] are not clear.

The ability to displace the nucleotide [ATP/ADP] is an important feature of G-actin. The amino acids, which stabilize the interactions with the nucleotide are highly conserved. However, according to the intrinsic fluorescence spectrum of mant-ATP-G-actin [Fig.4.23], the substitution Ser155Ala in slow actin changes the hydrophobicity of the nucleotide-binding pocket. The higher rate of displacement of ATP in slow muscle actin, when compared to salmon fast actin implies that the long-range interactions either by changing the interactions with the nucleotide or the metal ion, has had an impact on the strength of the nucleotide binding to molecule.

It is well documented that actin is an old highly conserved protein molecule. From the species analyzed [Chapter 5], it can be suggested that the slow muscle actin gene expresses randomly only in aquatic species. The non-conservative substitutions found in slow muscle actin can be seen in a few other species [see Table 5.5]. In particular, the charged substitution thought to be found only in Salmon. However, recently, it has been determined that Atlantic herring slow muscle actin also has this charge substitution [unpublished data from Heeley's lab]. Therefore, the charge substitution at 360 could be used as a marker for slow muscle actins. However, the evolutionary studies which were conducted using actin nucleotide sequences revealed that salmon slow muscle actin isoform is more closely related to puffer fish cardiac actin 1 isoform than it is to other sarcomeric actins. In addition, salmon fast actin isoform is clustered together with puffer fish skeletal alpha actin 1 isoform. The combination of this data with the taxonomical distribution of these selected species indicates that slow actin starts to express in slow twitch muscle as a result of the gene duplication which has been taken place prior to the divergence of bony vertebrates [euteleostomi] from cartilaginous fish [chondrichthyes]. The fact that it is then entered into clupeocephalians but not into tetrapodes, maybe due to structural, functional and/or environmental factors that affect on the expression of this isoform. However, it is difficult to gather more information pertaining to its distribution due to lack of slow muscle actin amino acid sequences in the data base.

Finally, it can be concluded that the amino acid substitutions [both conservative and non-conservative] observed in variant forms of actin and tropomyosin have short or long

range interactions with other thin filament proteins that may have caused them to perform its function to a different extent. Secondly, the charge substitution of salmon slow muscle actin at residue 360 can be used as a marker to identify slow muscle actin. However, further studies on slow muscle actin isoform amino acid sequences from other species are necessary to be done.

Future research work

It would be of interest to investigate the stability of salmonid isoTMs using circular dichroism and differential scanning colorimetry. This can be studied by thermal unfolding of isoactins in the presence of rabbit Tn and then with thin filament [either with rabbit actin or relevant salmonid isoactins] at the near and far-UV range. The interactions of F-actin affect the character of thermal unfolding of TM, leading to the appearance of a new Tm. Addition of Tn would change the Tm of F-actin bound TM. This experiment could be carried out in the presence and absence of Ca+2 and at different ionic strengths as well. To study the influence of isolated components of Tn, TnT, TnI and TnC could be added separately.

To determine the significance of the substitutions occurred in Tn binding region, mutational studies of recombinant TM could be carried out. The functional properties of the modified proteins could then be defined by actin affinity, TnT affinity and by regulation of reconstituted thin filaments. As a continuation of Tn binding with salmonid

TM isoforms, the experiment could be carried out using TnT bound affinity column material istead of whole Tn.

It is important to determine the unfolding regions in the presence of 8M urea and Gdn-HCl. This could be carried out by mapping the unfolded regions using enzymes such as trypsin and subtilisin. Further, size exclusion chromatography could be a valuable tool used to study the number of inactivated molecules at 4M urea concentration [in connection with Safer gel analysis] in each isoform.

The importance of conservative and non-conservative substitutions in the actin binding protein regions could be studied. For example, the charge substitution at 360 is in the binding site of profiline and hence a comparative study of profilin binding with salmonid actin will give insights to the orientation of this substitution in the sub domain-1

It is useful to study the nucleotide displacement of ATP-G-actin as a function of metal ion concentration [Mg^{+2} / Ca^{+2}]. Further, for a comparative study, the same experiment could be repeated using ADP-G-actin. The dissociation of nucleotide [either ATP or ADP] could be examined in the presence of EDTA using stop-flow apparatus.

Finally, as a continuation of the thin filament regulation studies on salmonid TM and actin isoforms at steady state, the same experiment could be repeated under pre-steady state conditions using stop-flow apparatus.

References

1. Heeley, D. H., Bieger, T., Walddleton, D. M., Hong, C., Jackman, D. M., McGowan, C., Davidson, W. S. and Beavis, R. C. (1995). Characterization of fast, slow and cardiac muscle tropomyosins from salmonid fish. *Eur. J. Biochem.* **232,** 226-234.
2. Sherwood, L. (1993). In Human Physiology, from Cells to Systems. (2nd edt.). New York west publishing company. Pg 213-240.
3. Bagshaw, C. R. (1993). In Muscle contraction. (2nd edt). New York, Chapman hall Publishers. Pg 5-10.
4. Ruegg, J. C. (1988). In calcium in muscle activation. (2nd edt). Springer-Verlag Publishers. Pg 5.
5. Brooke, M. H. and Kaiser, K. K. (1970). Muscle fibers-how many and what kind?. *Arch. Neurology* **23**, 369-379.
6. Huxley, A. F. and Niedergerke, R. (1954). Interference microscopy of living muscle fibers. *Nature* **173**, 971-972.
7. Huxley, A. F. and Hanson, J. (1954). Changes in the cross-striations of muscle contraction and their structural interpretation. *Nature* **173**, 973-976.
8. Bailey, K. (1946). Tropomyosin a new asymmetric protein component of muscle. *Nature*, **157**, 368.
9. Mak, A. S., Smillie, L. B. and Barany, M. (1978). Specific phosphorylation of serine 283 of alpha-tropomyosin from frog skeletal and rabbit skeletal and cardiac muscle. *Proc. Natl. Acad. Sci. USA* **75**, 3588-3592.

10. Woods, E. F. (1967). Molecular weight and subunit structure of tropomyosin B. *J.Biol.Chem.* **242**, 2859-2871.

11. Smillie, L.B. (1979). Structure and functions of tropomyosins from muscle and non-muscle sources. *Trends Biol. Sci.* **4**, 151-155.

12. Stone, D. and Smillie, L. B. (1978) The amino acid sequence of rabbit skeletal alpha-tropomyosin. The NH2-terminal half and complete sequence. *J.Biol.Chem.* **253**, 1137-1148.

13. Sodek, J., Hodges, R. S., Smillie, L. B. and Jurasek, L. (1972). Amino-acid sequence of rabbit skeletal tropomyosin and its coiled-coil structure. *Proc. Natl. Acad. Sci. USA* **69**, 3800-3804.

14. Crick, F. H. C. (1953). The packing of alpha helices; simple coiled coils. *Acta Crystallogr.* **6,** 689-697.

15. Cummins, P. and Perry, S. V. (1974). Chemical and immunochemical characteristics of tropomyosins from striated and smooth muscle. *Biochem. J.* **141**, 43-49.

16. Stewart, M. (2001). Structural basis for bending tropomyosin around actin in muscle thin filaments. *Proc. Natl. Acad. Sci. USA* **98,**8165-8166.

17. Lehrer, S. S. (1975). Intramolecular crosslinking of tropomyosin via disulfide bond formation: evidence for chain register. *Proc. Natl. Acad. Sci. USA* **72**, 3377-3381.

18. Stewart, M. (1975). Tropomyosin: evidence for no stagger between the chains. *FEBS Letts.* **53**, 5-7.

19. Johnson, P. and Smillie, L. B. (1975). Rabbit skeletal alpha-tropomyosin chains are in register. *Biochem. Biophys. Res. Commun.* **64**, 1316-1322.

20. Caspar, D. L. D., Cohen, C. and Longly, W. (1969) Tropomyosin: Crystal structure, polymorphism and molecular interactions. *J. Mol. Biol.* **41**, 87-94.

21. Cohen, C. and Szent-Gyorgyi, A. G. (1957). Optical rotation and helical polypeptide configuration in alpha-proteins. *J. Am. Chem. Soc.* **79**, 248.

22. McLachlan, A. D. and Stewart, M. (1975). Tropomyosin coiled coil interactions: evidence for an unstaggered structure. *J.Mol. Biol.* **98**, 293-304.

23. Lehrer, S. S. (1975). Intramolecular crosslinking of tropomyosin via disulfide bond formation: evidence for chain register. *Proc. Natl. Acad. Sci. USA* **72**, 3377-3381.

24. O'Shea, E. K., Klemm, J. D., Kim, P. S. and Alber, T. (1991). X-ray structure of the GCN4 leucine zipper, a two-stranded parallel-coiled coil. *Science* **254**, 539-544.

25. McLachlan, A. D. and Stewart, M. (1976). The 14-fold periodicity in α-tropomyosin and the interaction with actin *J.Mol. Biol.* **103**, 271-298.

26. Brown, J. H. , Kim, K. H. , Jun, G. , Greenfield, N. J. , Dominguez, R. , Volkmann, N. , Hitchcock-DeGregori, S. E. & Cohen, C. (2001) Deciphering the design of the tropomyosin molecule. *Proc. Natl. Acad. Sci. USA* **98**, 8496-8501.

27. Helfman, D. M., Feramisco, J. R., Ricci, W. M. and Hughes, S. H. (1984). Isolation and sequence of a cDNA clone that contains the entire coding region for chicken smooth-muscle alpha-tropomyosin. *J. Biol. Chem.* **259**, 14136-14143.

28. MacLeod, A. R., Houlker, C., Reinach, F. C. and Talbot, K. (1986). The mRNA and RNA-copy pseudogenes encoding TM30nm, a human cytoskeletal tropomyosin. *Nucleic Acids Res.* **14**, 8413-8426.

29. Mak. A. S., Smillie, L. B. and Stewart, G. R. (1980). A comparison of the amino acid sequences of rabbit skeletal muscle alpha- and beta-tropomyosins. *J. Biol. Chem.* **255**, 3647-3655.

30. Ooi, T., Mihashi, K. and Kobayashi, H. (1962). On polymerization of tropomyosin. *Arch. Biochem. Biophys.* **98**, 1-11.

31. Sousa, A. D. and Farah, C. S. (2002). Quantitative analysis of tropomyosin linear polymerization equilibrium as a function of ionic strength. *J.Biol.Chem.* **277**, 2081-2088.

32. Cohen, C., Caspar, D. L. D., Parry, D. A. D. and Lucas, R. M. (1971). Tropomyosin crystal dynamics. *Cold spring harbor* 205-216.

33. Ueno, H., Tawada, Y. and Ooi, T (1976). Porperties of non-polymerizable tropomyosin obtained by carboxypeptidase A digestion. *J. Biochem. (Tokyo)* **80**, 283-290.

34. Johnson, P. and Smillie, L. B. (1977). Polymerizability of rabbit skeletal tropomyosin: effects of enzymatic and chemical modifications. *Biochemistry* **16**, 2264-2269.

35. Walsh, T. P., Trueblood, C. E., Evans, R. and Webber, A. (1985) Removal of tropomyosin overlap and the co-operative response to increasing calcium concentrations of the acto-subfragment-1 ATPase. *J. Mol. Biol.* **182**, 265-269.

36. Hitchcock-DeGregori S. E and Heald, R.W. (1987). Altered actin and troponin binding of amino terminal variants of chicken striated muscle alpha-tropomyosin expressed in *Escherichia coli*. *J.Biol.Chem.* **262**, 9730-9735.

37. Heald, R.W. and Hitchcock-DeGregori S. E. (1988). The structure of the amino terminus of tropomyosin is critical for binding to actin in the absence and presence of troponin. *J.Biol.Chem.* **263**, 5254-5259.

38. Cho, Y. J. and Hitchcock-DeGregori S. E. (1990). The amino terminus of the muscle tropomyosin is a major determinant for function. *J.Biol.Chem* **265**, 538-545.

39. Mak, A. S. and Smillie, L. B. (1981). Non-polymerizable tropomyosin preparation, some properties and F-actin binding. *Biochem. Biophys. Res. Commun.* **101**, 208-214.

40. Monteiro, P .B., Lataro, R. C., Ferro, J. A. and Reinach, F. C. (1994). Functional alpha – tropomyosin produced in *Escherichia coli*. A dipeptide extension can substitute the amino-terminal acetyl-group. *J.Biol.Chem* **269**, 10461-10466.

41. Moraczewska, J. and Hitchcock-DeGregori S. E. (2000). Independent functions for the N- and C- termini in the overlap region of tropomyosin. *Biochemistry* **39**, 6891- 6897.

42. Graceffa, P and Lehrer, S. S. (1980). The excimer fluorescence of pyrene-labelled tropomyosin. A probe of conformational dynamics. *J.Biol.Chem* **255**, 11296-11300.

43. Sano, K., Maeda, K., Taniguchi, H. and Meada, Y. (2000). Amino acid replacements in an internal region of tropomyosin alter the properties of entire molecule. *Eur. J. Biochem.* **267**, 4870-4877.

44. Phillip, G. N. Jr., Fillers, J. P. and Cohen, C. (1986). Tropomyosin crystal structure and muscle regulation. *J.Mol.Biol.* **192**, 111-131.

45. Whitby, F. G. and Phillip, G. N. Jr. (2000). Crystal structure of tropomyosin at 7.0 ^{0}A resolution. *Proteins* **38**, 49-59.

46. Bailey, K. (1948). Tropomyosin: a new asymmetric protein component of muscle. *Biochem.J.* **43**, 271-275.

47. Astbury, W. T., Reed, R. and Spark, L. C. (1948). An X-ray and electron microscope study of tropomyosin. *Biochem. J.* **43**, 282-287.

48. Wakabayashi, T., Huxley, H. E., Amos, L. A. and Klug, A. (1975) Three-dimensional image reconstruction of actin-tropomyosin complex and actin-tropomyosin-troponin T-troponin I complex. *J.Mol.Biol.***93**, 477-484.

49. Li, Y., Mui, S., Brown, J. H., Strand, J., Reshetnikova, L., Tobacman, L. S. and Cohen, C. (2002). The crystal structure of the C-terminal fragment of striated muscle alpha tropomyosin reveals a key troponin T recognition site. *Proc. Natl. Acad. Sci. USA* **99**, 7378-7383.

50. Stewart, M. and Robert, G. C. (1983). Nuclear magnetic resonance evidence for a flexible region at the C-terminus of alpha tropomyosin. *J.Mol.Biol.* 166, 219-225.

51. Phillip, G. N. Jr., Fillers, J. P. and Cohen. C. (1980). Motions of tropomyosin: crystal as metaphor. *Biophys. J.* **32**, 485-502.

52. Greenfield, N. J., Swapna, G. V., Huang, Y., Palm, T., Graboski, S., Montelione, G. T. and Hitchcock-DeGregori S. E. (2003). The structure of the carboxyl terminus of striated alpha-tropomyosin in solution reveals an unusual parallel arrangement of interacting alpha helices. *Biochemistry* **42**, 614-619.

53. Mo, J. M., Holtzer, M. E. and Holtzer, A. (1991) Kinetics of self-assembly of -αα-tropomyosin coiled coils from unfolded chains. *Proc. Natl. Acad. Sci. USA* **88**, 916-920.

54. Kammerer, R. A., Schulthess, T., Landwehr, R., Lustig, A., Engle, J., Aebi, U. and Steinmetz, M. O. (1998) An autonomous folding unit mediates the assembly of two-stranded coiled coils. *Proc. Natl. Acad. Sci. USA* **95**, 13419-13424.

55. Pato, M. D., Mak, A. S. and Smillie, L. B. (1981). Fragments of rabbit striated muscle alpha-tropomyosin. I. Preparation and characterization. *J.Biol.Chem* **256**, 593-601.

56. Holtzer, M. E. and Holtzer, A. (1990). Alpha helix to random coil transitions of two-chain coiled-coils: experiments on the thermal denaturation of isolated segments of alpha-alpha tropomyosin. *Biopolymers* **30**, 985-993.

57. Potekhin, S. A. and Privalov, P. L. (1982). Co-operative blocks in tropomyosin. *J.Mol.Biol* **159**, 519-535.

58. Holtzer, M. E. and Holtzer, A. (1991). Uncooperative block in the tropomyosin coiled coil. *J. Am. Chem. Soc.* **113**, 7444-7445.

59. Holtzer, M. E. Crimmins, D. L. and Holtzer, A. (1995). Structural stability of short sequences of tropomyosin chain. *Biopolymers* **35**, 125-136.

60. Holtzer, M. E., Mints, L., Hogue, A. R., d'Avignon, D. A. and Holtzer, A. (2001) CD and 13Cα-NMR studies of folding equilibria in a two-stranded coiled coil formed by residues 190-254 of α-tropomyosin. B*iopolymers* **59**, 257-265.

61. Lee, D. L., Lavigne, P. and Hodges, R. S. (2001). Are trigger sequences essential in the folding of two-stranded α-helical coiled-coils?. *J.Mol.Biol* **306**, 539-553.

62. Paulucci, A. A., Hicks, L., Machado, A. M., Miranda, T. M., Kay, C. M. and Farah, C. S. (2002). Specific sequences determine the stability and cooperativity of folding of the C-terminal half of tropomyosin *J.Biol.Chem.* **277**, 39574-39584.

63. Woods, E. F. (1966). Dissociation of tropomyosin by urea. *J. Mol. Biol.* **16**, 581-584.

64. Ohyashiki, T., Kanaoka, Y. and Sekine, T. (1976). Studies on calcium ion-induced conformational changes in the actin-tropomyosin-troponin system by fluorimetry. Changes in the conformation of tropomyosin associated with functional states. *Biochim. Biophys. Acta* **420**, 27-36.

65. Phillip, G. N. Jr. and Chacko, S. (1996). Mechanical properties of tropomyosin and implications on muscle regulation. *Biopolymers*. **38**, 89-95.

66. Ebashi, S. and Ebashi, F. (1964). A new protein component participating in the super-precipitation of myosin B. *J. Biochem. (Tokyo).* **55**, 604.

67. Yang, Y. Z., Korn, E. D. and Eisenberg, E. (1979). Cooperative binding of tropomyosin to muscle and acanthamoeba actin. *J. Biol. Chem.* **254**, 7137-7140.

68. Lehrer, S. S., Golitsina, N. L. and Geeves, M. A. (1997). Actin-tropomyosin activation of myosin subfragment-1 ATPase and thin filament cooperativity: the

role of tropomyosin flexibility and end-to-end interactions. *Biochemistry* **36**, 13449-13454.

69. Bremel, R. D., Murray, J. M. Webber, A. (1973). Manifestation of cooperative behaviour in the regulated actin filament during actin-activated ATP hydrolysis in the presence of calcium. *Cold Spring Harbor Symp. Quant. Biol.* **37**, 267-275.
70. Cummins, P. and Perry, S. V. (1973). The subunits and biological activity of polymorphic forms of tropomyosin. *Biochem. J.* **133**, 765-777
71. Lees-Miller, J. P. and Helfman, D. M. (1991). The molecular basis for tropomyosin isoform diversity. *Bioessays* **13**, 429-437
72. Drees, B., Brown, C., Barrel, B. G. and Bretscher, A. (1995). Tropomyosin is essential in yeast, yet the TPM1 and TPM2 products perform distinct functions. *J. Cell. Biol.* **128**, 383-392.
73. Pittenger, M. F., Kazzaz, J. A. and Helfman, D. M. (1994). Functional properties of non-muscle tropomyosin isoforms. *Curr. Opin. Cell. Biol.* **6**, 96-104.
74. Helfman, D. M., Cheley, S., Kuismanen, E., Finn, A. and Yamawaki-Katoaka, Y. (1986). Non-muscle and muscle tropomyosins are expressed from a single gene by alternate splicing and polyadenylation. *Mol. Cell Biol.* **6**, 3582-3595.
75. Ruiz-Opazo, N. and Ginard, G. B. (1987). Alpha-tropomyosin gene organization. Alternative splicing of duplicated isotype-specific exons accounts for the production of smooth and striated muscle isoforms. *J. Boil. Chem.* **262**, 4755-4765.

76. Gunning, P., Gordon, M., Wade, R., Gailman, R., Lin, C. S. and Hardeman, E. (1990). Differential control of tropomyosin mRNA levels during myogenesis suggests the existence of an isoform competition- autoregulatory compensation mechanism. *Dev. Biol.* **138**, 443-453.

77. Heeley, D. H., Dhoot, D. K. and Perry, S. V. (1985). Factors determing the subunit composition of tropomyosin in mammalian muscle. *Biochem. J.* **226**, 461-468

78. Heeley, D. H., Dhoot, D. K., Frearson, N., Perry, S. V. and Vrbova, G. (1983). The effect of cross innervation on the tropomyosin composition of rabbit skeletal muscle. *FEBS Letts.* **152**, 282-286.

79. Amphlett, G. M., Syska, H. and Perry, S. V. (1976). The polymorphic forms of tropomyosin and troponin I in developing rabbit skeletal muscle. *FEBS Letts.* **63**, 22-26.

80. Palmiter, K. A., Kitada, Y., Muthuchamy, M., Wieczorek, D. F. and Solaro, R. J. (1996) Exchange of β- for α-Tropomyosin in hearts of transgenic mice induces changes in thin filament response to Ca^{2+}, strong cross-bridge binding, and protein phosphorylation *J. Biol. Chem.* **271,** 11611-11614.

81. Wolska, B. M., Keller, R. S., Evans, C. C., Palmiter, K. A., Phillip, R. M., Muthuchamy, M., Oehlenschlager, J., Wieczorek, D. F., de Tombe, P. P. and Solaro, R. J. (1999) Correlation Between Myofilament Response to Ca^{2+} and Altered Dynamics of Contraction and Relaxation in Transgenic Cardiac Cells That Express ß-Tropomyosin. *Circ. Res.* **84**, 745-751.

82. Straub, F. B. (1942). Actin. *Stud. Szeged.* **2**, 3-15.

83. Sheterline, P. and Sparrow, J. C. (1994). In Actin. Vol 1, London academic press Pg14-18.

84. Weeds, A. (1982). Actin binding proteins-regulators of cell architecture and motility. *Nature (London)* **296**, 811-816.

85. Nyman, T., Schuler, H., Korenbaum, E., Schutt, C. E., Karlsson, R. and Lindberg, U. (2002). The role of MeH73 in actin polymerization and ATP hydrolysis . *J. Mol. Biol.* **317**, 577-589.

86. Kalhor, H. R., Niewmierzycka, A., Faull, K. F., Yao, X., Grade, S., Clarke, S. and Rubenstein, P. A. (1999). A highly conserved 3-methylhistidine modification is absent in yeast actin. *Arch. Biochem. Biophys.* **370**, 105-111.

87. Carlier, M. P., Pantaloni, D. and Korn E.D. (1986). Fluorescence measurements of the binding of cations to high-affinity and low-affinity sites on ATP-G-actin. *J. Biol. Chem.* **261**, 10778-10784.

88. Asakura, S. (1961). The interactions between G-actin and ATP. *Arch. Biochem. Biophys.* **92**, 140-149.

89. Strohman, R. C. and Somorodin, A. J. (1962). The requirements for adenosine triphosphate binding to globular actin. *J. Biol. Chem.* **237**, 363-370.

90. Brenner, S. L. and Korn, E. D. (1984). Evidence that F-actin can hydrolyze ATP independent of monomer-polymer end interactions. *J. Biol. Chem.* **259**, 1441-1446.

91. Wegner, A. (1976). Head to tail polymerization of actin. *J. Mol. Biol.* **108**, 139-150.

92. Carlier, M. F. (1991) Actin: protein structure and filament dynamics. *J. Biol. Chem.* **266**, 1-4.

93. Iyengar, M. R. and Weber, H. H. (1964). The relative affinities of nucleotides to G-actin and their effects. *Biochim. Biophys. Acta* **86**, 543-553.

94. Higashi, S. and Oosawa, F. (1965). Conformational changes associated with polymerization and nucleotide binding in actin molecules. *J. Mol. Biol.* **12**, 843-865.

95. Cooke, R. and Murdoch, L. (1973). Interaction of actin with analogs of adenosine triphosphate. *Biochemistry* **12**, 3927-3932.

96. Cooke, R. (1975). The role of the bound nucleotide in the polymerization of actin. *Biochemistry* **14,** 3250-3256.

97. Lal, A. A., Brenner, S. L. and Korn, E. D. (1983). The kinetics of ADP-actin polymerization. *J. Cell Biol.* **97**, 289a

98. Hayashi, T. and Rosenbluth, R. (1962). Actin polymerization by direct transphosphorylation. *Biochem. Biophys. Res. Commun.* **8**, 20-23.

99. Carlier, M. P., Pantaloni, D. and Korn E.D. (1986). The effects of Mg+2 at the high affinity and low affinity sites on the polymerization of actin and associated ATP hydrolysis. *J. Biol. Chem.* **261**, 10785-10792.

100. Pollard, T. D. and Craig, S. W. (1982). Mechanism of actin polymerization. *Trends Biochem. Sci.* **7**, 55-58.

101. Suetsugu, S., Miki, H. and Takenawa, T. (2002). Spatial and temporal regulation of actin polymerization through Arp2/3 complex and WASP? WAVE proteins. *Cell motility and the cytoskeleton.* **51**, 113-122.

102. Cooper, J. A., Buhle, E. J., Jr., Walker, S. B., Tsong, T. Y. and Pollard, T. D. (1983). Kinetics evidence for a monomer activation step in actin polymerization. *Biochemistry* **22**, 2193-2202.

103. Tobacman, L. S. and Korn E.D. (1983). The kinetics of actin nucleation and polymerization. *J. Biol. Chem.* **258,** 3207-3214.

104. Frieden, C. (1983). Polymerization of actin: mechanism of the Mg^{+2} induced process at pH 8 and 20^0C. *Proc. Natl. Acad. Sci. USA* **80**, 6513-6517.

105. Woodrum, D. T., Rich, S. A. and Pollard, T. D. (1975). Evidence for the biased bidirectional polymerization of actin using heavu meromyosin produced by an improved method. *J. Cell Biol.* **67**, 231-237.

106. Pollard, T. D. (1986). Rate constants for the reactions of ATP- and ADP-actin with the ends of actin filaments. *J. Cell Biol.* **103**, 2747-2754.

107. Maruyama, K. (1981). Effects of trace amounts of Ca^{+2} and Mg^{+2} on the polymerization of actin. *Biochem. Biophys. Acta.* **667**, 139-142.

108. Frieden, C., Lieberman, D. and Gilbert, H. R. (1980). A fluorescent probe for conformational changes in skeletal muscle G-actin. *J. Biol. Chem.* **255**, 8991-8993.

109. Frieden, C. (1982). The Mg^{+2} induced conformational change in rabbit skeletal muscle G-actin. *J. Biol. Chem.* **257**, 2882-2886.

110. Lal, A. A., Korn, E. d., and Brenner, L. C. (1984) Rate constants for actin polymerization in ATP determined using cross-linked actin trimers as nuclei. *J. Biol. Chem.* **259**, 8794-8800.

111. Kasai, M., Asakura, S. and Oosawa, F. (1962). The cooperative nature of G-F transformation of actin. *Biochem. Biophys. Acta.* **57**, 22-31.

112. Dancker, P. and Low, I. (1977). Dual effect of Ca^{+2} on ultrasonic ATPase activity and polymerization of muscle actin. *Biochem. Biophys. Acta.* **484**, 169-176.

113. Avissa, N., Kaminsky, E., Leibovich, S. J. and Oplatka, A. (1979). Rabbit skeletal muscle F-actin can be stable at low ionic strength, provided trace amounts of Ca^{+2} are absent. *Biochem. Biophys. Acta.* **577**, 267-272.

114. Selden, L. A., Estes, J. E. and Gershman, L. C. (1983). The tightly bound divalent cation regulates actin polymerization. *Biochem. Biophys. Res. Commun.* **116**, 478-485.

115. Barden, J. A. and dos Remedios, C. G. (1985). Conformational changes in actin resulting from Ca2+/Mg2+ exchange as detected by proton NMR spectroscopy. *Eur. J. Biochem.* **146**, 5-8.

116. Martonosi, A., Molino, C. M. and Gergely, J. (1964). The Binding of Divalent Cations to Actin. *J. Biol. Chem.* **239,** 1057-1064.

117. Strzelecka – Golaszewska, H., Prochniewicz, E. and Drabikowski, W. (1978). Interaction of actin with divalent cations. 1. The effect of various cations on the physical state of actin. *Eur. J. Biochem.* **88,** 219-227.

118. Smith, P. R., Fowler, W. E., Pollard, T. D. and Aebi, U. (1983). Structure of actin molecule determined from electron micrographs of crystalline actin sheets with a tentative alignment of the molecule in the actin filament. *J. Mol. Biol.* **167**,641-660.

119. Kabsch, W., Mannherz, H. G., Suck, D., Pai, E. F. and Holmes, K. C. (1990). Atomic structure of the actin: DNase I complex. *Nature.* **347**, 37-44.

120. Mannherz, H. G., Kabsch, W. and Leberman, J. (1977). Crystals of skeletal muscle actin: Pancreatic DNAase I complex. *FEBS Letts.* **73**, 141-143.

121. McLaughlin, P. J., Gooch, J. T., Mannherz, H. G. and Weeds, A. G. (1993). Structure of gelsolin segment 1-actin complex and the mechanism of filament severing. *Nature.* **364**, 685-692.

122. Schutt, C. E., Myslik, J. C., Rozycki, M. D., Goonesekere, N. and Lindberg, U. (1993). The structure of crystalline profilin: β-actin. *Nature.* **365**, 810-816.

123. Otterbein, L. Graceffa, P. and Dominguez, R. (2001). The crystal structure of G-actin (abstract). *Biophys. J.* **80**, 172a

124. Otterbein, L. Graceffa, P. and Dominguez, R. (2001). The crystal structure of uncomplexed actin in the ADP state. *Science* **293**, 708-711.

125. Kinosian, H. J., Selden, L. A., Estes, J. E. and Gershman, L. C. (1993). Nucleotide binding to actin. Cation dependence of nucleotide dissociation and exchange. *J. Biol. Chem.* **268**, 8683-8691.

126. Tirion, M. M., Benavraham, D., Lorenz, M. and Holmes, K. C. (1995). Normal modes as refinement parameters for the F-actin model. *Biophys. J.* **68**, 5-12.

127. Bork, P., Sander, C., Valencia, A. (1992). An ATPase domain common to prokaryotic cell cycle proteins, sugar kinases, actin and hsp70 heat shock proteins. *Proc. Natl. Acad. Sci. USA* **89**, 7290-7294.

128. Maruyama, K. and Gergely, J. (1961) Removal of the bound calcium of G-actin by ethylenediaminetetraacetate (EDTA). *Biochem. Biophys. Res. Commun.* **6**, 245-249.

129. Lewis, M. S., Maruyama, K., Carrol, D. R., Kominz, D. R. and Laki, K. (1963) Physical properties and polymerization reactions of native and inactivated G-actin. *Biochemistry* **2**, 34-39.

130. Strzelecka – Golaszewska, H., Venyaminov, S., Yu., Zmorzynski, S. and Mossakowska, M. (1985). Effects of various amino acid replacements on the conformational stability of G-actin. *Eur. J. Biochem.***147**, 331-342.

131. Lehrer, S. S. and Kerwar, G. (1972) Intrinsic fluorescence of actin *Biochemistry* **11**, 1211-1217.

132. Kuznetsova, I. M., Khaitlina, S., Yu., Konditerov, S. N., Surin, A. M. and Turoverov, K. K. (1988) Changes of structure and intramolecular mobility in the course of actin denaturation. *Biophys. Chem.* **32**, 73-78.

133. Moore, P. B., Huxley, H. E. and deRosier, D. J. (1970). Three-dimensional reconstruction of F-actin, thin filaments and decorated thin filaments. *J. Mol. Biol.* **50**, 279-295.

134. Holmes, K. C., Popp, D., Gebhard, W. and Kabsch, W. (1990). Atomic model of the actin filament. *Nature* **347**, 44-49.

135. Lorenze, M., Popp, D. and Holmes, K. C. (1993). Refinement of the F-actin model against X-ray fiber diffraction data by the use of a directed mutation algorithm. *J. Mol. Biol.* **234**, 826-836.

136. Milligan, R. A., Whittaker, M. and Safer, D. (1990). Molecular structure of F-actin and location of surface binding sites. *Nature* **348,** 217-221.

137. http://www.mpimf-heidelberg.mpg.de/ [Dr. K. C. Holmes web site]

138. Grabaraek, Z. and Gergely, J. (1987). Troponin I binds to the N-terminal 12-residues segment of actin. *Biophys. J.* **51**, 331a

139. Grabaraek, Z., tao, T., Mabucni, Y., Gong, B. J. and Gergely, J. (1988). Actin-tropomyosin cross linking with the use of active esters. *Biophys. J.* **53**, 590a.

140. Rubenstein, P. A. (1990). The functional importance of multiple actin isoforms. *Bioessays* **12,** 309-315.

141. Sutoh, K. and Hatano, S. (1986). Actin-fragmin interactions as revealed by chemical cross-linking. *Biochemistry* **25**, 435-440.

142. Rayment, I., Holden, H. M., Whittaker, M., Yohn, C. B., Lorenz, M., Holmes, K. C. and Milligan, R. A. (1993). Structure of actin – myosin complex and its implications for muscle contraction. *Science* **261**, 58-65.

143. Shroder, R. R., Manstein, D. J., Jahn, W., Holden, H. M., Rayment, I., Holmes, K. C. and Spudich, J. A. (1993). Three-dimensional atomic model of F actin decorated with *Dictyostelium* myosin S1. *Nature.* **364**, 171-174.

144. Hegyi, G., Premecz, G., Sain, B. and Muhlrad, A. (1974) Selective carbethoxylation of the histidine residues of actin by diethylpyrocarbonate. *Eur. J. Biochem.* **44**, 7-12.

145. Bender, N., Fasold, H., Kenmoku, A., Middlehoff, G. and Volk, K. E. (1976) The selective blocking of the polymerization reaction of striated muscle actin leading to a derivative suitable for crystallization. Modification of Tyr-53 by 5-diazonium-(1H)tetrazole. *Eur. J. Biochem.* **64**, 215-218.

146. Burtnick, L. D. (1984). Modification of actin with fluorescein isothiocyanate. *Biochim, Biophys. Acta* **791**, 57-62.

147. Clermont, G. P. J., Machesky, L. M., Doberstein, S. K. and Pollard, T. D. (1991). Mechanism of the interaction of human platelet profilin with actin. *J. Cell Biol.* **113**, 1081-1089.

148. Pope, B., Way, M. and Weeds, A. G. (1991). Two of the three actin binding domains of gelsolin bind to the same subdomain of actin. Implication of capping and severing mechanisms. *FEBS Lett.* **280**, 70-74.

149. Hasegawa, T., Takahashi, S., Hayashi, H. and Hatano, S. (1980). Fragmin: a calcium ion sensitive regulatory factor on the formation of actin filaments. *Biochemistry* **19**, 2677-2683.

150. Bretscher, A. (1981) Fimbrin is a cytoskeletal protein that crosslinks F-actin in vitro. *Proc. Natl. Acad. Sci. USA* **78,** 6849-6853.

151. Bryan, J. and Kane, R. E. (1978) Separation and interaction of the major components of sea urchin actin gel. *J. Mol. Biol.* **125**, 207-224.

152. Zhu, X., Zeng, X., Huang, B. and Hao, S. (2004). Actin is closely associated with RNA polymerase II and involved in activation of gene transcription. *Biochem. Biophys. Res. Commun.* **321**, 623-630.

153. Garrels, J. I. and Gibson, W. (1976). Identification and characterization of multiple forms of actin. *Cell* **9**, 793-805.

154. Vanderkerckhove, J. and Weber, K. (1978a). At least six different actins are express in a higher mammal: an anlysis based on the amino acid sequence of the amino terminal tryptic peptide. *J. Mol. Biol.* **126**, 783-802.

155. Vanderkerckhove, J. and Weber, K. (1978b). Actin amino acid sequences. Comparison of actins from calf thymus, bovine brain, and SV40-transformed mouse 3T3 cells with rabbit skeletal muscle actin. *Eur. J. Biochem.* **90**, 450-462.

156. Vanderkerckhove, J. and Weber, K. (1978c). The amino acid sequence of *Physarum* actin: mammalian cytoplasmic actins are more related to actin from *Physarum polycephalum* than to mammalian skeletal muscle actins. *Nature* **276**, 720-721.

157. Vanderkerckhove, J. and Weber, K. (1979a). The complete amino acid sequences of actins from bovine aorta, bovine heart, bovine fast skeletal muscle and rabbit slow skeletal muscle: a protein chemical analysis of muscle actin differentiation. *Differentiation.* **14**, 123-133.

158. Vanderkerckhove, J. and Weber, K. (1979b). The amino acid sequence of actin from chicken skeletal muscle and chicken gizzard smooth muscle. *FEBS Letts.* **102**, 219-222.

159. Vanderkerckhove, J. and Weber, K. (1978). Mammalian cytoplasmic actins are the products of at least two genes and differ in primary structure in at least 25 identified positions from skeletal muscle actins. *Proc. Natl. Acad. Sci. USA* **75**, 1106-1110.

160. Buckingham, M. E. (1985). Actin and myosin multigene families: their expression during the formation of skeletal muscle. *Essays Biochem.* **20**, 77-109.

161. Mounier, N., Gouy, M., Mouchiroud, D and Prudhomme, J. C. (1992). Insect muscle actins differ distinctly from invertebrate and vertebrate cytoplasmic actins. *J. Mol. Evol.* **34,** 406-415.

162. Pollard, T. D. and Cooper, J. A. (1986). Actin and actin binding proteins: a critical evaluation of mechanisms and functions. *Annu. Rev. Biochem.* **55**, 987-1035.

163. Herman, I. M. (1993). Actin isoforms. *Curr. Biol.* **5**, 48-55.

164. Ebashi, S. and Endo, M. (1968). Calcium and muscle contraction. *Prog. Biophys. Mol. Biol.* **18,** 123-183.

165. Hitchcock, S. E., Huxley, H. E. and Szent-Gyorgyi, A. G. (1973). Calcium sensitivity binding of troponin to actin-tropomyosin: a two-site model for troponin action. *J. Mol. Biol.* **80,** 825-836.

166. Margossian, S. S. and Cohen, C. (1973). Structural interpretation of the two-site binding of troponin on the muscle thin filament *J. Mol. Biol.***149**, 541-550.

167. Potter, J. D. and Gergely, J. (1974). Troponin, tropomyosin and actin interactions in the Ca^{+2}: regulation of muscle contraction. *Biochemistry* **13**, 2697-2703.

168. Pearlstone, J. R. and Smillie, L. B. (1983). Effects of troponin I plus –C on the binding of troponin T and its fragments to alpha tropomyosin. Ca^{+2} sensitivity and cooperativity. *J. Biol. Chem.* **258,** 2534-2542.

169. Ebashi, S. (1960). Calcium binding and relaxation in the actomyosin system. *J. Biochem. (Tokyo).* **48,** 150-151.

170. Greaser, M. L. and Gergely, J. (1971). Reconstitution of troponin activity from three protein components. *J. Biol. Chem.* **246**, 4226-4233.

171. Malnic, B. and Reinach, F. C. (1994). Assembly of functional skeletal muscle troponin complex in *E.coli. Eur. J. Biochem.* **222,** 49-54.

172. Flicker, P. F., Phillips, J. G. N. and Cohen, C. (1982) Troponin and its interactions with tropomyosin: An electron microscope study. *J. Mol. Biol.***162**, 495-501.

173. White, S. P., Cohen, C. and Phillips, G. N. Jr (1987). Structure of co-crystals of tropomyosin and troponin. *Nature* **353**, 826-828.

174. Takeda, S., Yamashita, A., Maeda, K. and Maeda, Y. (2003). Structure of the core domain of human cardiac troponin in the Ca+2 saturated form. *Nature* **424**, 35-41.

175. Hartshorne, D. J. and Mueller, H. (1968). Fractionation of troponin into two distinct proteins. *Biochem. Biophys. Res. Commun.* **31**, 647-653.

176. Schaub, M. C. and Perry, S. V. (1969). The relaxing protein system of striated muscle. Resolution of the troponin complex into inhibitory and calcium ion sensitizing factors and their relationship to tropomyosin. *Biochem. J.* **115**, 993-1004.

177. Zot, A. S. and Potter, J. D. (1987). Structural aspects of troponin-tropomyosin regulation of skeletal muscle contraction. *Ann. Rev. Biophys. Chem.* **16**, 535-559.

178. Herzberg, O. and James, M. N. G. (1985). Structure of the calcium regulatory muscle protein troponin C at 2.8 A^0 resolution. *Nature* **313**, 653-659.

179. Sundaralingam, M., Bergstrom, R., Straburg, G., Rao, S. T., Roychowdhury, P., Greaser, M. and Wang, B. C. (1985). Molecular structure of troponin C from chicken skeletal muscle at 3.0 A^0 resolution. *Science* **227**, 945-948.

180. Herzberg, O. and James, M. N. G. (1988). Refined crystal structure of troponin C from turkey skeletal muscle at 2.0 A^0 resolution. *J. Mol. Biol.* **203**, 761-779.

181. Straburg, G., Rao, S. T., Pysalska, D., Drendel, W., Greaser, M. and Sundaralingam, M. (1988). Refined structure of chicken skeletal muscle troponin C in the two-calcium state at 2.0 A^0 resolution. *J. Biol. Chem.* **263**, 1628-1647.

182. Collins, J. H. (1974) Homology of myosin light chains, troponin-C and parvalbumins deduced from comparison of their amino acid sequences. *Biochem. Biophys. Res. Commun.* **58,** 301-308.

183. Kretsinger, R. H. and Barry, C. D. (1975). The predicted structure of the calcium binding component of troponin. *Biochem. Biophys. Acta* **405,** 40-52.

184. Slupsky, C. M. and Sykes, B. D. (1995). NMR solution structure of calcium – saturated skeletal muscle troponin C. *Biochemistry* **34**, 15953-15964.

185. Potter, J. D. and Gergely, J. (1975). The calcium and magnesium binding sites on troponin and their role in the regulation of myofibrillar ATPase. *J. Biol. Chem.* **250,** 4628-4633.

186. Potter, J. D., Seidel, J. C., Leavis, P. C., Lehrer, S. S. and Gergely, J. (1976) Effect of Ca2+ binding on troponin C. Changes in spin label mobility, extrinsic fluorescence, and sulfhydryl reactivity. *J. Biol. Chem.* **251**, 7551-7556.

187. Leavis, P. C., Rosenfeld, S. S., Gergely, J. and Drabikowski, W. (1978). Proteolytic fragments of troponin C: location of high and low affinity Ca^{+2} binding sites and interactions with troponin I and troponin T. *J. Biol. Chem* **253**, 5452-5459.

188. Holroyde, M. J., Roberston, S. P., Johnson, J. D., Solaro, R. J. and Potter, J. D. (1980) The calcium and magnesium binding sites on cardiac troponin and their role in the regulation of myofibrillar adenosine triphosphatase. *J. Biol. Chem.***255**, 11688-11693.

189. Wang, C. L. A., Zhan, Q., Tao, T. and Gergely, J. (1986). Effects of pH changes and binding of troponin I on the structure of troponin C. *Biophys. J.* **49**, 48a

190. Drakenberg, T., Forsen, S., Thulin, E. and Vogel, H. J. (1987). The binding of Ca^{+2}, Mg^{+2} and Cd^{+2} to tryptic fragments of skeletal muscle troponin C. Cadmium-113 and proton NMR studies. *J. Biol. Bhem.* **262**, 672-678.

191. Wang, C. L. A. and Gergely, J. (1986). Modulation of the interaction between the two halves of troponin C by the other troponin subunits. *Eur. J. Biochem.* **154**, 225-228.

192. Grabarek, Z., Leavis, P. C. and Gergely, J. (1986). Calcium binding to the low affinity sites in troponin C induces conformational changes in the high affinity domain. A possible route of information transfer in activation of muscle contraction. *J. Biol. Chem.***261**, 608-613.

193. Johnson, J. D., Charlton, S. C. and Potter, J. D. (1979). A fluorescence stopped flow analysis of Ca2+ exchange with troponin **C**. *J. Biol. Chem.***254**, 3497-3502.

194. Johnson, J. D., Robinson, D. E., Robertson, S. P., Schwartz, A. and Potter, J. D. (1981) In Regulation of muscle contraction: Excitiation-contraction coupling (Grinnel, A., ed), Academic Press, New York, Pg. 241-257.

195. Horwitz, J., Bullard, B. and Mercola, D. (1979). Interaction of troponin subunits. The interaction between the inhibitory and tropomyosin-binding subunits. *J. Biol. Chem.***254**, 350-355.

196. Perry, S. V., Cole, H., Head, J. F. and Wilson, F. J. (1972). Localization and mode of action of the inhibitory protein component of the troponin complex. *Cold Spring Harbor Symp. Quant. Biol.* **37,** 251-257.

197. Hitchcock, S. E. (1975). Regulation of muscle contraction. Binding of troponin C involved in calcium ion dependent interaction with troponin I. *Eur. J. Biochem.* **52,** 255-263.

198. Weeks, R. A. and Perry, S. V. (1978). Characterization of a region of the primary sequence of troponin C involved in calcium ion-dependent interaction with troponin I. *Biochem. J.* **173,** 449-457.

199. Chong, P. C. S., Asselberg, P. J. and Hodges, R. S. (1983). Inhibition of rabbit skeletal muscle acto S1-ATPase by troponin T. *FEBS Lett.* **153**, 372-376.

200. Moir, A.J.G., Wilkinson, J. M. and Perry, S. V.(1974). The phosphorylation sites of troponin I from cardiac muscle. *FEBS Lett.* **42,** 253-257.

201. Cole, H. A. and Perry, S. V. (1975). The phosphorylation of troponin I from cardiac muscle. *Biochem. J.* **149**, 525-533.

202. Syska, H., Wilkinson, J. M., Grand, R. J. A. and Perry, S. V. (1976). The relationship between biological activity and primary structure of troponin I from white skeletal muscle of the rabbit. *Biochem. J.* **153**, 375-387.

203. Talbot, J. A. and Hodges, R. S. (1979). Synthesis and biological activity of an icosapeptide analog of the actomyosin inhibitory region of troponin I. *J. Biol. Chem.* **254**, 3720-3723.

204. Cachia, P. J., Sykes, B. D. and Hodges, R. S. (1983). Calcium dependent inhibitory region of troponin. A proton magnetic resonance study on the interaction between troponin C and the synthetic peptide Nα-acetyl [F-phenylalanine 106] TnI (104-115) amide. *Biochemistry*. **22,** 4145-4152.

205. Van Eyk, J. E., Kay, C. M. and Hodges, R. S. (1991). A comparative study of the interaction of synthetic peptides of the skeletal and cardiac troponin I inhibitory region with skeletal and cardiac troponin C. *Biochemistry*. **30**, 9974-9981.

206. Huang, T. S., Bylund, D. B., Stull, j. and Krebs. E. (1974). The amino acid sequences of the phosphorylated sites in troponin-I from rabbit skeletal muscle. *FEBS letts*. **42**, 249-252.

207. Robertson, S. P., Johnson, J. D., Holroyde, M. J., Kranlas, E. G., Potter, J. D. and Solaro, R. J. (1982) The effect of troponin I phosphorylation on the Ca2+-binding properties of the Ca2+-regulatory site of bovine cardiac troponin. *J. Biol. Chem.* **257**, 260-263.

208. Campbell, A. P. and Sykes, B. D. (1991b). Interactions of troponin I and troponin C: Use of the two-dimensional NMR transferred nuclear Overhauser effect to determine the structure of the inhibitory troponin I peptide when bound to skeletal troponin C. *J. Mol. Biol.* **222**, 405-421.

209. Li, M. X., Spyracopoulos, L. and Sykes, B. D. (1999). Binding of cardiac troponin-$I_{147-163}$ induces a structural opening in human cardiac troponin-C. *Biochemistry* **38**, 8289-8298.

210. Pearlstone, J. R., Carpenter, M. R. and Smillie, L. B. (1986). Amino acid sequence of rabbit cardiac troponin T. *J. Biol. Chem.* **261,** 16795-16810.

211. Gusev, N. B., Barskaya, N. V., Verin, A. D., Duzhenkova, I. V., Khuchua, Z. A. and Zheltova, A. O. (1983). Some properties of cardiac troponin T structure. *Biochem. J.* **213**, 123-129.

212. Pearlstone, J. R. and Smillie, L. B. (1977). The binding site of rabbit skeletal alpha- tropomyosin on troponin T. *Can. J. Biochem.* **55**, 1032-1038.

213. Moir, A. J. G., Cole, H. A. and Perry, S. V. (1977). The phosphorylation sites of troponin T from white skeletal muscles and the effects of interaction with troponin C on their phosphorylation by phosphorylase kinase. *Biochem. J.* **161**, 371-382.

214. Heeley, D. H. (1994). Investigation of the effects of phosphorylation of rabbit striated muscle alpha-alpha- tropomyosin and rabbit skeletal muscle troponin T. *Eur. J. Biochem.* **221**, 129-137.

215. Mak, A. S. and Smillie, L. B. (1981). Structural interpretation of the two-site binding of troponin on the muscle thin filament. *J. Mol. Biol.***149**, 541-550

216. Dennis B. (2001). In *Cell Movements- from molecules to motility.* (2nd edn.) , Garland Publishes.

217. Sellers, J. R. (1999) in *Myosins*, (2nd edn.), Oxford Univ. Press, Oxford, U.K., Pg. 1-7.

218. Korn, E. D. (2000). Coevolution of head, neck and tail domains of myosin heavy chains. *Proc. Natl. Acad. Sci. USA* **97**, 12559-12564.

219. Cheney, R. E., Riley, M. A. and Mooseker, M. S. (1993). Phylogenetic analysis of myosin super family. *Cell Motil. Cytoskeleton* **24**, 215-223.

220. Weeds, A. G. (1969). Light chains of myosin *Nature* **223**, 1362-1364.

221. Weeds, A. G. and Lowey, S. J. (1971). Substructure of the myosin molecule. II. The light chains of myosin *J. Mol. Biol.* **61**, 701-725.

222. Titus, M. A. (1993). Myosins. *Curr. Opin. Cell Biol.* **5,** 77-81.

223. Titus, M. A. (1997). Motor proteins: Myosin V-the multi-purpose transport motor. *Curr. Biol.* **7,** R301-R304.

224. Gazith, J. S., Himmelfarb, S. and Harrington, W. F. (1970). Studies on the subunit structure of myosin *J. Biol. Chem.***245**, 15-22.

225. Wagner, P. D. and Weeds, A. G. (1977). Studies on the role of myosin alkali light chains. Recombination and hybridization of light chains and heavy chains in subfragment –1 preparations *J. Mol. Biol.* **109**, 455-470.

226. Dreizen, P. and Gershman, L. C. (1970). Relation of structure to function in myosin. II. Salt denaturation and recombination experiments. *Biochemistry* **9,** 1688-1693.

227. Kim, H. D. and Mommaerts, W. F. H. M. (1971). On the reconstitution of rabbit myosin from fast and slow muscle. *Biochim. biophys. Acta* **245**, 230-234.

228. Leger, J. J. and Marotte, F. (1975). The effects of concentrated salt solutions on the structure and the enzymatic activity of myosin molecules from skeletal and cardiac muscles. *FEBS Lett.* **52,** 17-21.

229. Frank, G. and Weeds, A. G. (1974). The amino-acid sequence of the alkali light chains of rabbit skeletal- muscle myosin. *Eur. J. Biochem.* **44**, 317-334.

230. Hayashibara, T. and Miyanishi, T. (1994). Binding of the amino-terminal region of myosin alkali 1 light chain to actin and its effect on actin-myosin interaction. *Biochemistry* **33**, 12821-12827.

231. Lowey, S., Waller, G. S. and Trybus, K. M. (1993). Function of skeletal muscle myosin heavy and light chain isoforms by an in vitro motility assay. *J. Biol. Chem.* **268**, 20414-20418.

232. Timson, D. J., Trayer, H. R. and Trayer, I. P. (1998). The N-terminus of A1-type myosin essential light chains binds actin and modulates myosin motor function. *Eur. J. Biochem* **255**, 654-662.

233. Weeds, A. G. and Frank, G. (1972). Structural studies on the light chains of myosin. *Cold Spring Harbor Symp. Quant. Biol.* **37**, 9-14.

234. Rayment, I., Rypniewski, W. R., Schmidt-Base, K., Smith, R., Tomchick, D. R., Benning, M. M., Winkelmann, D. A., Wesenberg, G. and Holden, H. M. (1993). Three-dimensional structure of myosin subfragment-1: a molecular motor. *Science* **261**, 50-58.

235. Schroder, R. R., Manstein, D. J., Jahn, W., Holden, H. M., Rayment, I., Holmes, K. C. and Spudich, J. A. (1993). Three-dimensional atomic model of F-actin decorated with Dictyostelium myosin S1. *Nature* **364**, 171-174.

236. Mornet, D., Pantel, P., Audemard, E. and Kassab, R. (1979). A limited tryptic cleavage of chymotryptic S-1: an approach to the characterization of the actin site in myosin heads. *Biochem. Biophys. Res. Commun.* **89**, 925-932.

237. Mornet, D., Ue, K. and Morales, M. F. (1984). Proteolysis and the domain organization of myosin subfragment 1. *Proc. Natl. Acad. Sci. USA* **81**, 736-739.

238. Kelley, C. A. and Adelstein, R. S. (1995). Characterization of myosin II isoforms containing insertions of amino acids in the flexible loop near the ATP-binding pocket. *Biophys. J.***68,** 225S

239. Kurzawa-Goertz, S. E., Perreault-Micale, C. L., Trybus, K. M., Szent-Gyorgyi, A. G. and Geeves, M. A. (1998). Loop I Can Modulate ADP Affinity, ATPase Activity, and Motility of Different Scallop Myosins. Transient Kinetic Analysis of S1 Isoforms. *Biochemistry* **37**, 7517-7525.

240. Uyeda, T. Q., Ruppel, K. M. and Spudich, J. A. (1994). Enzymatic activites correlate with chimeric substitutions at the actin-binding face of myosin. *Nature* **368**, 567-569.

241. Furch, M., Geeves, M. A. and Manstein, D. J. (1998). Modulation of actin affinity and actomyosin adenosine triphosphatase by charge changes in the myosin motor domain. *Biochemistry* **37**, 6317-6326.

242. Weeds, A. G. and Taylor, R. S. (1975). Separation of subfragment-1 isoenzymes from rabbit skeletal muscle myosin. *Nature* **257**, 54-56.

243. Reisler, E., Burke, M. and Harrington, W. F. (1974). Cooperative role of two sulfhydryl groups in myosin adenosine triphosphatase. *Biochemistry* **13,** 2014-2022.

244. Sekine, T. and Yamaguchi, M. (1963). Effect of ATP on the binding of N-ethylmaleimide to SH groups in the active site of myosin ATPase. *J. Biochem* **54**, 196-198.

245. Kielley, W. W. and Bradley, L. B. (1956). The relationship between sulfhydryl groups and the activation of myosin adenosinetriphosphatase. *J. Biol. Chem* **218,** 653-659.

246. Elzinga, M. and Collins, J. H. (1977). Amino acid sequence of a myosin fragment that contains SH-1, SH-2, and N^{τ}-methylhistidine. *Proc. Natl. Acad. Sci. USA* **74**, 4281-4284.

247. Balint, M., Wolf, I., Tarcsafalvi, A., Gergely, J. and Sreter, F. A. (1978). Location of SH-1 and SH-2 in the heavy chain segment of heavy meromyosin. *Arch. Biochem. Biophys.* **190**, 793-799.

248. Wells, J. A. and Yount, R. G. (1979). Active site trapping of nucleotides by crosslinking two sulfhydryls in myosin subfragment 1. *Proc. Natl. Acad. Sci. USA* **76**, 4966-4970.

249. Kubo, S., Tokura, S. and Tonomura, Y. (1960). On the active site of myosin A-adenosine triphosphatase. I. Reaction of the enzyme with trinitrobenzenesulfonate. *J. Biol. Chem* **235**, 2835-2839.

250. Fabian, F.and Muhlrad, A. (1968). Effect of trinitrophenylation on myosin ATPase. *Biochem. Biophys. Acta* **162**, 596-603.

251. Huxley, H. E. (1963). Electron microscope studies on the structure of natural and synthetic protein filaments from striated muscle. *J. Mol. Biol.***7**, 281-308.

252. Taylor, K. A. and Amos, L. A. (1981). A new model for the geometry of the binding of myosin crossbridges to muscle thin filaments. *J. Mol. Biol* **147**, 297-324

253. Wakabayashi, T. and Toyoshima, C. (1981). Three-dimensional image analysis of the complex of thin filaments and myosin molecules from skeletal muscle. II. The multi-domain structure of actin-myosin SI complex. *J. Biochem.* **90**, 683-701.

254. Mendelson, R. and Kretzschmar, K. M. (1980). Structure of myosin subfragment 1 from low-angle x-ray scattering. *Biochemistry* **19**, 4103-4108.

255. Elliot, A. and Offer, G. (1978). Shape and flexibility of the myosin molecule. *J. Mol. Biol* **123**, 505-519.

256. Craig, R., Szent-Gyorgyi, A. G., Beese, L., Flicker, P., Vibert, P. and Cohen, C. (1980). Electron microscopy of thin filaments decorated with a Ca^{2+}-regulated myosin. *J. Mol. Biol* **140,** 35-55.

257. Malhotra, A., Huang, S. and Bhan, A. (1979). Subunit function in cardiac myosin: effect of removal of Lc2 (18,000 molecular weight) on enzymic properties. *Biochemistry* **18**, 461-467.

258. Sellers, J. R. and Alelstein, R. A. (1987) In *The Enzymes,* Vol. 18, Academic San Diego publishes. Pg 381-418.

259. Trybus, K. M., Huiatt, T. M. and Lowey, S. (1982). A bent monomeric conformation of myosin from smooth muscle. *Proc. Natl. Acad. Sci. USA* **79**, 6151-6155.

260. Ikebe, M., Hinkins, S. and Hartshorne, D. J. (1983). Correlation of enzymatic properties and conformation of smooth muscle myosin. *Biochemistry* **22**, 4580-4587.

261. Franzini-Armstrong, C. and Peachy, L. D. (1981). Striated muscle contractile and mechanisms. *J. Cell Biol.* **91**, 166s-186s.

262. Huxley, A. F. and Simmons, R. M. (1971). Proposed mechanism of force generation in striated muscle. *Nature* **233**, 533-538.

263. Huxley, H. E. (1969). Mechanism of muscular contraction. *Science* **164**, 1356 – 1366.

264. Huxley, H. E. and Holmes, K. C. (1997). Development of synchrotron radiation as a high-intensity source for X-ray diffraction. *Synchrotron Radiat.* **4,** 366-379.

265. Huxley, H. E., Simmons, R. M., Faruqi, A. R., Kress, M., Bordas, J. and Koch, M. H. J. (1981). Millisecond tme-resolved changes in X-ray reflections from contracting muscle during rapid mechanical transients, recorded using synchrotron radiation. *Proc. Natl. Acad. Sci. USA* **78**, 2297-2301.

266. Irving, M., Lombardi, V. and Piazzesi, G. (1992). Myosin headmovements are synchronous with the elementary force generating process in muscle. *Nature* **357**, 156-158.

267. Cooke, R. (1986). The mechanism of muscle contraction. *Crit. Rev. Biochem.* **21**, 53-118.

268. Sabido-David, C., Hopkins, S. C., Saraswat, L. D., Lowey, S., Goldman, Y. E. and Irving, M. (1998). Orientation changes of fluorescent probes at five sites on the myosin regulatory light chain during contraction of single skeletal muscle fibres. *J. Mol. Biol.* **279**, 387-402.

269. Lymn, R. W. and Taylor, E. W. (1971). Mechanism of adenosine triphosphate hydrolysis by actomyosin. *Biochemistry* **10,** 4617-4624.

270. Chalovich, J. M. and Eisenberg, E. (1982). Inhibition of actomyosin ATPase activity by troponin-tropomyosin without blocking the binding of myosin to actin. *J. Biol. Chem.,* 257, 2432-2437.

271. Holmes, K. C. (1995). The actomyosin interaction and its control by tropomyosin. *Biophys. J.* **68**, 2s-7s.

272. Eisenberg, E. and Green, L. E. (1980). The relation of muscle biochemistry to muscle physiology. *Annu. Rev. Physiol.* **42**, 293-309.

273. Hill, T. L., Eisenberg, E. and Greene, L. E. (1980). Theoretical model for the cooperative equilibrium binding of myosin subfragment-1 to the actin-troponin-tropomyosin complex. *Proc. Natl. Acad. Sci. USA* **77**, 3186-3190.

274. McKillop, D. F. and Geeves, M. A. (1993). Regulation of the interaction between actin and myosin subfragment-1: evidence for the three states of the thin filament. *Biophys. J.* **65**, 693-701.

275. Geeves, M. A. and Conibear, P. B. (1995). The role of three-state docking of myosin S1 with actin in force generation. *Biophys. J.* **68**, 194s-201s.

276. Lehman, W., Craig, R. and Vibert, P. (1994). Ca^{+2}-induced tropomyosin movement in *Limulus* thin filaments revealed by three-dimensional reconstruction. *Nature* **368**, 65-67.

277. Poole, K. V. g., Evans, G., Rosenbaum, G., Lorenz, M. and Holmes, K. C. (1995). The effect of cross-bridges on the calcium sensitivity of the structural change of the regulated thin filament. *Biophys. J.* **68,** 365a.

278. Xu, C., Craig, R., Tobacman, L., Horowitz, R and Lehman, W. (1999). Tropomyosin positions in regulated thin filament revealed by cryoelectron microscopy. *Biophys. J.* **77**, 985-992.

279. Craig, R. and Lehman, W. (2001). Cross-bridge and tropomyosin positions observed in native, interacting thick and thin filaments. *J. Mol. Biol.***311**, 1027-1036.

280. Heeley, D. H., Belknap, B. and White, H. D. (2002). Mechanism of regulation of phosphate dissociation from actomyosin-ADP-Pi by thin filament proteins. *Proc. Natl. Acad. Sci. USA* **99**, 16731-16736.

281. Heeley, D. H., Belknap, B. and White, H. D. (2006). Maximal activation of skeletal muscle thin filaments requires both rigor myosin S1 and calcium. *J. Biol. Chem.*, **281**, 668-676.

282. Stein, L. A., Chock, P. B. and Eisenberg, E. (1984) The rate-limiting step in the actomyosin adenosine triphosphatase cycle. *Biochem.* **23**, 1555-1563.

283. Bollag, D. M. and Edelstein, S. J. (1991) In Protein Methods. New York, NY; Toronto: Wiley-Liss, pp47.

284. Cartson, M. E. and Mommearts, W. F. H. M. (1963). A study of actin by means of starch gel electrophoresis. *Biochemistry* **2,** 28-32.

285. Spudich, J. A. and Watt, S. (1971). The regulation of rabbit skeletal muscle contraction. *J.Biol.Chem.* **246,** 4866-4871.

286. Smillie, L.B. (1982) Preparation and identification of alpha and beta tropomyosins. *methods Enzymol.* **85**, 234-241.

287. Potter, J. D. (1982). Purification of skeletal troponin. *methods Enzymol.* **85**, 241-263.

288. Perry, S. V. (1955). Myosin adenosine-triphosphatase. m*ethods enzymol.* **2**, 582-588.

289. Laemmli, U. K. (1970). Cleavage of structural proteins during assembly of the head of bacteriophage T4. *Nature* **227**, 680-685.

290. Perrie, W. T. and Perry, S. V. (1970). An Electrophoretic study of the low-molecular weight components of myosin. *Biochem. J.* **119**, 31-38.

291. Safer, D. (1989). An electrophoretic procedure for detecting proteins that bind actin monomers. *Anal.Biochem.* **178**, 32-37.

292. Towbin, H., Staehelin, T. and Gordon, J. (1979). Electrophoretic transfer of proteins from polyacrylamide gels to nitrocellulose sheets:procedure and some applications. *Proc. Natl. Acad. Sci. USA* **76**, 4350-4354.

293. Heeley, D. H., Watson, M. H., Mak, A. S., Dubord, P. and Smillie, L. B. (1989). Effect of phosphorylation on the interaction and functional properties of rabbit striated muscle αα-tropomyosin. *J. Biol. Chem.* **264**, 2424-2430.

294. Moraczewska, J., Strzelcka-Golaszewska, H., Moens, P. D. J. and Dos Remedios, C. G. (1996). Structural changes in subdomain 2 of G-actin observed by fluorescence spectroscopy. *Biochem. J.* **317**, 605-611.

295. Hartshorne, D. J. and Mueller, H. (1969). The preparation of tropomyosin and troponin from natural actomyosin. *Biochim Biophys. Acta* **175**, 301-319.

296. Young, D. M., Himmelfrab, S. and Harrington, W. F. (1965). On the structural assembly of the polypeptide chains of heavy meromyosin. *J. Biol. Chem.* **240**, 2428-2436.

297. Young, D. M., Himmelfrab, S. and Harrington, W. F. (1964). The Relationship of the Meromyosins to the Molecular Structure of Myosin. *J. Biol. Chem.* **239**, 2822-2829.

298. Houk, T. W. and Ue, K. (1974). The measurement of actin concentration in solution : a comparison of methods. *Anal.Biochem.* **62,** 66-74.

299. Bradford, M.M. (1976). A rapid and sensitive method for the quantitation of microgram quantities of protein utilizing the principle of protein-dye binding, *Anal.Biochem.* **72**, 248-254.

300. Heeley, D.H. and Hong, C. (1994). Isolation and characterization of tropomyosin from fish muscle, *Comp.Biochem.physiol.* **108B**, 95-106.

301. Penke, B., Ferenczi,R. and Kovacs, K. (1974). A new acid hydrolysis method for determining tryptophan in peptides and proteins, *Anal.Biochem* **60**, 45 –50.

302. Moore, S. (1963). On the determination of cystine as cysteic acid, *J.Biol.Chem* **238**, 235-237.

303. Crestfield, A.M., Moore, S. and Stein, W.H. (1963). The preparation and enzymatic hydrolysis of reduced and S-carboxymethylated proteins, *J.Biol.Chem* **238**, 622-627.

304. Ellman, G. L. (1959). Tissue sulfhydryl groups. *Arch. Biochem. Biophys.* **82**, 70-77.

305. Bornstein, P. (1970). Structure of α1-CB8, a large cyanogens bromide produced fragment from the α1 chain of rat collagen. The nature of a hydroxylamine-sensitive bond and composition of tryptic peptides. *Biochemistry* **9**, 2408-2421.

306. Hynes, G. S. and Willison, K. R. (2000). Individual subunits of the eukaryotic cytosolic chaperonin mediate interactions with binding sites located on subdomains of β-actin. *J.Biol.Chem.* **275**, 18985-18994.

307. Pollard, T. D. (1986). Rate constants for the reaction of ATP-and ADP-actin with the ends of actin filaments. *J. Cell Biol.* **103,** 2747-2754.

308. Strzelecka-Golaszewska, H., Moraczewska, J., Khaitlina, S.Y. & Mossakowska, M. (1993) Localization of the tightly bound divalent-cation-dependent and nucleotide-dependent conformation changes in G-actin using limited proteolytic digestion. *Eur J. Biochem.* **211**, 731–739.

309. Brown, S. E. and Knudson, D. L. (1991). 96 well plates for recombinant library maintenance and dot blot production. *BioTechniques* **10**, 719-722.

310. Sambrook, J., Fritsch, E. F. and Maniatis, T. (1989). *Molecular cloning: A laboratory manual*, 2nd ed. Cold Spring Harbor Laboratory Press, Cold Spring Harbor NY.

311. Southern, E. M. (1975). Detection of specific DNA sequences among DNA fragments separated by gel electrophoresis. *J. Mol. Biol.* **98**, 503-517.

312. Sanger, F., Nicklen, S. and Coulson, A. R. (1977). DNA sequencing with chain terminating inhibitors. *Proc. Natl. Acad. Sci. USA* **74**, 5463-5467.

313. Lehrer, S. S. and Morris, E. P. (1982). Dual effects of tropomyosin and troponin-tropomyosin on actomyosin subfragment 1 ATPase. *J. Biol. Chem.* **257**, 8073-8080.

314. Ribolow, H. and Barany, M.(1977). Phosphorylation of tropomyosin in live frog muscle. *Arch. Biochem. Biophys.* **179**, 718-720.

315. Barany, M. and Barany, K. (1980). Phosphorylation of the myofibrillar proteins. *Annu. Rev. Physiol.* **42**, 275-292.

316. Montarass D, Fiszman MY and Gros F (1981) Characterisation of the tropomyosin present in various chick embryo muscle types and in muscle cells differentiated *in vitro*. *J Biol Chem* **256:** 4081-4086.

317. Montgomery K and Mak AS (1984) In vitro phosphorylation of tropomyosin by a kinase from chicken embryo. *J Biol Chem* **259:** 5555-5560.

318. Perry, S. V., Cole, H. A., Morgan, M., Moir, A. J. G. and Pires, E. (1975). Phosphorylation of the proteins of the myofibril. *Proc. 9th Meet. Fed. Eur. Biochem. Soc., Amsterdam: North-Holland.* pp. 163-176.

319. Pratje, E. and Heilmeyer, L. M. G. Jr. (1972). Phosphorylation of rabbit muscle troponin and actin by a 3',5'-cAMP-dependent protein kinase. *FEBS Letts.* **27**, 89-93.

320. Stull, J. T. and Buss, J. E. (1977). Phosphorylation of cardiac troponin by cyclic adenosine 3',5'-monophosphate dependent protein kinase. *J. Biol. Chem.* **252**, 851-857.

321. Heeley, D. H., Watson, M. H., Mak, A. S., Dubord, P. and Smillie, L. B. (1989). Effect of phosphorylation on the interaction and functional properties of rabbit striated muscle αα-tropomyosin. *J. Biol. Chem.* **264**, 2424-2430.

322. Sano, K., maeda, K., Oda, T. and Maeda, Y. (2000). The effect of single residue substitutions of Serine-283 on the strength of head to tail interaction and actinbinding properties of rabbit skeletal muscle alpha-tropomyosin. *J. Biochem.* **127**, 1095-1102.

323. Greenfield, N.J., Palm, T. and Hitchcock-DeGregori, S. E.(2002). Structure and interactions of the carboxyl terminus of striated muscle α-tropomyosin: It is important to be flexible. *Biophys. J.* **83,** 2754-2766.

324. Hayley, M. (2004). Thermal stability: Characterization of makoshark skeletal tropomyosin. MSc thesis.

325. Murray, J. M., Knox, M. K., Trueblood, C. E. and Weber, A. (1980). Do tropomyosin and myosin compete for actin sites in the presence of calcium?. *FEBS Letts.* **114,** 169-173.

326. Williams, D. L., Green, L. E. and Eisenberg, E. (1988). Cooperative turning on of myosin subfragment 1 adenosine triphosphatase activity by the troponin-tropomyosin-actin complex. *Biochemistry* **27**, 6987-6993.

327. Eaton, B. L., Kominz, D. R. and Eisenberg, E. (1975). Correlation between the inhibition of the acto-heavy meromyosin ATPase and the binding of tropomyosin to F-actin. Effects of Mg^{2+}ion, potassium chloride troponin I, and troponin C. *Biochemistry* **14**, 2718-2725.

328. Greene, L. E. and Eisenberg, E. (1980). Cooperative binding of myosin subfragment-1 to the actin-troponin-tropomyosin complex. *Proc. Natl. Acad. Sci. USA* **77**, 2616-2620.

329. Hill, L. E., Mehegan, J. P., Butters, C. A. and Tobacman, L. S. (1992). Analysis of troponin-tropomyosin binding to actin. Troponin does not promote interactions between tropomyosin molecules. *J. Biol. Chem.* **267**, 16106-16113.

330. Murray, J. M., Weber, A. and Knox, M. K. (1981). Myosin subfragment 1 binding to relaxed actin filaments and steric model of relaxation. *Biochemistry* **20**, 641-649.

331. Willadsen, K. A., Butters, C. A., Hill, L. E. and Tobacman, L. S. (1992). Effects of the amino-terminal regions of tropomyosin and troponin-T on thin filament assembly. *J. Biol. Chem.* **267**, 23746-23752.

332. Pittenger, M. F.and Helfman, D. M. (1992) In vitro and in vivo characterization of four fibroblast tropomyosins produced in bacteria: TM-2, TM-3, TM-5a, and TM-5b are co-localized in interphase fibroblasts. *J. Cell Biol.* **118**, 841-858.

333. Cho, Y. J. and Hitchcock-DeGregori S. E. (1991). Relationship Between Alternatively Spliced Exons and Functional Domains in Tropomyosin. *Proc. Natl. Acad. Sci. USA* **88,** 10153-10157.

334. Green, L. E., Williams, D. L., Jr. and Eisenberg, E. (1987). Regulation of actomyosin ATPase activity by troponin-tropomyosin: Effect of the binding of the myosin subfragment 1 (S-1)· ATP complex. *Proc. Nat. Acad. Sci. USA.* **84**, 3102-3106.

335. Butters, C. A., Willadsen, K. A., and Tobacman, L. S. (1993). Cooperative interactions between adjacent troponin-tropomyosin complexes may be transmitted through the actin filament. *J. Biol. Chem.* **268**, 15565-15570.

336. Chalovich, J. M., Chock, P. B. and Eisenberg, E. (1981). Mechanism of action of troponin . tropomyosin. Inhibition of actomyosin ATPase activity without inhibition of myosin binding to actin. *J. Biol. Chem.* **256**, 575-578.

337. Gaffin, R. D., Gokulan, K., Sacchettini, J. C., Hewett, T., Klevitsky, R., Robbins, J. and Muthuchamy, M. (2004). Charged residue changes in the carboxy-terminus of α-tropomyosin alter mouse cardiac muscle contractility. *J. Physiol.* **556**, 531-543.

338. Gaffin, R. D., Tong, C., Zawieja, D. C., Hewett, T., Klevitsky, R., Robbins, J. and Muthuchamy, M. (2004). Charged residue alterations in the inner-core domain and carboxyl terminus of α-tropomyosin differentially affects mouse cardiac muscle contractility. *J. Physiol.* **561**, 777-791.

339. Jagatheesan, G., Rajan, S., Petrasheskaya, N., Schwartz, A., Boivin, G., Vahebi, S., DeTombe, P., Solaro, R. J., Labitzket, E., Hillard, G. and Wieczorek, D. F. (2003). Functional importance of the carboxyl terminal region of striated muscle tropomyosin. *J. Biol. Chem.* **278**, 23204-23211

340. Farah, C.S. and Reinach, F. C. (1999). Regulatory properties of recombinant tropomyosins containing 5-hydroxytryptophan: Ca+2 binding to troponin results in a conformational change in a region of tropomyosin outside the troponin binding site. *Biochemistry* **38**, 10543-10551.

341. Pardee, J.D. and Spudich, J.A. (1982). Mechanism of K+-induced actin assembly. *J. Cell Biol.* **93,** 648-654.

342. Pollard. T. P. and Weeds, A. G. (1984). The rate constant for ATP hydrolysis by polymerized actin. *FEBS Letts.* **170**, 94-98

343. Carlier, M. G., Panataloni, D. and Korn, E. D. (1984). Evidence for an ATP cap at the ends of actin filaments and its regulation of the F-actin steady state. *J. Biol. Chem.* **259**, 9983-9986.

344. Zimmerle, C. T. and Frieden, C.(1988). Effect of pH on the mechanisms of actin polymerization. *Biochemistry* **27**, 7766-7772.

345. Chen, X., Cook, K. and Rubenstein, P. A. (1993). Yeast actin with a mutation in the " hydrophobic plug" between subdomain 3 and 4 (L266D) displays a cold sensitive polymerization defect. *J. Cell Biol.* **123**, 1185-1195.

346. Konno, K. and Morales, M. F. (1985). Exposure of actin thiols by the removal of tightly held calcium ions. *Proc. Natl. Acad. Sci. USA* **82**, 7904-7908.

347. Chik, J. K., Lindberg, U. and Schutt, C. E. (1996). The structure of an open state of beta-actin at 2.65 A0 resolution. *J. Mol. Biol.* **263,** 607-623

348. Schutt, C. E., Myslik, J. C., Rozycki, M. D., Goonasekere, N. C. W. and Lindberg, U. (1993). The structure of the crystalline profiling-beta-actin. *Nature* **365**, 810-816.

349. Eaton, B. L. (1976). Tropomyosin binding to F-actin induced by myosin heads. *Science* **192,** 1337-1349.

350. Dominguez, R. (2004). Actin binding proteins-unifying hypothesis. Trends in Biochem. Sci. **29**, 572-578.

351. Feng, L., Kim, e., Lee, W., Miller, C. J., Kuang, B., Reisler, E. and Rubenstein, P. A. (1997). Fluorescence probing of yeast actin subdomain ¾ hydrophobic loop. *J. Biol. Chem.* **272**, 262-274.

352. Schutt, C. E., Lindberg, U., Myslik, J. and Strauss, N. (1989). Molecular packing in profiling:actin crystals and its implications. *J. Mol. Biol.* **209**, 735-746.

353. Orlova, A. and Egelman, E. H. (1992). Structural basis for the destabilization of F-actin by phosphate release following ATP hydrolysis. *J. Mol. Biol.* **245**, 582-597.

354. Schwyter, D.H., Kron, S.J., Toyoshima, Y.Y., Spudich, J.A. and Reisler, E. (1990). Subtilisin cleavage of actin inhibits *in vitro* sliding movement of actin filaments over myosin. *J. Cell Biol.* 111, 465-470.

355. Konno, K. (1987). Functional, chymotryptically split actin and its interaction with myosin subfragment 1 *Biochemistry* **26**, 3582-3589.

356. Khaitlina, S.Y., Collins, J. H., Kuznetseva, I. M., Pershina, V. P, Synakevich, I. G., Turoverov, K. K. and Usmanova, A. M. (1991). Physico-chemical properties of actin cleaved with bacterial protease from *E. coli* A2 strain. *FEBS Letts.* **279**, 49-51.

357. Jacobson, G. R. and Rosenbusch, J. P. (1976). ATP Binding to a Protease-Resistant Core of Actin. *Proc. Natl. Acad. Sci. USA* **73**, 2742-2746.

358. Vahdat, A., Miller, C., Phillips, M., Muhlrad, A. & Reisler, E. (1995) A novel 27/16 kDa form of subtilisin cleaved actin: structural and fonctional consequences of cleavage between Ser 234 and Ser 235. *FEBS Lett.* **365**, 149-151.

359. Schuler, H., Nyakern, M., Schutt, C. E., Lindberg, U. and Karlsson, R. (2000). Mutational analysis of arginine 177 in the nucleotide binding site of beta-actin. *Eur. J. Biochem.* **267**, 4054-4062.

360. Schuler, H., Korenbaum, E., Schutt, C. E., Lindberg, U. and Karlsson, R. (1991). Mutational analysis of Ser14 and Asp157 in the nucleotide binding site of beta-actin. *Eur. J. Biochem.* **265**, 210-220.

361. Yao, X., Grade, S., Wriggers, W. and Rubenstein, P. A. (1999). His73, often methylated is an important structural determinant for actin. *J. Biol. Chem.* **274,** 37443-37449.

362. Kim, E., Miller, C. J., Motoki, M., Seguro, K., Muhlrad, A. and Reisler, E. (1996). Myosin-induced changes in F-actin - fluorescence probing of subdomain 2 by dansyl ethylenediamine attached to Gln41. *Biophys. J.* 70, 1439-1446.

363. Khaitlina, S.Y., Moraczewska, J. and Strzelecka-Golaszewska, H. (1993). The actin/actin interactions involving the N terminus of the DNase-I-binding loop are crucial for stabilization of the actin filament. *Eur. J. Biochem.* 218, 911-920.

364. Pantaloni, D., Carlier, M. F., Coue, M., Lal, A. A., Brenner, S. L. and Korn, E. D. (1984). The critical concentration of actin in the presence of ATP increases with the number concentration of filaments and approaches the critical concentration of actin. ADP. *J. Biol. Chem.* **259**, 6274-6283.

365. Schuler, H., Lindberg, U., Schutt, C. E. and Karlsson, R. (2000). Thermal unfolding of G-actin monitored with the DNase I inhibition assay: Stabilities of actin isoforms. *Eur. J. Biochem.* **267**, 476-486.

366. Chen, X., Peng, J., Pedram, M., Swenson, C. A. and Rubenstein, P. A. (1995). The effect of the S14A mutation on the conformation and thermostability of Saccharomyces serevisiae G-actin and its interaction with adenine nucleotide. *J. Biol. Chem.* **270**, 11415-11423.

367. Turoverov, K. K., Biktasshev, A. G., Khaitlina, Yu, S. and Kuznetsova, I. M. (1999). The structure and dynamics of partially folded actin. *Biochemistry* **38**, 6261-6269.

368. Bertazzon, A. Tian, G. H., Lamblin, A. and Tsong, T. Y. (1990). Enthalpic and entropic contributions to actin stability: calorimetry, circular dichroism, and fluorescence study and effects of calcium. *Biochemistry* **29**, 291-298.

369. Kuznetsova, I. M., Biktashev, A. G., Khaitlina, Yu, S., Vassilenko, K. S., Turoverov, K. K. and Uversky, V. N. (1999). Effect of self-association on the structural organization of partially folded proteins: Inactivated actin. *Biophys. J.* **77,** 2788-2800.

370. Kuznetsova, I. M., Stepanenko, O. V., Povarova, O. I., Biktashev, A. G., Verkhusha, V. V., Shavlovsky, M. M. and Turoverov, K. K. (2002). The place of inactivated actin and its kinetics predecessor in actin folding-unfolding. *Biochemistry* 41, 13127-13132.

371. Turoverov, K. K., Verkhusha, V. V., Shavlovsky, M. M., Biktashev, A. G., Povarova, O. I. and Kuznetsova, I. M. (2002). Kinetics of unfolding induced by guanidine hydrochloride. *Biochemistry* **41**, 1041-1019.

372. Mazhul, V. M., Zaiitseva, E. M., Shavlovsky, M. M., Stepanenko, O. V., Kuznetsova, I. M. and Turoverov, K. K. (2003). Monitoring of actin unfolding by room temperature tryptophan phosphorescence. *Biochemistry* **42**, 13551-13557.

373. Waechter, F. and Engle, J. (1977). Association kinetics and binding constants of nucleoside triphosphates with G-actin. *Eur. J. Biochem.* **74**, 227-232.

374. Nagy, B. and Strzelecka-Golaszewska, H. (1972). Optical rotatory dispersion and circular dichroic spectra of G-actin. *Arch. Biochem. Biophys.* **150,** 428-435.

375. Kuznetsova, I. M., Khaitlina, Yu, S., Konditerov, S. N., Surin, A. M. and Turoverov, K. K. (1988). Changes of structure and intramolecular mobility in the course of actin denaturation. *Biophys. Chem.***32,** 73-78.

376. Le Bihan, T. and Gicquaud, C. (1993). Kinetic Study of the Thermal Denaturation of G Actin Using Differential Scanning Calorimetry and Intrinsic Fluorescence Spectroscopy.*Biochem. Biophys. Res. Commun.* **194**, 1065-1073.

377. Nowak, E., Strzelecka-Golaszewska, H. and Goody, R. S. (1988). Kinetics of nucleotide and metal ion interaction with G-actin. *Biochemistry* **27,** 1785-1792.

378. Frieden, C. and Patane, K. (1988). Mechanism for nucleotide exchange in monomeric actin. *Biochemistry* **27,** 3812-3820.

379. Nowak, E. and Goody, R. S. (1988). Kinetics of adenosine 5'-triphosphate and adenosine 5'-diphosphate interaction with G-actin. *Biochemistry* **27**,8613-8617.

380. Kinosian, H. J., Selden, L. A., Estes, J. E. and Gershman, L. C. (1991). Thermodynamics of actin polymerization. Influence of the tightly bound cation. *Biochim. Biophys. Acta.* **1077**, 151-158.

381. Neidl, C. and Engel, J. (1979). Exchange of ADP, ATP and 1: N6-ethenoadenosine 5'-triphosphate at G- actin. Equilibrium and kinetics. *Eur. J. Biochem.* **101**, 163-169.

382. Wanger, M. and Wegner, A. (1983). Similar affinities of ADP and ATP for G-actin at physiological salt concentrations. *FEBS Letts.* **162,** 112-116.

383. Selden, L. A., Gershman, L. C., Kinosian, H. J. and Estes, J. E. (1987). Conversion of ATP-actin to ADP-actin reverses the affinity of monomeric actin for Ca^{2+} vs Mg^{2+}. *FEBS Lett.* **217**, 89-93.

384. Strzelecka-Golaszewiska, H. (1973). Relative affinities of divalent cation to the site of the tight calcium binding in G-actin. *Biochim. Biophys. Acta* **310**, 60-69.

385. Gershman, L. C., Selden, L. A. and Estes, J. E. (1986). High affinity binding of divalent cation to actin monomer is much stronger than previously reported. *Biochem. Biophys. Res. Commun.* **135**, 607-614.

386. Duke, J., Takashi, R., Ue, K. and Morales, M. F. (1976). Resiprocal reactivities of specific thiols when actin binds to myosin. *Proc. Natl. Acad. Sci. USA* **73**, 302-306.

387. Johara, M., Toyoshima, Y. Y., Ishuima, A., Kojima, H., Yanagida, T., and Sutoh, K. (1993). Charge-reversion mutagenesis of Dictyostelium actin to map the surface recognized by myosin during ATP driven sliding motion. *Proc. Natl. Acad. Sci. USA* **90**, 2127-2131.

388. Egelman, E. H. and Orlova, A. (1995). New insights into actin filament dynamics. *Curr. Opin. Struct. Biol.* **5**, 172-180.

389. Sablin, E. P., Dawson, J. F., Vanlock, M. S., Spudich, J. A., Egelman, E. H. and Fletterick, R. J. (2002). How does ATP hydrolysis control actin's associations?. *Proc. Natl. Acad. Sci. USA* **99**, 10945-10947.

390. Lorenz, M., Poole, K. J. V., Popp, D., Rosenbaum, G. and Holmes, K. C. (1995). An atomic model of the unregulated thin filament obtained by X-ray fiber diffraction on oriented actin-tropomyosin gels. *J. Mol. Biol.* **246**, 108-119.

391. Korman, V. L. and Tobacman, L. S. (1999). Mutations in actin sub-domain 3 that impair thin filament regulation by troponin and tropomyosin. *J. Biol. Chem.* **274,** 22191-22196.

392. Kovilur, S., Jacobson, J. W., Beach, R. L., Jeffey, W. R. and Tomlinson, C. R. (1993) Evolution of the Chordate Muscle Actin Gene *J. Mol. Evol.* **36,** 361-368.

393. Kusakabe, T., Araki, I., Satoh, N.and Jeffery, W. R. (1997b). Evolution of chordate actin genes: evidence from genomic organization and amino acid sequences. *J Mol Evol* **44,** 289-298.

394. Miwa, T., Manabe, Y., Kurokawa, K., Kamada, S., Kanda, N., Brung, G., Ueyama, H. and kakunaga, T. (1991). Srtucture, chromosome location, and

expression of human smooth muscle (enteric type) gamma actin gene: evolution of six human actin genes. *Mol. Cell Biol.* **11**, 3296-3306.

395. Moos, M. and Gallwitz, D. (1983). Structure of two human beta actin related processed genes one of which is located next to a simple repetitive sequence. *EMBO J.* **2,** 757-761.

396. Ng, S., Gunning, P., Eddy, R., Ponte, P., Leavitt, J., Shows, T. and Kedes, L. (1985). Evolution of the functional human beta actin gene and its multi-pseudogene family: conservation of non-coding regions and chromosomal dispersion of pseudogene. *Mol. Cell Biol.* **5**, 2720-2732.

397. Chang, K. S., Rothblum, K. N. and Schwartz, R. J. (1985). The complete sequence of the chicken alpha cardiac actin gene: a highly conserved vertebrate gene. *Nucl. Acids Res.* **13,** 1223-1237.

398. Fornwald, J. A., Kuncio, G., Peng, I. And Ordahl, C. P. (1982). The complete nucleotide sequence of the chick alpha actin gene and its evolutionary relationship to the actin gene family. *Nucl. Acids Res.***10**, 3861-3876.

399. Mohun, T. J., Garret, N. and Gurdon, J. B. (1986). Upsream sequences required for tissue specific activation of the cardiac actin gene in Xenopus laevis embryos. *EMBO j.* **5**, 3185-3193.

400. Carroll, S.L., Bergsma, D. J. and Schwartz, R. J.(1986). Structure and complete nucleotide sequence of chicken a-smooth muscle (aortic) actin gene. *J. Biol. Chem.* **261**, 8965-8976.

401. Bergsma, D. J., Chang, K. S. and Schwartz, R. J. (1985). Novel chicken actin gene: third cytoplasmic isoform. *Mol. Cell Biol.* **5,** 1152-1162.

402. Cox, R. D. and Buckingham, M. E. (1992). Actin and myosin genes are transcriptionally regulated during mouse skeletal muscle development. *Dev. Biol.* **149,** 228-234.

403. Vanderkerckhove, J., Franke, W. W. and Weber, K. (1981). Diversity of expression of non-muscle actin in amphibians. *J. Mol. Biol.* **152,** 413-426.

404. Lassar, A. B., Buskin, J. N., Lockshon, D., Davis, R. L., Apones, S., Hauschka, S. D. and Weintraub, H. (1989). MyoD is a sequence –specific DNA binding protein requiring a region of *myc* homology to bind to the muscle creatine kinase enhancer. *Cell* **58,** 823-831.

405. Weintraub, H., Davis, R. L., Tapscott, S., Thayer, M., Krause, M., Benezra, R., Blackwell, T. K., Turner, D., Rupp, R., Hollenberg, S., Zhuang, Y. and Lassar, A. B. (1991). The myoD gene family: nodel point during specification of the muscle cell lineage. *Science* **251**, 761-766.

406. Lee, T. C., Shi, Y. and Schwartz, R. J. (1992). Displacement of BrdUrd-induced YY1 by serum response factor activates skeletal alpha actin transcription in embryonic myoblasts. *Proc. Natn. Acad. Sci. USA* **89**, 9814-9818.

407. Moss, J. B., McQuinn, T. C. and Schwartz, R. J. (1994). The avian cardiac alpha actin promoter is regulated through a pair of complex elements composed of E boxes and serum response elements that bind both positive-and negative-acting factors. *J. Biol. Chem.* **269,** 12731-12740.

408. Mudalige, A. K. A. W., Jackman, D. M., Waddleton, D. M. and Heeley, D. H. (2007). A vertebrate slow muscle actin isoform [in press, FEBS]

409. Carey, F. G. and Teal, J. M. (1966). Heat conservation in tuna fish muscle. *Proc. Natn. Acad. Sci. USA* **56**, 1464-1469.

410. Carey, F. G., Teal, J. M., Kanwisher, J. W., Lawson, K. D. and Beckett, J. S. (1971). Warm-bodied fish. *Am. Zool.* **11,** 135-143.

411. Graham, J. B., Koehrn, F. J. and Dickson, K. A. (1983). Distribution and relative proportions of red muscle in scombrid fishes: consequences of body size and relationships to locomotion and Endothermy. *Can. J. Zool.* **61**, 2087-2096.

412. Carey, F. G. and Lawson, K. D.(1973). Temperature regulation in free-swimming bluefin tuna. *Comp. Biochem. Physiol.* **44A**, 375-392.

413. Thopson, J. D., Higgins, D. G., and Gibson, T. J. (1994). CLUSTAL W: improving the sensitivity progressive multiple sequence weighting, position specific gap penalties and weight matrix choice. *Nucleic acids Res.* **22**, 4673-4680.

414. Saitou, N. and Nei, M. (1987). The neighbor-joining method: a new method for reconstructing phylogenetic trees. *Mol. Biol. Evol.* **4,** 406-425.

415. Collins, J. H. and Elzinga, M. (1975). The primary structure of actin from rabbit skeletal muscle. Completion and analysis of the amino acid sequence. *J. Biol. Chem.* **250**, 5915-5920.

416. Zakut, R., Shani, M., Givol, D., Neuman, S., Yaffe, D. and Nudel, U. (1982). Nucleotide sequence of the rat skeletal muscle actin gene. *Nature* **298,** 857-859.

417. Hu, M. C., Sharp, S. B. and Davidson, N. (1986). The complete sequence of the mouse skeletal alpha-actin gene reveals several conserved and inverted repeat sequences outside of the protein coding region. *Mol. Cell Biol.* **6,** 15-25.

418. Reecy, J. M., Bidwell, C. A., Briley, G. P. and Grant, A. L. (1996). Structure and regulation of the porcine skeletal alpha-actin-encoding gene. *Gene* **21**, 23-8.

419. Hanauer, A. Levin, M., Heilig, R., Daegelen, D. Khan, A. and Mandel, J. L. (1983). Isolation and characterization of cDNA clones for human skeletal muscle alpha-actin. *Nucleic Acids Res.* **11**, 3503-3516.

420. Stutz, F. and Spohr, G. (1986). Isolation and characterization of sarcomeric actin genes expressed in *Xenopus laevis* embryos. *J. Mol. Biol.* **187,** 349-361.

421. Venkatesh, B., Tay, B. H., Elgar, G. and Brenner, S. (1996). Isolation, characterization and evolution of nine puffer fish (Fugu rubripes) actin genes. *J. Mol.Biol.***259**, 655-665.

422. Ponte, P., Gunning, P., Balu, H. and Kedes, L. (1983). Human actin genes are single copy for alpha skeletal and alpha cardiac actins but multicopy for beta and gamma cytoskeletal genes: 3' untranslated regions are isotype specific but are conserved in evolution. *Mol. Cell Biol.* **3,** 1783-1791.

423. Kost, T. A., Theodorakis, N. and Hughes, S. H.(1983). The nucleotide sequence of the chick cytoplasmic ß-actin gene. *Nucl. Acids Res.***11**, 8287-8301.

424. Ordahl, C. P. and Cooper, T. A. (1983) Strong homology in promoter and 3'-untranslated regions of chick and rat alpha-actin genes. *Nature* **303,** 348-349.

425. Van Den Berg, J., Van Ooen, A., Mantei, N., Schmbock, A., Grosveld, G., Flavell, R. A. and Weissman, C. (1978). Comparison of cloned rabbit and mouse beta-globin genes showing strong evolutionary divergence of two homologous pairs of introns. *Nature* **276**, 37-44.

426. Kuma, K., Iwabe, N. and Miyata, T. (1995). Functional constraints against variations from tissue level: slowly evolving brain specific genes demonstrated by protein kinase and immunoglobulin supergen family. *Mol. Biol. Evol.* **12**, 123-130.

427. Doolottle, R. F. (1995). The origins and evolution of eukaryotic proteins. *Philos Trans R Soc Lond B Biol Sci.* **29**, 235-240.